UNIVERSITY OF LONDON THESIS

Degree PhD Year 2007 Name of Author SHAWCROSS, Deborah Lindsay

Ammonia, Infection and Inflammation in Hepatic Encephalopathy

By

Debbie L. Shawcross

Thesis submitted for the degree of Doctor of Philosophy

Liver Failure Group
Institute of Hepatology
Royal Free & University College London Medical School
University College London

Submitted September 2006
Revised June 2007

ProQuest LLC
789 East Eisenhower Parkway
P.O. Box 1346
Ann Arbor, MI 48106-1346

'There are in fact two things, science and opinion; the former begets knowledge, the latter ignorance'

Hippocrates

This thesis is dedicated to all the members and collaborators of the Liver Failure Group, past and present, whose support and friendship will never be forgotten.

I declare that the work presented in this thesis is my own and that no conflicts of interest exist.

ABSTRACT

For over a century, we have known that ammonia is important in the pathogenesis of hepatic encephalopathy. Studies in patients with acute liver failure have shown rapid progression to severe encephalopathy in those patients with evidence of a systemic inflammatory response, suggesting a possible link between inflammation and encephalopathy. In view of the growing evidence to support the role of inflammation in increasing the susceptibility of the brain to the effects of hyperammonemia in liver disease, 3 hypotheses were explored: **1:** Inflammation and infection are important in hepatic encephalopathy. **2:** Inflammation and infection act synergistically with ammonia. **3:** Ammonia makes the immune system more susceptible to infection.

In the first of 2 clinical studies, inflammation was shown to be an important determinant of the presence and severity of minimal hepatic encephalopathy. In a second study, significant deterioration of neuropsychological test scores in patients with cirrhosis following induced hyperammonemia during the inflammatory state, but not after its resolution, suggested that inflammation may be important in modulating the cerebral effect of ammonia in liver disease, supporting the first hypothesis. Ammonia and inflammation were shown to be synergistic in the bile duct ligated rat which showed increased brain water and astrocyte swelling exacerbated by endotoxin and accompanied by a rise in nitric oxide and brain nitrotyrosine, but not in plasma ammonia, suggesting nitric oxide may play an important synergistic role in the pathogenesis of hepatic encephalopathy.

Ammonia was shown to impair neutrophil function by reducing phagocytosis, inducing spontaneous respiratory burst and cell swelling. The $p38^{-MAPK}$ pathway was shown to be important and a $p38^{-MAPK}$ agonist prevented neutrophils from swelling in the presence of ammonia and improved phagocytosis. While cultures of muscle cells were a potentially interesting direction to take to investigate the effect of inflammation on the muscle uptake of ammonia, unfortunately the resulting data demonstrated a low glutamine synthetase activity. In conclusion, these studies illustrate the important factors that modulate the manifestation of symptoms of hepatic encephalopathy in cirrhosis, the most important of which is the synergistic role of inflammation and ammonia. Furthermore, the ammonia-induced impairment of neutrophil function may, in part, account for the increased susceptibility to infection found in patients with cirrhosis.

CONTENTS

ABBREVIATIONS

aa – Amino Acid

ACLF – Acute-on-Chronic Liver Failure

ADP – Adenosine Diphosphate

ALF – Acute Liver Failure

AMT – Amino-1,2,4-triazole

APACHE – Acute Physiology and Chronic Health Evaluation

ATP – Adenosine Triphosphate

BDL – Bile Duct Ligated

CRP – C- Reactive Protein

ddH_2O – Double Distilled Water

DMSO – Dimethyl Sulfoxide

DFMO – Dimethylfluoro Ornithine

DSST – Digit Symbol Substitution Test

EPO – Eosinophil Myeloperoxidase

Erk - Extracellular signal-regulated kinase

fMLP - Formyl-Methionine-Leucine-Phenylalanine

GABA – Gamma Butyric Acid

GLN – Glutamine

GLU – Glutamate

GLUT-1 – Glucose Transporter

GLT -1 – Glutamate Transporter

GS – Glutamine Synthetase

cGMP – Cyclic Guanosine Monophosphate

HE – Hepatic Encephalopathy

ICAM – Intercellular Adhesion Molecule

IL – Interleukin

IL-1β – Interleukin–1–beta

IL-6 – Interleukin-6

IFN-γ – Interferon-gamma

ICP – Intracranial Pressure

Jnk – Jun-kinase

L-NAME – Nitro-L-arginine Methylester

LOLA – L-ornithine-L-aspartate

LPS – Lipopolysaccharide

MEK – Mitogen extracellular kinase

MHE – Minimal Hepatic Encephalopathy

MKK – MAP kinase kinase

MPO – Myeloperoxidase

NADPH - Nicotinamide Adenine Dinucleotide Phosphate

NH_3 – Ammonia

NH_4Cl – Ammonium Chloride

NMDA – N-methyl-D-aspartate

NO – Nitric Oxide

NO_x – Nitrite/Nitrate

eNOS – Endothelial Nitric Oxide Synthase

iNOS – Inducible Nitric Oxide Synthase

nNOS – Neuronal Nitric Oxide Synthase

OKG – Ornithine Ketoglutarate

PBS – Phosphate Buffered Saline

PE – Phycoerythrin

PHES – Psychometric Hepatic Encephalopathy Score

PMA - Phorbol 12-myristate 13-acetate

$p38^{-MAPK}$ – p38 mitogen activated protein kinase

RNA – Ribonucleic Acid

SD – Standard Deviation

SEM – Standard Error of the Mean

SIRS – Systemic Inflammatory Response Score

TGF-β – Transforming Growth Factor-Beta

TIPSS – Transjugular Intrahepatic Portosystemic Shunt

TNF-α – Tumour Necrosis Alpha

TRB – Trails B Test

WBC – White Blood Cell Count

TABLE LISTING

CHAPTER 1

Introduction

CHAPTER 3

Role of ammonia, infection and inflammation in hepatic encephalopathy in cirrhosis

CHAPTER 4

The effect of inflammation on the brain in a rat model of cirrhosis

CHAPTER 5

The effect of ammonia on neutrophil function: an observational study

CHAPTER 7

An Investigation into the Influence of Inflammation on the Ammonia Uptake in Muscle

FIGURE LISTING

CHAPTER 1

Introduction

CHAPTER 2

Hypothesis and Aims

CHAPTER 3

Role of ammonia, infection and inflammation in hepatic encephalopathy in cirrhosis

CHAPTER 4

The effect of inflammation on the brain in a rat model of cirrhosis

CHAPTER 5

The effect of ammonia on neutrophil function: an observational study

CHAPTER 6

The effect of ammonia on neutrophil function: an investigation into a $p38^{MAPK}$ dependent mechanism

CHAPTER 7

An Investigation into the Influence of Inflammation on the Ammonia Uptake in Muscle

CHAPTER 8

Summary

Chapter 1

INTRODUCTION

1.1 THE FOUNDATION STONES OF HEPATIC ENCEPHALOPATHY

The word ammonia was derived from Amen, an Egyptian God described in Egyptian mythology (1) (Figure 1.1). To the Greeks, Amen was known as Ammon whose temple and oracle were situated at an oasis in the Libyan desert near Memphis. Camel urine was collected in a cesspool close to the temple and it was widely believed that "man and all life rose spontaneously from a sea of ammonia"; camel urine, soot and sea salt were heated together to from *sal ammoniac* (or "salt of Ammon") (2).

Amen – Egyptian Mythical God

Figure 1.1

Image obtained from aol Egypt Art images

Heating of *sal ammoniac* with alkali resulted in the production of ammonia gas leading the Swedish chemist Tobern Olaf Bergman to coin the term "ammonia" in 1782. Ammonia was subsequently widely used as the active ingredient of smelling salts used to revive ladies of that period who were "faint of heart and light of head".

In the 1890's, Marcel Nencki was chief chemist at the Imperial Institute of Experimental Medicine in St Petersburg. Ivan Pavlov was a physiologist in the same institution. Pavlov was awarded the Nobel Prize in 1904 for developing the concept of the 'conditional reflex' in the classic experiment in which he trained a dog to salivate at the sound of a bell. Pavlov was a great manager and thinker rather than an experimentalist *per se*, and coordinated a hugely successful laboratory enterprise nicknamed 'Pavlov's Physiology Factory'. (3) But as is often the case in science, the contribution of Nencki in the development of this hypothesis was overshadowed by the more well-renowned and established Ivan Pavlov. Nevertheless, the 'Nencki Institute of Experimental Biology' was set up in 1918 in Poland and stands in honour to this great man's work where neurobiology and biochemistry research continues on even to this day. (Figure 1.2).

Figure 1.2

Nencki image obtained from Bioanalytical.com calendar 2000.
Pavlov image obtained from Twisted History (Copyright 2000 Armour Van Horn).

Their first published collaborative work in 1893 described the physiological consequences of a portacaval shunt in dogs, a surgical procedure first described by Eck in 1879 ('Eck's fistula'). (4) Such dogs developed neurobehavioral changes in 10 days to 6 weeks post-surgery; symptoms included aggression, irritability, ataxia, convulsions and coma. Symptoms worsened after feeding of meat but not after ingestion of milk or bread leading the investigators to coin the phrase "meat intoxication syndrome". They went on to perform nitrogen balance studies in which they discovered an excess of "carbamin saere" (carbamic acid [$H_2NC(=O)OH$]) in the urine. (5) Carbamic acid is a hypothetical acid that exists only in the form of its esters and salts, mainly the salt ammonium carbamate. Subsequently they showed that normal dogs administered "carbamin saere" developed neurobehavioral symptoms in a dose-dependent fashion. Portacaval shunted dogs given relatively small doses of "carbamin saere" developed profound neurobehavioral changes associated with increased urinary ammonia excretion. Similar findings were observed following a meal of meat. They concluded that ammonia is metabolized to urea by the liver but this process is impaired in dogs with a portacaval shunt. Studies in the Pavlov laboratory were repeated in 1896 (6) and the following is a copy of their original abstract published in german in The Archives of Experimental Pathology and Pharmacology followed by the English translation:

ORIGINAL ABSTRACT FROM THE PAVLOV LABORATORY

Die nachfolgenden Untersuchungen bilden eine Vervollständigung und bis zu gewissem Grade einen Abschluss der im XXXII. Bande des Archives von M. Hahn, O. Massen, M. Nencki und J.P Pawlow publicirten Untersuchung über die Eck'sche Fistel zwischen der unteren Hohlvene und der Pfortader und ihre Folgen für den Organismus. Wir zeigten dort, dass nach erfolgreicher Anlegung der Venenfistel bei den Hunden frühestens nach 10 Tagen, meistens erst nach einigen Wochen sich charakteristische Krankheitssymptome einstellten, wobei wir folgende Stoffwechselveränderungen constatirten:

1. *Eine Verminderung der Harnstoffausscheidung bei Hunden, denen die Venenfistel angelegt und ausserdem die Leberaterie unterbunden war.*
2. *Eine vermehrte Ammoniakausscheidung im Harn und Unvermögen aus der in den Magen eingeführten Carbaminsäure Harnstoff zu bilden.*
3. *Die willkürliche Hervorrufung der Vergiftungssymptome durch reichliche Zufuhr stickstoffhaltiger Nahrung oder Ammoniaksalzen.*
4. *Eine Vermehrung der Harnsaüre im Harn.*

ENGLISH TRANSLATION

The following investigations complete and, to a certain degree, conclude the study, published in Vol. XXXII of the Archives, by M. Harn, O. Massen, M. Nencki and J.P Pavlov on an Eck's fistula between the inferior vena cava and the portal vein, and its consequences for the organism. There we demonstrated that, after successfully constructing the venous fistula in dogs, characteristic disease symptoms occurred at the earliest 10 days, but more often after several weeks, which resulted in the following metabolic changes:

1. *A decrease of urea excretion in dogs in which the fistula had been constructed and the hepatic artery had been ligated.*
2. *An increased excretion of ammonia in the urine and an inability to form urea from carbamic acid which had been infused into the stomach.*
3. *The arbitrary inducement of symptoms of poisoning through a plentiful supply of nitrogen-containing food or of salts of ammonia.*
4. *An increase of uric acid in the urine.*

A summary of the results of each of these original experiments translated from the 1896 publication (6) to include a calculation of the blood ammonia (mmol/L) are shown in Table 1.1 (7)

Table 1. Experimental Details

Expt no.	Experimental condition	Animal	Time after eating (h)	Organ/blood vessel measured	Blood ammonia (mmol/***l)	Tissue ammonia (mg/100 g)
1	Meat and milk meal	Dog	3	Femoral artery	1.1	
2	Meat and milk meal	Dog	4 1/2	Carotid artery	0.9	
3	Meat and milk meal	Dog	7	Inferior vena cava	0.67	
				Portal vein	3.41	
				pancreaticoduodenal		
4	Meat meal	Dog	7	vein	7.31	
				Mesenteric vein	5.3	
				Inferior vena cava	1.16	
5	Meat and oatmeal soup	Dog	9	Haemorrhoidal vein	3.53	
				Mesenteric vein	2.92	
6	Meat meal	Dog	2	Gastric mucosa		37.1
				Intestinal mucosa		23
				Liver		22.8
				Muscle		9.2
				Pancreas		8.8
7 and 8	Meat meal	Dog	4 and 5	Gastric mucosa		43.2
				Gastric contents		9.9
				Intestinal mucosa		28.9
				Intestinal contents		22.4
9	Meat meal	Dog	6	Lymph	0.35	
10 and 11	Meat and sausage meal	Dog	5	Portal vein	2.13	
				Hepatic vein	1.22	
				Urine	85.24	
12	Meat after 6-day fast	Dog	5	Portal vein	2.13	
				Hepatic vein	0.91	
13	5-day fast	Dog		Mesenteric vein	0.73	
				Inferior vena cava	1.71	

Table 1. Continued

Expt no.	Experimental condition	Animal	Time after eating (h)	Organ/blood vessel measured	Blood ammonia (mmol/***l)	Tissue ammonia (mg/100 g)
14	2-day fast	Dog		Gastric mucosa		21.5
				Intestinal mucosa		16.2
				Muscle		4.6
		2				
15	Vegetables	Rabbits		Gastric mucosa		8.5
				Gastric contents		3.2
				Liver		4.2
				Muscle		5.3
				Carotid artery	0.85	
16	Hay	Sheep		Liver		13.9
				Kidney		8.6
				Muscle		3.5
				Portal vein	2.01	5.9
				Inferior vena cava	1.77	
				Carotid artery	0.67	
				Brain white/grey		
17	Hay	Horse		Matter		5.9/8.3
				Liver		21.6
18	Performed by Prof Cybulski in Cracow			Portal vein blood flow	2.35–2.7 cc/s(9090cc/h)	
19	Oesophagostomy and gastrostomy	Dog		Gastric mucosa	25.69	
				Gastric juice	2.44	
					3.35	
20	Portacaval fistula	Dog		Carotid artery		
				Gastric mucosa		42.6
				Liver		20
				Muscle		15.6
				Brain		20.9
				Kidneys		19.2
				Urine	127.42	

Nencki and Pavlov were able to conclusively demonstrate that in the fasting state, arterial ammonia was unchanged but following a high protein meal the ammonia in the portal vein (and its tributaries) rose 3 - 4 fold higher than that of the systemic circulation. The ammonia content of the blood and tissues depended on protein intake (higher after meat than vegetable protein). In addition to the liver, all organs, in particular the muscles had higher ammonia contents than blood from the systemic circulation.

In the portacaval shunted dog, the arterial ammonia only rose after a protein meal and this was accompanied by increased urinary excretion of ammonia. After ammonia ingestion, the dog became comatose and died. This was associated with the arterial ammonia concentration approaching that normally found in the portal vein and the ammonia content of the brain was four times that of normal which led them to attribute the behavioural symptoms to ammonia. This is likely to be the first ever description of a link between ammonia and the different stages of hepatic encephalopathy, progressing from full wake fullness through to stupor to coma.

Interestingly, they also measured the ammonia content within the gastric mucosa and intestinal mucosa and gastric juice. They showed that even in a prolonged fasted state the ammonia content within the gastric mucosa was high. They found it difficult to interpret these findings at the time but in the light of current research these early observations were also highly significant. This may be related to the fact that ammonia inhibits gastric acid secretion and may be important in its modulation, (8) but could also be related to the fact that over 80% of dogs are infected with H. pylori, an organism known to hydrolyse urea to produce ammonia (9). Although recent studies (10) suggest that the H. pylori infection is not a major contributing factor to fasting blood ammonia levels or parameters assessing minimal hepatic

encephalopathy in cirrhosis, this may account for their findings, but could also signify that the gastric mucosa is a passive ammonia trap from the blood rather than being obtained directly from the food.

1.2 INTERORGAN AMMONIA METABOLISM

Recent studies have complemented the work of Nencki and Pavlov, suggesting that the gut produces ammonia which is metabolised in the liver and that almost all organ systems are involved in ammonia metabolism (Table 1.2).

Early clinical and experimental literature suggested that colonic bacterial flora is the main source of ammonia production in the body. (11) Colonic bacteria produce ammonia by splitting urea and possibly amino acids. (12) However, this hypothesis does not explain hyperammonemia and hepatic encephalopathy in germ-free dogs with a portacaval shunt, (13) the high portal-venous ammonia concentration in germ-free rats or hyperammonemia in germ-free hepatectomized rats. (14) The alternative explanation is that hyperammonemia in germ-free animals is the result of intestinal breakdown of amino acids, especially glutamine. (15) The intestines have a high glutaminase activity, predominantly located in the enterocytes, and only a little glutamine synthetase activity, making it a major glutamine-consuming organ.

In 1960, Owen et al. (16) demonstrated that the kidney is an important source of blood ammonia in patients with liver disease, and Webster and Gabuzda in 1958 (17) demonstrated that ammonia was taken up by the muscle and brain in hepatic coma. Lockwood et al. (18) were then able to confirm the initial finding of Nencki that ammonia is metabolised in muscle. Owen et al. (19) and Dejong et al. (20) were then able to confirm Nencki's initial observation that ammonia is raised in the kidney in a portacaval shunted animal model. Olde Damink et al. (21) determined the contribution of the main ammonia producing and consuming organs to whole body ammoniagenesis.

Table 1.2

The translation of the different pathophysiological observations of Nencki and Pavlov into actual therapy of Hepatic Encephalopathy.

A. Interorgan Ammonia Metabolism

Nencki, Pavlov, Zaleski Observation:	Current/Proposed Treatment:
1. Portal venous ammonia is greater than arterial ammonia.	Lactulose and antibiotics
2. Ammonia is metabolised in the muscle.	L-ornithine L-aspartate
3. The ammonia concentration is raised in the gastric mucosa even in the fasting state.	?? H. Pylori eradication therapy
4. Ammonia is raised in the kidney of the portacaval shunted dog compared to a healthy one.	Volume Expansion Gut Lavage

B. Animal Behaviour and Brain Ammonia

Nencki, Pavlov, Zaleski Observation:	Proposed Mechanisms:	Current/Proposed Treatment:
1. The blood brain barrier ammonia concentration is four times as high as that in the systemic circulation. 2. Similar arterial concentrations cause HE in portacaval shunted dogs, but not in control animals.	1. Direct ammonia toxicity (cerebral energy failure).	-
	2. Astrocyte swelling.	Hypothermia
	3. Ammonia-glutamine-brain swelling hypothesis.	Mannitol Hypertonic saline
	4. Altered gene expression.	Hypothermia
	5. Increased cerebral blood flow.	Hypothermia

Fasted, metabolically stable patients with cirrhosis who underwent transjugular intrahepatic portosystemic shunt (TIPSS) portography were studied. The results suggested that hyperammonemia was mostly due to portosystemic shunting and renal ammonia production. Skeletal muscle removed more ammonia than liver. However, the amount of nitrogen that was taken up by skeletal muscles in the form of ammonia was much less than the amount of nitrogen that was released in the form of glutamine. Glutamine released from skeletal muscle can be taken up in the portal drained viscera and in the kidneys, where it can be metabolised to ammonia, thereby abolishing the effect on muscle ammonia uptake on whole body ammonia removal. Increased hepatic urea synthesis, urinary ammonia excretion, and probably increased peripheral breakdown of arginine were the only ways in which the body removed ammonia.

Upper gastrointestinal bleeding in cirrhosis is associated with enhanced ammoniagenesis. Olde Damink et al. (22) also reported the results of a study to evaluate interorgan metabolism of ammonia following a 'simulated' upper gastrointestinal bleed by the administration of an amino acid solution that mimics haemoglobin amino acid composition in patients with cirrhosis and a TIPSS. During the simulated bleed arterial concentrations of ammonia increased significantly. There was no change in ammonia production from the portal drained viscera but renal ammonia production increased 6-fold. In contrast to an unchanged ammonia removal by the liver, a significant increase in muscle ammonia removal was observed. In another study, cirrhotics with an acute upper gastrointestinal bleed that underwent TIPSS insertion were studied. Ammonia was only produced by the kidneys and not by the splanchnic area, suggesting that enhanced renal ammonia release played an important role in the hyperammonemia that followed an upper gastrointestinal bleed in patients with cirrhosis. During the hyperammonemic state, the muscle was the

major site of ammonia removal. (22) Figure 1.3 illustrates the inter-organ trafficking of ammonia in a normal individual and one with cirrhosis.

Some 50 years later after Nencki and Pavlov's initial observation in dogs, Gabuzda et al. (23) noted that patients with cirrhosis and ascites treated with cation-exchange resins that absorbed sodium but released ammonium ions developed episodic hepatic encephalopathy. Phillips et al. (24) then went on to describe the behavioural alterations and a syndrome of impending hepatic coma in cirrhotics given certain nitrogenous substances. The severity of hepatic encephalopathy was then shown to broadly relate to the blood ammonia level in 2 large studies. (25;26)

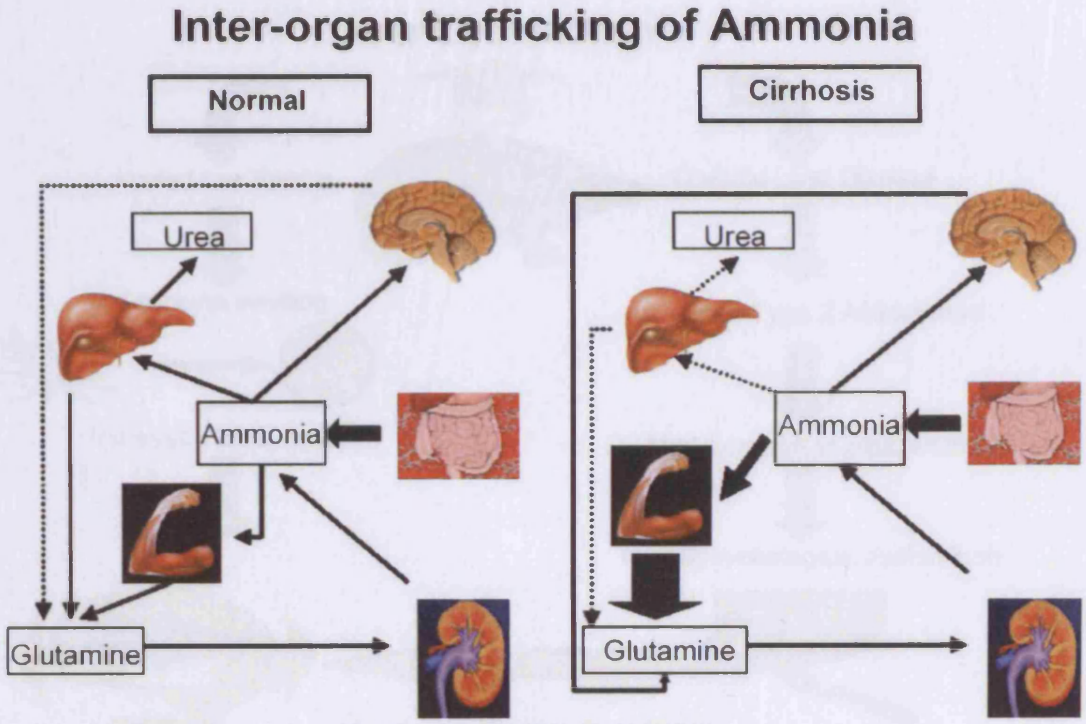

Figure 1.3

Inter-organ trafficking of ammonia in health and in cirrhosis

In healthy individuals, the liver removes ammonia by detoxification into urea. In patients with cirrhosis, the metabolic capacity of liver is reduced, resulting in hyperammonemia. The muscle then becomes an important organ of ammonia detoxification by trapping it in glutamine. Glutamine acts as a temporary buffer that can both regenerate ammonia in the enterocytes and excrete ammonia via the kidneys.

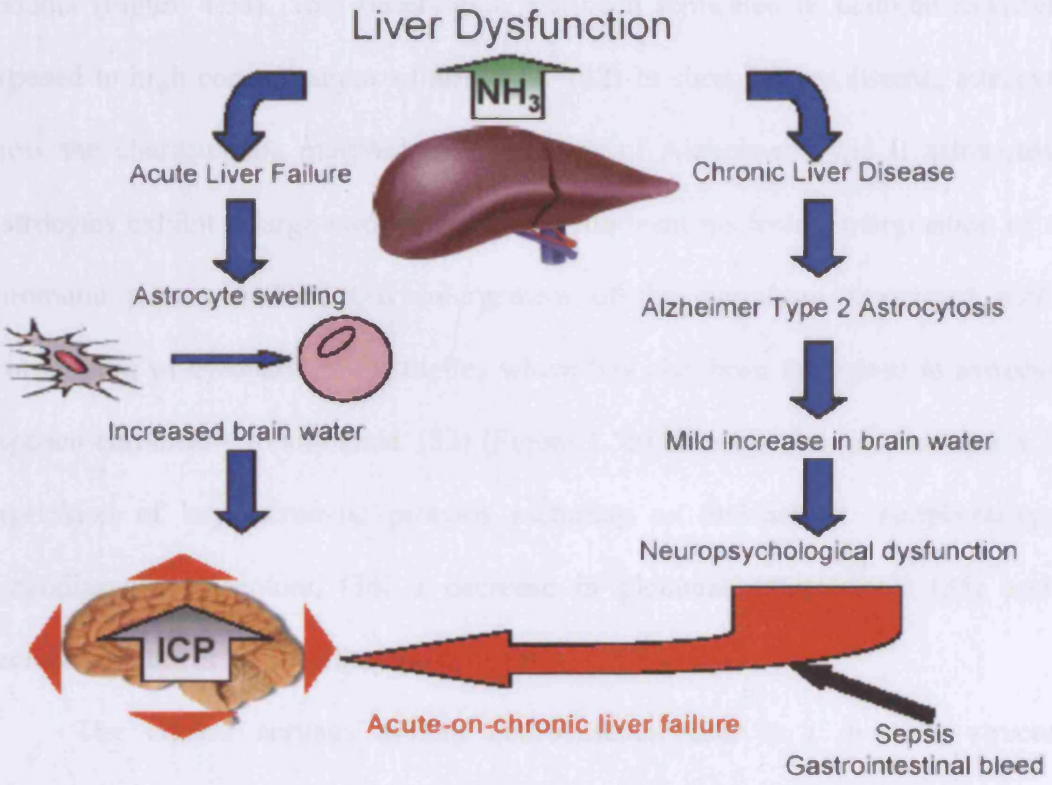

Figure 1.4

The cell that is most important in the pathogenesis of hepatic encephalopathy is the astrocyte. This diagram illustrates that acute and chronic liver dysfunction both result in increased brain water and that an acute insult on a background of chronic liver disease can result in acute cerebral oedema and raised intracranial pressure (NH_3: ammonia; ICP:intracranial pressure).

1.4 NEUROPATHOLOGY

In acute liver failure, astrocytes swell and patients develop cytotoxic brain oedema (Figure 1.5a). This observation has been replicated in cultured astrocytes exposed to high concentrations of ammonia. (32) In chronic liver disease, astrocytes show the characteristic morphological features of Alzheimer Type II astrocytosis. Astrocytes exhibit a large swollen nucleus, prominent nucleolus, margination of the chromatin pattern and marked enlargement of the cytoplasm associated with a proliferation of cytoplasmic organelles which has also been replicated in astrocytes exposed chronically to ammonia. (33) (Figure 1.5b) There is also an alteration in the expression of key astrocytic proteins including an increase in 'peripheral-type' benzodiazepine receptors, (34) a decrease in glutamate transporters (35) and a decrease in glial acidic fibrillary protein. (36)

The central nervous system neurovascular unit is a dynamic structure consisting of vascular endothelial cells, pericytes, and closely juxtaposed astrocytes and neurons. Contact and communication between these cells modulates cerebral blood flow and influence permeability properties of the blood brain barrier. (37) The blood brain barrier remains anatomically intact in hepatic encephalopathy but studies using positron emission tomography reveal an increase in the permeability-surface area to ammonia with increasing severity of disease. (38) A recent study has shown that the removal of astrocytes from culture resulted in increased permeability to small tracers across the brain endothelial cell monolayer and an opening of the tight junctions which was not accompanied by the loss of tight junction proteins such as claudin and occludin. (39)

(a)

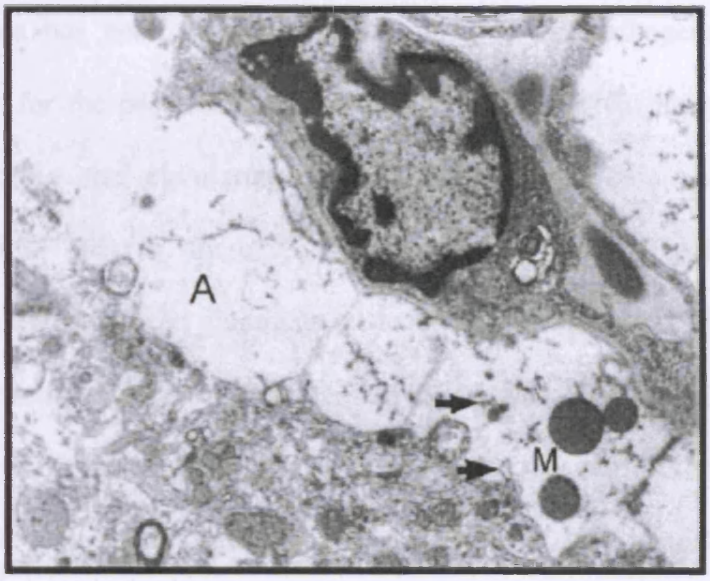

(b)

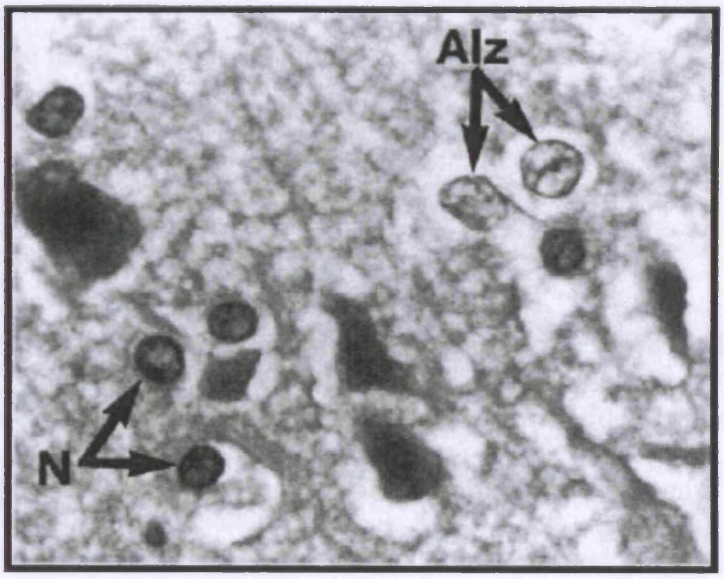

Figure 1.5

(a) Electron micrograph of the brain from a patient dying from acute liver failure showing a swollen astrocyte (A) (M:mitochondria).
(b) Histopathology of the brain from a patient dying from cirrhosis showing evidence of type II astrocytosis (Alz) and a normal neuron (n) from Kato, Hughes, Keays & Williams, 1992. (40)

1.5 PATHOGENESIS OF HEPATIC ENCEPHALOPATHY

Ammonia has been thought to be central in the pathogenesis of hepatic encephalopathy for the past 100 years and most of the current therapies are based around modulating the circulating levels of this neurotoxin. Disturbances in neurotransmission due to increased γ-aminobutyric acid (GABA) (increased neuroinhibition) (41), reduced glutamate (reduced neuroexcitation) (42) and increased endogenous benzodiazepines and neurosteroids (43;44) have been thought to be important but current data suggest that at least some of these effects may be mediated by ammonia. (45) Altered cerebral blood flow is thought to be important but it is not clear whether this is mediated through ammonia or secondary to superimposed inflammation. There is emerging literature suggesting that inflammation and its mediators may be important in the pathogenesis of hepatic encephalopathy.

1.5.1 THE AMMONIA HYPOTHESIS

Important direct evidence showing that ammonia is taken up by the brain in patients with liver disease and hyperammonemia was provided by Lockwood et al. (46) Using positron emission tomography with ^{13}N-Ammonia, he elegantly demonstrated that uptake of ammonia into the brain of patients with hepatic encephalopathy was significantly higher than in healthy volunteers and that the arterial concentrations of ammonia may increase the uptake of ammonia in the brain through an increase in the permeability of the blood brain barrier to ammonia. (38) In experimental animals with acute liver failure, brain ammonia flux may be up to 45-fold higher than normal. (47) These observations support those in acute liver failure

patients where arterial ammonia levels of >150 μmol/L predict a greater likelihood of dying from brain herniation. (48)

1.5.1.1 AMMONIA-GLUTAMINE BRAIN SWELLING HYPOTHESIS

In the presence of liver dysfunction, urea synthesis is impaired and the brain acts as a major alternative ammonia detoxification pathway. Astrocytes, which provide physical and nutritional support for neurons also eliminate ammonia by the synthesis of glutamine through amidation of glutamate. Accumulation of glutamine in astrocytes, induced by hyperammonemia, produces osmotic stress and causes the astrocytes to swell. (49) Evidence of an increase in brain water in minimal hepatic encephalopathy has been provided in humans through studies using magnetic resonance imaging which show decreased magnetization transfer ratio indicating increased brain water. This was shown to correlate with neuropsychological function and the abnormality was reversed by liver transplantation. (50) More recently, hyperammonemia induced by the oral administration of an amino acid solution in patients with cirrhosis was shown to result in significant deterioration in neuropsychological function, an increase in brain glutamine levels and a reduction in the magnetic transfer ratio suggesting an increase in brain water. (51) This study provided further support for the ammonia-glutamine brain water hypothesis of hepatic encephalopathy. The effect of hyperammonemia is likely to be determined by the ability of the astrocytes to maintain osmotic equilibrium by losing osmolytes like myo-inositol in response to the ammonia-induced increase in glutamine. (52) Therefore, patients with co-existing hyponatremia (53) or chronic hyperammonemia,

which resulted in depleted myo-inositol stores, may be more sensitive to the effects of induced hyperammonemia (Figure 1.6.1 & 1.6.2).

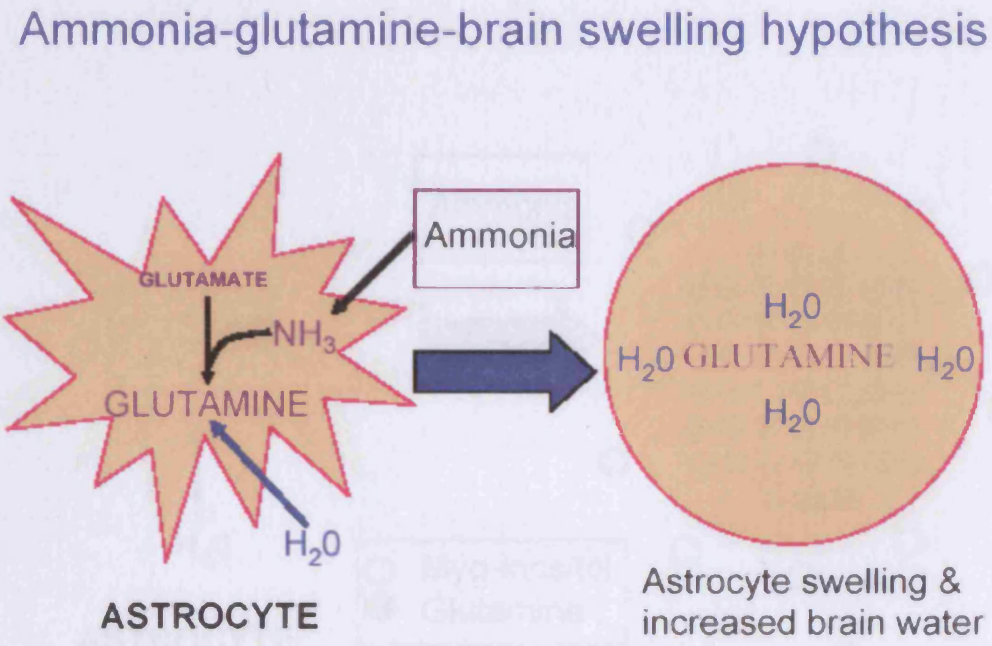

Figure 1.6.1

A diagrammatic representation of the ammonia-glutamine-brain swelling hypothesis. Astrocytes are the site of ammonia detoxification in the brain and eliminate ammonia by the synthesis of glutamine through amidation of glutamate. The glutamine is retained and its osmotic effect within the astrocyte causes it to take up water causing it to swell.

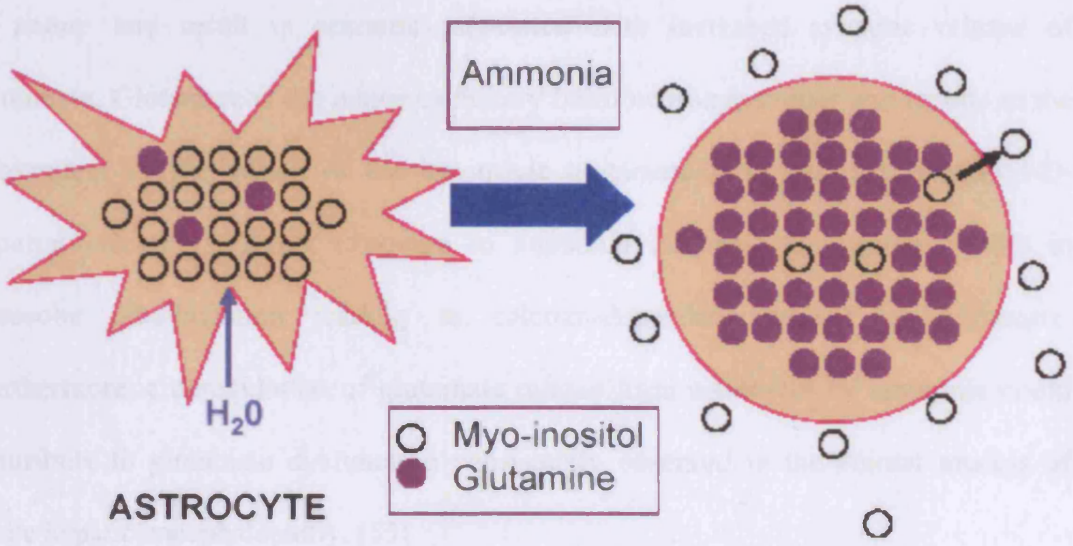

Figure 1.6.2

A diagrammatic representation to show the role of myo-inositol as an osmotic regulator within the astrocyte. As glutamine accumulates within the astrocyte, myo-inositol exits to try to redress the osmotic balance within the cell and prevent cerebral oedema.

1.5.1.2 DIRECT AMMONIA TOXICITY

Ammonia, when present in high concentrations, has the potential to adversely affect the central nervous system particularly through modulation of inhibitory and excitatory neurotransmission. (54)

In acute liver failure, the manifestation of hyperammonemia may be excitatory in nature and result in seizures associated with increased synaptic release of glutamate. Glutamate is the major excitatory brain neurotransmitter and results in the subsequent overactivation of the ionotropic glutamate receptors, the N-methyl-D-aspartate receptors. Acute exposure to ammonia in astrocyte cultures results in cytosolic alkalinization leading to calcium-dependent release of glutamate. Furthermore, a deregulation of glutamate release from astrocytes by ammonia could contribute to glutamate dysfunction consistently observed in the animal models of acute hepatic encephalopathy. (55)

In chronic liver disease however, there appears to be shift in the balance between inhibitory and excitatory neurotransmission, towards a net increase in inhibitory neurotransmission. This may be due to a down-regulation of glutamate receptors resulting in decreased glutamatergic tone. In patients with hepatic encephalopathy, cerebral glutamate is decreased and down-regulation of glutamate binding sites on the postsynaptic neurons and astrocytes occurs, resulting in decreased neuroexcitation. (56) Furthermore, chronic hyperammonemia inactivates the glutamate transporter (GLT-1) in astrocytes. (57) For over 25 years now, it has been observed that there is increased GABAergic tone in patients with hepatic encephalopathy. GABA is the predominant inhibitory neurotransmitter in the brain and it was hypothesised that GABA accumulated in liver failure and crossed the blood

brain barrier. (41) This hypothesis has not been confirmed in some of the more recent studies. Recent hypotheses suggest that hyperammonemia may modulate the observed increase in GABAergic tone in liver disease. Hyperammonemia has been shown to inhibit astrocytic GABA uptake, increase neuronal chloride currents by a direct action on the $GABA_A$ receptor complex, to potentiate the binding of $GABA_A$ and central benzodiazepine receptor agonists to the $GABA_A$ receptor complex. (43;58) Recent studies have suggested that alterations in brain GABA content or receptor complex function may not be as important as the presence of neurosteroids with GABA agonist properties which may explain the increased GABAergic tone in hepatic encephalopathy. (59)

In rat models of chronic liver failure and hyperammonemia, it has been shown that ammonia impairs the glutamate-nitric oxide-cGMP pathway which is activated by the NMDA receptor and is important in learning. Moreover, chronic treatment with sildenafil, an inhibitor of the phosphodiesterase that degrades cGMP, normalises the function of the pathway and restores learning ability in rats with portacaval shunts or with hyperammonemia. This may at least in part, offer an explanation as to why patients with minimal hepatic encephalopathy have impairment in short term memory. (60)

1.5.1.3 AMMONIA AND BRAIN METABOLISM

Ammonia at millimolar concentrations also has the potential to impair brain energy metabolism, particularly as it is known to inhibit the tricarboxylic acid cycle enzyme ketoglutarate dehydrogenase. (61) However, brain energy metabolism does not appear to be impaired in chronic liver disease until the very late stages when

isoelectric electroencephalography traces become abnormal. (62) Nevertheless, cerebral spinal fluid lactate is increased in patients with hepatic encephalopathy (63) and in animal models of chronic liver disease and ammonia precipitated encephalopathy (64). These contrasting observations may simply reflect the limitation of isoelectric electroencephalography as a tool to monitor hepatic encephalopathy in chronic liver disease.

However, using nuclear magnetic resonance studies in the hepatic devascularised rat model of acute liver failure, Zwingmann et al. (65) demonstrated 2 to 4.5 fold increase in total brain glutamine and lactate in the early pre-coma stages of hepatic encephalopathy. In the more severe coma stage associated with brain oedema there was a further significant increase in brain lactate. ^{13}C isotopomer analysis showed a selective increase of *de novo* synthesis of lactate from [1-^{13}C] glucose resulting in a 2.5 fold increased fractional ^{13}C enrichment in lactate. [2-^{13}C] Glutamine, synthesised through the astrocytic enzyme pyruvate carboxylase increased 10 fold in the pre-coma stages of hepatic encephalopathy but there was no further increase in the coma stages. ^{13}C-label incorporation into [4-^{13}C] glutamate, synthesised mainly through neuronal pyruvate dehydrogenase, was selectively reduced in the coma stages whilst brain GABA synthesis remained unchanged. These observations indicate that increased brain lactate synthesis and impaired glucose oxidative pathways are important in the pathogenesis of brain oedema in acute liver failure.

1.5.1.4 ALTERED GENE EXPRESSION

Acute liver failure results in altered expression of several genes in the brain which code for important proteins involved in brain function. These are summarized in Table 1.3. These proteins include the glucose (GLUT-1) and glutamate (GLT-1) transporters, the astrocytic structural protein glial fibrillary acidic protein, the 'peripheral-type' benzodiazepine receptor and aquaporin IV which is a water-channel transmembrane protein. Loss of expression of GLT-1 results in increased extracellular glutamate. The monoamines serotonin and noradrenaline are also increased extracellularly following post-translational modifications to their receptors. (66) This altered monoaminergic function may also be responsible for the early neuropsychiatric symptoms of hepatic encephalopathy. (67) The increased expression and activation of the 'peripheral-type' benzodiazepine receptor results in altered brain excitability. As a mitochondrial protein, it plays an important role in the maintenance of astrocytic energy metabolism and uptake of cholesterol resulting in the synthesis of neurosteroids which have potent neuroinhibitory properties. (68) Increased expression of aquaporin IV may be important in regulation of water transport and hence alter brain water (69) and aquaporin knockout mice show reduced brain oedema and improved neurological outcome compared to wild type mice in models of brain oedema. (70) Portacaval anastomosis in the rat results in increased gene expression of the constitutive neuronal isoform of nitric oxide synthase in the brain. This may contribute to altered mental state through disturbances in cerebral blood flow. (71)

Table 1.3

A summary of the main astrocyte genes which are up and down-regulated in acute liver failure

Up-regulation	**Down-regulation**
'Peripheral-type' benzodiazepine receptor (PTBR)	GLT-1 (Glutamate transporter)
GLUT-1 (Glucose transporter)	Glial fibrillary acidic protein (GFAP)
Neuronal nitric oxide synthase (nNOS)	GLYT-1 (Glycine transporter)
Aquaporin IV	

1.5.2 AMMONIA AND CEREBRAL BLOOD FLOW

Cerebral blood flow is closely coupled to neuronal activity and is modified by afferent projection fibres that release vasoactive neurotransmitters in the perivascular region, principally on the astrocyte endfeet that outline cerebral blood vessels enabling cerebral blood flow autoregulation. Cerebral vasoconstriction induced by increased calcium in astrocytic endfeet is generated through the phopholipase A2-arachidonic acid pathway generating 20-hydroxyeicosatetraenoic acid production. (72)

In acute liver failure, there is a loss of cerebral autoregulation, altered reactivity to carbon dioxide and cerebral hyperemia. Arterial concentrations of ammonia, its delivery to the brain and its metabolism are significantly higher in patients with acute liver failure and intracranial hypertension confirming the important role of ammonia in the pathogenesis of intracranial hypertension, although the underlying mechanisms are unclear. (73) The development of increased blood brain volume leads to a rise in intracranial pressure and this may facilitate the movement of water across the blood brain barrier in an osmotically altered brain. (74) As the astrocyte is involved in the normal coupling of neuronal activity with cerebral blood flow, (75) alterations in astrocyte function either directly or indirectly by increased brain ammonia concentrations are likely to affect cerebral blood flow. When methods are introduced to inhibit brain glutamine synthesis, such as using the glutamine synthetase inhibitor methionine sulfoximine, (76) a rise in cerebral blood flow is prevented. This observation supports the view that increased cerebral blood flow may be important in initiating brain swelling in this model. However, in humans with acute liver failure, the increase in cerebral blood flow is a later event. Patients

with acute liver failure that have severe encephalopathy and mildly increased intracranial pressure often have normal cerebral blood flow. Marked increases in intracranial pressure are associated with a concomitant rise in cerebral blood flow. (73)

In contrast, in chronic liver disease, the predominant picture is of cerebral vasoconstriction. (77) Regional differences in cerebral blood flow are also seen. Regional cerebral blood flow corresponds to functional impairment of the frontal cortex and cingulate gyrus. (78) Administration of an oral amino acid load to patients with cirrhosis that results in increased ammonia results in reduced regional cerebral perfusion in the temporal lobes, left superior frontal gyrus and right parietal and cingulate gyrus, and deterioration in memory tests. (79) These results attest to the intimate relationship that ammonia has with cerebral blood flow.

1.6 THE ROLE OF INFLAMMATORY MEDIATORS IN MODULATING THE MANIFESTATION OF HEPATIC ENCEPHALOPATHY

As is clear from the previous discussion, there is overwhelming evidence supporting the ammonia hypothesis of hepatic encephalopathy. However, in clinical practice a consistent correlation between the concentration of ammonia in the blood and the symptoms of hepatic encephalopathy cannot be confirmed. Sepsis is a frequent precipitating factor for the development of hepatic encephalopathy in patients with cirrhosis supporting the view that additional inflammation may play a role in the pathogenesis of hepatic encephalopathy (Figure 1.7). There is a growing body of evidence supporting the role of inflammation as being important in increasing the susceptibility of the brain to the effects of hyperammonemia. This concept and current views on its pathophysiologic basis will now be reviewed.

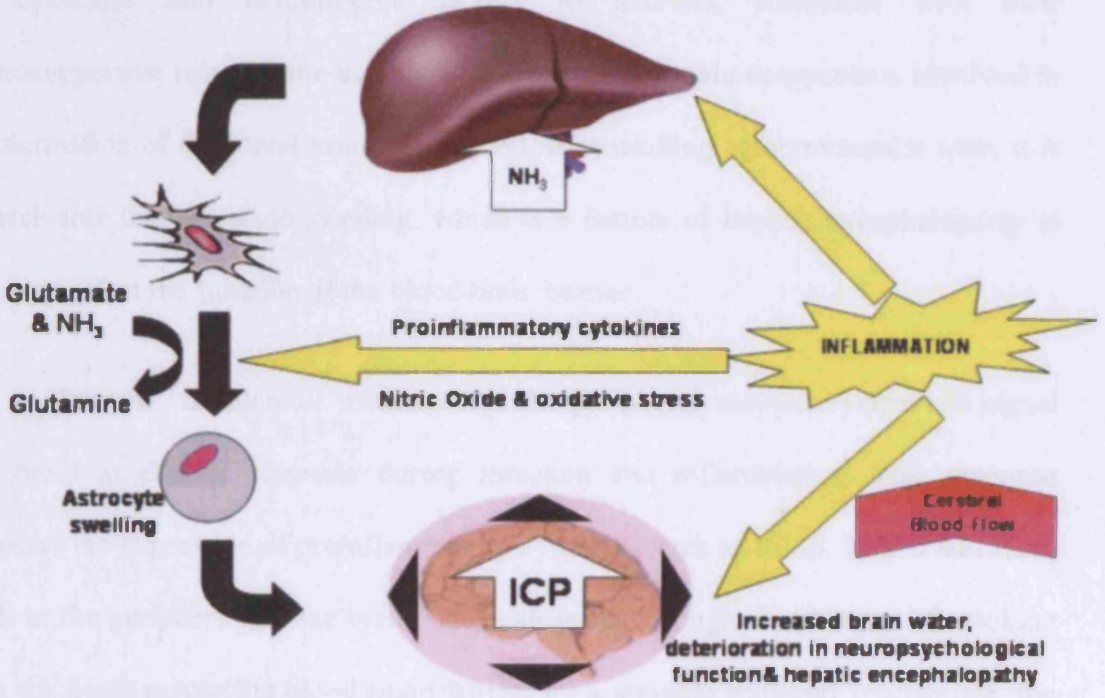

Figure 1.7

A diagrammatic representation of the relationship between inflammation and cerebral blood flow on the development and manifestation of hepatic encephalopathy. Astrocytes are the site of ammonia (NH_3) detoxification in the brain and eliminate ammonia by the synthesis of glutamine through amidation of glutamate. The resultant astrocytic swelling leads to increased brain water and raised intracranial pressure (ICP).

1.6.1 CYTOKINES, ASTROCYTES AND THE BLOOD BRAIN BARRIER

Astrocytes are considered to be the key cells involved in the pathogenesis of hepatic encephalopathy, as they have been found to be the cells that are most commonly seen to be affected histopathologically. Astrocytes secrete a full repertoire of cytokines and neurotrophic factors to neurons, consistent with their neurosupportive role. As the astrocytes are one of the main components involved in the formation of the blood brain barrier and in controlling cerebrovascular tone, it is conceivable that astrocyte swelling, which is a feature of hepatic encephalopathy is likely to affect the function of the blood brain barrier.

There is considerable evidence that the peripheral immune system can signal the brain to elicit a response during infection and inflammation. This response involves the expression of proinflammatory cytokines such as IL-1β, TNF-α and IL-6, both in the periphery and the brain. This can occur through direct entry of cytokine into the brain across the blood brain barrier by a storable transport mechanism, the interaction of cytokine with circumventricular organs such as the orgnum vasculosum of the lamina terminalis and area postrema (80) and activation of afferent neurons of the vagus nerve. (81) Sharshar et al. (82) showed that in patients dying with septic shock, neuronal and glial apoptosis occurs within the brain autonomic centres, which are strongly associated with iNOS expression in the endothelial cells. This may alter glutamatergic neurotransmission (83) and increase the number of 'peripheral-type' benzodiazepine receptors which may alter cellular osmotic homeostasis. (84) Cytokines may also modulate ammonia diffusion and it has been shown that TNF-α and IL-6 increase fluid phase permeability and ammonia diffusion in central nervous system-derived endothelial cells. (85) Brain endothelial cells have receptors for IL-1β

and TNF-α. These can transduce signals which can culminate in the intracerebral synthesis of nitric oxide and prostanoids. (80) Perivascular cells of macrophage origin may be a target for these cytokine effects. (86)

In the brain activated microglial cells and astrocytes produce cytokines in response to injury or inflammation. One of the early cytokines to be released is tumour necrosis alpha (TNF-α). TNF-α is involved in the induction of the cytokines interleukin 1 (IL-1) and interleukin 6 (IL-6). (87) It has been shown *in vitro* that the integrity of the blood brain barrier is compromised by IL-1β, mediated through the cyclooxygenase pathway within the endothelial cells. (88) In addition, the effect of TNF-α on human brain microvesicular endothelial cell permeability has the potential to compromise the blood brain barrier function. (89) Furthermore, in astrocyte cultures, interferon gamma (IFN-γ) upregulates inducible nitric oxide synthase (iNOS). (90)

Stimulation of astrocytes in culture with lipopolysaccharide also results in upregulation of iNOS that culminates in increased production of nitric oxide. (91) A similar phenomenon is observed with ammonia. Schleiss et al. have provided evidence of protein tyrosine nitration in ammonia-treated cultured astrocytes and also *in vivo* in brains of rats treated with an ammonia load. (92) Furthermore, the addition of ammonia to astrocyte cultures generates reactive oxygen species, a process involving the synthesis of glutamine. Treatment of astrocytes with glutamine also increases free radical production. (93) If phosphate-activated glutaminase is inhibited free radical production is blocked, suggesting that ammonia released by the hydrolysis of glutamine may be a factor. (94;95) As most of the glutamine in astrocytes is metabolised by mitochondrial phosphate-activated glutaminase, breakdown of

glutamine could result in release of high levels of ammonia in mitochondria, which may contribute to an increase in reactive oxygen species.

Increased levels of nitric oxide and reactive oxygen species may have compounded effects as peroxynitrite is formed from the combination of superoxide and nitric oxide. Peroxynitrite, in the presence of carbon dioxide can modify tissue proteins to form nitrotyrosine which may mediate nitric oxide-induced blood brain barrier damage. (96) Furthermore, an increase in the permeability of the inner mitochondrial membrane to small solutes (mitochondrial permeability transition) results from oxidative and nitrosative stress and ammonia has been recently shown to induce similar changes in cultured astrocytes. (97)

1.6.2 EVIDENCE FOR THE ROLE OF INFLAMMATION/INFECTION IN ACUTE LIVER FAILURE

Hippocrates was the first to write of the association between infection and impaired brain function in 400 BC and the association between infection and impaired brain function is well recognised. Septic encephalopathy can arise from the action of inflammatory mediators on the brain or a cytotoxic response by brain cells to these mediators. Septic encephalopathy is usually the sequelae of severe sepsis complicated by multiple organ failure and hypotension. (98) Severe sepsis causes plasma and brain amino acids to become deranged with a decrease in branched chain amino acids (e.g. isoleucine) and an increase in neutral amino acids in the brain similar to the findings in portosystemic encephalopathy. (99;100) In patients with sepsis it was shown that aromatic amino acids (e.g. phenylalanine) correlated with APACHE II scores and mortality. Scores were greater in shock patients with higher levels of ammonia and

sulphur containing amino acids with a higher mortality rate. (101) Oxidative stress is important in the pathogenesis of ammonia-induced neurotoxicity. In hyperammonemia, free-radical production may be mediated by NMDA-receptor activation (102) and ammonia-induced mitochondrial dysfunction (103) could also be a source of reactive oxygen species such as peroxynitrite. (96) Furthermore, antioxidants have beneficial effects in experimental animal models of hepatic encephalopathy and hyperammonemia. (104;105) As previously mentioned, hypothermia improves the outcome in acute liver failure. Hypothermia reduces free radical production which may account for some of its beneficial effects. (106) Takada et al. (107) have shown in a pig model of acute liver failure that animals administered lipopolysaccharide and amatoxin intraportally developed more pronounced intracranial hypertension than animals given amatoxin alone, even though ammonia concentrations were similar in both groups. In another pig model of acute liver failure induced by hepatic devascularisation, improvement in the severity of hepatic encephalopathy following treatment with albumin dialysis occurs independently of changes in ammonia. (108) Albumin dialysis probably achieves this effect through reduction in oxidative stress and restoring nitric oxide metabolism. These observations support a role for mechanisms other than ammonia in the pathogenesis of hepatic encephalopathy.

Studies in patients with acute liver failure have shown rapid progression to severe hepatic encephalopathy in those with evidence of a systemic inflammatory response, suggesting a possible link between inflammation and hepatic encephalopathy. (109;110) In addition, in patients with acetaminophen-induced acute liver failure, infection and/or the resulting systemic inflammatory response was shown to be an important factor in contributing to deterioration in the severity of

hepatic encephalopathy. (111) In the advanced stages of hepatic encephalopathy in acute liver failure, when patients have uncontrolled intracranial hypertension, the brain produces cytokines such as TNF-α, IL-1β and IL-6. (112;113)

In addition, it is likely that one of the mechanisms through which inflammation exerts its deleterious effect is by inducing alterations in cerebral blood flow through its effects on the expression of the NOS proteins. Accordingly, Aggarwal et al. (114) showed that patients with high intracranial pressure have elevated cerebral blood flow. More recently a direct correlation between the severity of inflammation and increased cerebral blood flow has been observed in acute liver failure. (73) Further evidence supporting the role of inflammation is derived from experimental interventions that reduce brain swelling by altering cerebral blood flow and inflammatory responses. In patients with uncontrolled intracranial hypertension and acute liver failure, moderate hypothermia reduces brain flux of TNF-α, IL-1β and IL-6 and cerebral blood flow contributing to reduction in intracranial pressure. (105;115) Removal of the necrotic liver in acute liver failure reduces circulating levels of proinflammatory cytokines such as TNF-α, IL-1β and IL-6, lowers cerebral blood flow resulting in a reduction in the severity of intracranial hypertension. (116)

1.6.3 EVIDENCE FOR THE ROLE OF INFLAMMATION/INFECTION IN CIRRHOSIS

A distinctive postmortem finding in human brains with hepatic encephalopathy is the presence of Alzheimer Type II astrocytosis (32) which characteristically contain increased amounts of lipofuscin pigment that consists of peroxidized lipids compatible with oxidative damage. (117) Nitric oxide has also been implicated in the pathogenesis of hepatic encephalopathy. Nitric oxide synthase activity has been shown to be elevated in experimental models of hepatic encephalopathy (118) and increased brain nitric oxide production was shown in portacaval-shunted rats given ammonia infusions (76) with evidence of nitrotyrosine accumulation in astrocytes. (119) (Figure 1.8) Studies in portacaval shunted rats administered an ammonia load have demonstrated a rise in cerebral blood flow that paralleled the increase in intracranial pressure and correlated directly with brain water content. (76;120) In cirrhosis, it has been shown that changes in regional cerebral blood flow lead to differences in cerebral ammonia uptake. (78) Cerebral blood flow is higher in the basal ganglia and cerebellum which correlates with increased ammonia extraction. (79)

Further support for interaction between ammonia and inflammation is provided in a recent paper by Liu et al (121), who showed that alteration of gut flora in patients with cirrhosis with the administration of fibre and probiotics was associated with improvement in the severity of minimal hepatic encephalopathy compared with a control group. They showed that this improvement in minimal hepatic encephalopathy was associated with a reduction in venous endotoxin and ammonia levels at day 30.

Patients with chronic liver disease are particularly prone to infection which is frequently a precipitant of hepatic encephalopathy. (122;123) Bacterial infections are of particular concern in patients with cirrhosis because they are poorly tolerated. (124) Sepsis and associated endotoxaemia occur in approximately 40% of hospitalized patients with cirrhosis and is a major cause of death. (125;126) The increased risk of infection is secondary to impairment of several host defence mechanisms including impaired neutrophil function. (127;128) The hemodynamic derangement of cirrhosis resembles that produced by endotoxin, (129) and bacteremia can greatly exacerbate this state, producing hypotension, hepatorenal syndrome, deterioration in mental status and increased portal hypertension with risk of variceal bleeding. Factors that predispose to bacterial infection include malnutrition with impaired cell-mediated immunity, decreased integrity of the bowel wall leading to bacterial translocation, and impaired phagocytic activity of the hepatic and splenic reticuloendothelial system resulting from portal hypertension. Tuftsin, a natural tetrapeptide known to stimulate phagocytosis by neutrophils, has also been shown to be reduced in cirrhosis. It is part of a specific carrier, leucokinin, which is cleaved by an enzyme, tuftsin endocarboxypeptidase, while circulating through the spleen. (130) Neutrophils from patients with superimposed acute alcoholic hepatitis have depressed phagocytosis, intracellular killing and metabolic activity, although they have a greater capacity for ingestion and killing of bacteria than neutrophils of patients with cirrhosis alone. (128) Our group has recently shown that neutrophil dysfunction with high resting oxidative burst and reduced phagocytic capacity is present in patients with cirrhosis and alcoholic hepatitis which was associated with a significantly greater risk of infection, organ failure and mortality (131).

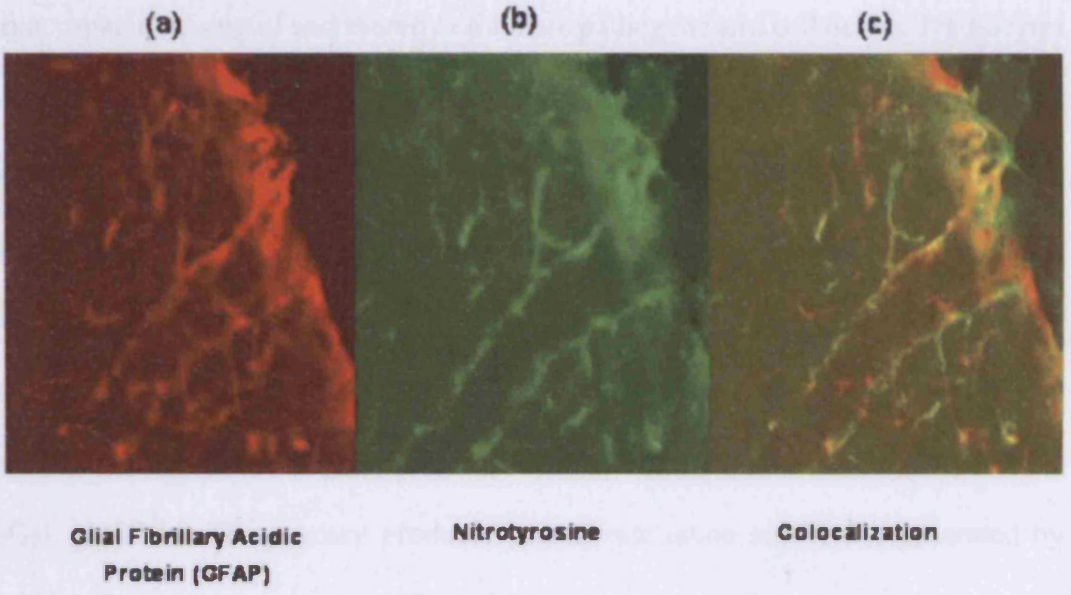

Figure 1.8

Slides showing staining for nitrotyrosine in the cerebral cortex of a portacaval shunted rat receiving an ammonia infusion (courtesy of Professor Andrei Blei, Northwestern University Feinberg School of Medicine, Chicago and published in Seminars in Liver Disease 2003; 23:259-69). (a) Shows glial fibrillary acidic protein (GFAP) positive astrocytes in the cerebral cortex, (b) shows nitrotyrosine staining in astrocytes and (c) reveals the overlap of GFAP and nitrotyrosine staining in cortical astrocytes.

1.7 NEUTROPHILS

Neutrophils account for 70% of all white blood cells [Figure 1.9] and along with macrophages comprise the professional phagocytes, being endowed with a unique capacity to engulf and thereby eliminate pathogens and cell debris. Phagocytes are equipped with specialised receptors to recognise their targets; this complex machinery initiates internalisation and mediates an assortment of degradative mechanisms that culminate in the killing and disposal of the engulfed particles. (132) During phagocytosis of microbial intruders, professional phagocytes of the innate immune system increase their consumption of molecular oxygen through the activity of an NADPH-oxidase that generates superoxide anion (O_2^-) and hydrogen peroxide (H_2O_2). (133;134) The primary products (superoxide anion and H_2O_2) generated by the NADPH-oxidase are not sufficiently reactive to account for the bactericidal effects, however, these oxygen metabolites give rise to yet other reactive oxygen species that are strongly anti-microbial. (135) The respiratory burst products are not only able to eradicate invading micro organisms, but unfortunately may also damage 'innocent bystanders;' leading to tissue destruction and associated inflammatory reactions. The reactive oxygen species generated by phagocytes function as regulators of other immune responsive cells (136) and for apoptotic processes. (137)

Neutrophil

Figure 1.9

Glutamine is an important fuel for neutrophils and enhances the function of these immune cells. (138) Glutamine is converted to glutamate, lactate and aspartate by a phosphate-dependent glutaminase [Figure 1.10] which is known to be inhibited by 2 mM ammonium chloride. (139) Furthermore, in rat neutrophils glutamine may give rise to substantial quantities of NADPH for superoxide production. (140) Ogle et al. (141) observed that the enhancement of human neutrophil action by glutamine was not due to increased phagocytosis and Moinard et al. demonstrated in stressed rats with a diet supplemented by glutamine, that respiratory burst is enhanced. (142) In a further study, they demonstrated that ornithine 2-oxoglutarate (OKG) was able to increase the chemotaxis of neutrophils 5 fold, but that arginine and glutamine administration failed to show the same effect. They also observed an increase in reactive oxygen species production. This is not dependent on glutamine production as it is unaffected by adding an inhibitor of glutamine synthetase (methionine sulphoxamine). Reactive oxygen species production due to OKG is mediated by nitric oxide, since the effect of OKG is abolished by S-methylthiourea, an inhibitor of inducible nitric oxide synthase. Furthermore, they observed that the respiratory burst was partially abolished by treatment with difluoromethylornithine (DFMO), an inhibitor of ornithine decarboxylase. They suggested that OKG may generate polyamines, which could mediate an increase in protein kinase C activity and thus stimulate reactive oxygen species production via activation of NADPH-oxidase. (143) The production of NADPH may be substantially increased by the polyamine pathway through an increase in glucose-6-phophate dehydrogenase (G6PD) activity, providing ample substrate for NADPH-oxidase. This is illustrated in Figure 1.11.

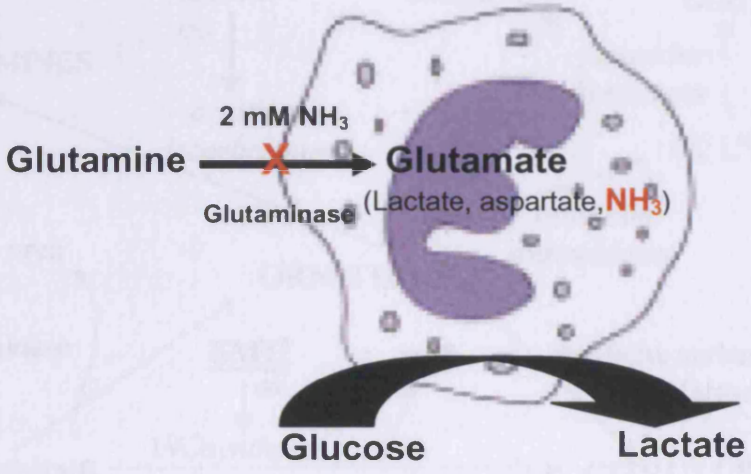

Figure 1.10

Diagrammatic illustration showing glutamine is an important fuel for neutrophils and enhances the function of these immune cells. Glutamine is converted to glutamate, lactate and aspartate by a phosphate-dependent glutaminase which is known to be inhibited by 2 mM NH_4Cl.

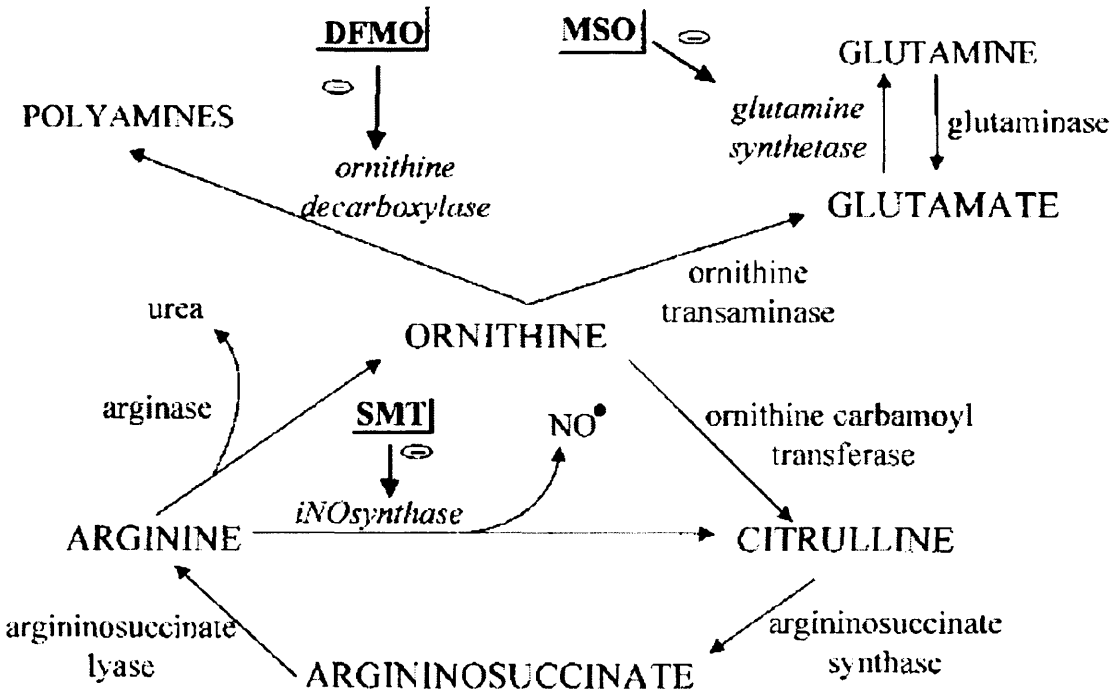

Figure 1.11

The metabolism of pharmaconutrients, the metabolic pathways and their inhibitors involved in neutrophil phagocytosis. (DFMO: difluoromethyl ornithine; MSO: methionine sulphoxamine; SMT: S – methylthiourea) taken from Moinard et al. Clinical Science 2002 ; 102 :288.

1.8 NEUTROPHIL MITOGEN-ACTIVATED KINASES

Mitogen-activated kinases (MAP kinases) are proline-directed serine and threonine protein kinases that are activated by dual specificity kinases by phosphorylation of threonine and tyrosine in a Thr-Xaa-Tyr motif in a loop near the active site. (144;145) The three types are defined by the intervening Xaa amino acid. In the extracellular signal-regulated kinases (ERK), the amino acid is glutamate; in the jun-kinases (JNK) it is proline and in the p38-MAP kinases ($p38^{-MAPK}$), it is glycine.

The $p38^{-MAPK}$ signaling pathway plays an important role in inflammation and other physiological processes. Specific inhibitors of $p38^{-MAPK}$ block production of the major inflammatory cytokines tumour necrosis factor α (TNF-α) and interleukin 1 (IL-1), and other inflammatory enzymes such as cyclooxygenase-2 (COX-2). These inhibitors are pyridinyl imidazole compounds e.g. SB203580 or SB202190. A major function of the $p38^{-MAPK}$ pathway is post-transcriptional control of inflammatory gene expression. Many of the messenger RNA's (mRNA) are unstable or untranslatable and signaling in the $p38^{-MAPK}$ pathway counteracts these and stabilizes the mRNA by preventing otherwise rapid de-adenylation. (146) There are 4 subtypes of $p38^{-MAPK}$: α, β, γ and δ. All are activated by upstream kinases – MAP kinase kinase (MKK) 3 or MMK6, in response to inflammatory and stressful stimuli. The α, β and δ forms are widely expressed, whereas γ is limited to muscle. $p38^{-MAPK}$ α was first isolated as a 38 kDa protein rapidly tyrosine phosphorylated in response to lipopolysaccharide stimulation. (147;148) It is strongly expressed in monocytes, macrophages, CD4 T cells, neutrophils and endothelial cells, strongly suggestive of a pivotal role in the immune system. Macrophages, CD4 T cells and neutrophils all express comparable

levels of α and δ, but the inhibitors of p38^{-MAPK} only inhibit α and β forms. The role of γ and δ in inflammation is unknown. (149)

Inflammatory stimuli activate four major signaling intracellular signaling pathways: the nuclear factor-κB (NFκB) and the 3 MAPK kinase pathways (p38^{-MAPK}, ERK and JNK). All 4 pathways drive transcription of inflammatory genes. It has been shown that the protein p38^{-MAPK} is an important kinase regulating apoptosis in neutrophils exposed to stress, hypoxia and lipopolysaccharide.(150) Furthermore, toll-like receptors play an important role in promoting clearance of bacteria through the up-regulation of macrophage phagocytic activity through p38^{-MAPK}. (151) Phagocytosis of apoptotic cells results in the production of transforming growth factor-β (TGF- β), which plays an important role in the resolution of inflammation. TGF- β prevents proinflammatory cytokine production through inhibition of p38^{-MAPK}. Crosstalk between ERK and p38^{-MAPK} is essential for this process. (152) Other inflammatory response proteins depend upon p38^{-MAPK} signaling for their production besides TNF-α, IL-1 and COX-2. Interleukin-6 (IL-6) and interleukin-8 (IL-8) stability is regulated by p38^{-MAPK} and monocytes chemoattractant protein-1, IL-12p40, granulocyte macrophage colony-stimulating factor, vascular endothelial growth factor and inducible nitric oxide synthase are all p38^{-MAPK} dependent. (146)

The pathway is also activated by cell stress, growth factors, G-protein coupled receptors and other stimuli, which might include ammonia. Inhibition of p38^{-MAPK} decreases survival of neutrophils, possibly by phosphorylating caspases 3 and 8. (153) This could thus modulate apoptosis. Glutamine exerts many of its biological effects through a swelling-induced activation of ERK and p38^{-MAPK} signaling. p38^{-MAPK} and ERK are osmosensors which are activated in response to increased cell hydration or swelling. (154-157) [Figure 1.12] A diagram of how these receptors and signals

interact, and how the neutrophil lyses the bacteria with reactive oxygen species within a phagosome is illustrated in Figure 1.13.

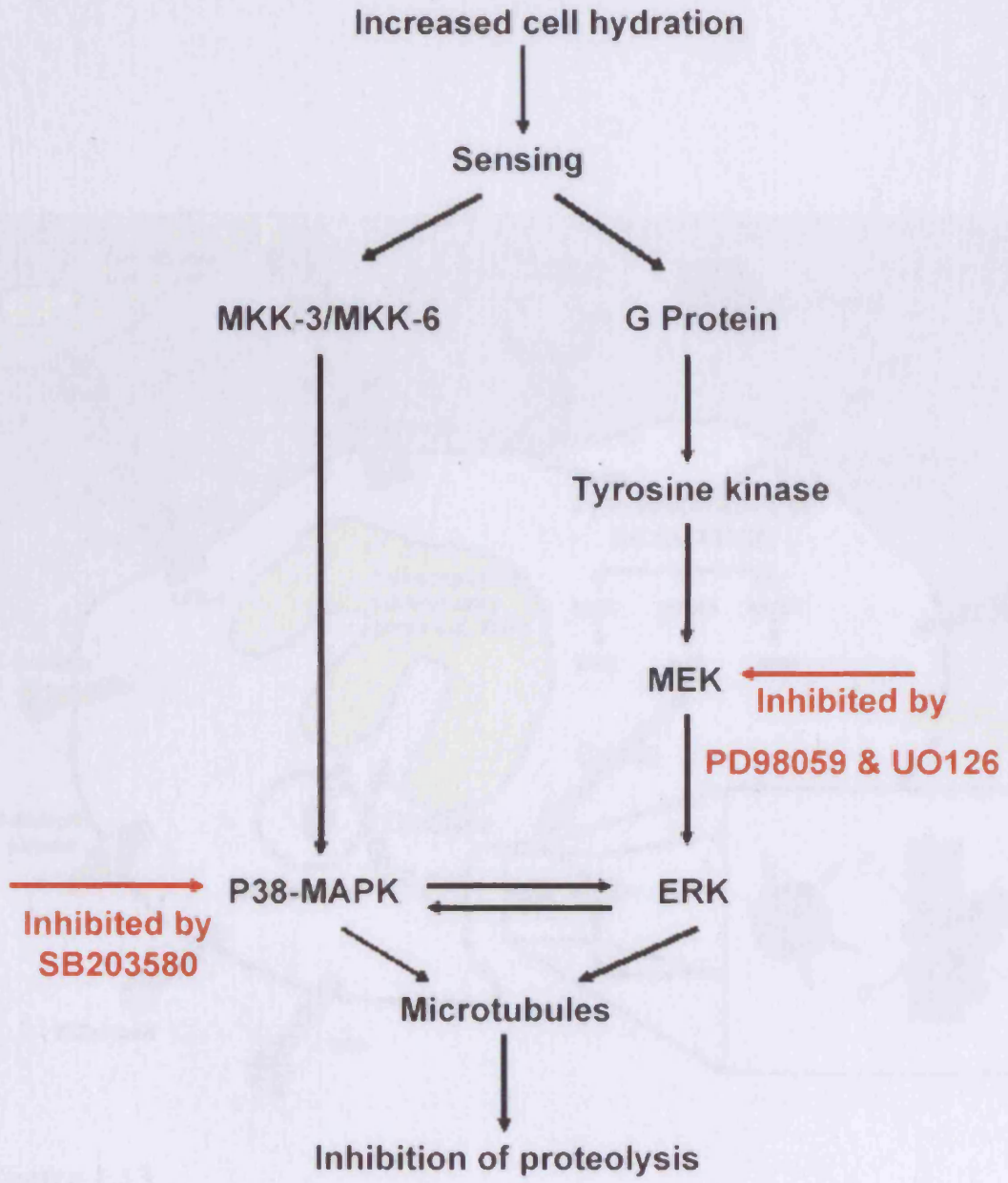

Figure 1.12

Diagrammatic representation of the mechanism by which the cell senses an increase in hydration by the $p38^{-MAPK}$ and ERK-dependent pathways. $p38^{-MAPK}$ can be inhibited by SB203680 and ERK can be inhibited by UO126.

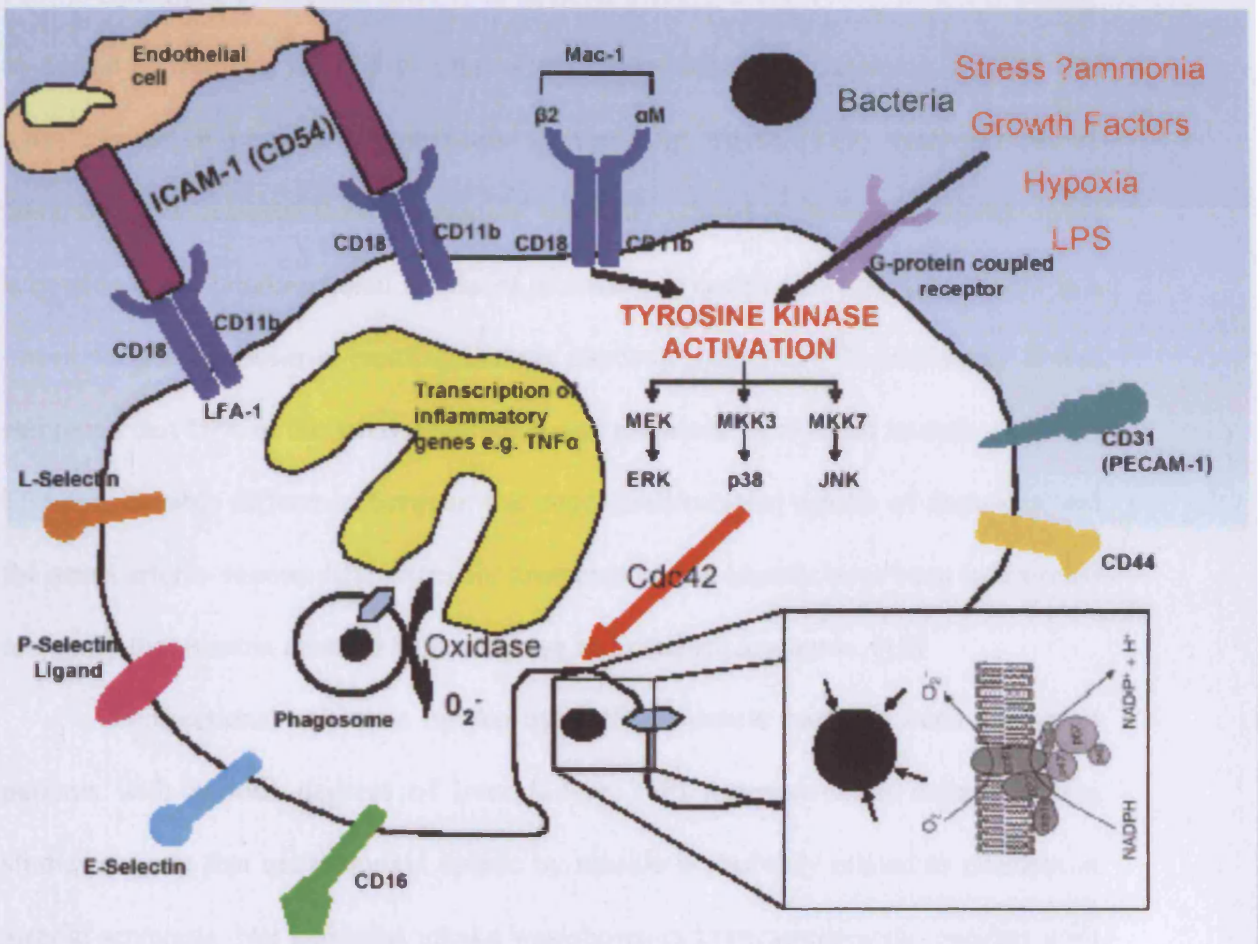

Figure 1.13

A diagram to summarise how the neutrophil receptors and signaling pathways interact in response to stress or a bacterial challenge, and of neutrophil lysis of an engulfed bacteria within a phagosome.

1.9 THE ROLE OF MUSCLE IN AMMONIA METABOLISM IN ACUTE AND CHRONIC LIVER FAILURE

Glutamine synthetase activity in skeletal muscle is low (158), and it is mainly by virtue of its mass relative to other glutamine synthetase containing organs, that muscle is one of the principle glutamine synthesizing organs. (159) Ammonia can be taken up by or released from the muscle, probably related to purine nucleotide cycle activation (160) Unidirectional uptake of ammonia in healthy humans was shown in a tracer study using positron-emitting isotope enriched ammonia (^{13}N-ammonia). It was estimated that 50% of the arterial ammonia was extracted by skeletal muscle. (18;161) The considerable difference between the large unidirectional uptake of ammonia and the small arterio-venous differences for ammonia across muscle have been interpreted to signify that muscle must continuously use and produce ammonia. (18)

Unidirectional ammonia uptake by skeletal muscle has also been shown in patients with various degrees of liver failure. (18) Arterio-venous catheterization studies suggest that net ammonia uptake by muscle is probably related to changes in arterial ammonia. Net ammonia uptake was shown in hyperammonemic patients with decompensated cirrhosis in arterio-venous difference measurements across the forearm (17;159;162;163) and leg. (164) A good correlation between arterial ammonia concentrations and muscle ammonia uptake was observed in patients in hepatic coma with (17) or without (162) active upper gastrointestinal bleeding. This is also seen in patients with decompensated cirrhosis (165) and gross muscle wasting (159) but not in compensated patients with normal muscle mass. (17;159) Furthermore, the fractional extraction of ammonia was reduced in patients with muscle wasting, (159) suggesting an important role for cirrhotic patients maintaining

adequate muscle mass. Leg ammonia consumption correlates with glutamine production in acute liver failure suggesting that skeletal muscle participates in ammonia detoxification. The total muscle amino acid production was 10 times higher than the uptake of ammonia, indicating that the production of glutamine was not only the result of ammonia consumption, but also the result of net muscle catabolism. (166) Furthermore, it has been demonstrated that in acute liver failure the gene for glutamine synthetase is significantly up regulated (measuring messenger RNA) compared to the level of gene transcription for β-actin ($p < 0.05$) [Figure 1.14]. (167)

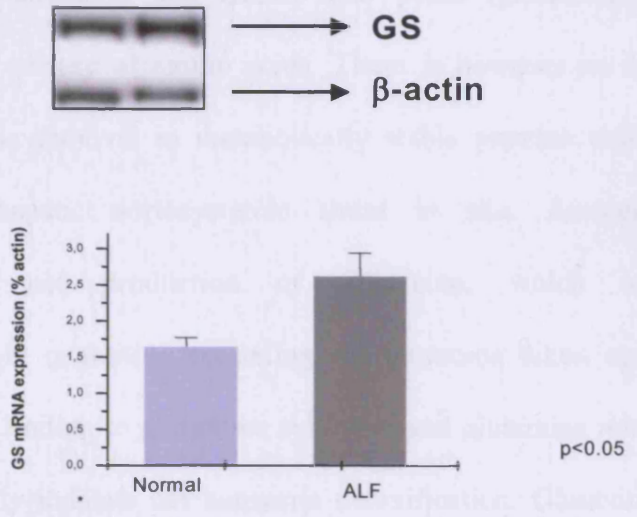

Figure 1.14

A diagram to show upregulation of muscle glutamine synthetase gene and protein induction in acute liver failure taken from Desjardins et al. 1999 (167).

Enhanced ammonia consumption by skeletal muscle has been shown in vivo after ammonia infusion in healthy rats (168), monkeys (169), dogs (169;170) and pigs. (171) The ammonia consumption enhanced glutamine production in only some of these studies (169;171), whilst glutamine production remained unchanged in others. (168;170) Muscle glutamine release was two to four-fold higher in chronic portacaval shunted rats compared with healthy controls, whereas the corresponding net ammonia uptake was not observed. (172) This is most likely due to enhanced muscle catabolism. Furthermore, part or all of the ammonia may be trapped in augmented tissue ammonia and amino acid pools (glutamine). This may not necessarily induce release of amino acids. There is however an important role for muscle in ammonia removal in metabolically stable patients with cirrhosis and a transjugular intrahepatic portosystemic shunt in situ. Ammonia uptake was accompanied by net production of glutamine, which increased during hyperammonemia in quantities exceeding the ammonia taken up. (21) Ammonia uptake by muscle, leading to glutamine synthesis and glutamine release from muscle does not necessarily indicate net ammonia detoxification. Glutamine released from skeletal muscle can be taken up in the splanchnic tissues or in the kidneys and can be metabolised to ammonia, abolishing the effect on whole body ammonia removal. Glutamine acts thereby as a non-toxic nitrogen carrier, without contributing to net nitrogen removal from the systemic circulation. Skeletal muscle metabolism probably plays an important role in ammonia metabolism in acute and chronic liver failure. This is mainly because total body skeletal muscle mass probably constitutes quantitatively, *in toto*, the most important localisation of the enzyme glutamine synthetase.

1.10 AMMONIA LOWERING STRATEGIEG TARGETING THE MUSCLE

Ammonia lowering interventions are limited, however, L-ornithine-L-aspartate (LOLA), the stable salt of the amino acids ornithine and aspartic acid, has been shown to reduce blood ammonia concentration and improve psychometric performance in patients with hyperammonemia and hepatic encephalopathy when administered intravenously. (173-176) LOLA is believed to act by stimulating the urea cycle and glutamine synthesis to effect ammonia detoxification, (176;177) though direct evidence for the mechanism of action is lacking.

It has been proposed that ornithine improves the rate of the urea cycle [Figure 1.15], especially through the enzyme carbamyl phosphate synthetase. Carbamyl phosphate synthetase catalyses the conversion of bicarbonate, ATP, and ammonia into carbamyl phosphate, this reaction is the first step in the urea cycle. The putative action of aspartate is unclear, though it is known to be a substrate for the enzyme asparagine synthetase which catalyses the reaction between ammonia and aspartate forming asparagine [Figure 1.16].

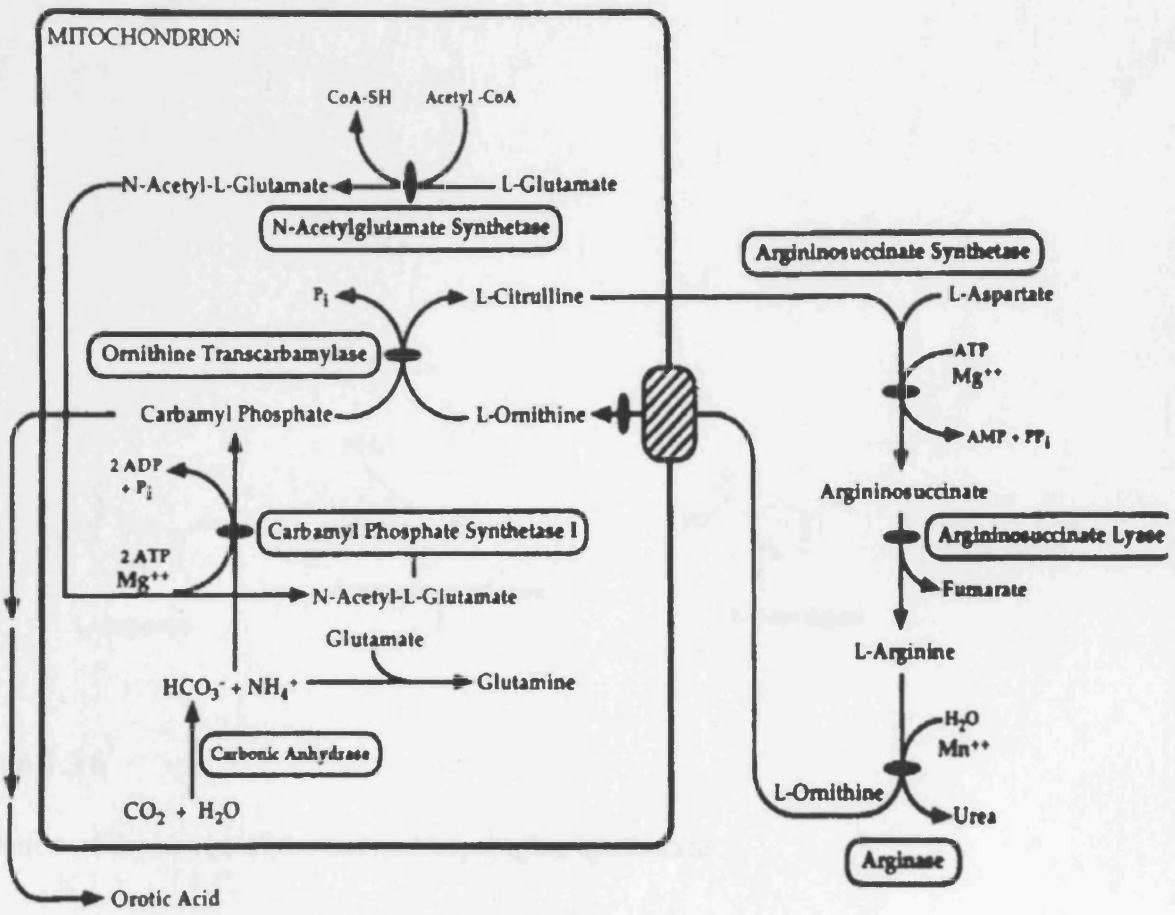

Figure 1.15

The urea cycle

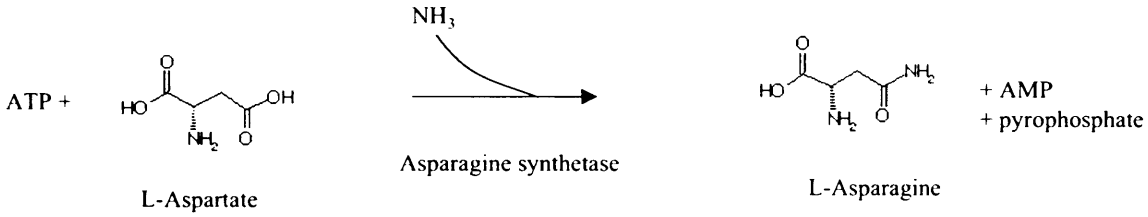

Figure 1.16

Illustration of the action of the enzyme asparagine synthetase

It should however be noted that ammonia uptake by muscle, leading to glutamine synthesis does not necessarily indicate ammonia detoxification. Glutamine released from muscle may be subsequently taken up by the splanchnic tissues or the kidneys and re-metabolised to ammonia.

The increased muscle levels of glutamine synthetase require sufficient substrate to effectively reduce circulating ammonia. In this regard LOLA offers a significant resource in that for each LOLA administered three molecules of glutamate are potentially generated [Figure 1.17]

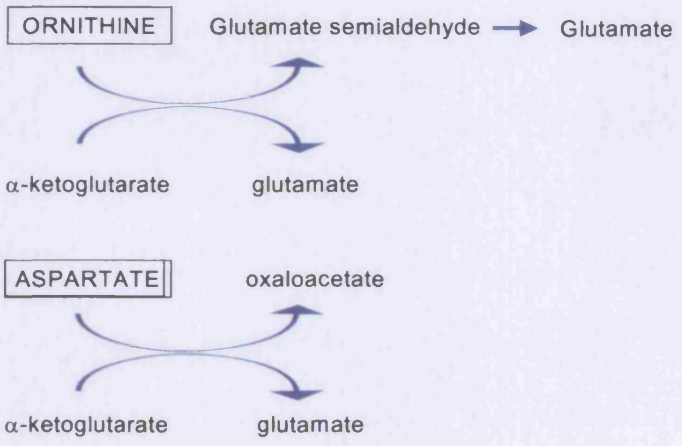

Figure 1.17

A diagram to show the metabolic conversion of LOLA to glutamate

By increasing the amount of glutamate as substrate for glutamine synthetase, in the presence of a ready supply of ammonia, the reaction would be driven to produce glutamine, thereby effectively lowering the systemic ammonia levels. This effect has been shown in a rat model of acute liver failure. When rats were administered LOLA, glutamate production was significantly increased ($p<0.001$) approximately four fold compared to rats given saline. (176)

1.11 SUMMARY

The current perspectives on the molecular pathogenesis of hepatic encephalopathy have been described. The importance of the role of ammonia has been highlighted with respect to both its direct neurotoxicity and on brain swelling through its detoxification to glutamine in the astrocyte, the cell most often implicated in the pathogenesis of hepatic encephalopathy. In fact, one might say that the key to understanding the pathogenesis of hepatic encephalopathy is to explore the story of the 'sick astrocyte'. The factors that are believed to be critical in modulating the manifest symptoms of hepatic encephalopathy have been reviewed; the most important of which is the potential synergistic role of inflammation in modulating the cerebral effects of ammonia. Furthermore, the production of reactive oxygen species and increased protein tyrosine nitration may alter astrocyte function and contribute or precipitate episodes of hepatic encephalopathy.

We have also described the inter-organ trafficking of ammonia. In healthy individuals the liver removes ammonia by detoxification into urea. However, in patients with cirrhosis, the metabolic capacity of the liver is reduced. The muscle then becomes an important organ of ammonia detoxification. Furthermore, we have given evidence for the role of inflammation in acute and chronic liver failure and how potentially such inflammation could alter the inter-organ metabolism of ammonia.

Finally, we have discussed the role of neutrophils in inflammation and infection. These are the cells which are endowed with a unique capacity to engulf and eliminate pathogens and to produce reactive oxygen species, which eradicate invading microorganisms but also lead to tissue destruction and associated inflammatory reactions.

In patients with cirrhosis, hyperammonemia is commonly associated with hepatic encephalopathy and accompanies gastrointestinal bleeding, both conditions being associated with a high incidence of sepsis and mortality.

Despite this extensive literature base, only the tip of the iceberg has so far been uncovered in terms of understanding the operative mechanisms involved in the pathogenesis of hepatic encephalopathy in relation to ammonia, infection and inflammation.

Chapter 2

Hypothesis And Aims

2.1 HYPOTHESIS

Ammonia has a central role in the pathogenesis of hepatic encephalopathy, albeit not as a simple, single-factor relationship. There is a growing evidence base to support the role of inflammation as being important in increasing the susceptibility of the brain to the effects of ammonia in liver disease. Therefore in an attempt to understand the complexity of the relationship to hepatic encephalopathy the following hypotheses were formulated:

1. Inflammation and infection are pivotal in the pathogenesis of hepatic encephalopathy (Figure 2; Q1).
2. Ammonia and inflammation/infection act synergistically in the pathogenesis of hepatic encephalopathy (Figure 2; Q2).

If inflammation modulates the cerebral effect of ammonia, then another key question to ask is whether the relationship is a two way one i.e, can the presence of ammonia itself influence the presence of infection or inflammation? If one takes a step back from this supposition, then it might be logical to question whether ammonia itself may impair immunity and predispose an individual to the development of infection or sepsis. This led onto the development of a third hypothesis:

3. Ammonia impairs neutrophil function (Figure 2; Q3).

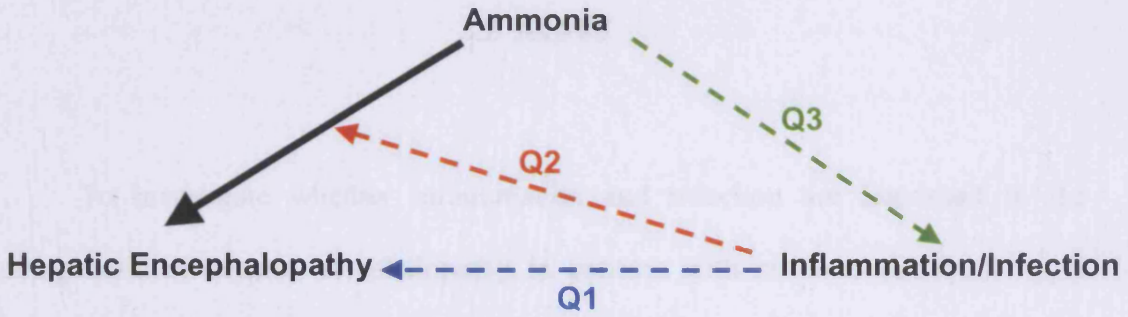

Figure 2.1

Hypothesis

If inflammation modulates the cerebral effects of ammonia, then the last key question to answer is how is the metabolism of ammonia affected by the presence of inflammation or infection? The muscle is an important organ in total body ammonia metabolism. As described earlier, the muscle may be an important site for ammonia detoxification and a potential therapeutic target for ammonia reduction in liver disease. By exploring how the muscle metabolism of ammonia is modulated by inflammation, potential mechanisms might be further elucidated.

Thus these hypotheses encompass the role of inflammation/infection on the metabolism of ammonia in the brain and muscle and explore how ammonia may impact on neutrophils whose function is critical in fighting microbial invasion and inducing inflammation.

2.2 AIMS

1. To investigate whether inflammation and infection are important in the pathogenesis of hepatic encephalopathy in patients with cirrhosis (Question 1), 2 clinical studies were performed [Chapter 4]. Minimal hepatic encephalopathy is common in cirrhosis (178) but its full pathophysiologic basis remains to be completely defined. In the first of these studies, an evaluation was made of whether the presence of minimal hepatic encephalopathy is associated with the severity of liver disease, ammonia levels or the presence of inflammation and the factors determining neuropsychological deterioration accompanying induction of hyperammonemia were assessed. Studies in acute liver failure show a correlation between evidence of a systemic inflammatory response and progression of hepatic encephalopathy (73;109;110) but this has not previously been described in cirrhosis. Therefore, in the second study, the hypothesis that inflammatory mediators, such as nitric oxide and proinflammatory cytokines, may exacerbate the neuropsychological effects of hyperammonemia in cirrhosis was tested. Patients with cirrhosis were studied 24-36 hours after admission with clinical evidence of infection, and following its resolution.

2. To investigate whether ammonia and inflammation/infection act synergistically in the pathogenesis of hepatic encephalopathy (Question 2), the pathological changes that occur in the brain of mildly hyperammonaemic animals with an induced liver disease leading to rapid hepatic liver fibrosis were studied. This was done using the bile duct ligated rat model, with and without an added bacterial endotoxin insult, through the administration of lipopolysaccharide.

3. Pilot studies performed by our group suggested that phagocytosis and oxidative burst in normal neutrophils may be impaired by micromolar concentrations of ammonia. The exact mechanism of action underlying this is unclear but could conceivably involve the inhibition of glutaminase. However, published data suggests that glutaminase is usually inhibited by millimolar rather than micromolar concentrations of ammonium chloride (139) which might suggest alternative mechanisms. It is also known that in astrocyte cultures, exposure to ammonia results in cytosolic alkalinization leading to calcium-dependent release of glutamate. (55) It is therefore reasonable to postulate that ammonia may cause cytosolic alkalinization in neutrophils as well. Ammonia freely passes into the neutrophil cytosol and one possibility is that it may alter the activity of intracellular signalers such as mitogen-activated protein (MAP) kinases, p38-MAP kinase ($p38^{-MAPK}$), Jun-kinase (JNK) and extracellular signal-regulated kinase (ERK) (179). The aim of this third study was therefore to characterize some aspects of neutrophil morphology and function in the presence of ammonia, such as phagocytosis and oxidative burst in a series of observational studies. This led onto a mechanistic study in which the hypothesis was developed that $p38^{-MAPK}$ signaling may be involved in the ammonia-induced impairment of neutrophil function. The impact of modulators of $p38^{-MAPK}$ activity influence on ammonia-induced phagocytosis were investigated and comparable experiments on resting respiratory burst in unstimulated neutrophils were performed.

4. To explore how the muscle metabolism of ammonia is modulated by inflammation, a series of studies were performed using chick embryo primary muscle cell cultures and later with cultures of the immortilized murine myofibroblast cell line C2C12 exploring whether ammonia metabolism, as measured by stable amino acid

isotopes, could be altered by the addition of an inflammatory stimulus such as lipopolysaccharide.

Chapter 3

Role of ammonia, infection and inflammation in hepatic encephalopathy in cirrhosis

3.1 CLINICAL STUDY METHODS

3.1.1 SIMULATION OF AN UPPER GASTROINTESTINAL BLEED

3.1.1.1 ORAL AMINO ACID SOLUTION

In 1963 Bessman and Hawkins published their findings to show that ingestion of packed red blood cells causes a statistically significant greater rise in blood ammonia than plasma protein. (165) They concluded that in view of the fact that 95% of the protein in an erythrocyte is haemoglobin, then this is likely to be a specific effect of this protein. The amino acid composition of the haemoglobin molecule is shown below in Table 3.1 (180).

The Amino Acid Composition of Haemoglobin Molecule (180)

Leucine	99.8	Glutamate	33.3	Aspartate	41.6
Isoleucine	0	Asparagine	27.7	Alanine	99.8
Valine	85.9	Glutamine	11.1	Cysteine	8.3
Glycine	55.4	Methionine	8.3	Serine	44.4
Tryptophan	8.3	Arginine	16.6	Phenylalanine	41.6
Threonine	44.4	Tyrosine	16.6	Histidine	52.7
Lysine	61.0	Proline	38.8		

NOTE. Expressed as mmol per 100 gram amino acid solution.

Table 3.1

3.1.1.2 INDUCED HYPERAMMONEMIA

Hyperammonemia was induced by simulation of an upper gastrointestinal bleed was by administration of an oral bolus of 75 grams of a specifically prepared solution (Nutricia Cuijk, The Netherlands, Product Number: 24143) that mimics the amino acid composition of the hemoglobin molecule (79;180). The solution was freshly made in 200 mls of water and xanthum gum was added to prevent sedimentation. The placebo solution looked identical and was comprised of xanthum gum only.

3.1.1.3 ETHICAL CONSIDERATIONS

Studies were undertaken with the approval of the Hospital Research Ethics Committee and the written informed consent was obtained from each patient before enrollment in the study in accordance with the Declaration of Helsinki (1989) of the World Medical Association. Administration of 75 grams of an amino acid solution mimicking the composition of the hemoglobin molecule to patients with cirrhosis has been shown to be safe and no significant complications were observed in previous studies (22;51;79). Others have used different formulations to produce hyperammonemia in patients (173;181-183); these approaches were also shown to produce ammoniagenesis without any significant adverse effects.

3.1.2 MEASUREMENT OF NEUROPSYCHOLOGICAL FUNCTION

A construct-driven neuropsychological test battery was designed. A critical factor in developing this evaluation was the total time period needed to complete the battery, so it could be used as a tool to assess changes in neuropsychological function in response to the administration of the amino acid solution. The following cognitive

domains were tested: concentration, memory, visuospatial-construction skills and motor function. The neuropsychological test battery consisted of: Trails B Test; (184) the Digit symbol substitution test; (185) the immediate story recall subtest of the Randt test battery; (186) and choice reaction time. (187) The total time required to perform this battery of tests was less than 20 minutes. The tests were performed immediately before the administration of the amino acid solution, and at 2 and 4 hours afterwards (except Trails B test which was only performed at 0 and 4 hours). The neuropsychological tests were performed by the same investigator (Dr Rajiv Jalan) and the patients had one practice session of each test. All the tests have been well validated and parallel forms were used.

3.1.2.1 TRAILS B TEST

This test is a derivative of the Trail Making Test (184) and measures visual conceptual and visuomotor tracking. Patients were asked to connect subsequent numbers with letters. The test has to be completed within 420 seconds.

3.1.2.2 THE DIGIT SYMBOL SUBSTITUTION TEST

The test is part of the Wechsler Adult Intelligence Schedule. (185) This test is used to assess visuomotor co-ordination and vigilance. The subject substituted a symbol for a digit from a code that was visible throughout the test. A different code was used for each test to control for the effect of learning. The test score was the number of symbols correctly substituted in 90 seconds.

3.1.2.3 REACTION TIME

This test is part of the Continuous Performance Task (186) and measures motor function, sustained concentration and the ability to suppress inappropriate responses. The patients saw a sequence of letters (X, M, T, E) on a computer display at a rate of one letter every 1.5 seconds. The task was to press the space bar of the computer as quickly as possible every time the letter E appeared, except when it was immediately preceded by the letter X. Patients were presented with 10 Es requiring a response and 10 Es preceded by Xs not requiring a response. The average reaction time was recorded.

3.1.2.4 IMMEDIATE STORY RECALL SUBTEST OF THE RANDT MEMORY TEST

This measures immediate memory function and is a subtest of the Randt memory test, which measures various aspects of memory function and include rote, associative, discourse and incidental memory as well as recall. (187) This test measures recall of 20 words from a paragraph that has an emotionally charged substance and includes fire and disaster. This single presentation takes about 15 seconds. The patient was then asked to recall the short story immediately after it had been read to them. After this the gist of the story was requested both immediately and also after 20 minutes. One point was awarded for each word that was recalled immediately after presentation (acquisition). For the gist score, credit was given for any block in which the precise word had been retrieved.

3.1.3 ANALYSIS OF PERIPHERAL VENOUS BLOOD

In the clinical studies, a peripheral venous blood sample was taken for analysis of white cell count (WCC), neutrophil count, C-reactive protein (CRP), ammonia, nitric oxide (NO_x), and interleukin- 6 (IL-6) at the beginning of each study immediately prior to the administration of the amino acid solution. Blood sampling was repeated at 4 hours after administration of the amino acid solution for analysis of ammonia.

3.1.3.1 WHITE CELL COUNT, NEUTROPHIL COUNT AND C-REACTIVE PROTEIN

These were measured by standard automated laboratory techniques in the haematology and chemical pathology laboratories, as part of a standard clinical care protocol.

3.1.3.2 METHOD OF AMMONIA DETERMINATION IN PLASMA USING A MODIFIED BETHELOT ASSAY (INDOPHENOL) (188)

Venous blood was taken and immediately placed in ice. Plasma was then obtained by centrifugation. All chemicals were supplied from Sigma-Aldrich and were of the highest laboratory grade.

1. Fifty μL of plasma was deproteinised by mixing immediately with 150 μL of 5% trichloroacetic acid.
2. This was then spun in a microcentrifuge at 11,200 g at 4 °C for 10 minutes.
3. Fifty μL of the supernatant was pipetted out onto a 96 well plate at 30 °C for 3 hours in 200 μL of a solution containing phenol (10mM), nitroprusside

(10mM), sodium hypochlorite (10mM) solution and sodium hydroxide (0.5mM).

4. The blue colour formed by reaction of ammonia with phenol and hypochlorite was then measured colorimetrically at 630nm. This was read in a 96 well plate reader (Tecan Sunrise, Salzburg, Austria).

5. Each sample was analysed in duplicate and compared to an ammonium chloride standard curve (Figure 3.1).

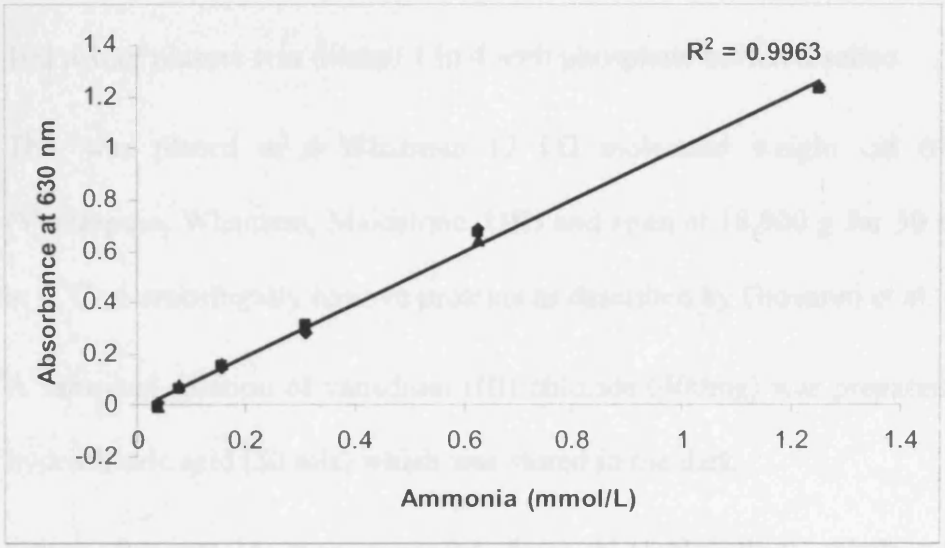

Figure 3.1

A typical ammonium chloride standard curve

3.1.3.3 METHOD FOR SIMULTANEOUS DETECTION OF NITRATE AND NITRITE (NO_X) IN PLASMA

Combined NO_2/NO_3 levels were determined from heparinised plasma samples, by a modified Greiss test (189) which had been obtained by centrifugation and stored at -80 °C. This determination predominantly represents the nitrate content in the sample, because the nitrite fraction alone is difficult to measure in this manner as its level is usually near the detection threshold of the assay (ca. 1 μM). All chemicals were supplied from Sigma-Aldrich (Poole, Dorset, UK) and were of the highest laboratory grade.

1. 100 μ/L of plasma was diluted 1 in 4 with phosphate buffered saline.
2. This was placed in a Whatman 12 kD molecular weight cut off filter (Vectaspoin, Whatman, Maidstone, UK) and spun at 18,900 g for 30 minutes at 4 °C to centrifugally remove proteins as described by Giovanni et al. (190)
3. A saturated solution of vanadium (III) chloride (400mg) was prepared in 1M hydrochloric acid (50 mls) which was stored in the dark.
4. Greiss Reagent A was prepared from N-(1-Naphthyl) ethylenediamine dihydrochloride (0.1% w/v) in double distilled water which was stored in the dark.
5. Greiss Reagent B was prepared from sulfanilamide (2% w/v) in 5% hydrochloric acid which was stored in the dark.
6. Fifty μ/L of the filtrate was pipetted out into a 96 well plate. To this were added 50 μ/L of vanadium (III) chloride solution, 50 μ/L of Greiss Reagent A, and 50 μ/L of Greiss Reagent B.

7. The plate was then left for 2 hours and read colorimetrically at 550nm on a 96 well plate reader (Tecan Sunrise, Salzburg, Austria) with accompanying Magellan 3 software. The nitrite/nitrate in the filtrate were determined against a sodium nitrite standard curve measured utilizing methods described by Miranda et al. (189)

8. Each sample was analysed in duplicate. Linear regression of the mean values of the absorbance at 550 nm for each standard set minus the blank values was utilized to determine the nitrite or total NO_x concentrations in samples. These values were then subtracted to give the nitrate concentration.

9. Nitrite alone was measured in a similar manner except that samples were only exposed to Greiss reagents A and B. Intra- and interassay coefficients of variation were 3.1% and 4.3% respectively.

3.1.3.4 MEASUREMENT OF INTERLEUKIN-6, INTERLEUKIN-1-β AND TUMOUR NECROSIS FACTOR-α.

Plasma was obtained by centrifugation and stored at -80 °C.

1. Capture antibodies for tumour necrosis factor (TNF-α), interleukin-6 (IL-6), interleukin-1-β (IL-1-β) (BioSource International, Nivelles, Belgium) were coated at 1 μg/ml onto 96 well Maxisorb (NUNC, Denmark) ELISA plates.
2. The plates were blocked with bovine serum albumin (Fraction V, Sigma, Poole, Dorset, UK) before the addition of 100 μl standard or sample together with biotin-conjugated detection antibody (50 μl; 0.4 μg/ml).

3. After incubation at room temperature for 2 hours and washing, streptavidin was added before incubation with substrate (o-phenylenediamine hydrochloride) in a borate-citrate buffer.
4. The reaction was stopped with 1.8M sulphuric acid and the optical density measured at 450nm referenced against 630nm. Individual standard curves were established and a lower limit for TNF-α detection set at 5 pg/ml. After a single batch analysis, the intra-assay coefficient of variation was 5.4%.

3.1.3.5 MEASUREMENT OF AMINO ACIDS

Plasma was obtained by centrifugation and deproteinised with sulphosalicylic acid for determination of amino acid concentration by high-performance liquid chromatography (Pharmacia, Woerden, The Netherlands). This was performed at The Department of Surgery, Maastricht University, Maastricht, The Netherlands by Dr H. van Eijk and Dr N.E.P Deutz. (191)

STUDY A

AN INVESTIGATION INTO THE ROLE OF AMMONIA AND INFLAMMATION IN MINIMAL HEPATIC ENCEPHALOPATHY

This study has been published:

Shawcross D.L, Wright G, Olde Damink S.W.M. and Jalan R. The role of ammonia and inflammation in minimal hepatic encephalopathy. Metabolic Brian Disease 2007; 22(1):125-38.

3.A.1 ABSTRACT

Background: Minimal hepatic encephalopathy is common in cirrhosis, but its pathophysiological basis remains undefined. This study was done to evaluate whether the presence of minimal hepatic encephalopathy was associated with severity of liver disease, ammonia levels or the presence of inflammation and assessed factors determining neuropsychological deterioration accompanying induction of hyperammonemia.

Methods: Eighty four patients with cirrhosis who had been administered a 'simulated bleed' were studied. A neuropsychological test battery was performed and blood taken for ammonia, WCC, CRP, NO_x and IL-6, before and after, induction of hyperammonemia by administration of a solution mimicking the amino acid composition of haemoglobin or placebo.

Results: The presence and severity of minimal hepatic encephalopathy were independent of severity of liver disease and ammonia concentration but markers of inflammation were significantly higher in those with minimal hepatic encephalopathy compared with those without. Induction of hyperammonemia produced deterioration in one or more neuropsychological tests by $\geq$1 SD in 73.3%. This was independent of the magnitude of change in plasma ammonia and severity of liver disease but was significantly greater in those with more marked inflammation.

Conclusion: These data suggest that inflammation is an important determinant of the presence and severity of minimal hepatic encephalopathy. The change in neuropsychological function following induced hyperammonemia is greater in those with more severe inflammation.

3.A.2 BACKGROUND

The occurrence of hepatic encephalopathy in cirrhosis seriously impairs daily functioning in both physical and psychological domains. This neuropsychiatric syndrome incorporates a spectrum of manifestations which include psychomotor dysfunction, impaired memory, increased reaction time, sensory abnormalities and poor concentration. When hepatic encephalopathy is severe in cirrhosis, patients may develop varying degrees of confusion and coma. (27) The term minimal hepatic encephalopathy is used to define individuals with cirrhosis who have no overt clinical features of hepatic encephalopathy, but who, nevertheless, have significant abnormalities on psychometric testing and in neuropsychological performance which may impact on their quality of life. Depending on the definition used the prevalence of minimal hepatic encephalopathy has been shown to vary between 30 - 84% in cirrhotic patients. (178)

Ammonia is thought to be central in the pathogenesis of hepatic encephalopathy. In patients with impaired capacity for detoxification of ammonia into urea, peripheral glutamine synthetase serves as a major alternative ammonia detoxification pathway. Glutamine synthesis also occurs within astrocytes and causes brain swelling. (45;119)

In a recently published study, we showed that simulating an upper gastrointestinal bleed by the oral administration of a specifically prepared amino acid solution identical to the amino acid profile of haemoglobin to patients with cirrhosis results in an increase in brain glutamine and brain water. (51) This pathophysiological change was associated with functional consequences manifested by worse neuropsychological performances compared with a placebo-treated group. This

provides a reproducible model to study the pathopysiological and functional effects of induced hyperammonemia.

Recent observations in patients with liver disease suggested that inflammatory response may be important in the pathophysiology of hepatic encephalopathy. In a preliminary study we have shown that induced hyperammonemia resulted in significantly greater deterioration in the psychotmetric tests in cirrhotic patients with ongoing infection compared with its effects after the infection had resolved. (192) These observations served as the basis of our hypothesis that inflammation may enhance the deleterious neuropsychiatric effects of ammonia.

The aims of this retrospective study in patients with cirrhosis who had been given an amino acid load in other study protocols, (51;52;79) were to determine the role of inflammation (in the absence of proven infection) in modulating the neuropsychiatric effects in cirrhotic patients with no evidence of overt hepatic encephalopathy. Furthermore, the study was designed in order to determine if induction of hyperammonemia causes neuropsychological deterioration in those who were are more inflamed at baseline.

3.A.3 STUDY PROTOCOL

3.A.3.1 ETHICAL CONSIDERATIONS

Studies were undertaken with the approval of the Hospital Research Ethics Committee and the written informed consent from each patient in accordance with the Declaration of Helsinki (1989) of the World Medical Association as detailed previously (3.1.1.3).

3.A.3.2 INCLUSION CRITERIA

Patients who had been previously enrolled in studies using an amino acid load, some of whom had been published (51;52;79) were retrospectively studied. All patients were recruited from the Edinburgh Royal Infirmary outpatient clinic and were included into the study if they had clinical, biochemical and histological evidence of cirrhosis. At the time of the study all patients were stable and did not have any evidence of overt infection on clinical assessment or overt hepatic encephalopathy as measured by the West Haven criteria (193). There had been no change in their clinical condition for the preceding 6 weeks and were not on any specific therapy for hepatic encephalopathy or on antibiotics. Patients who had previous or ongoing hyponatremia or renal impairment were not included.

3.A.3.3 EXCLUSION CRITERIA

Patients were excluded if they had clinical evidence of overt hepatic encephalopathy, diabetes, cardiovascular disease, renal dysfunction (serum creatinine >150 μmol/l), serum sodium <130 mmol/L, serum potassium <3.2 mmol/L or >5 mmol/L, concomitant neurological disease, recent gastrointestinal bleeding (within

the previous 4 weeks), antibiotic use, malignancy or pregnancy. Patients had to be abstinent from alcohol and benzodiazepines for at least 1 month prior to the study (ensured by random blood and urine testing x 2 prior to inclusion into the study).

3.A.3.4 STUDY PROTOCOL

All patients were studied after an overnight fast. The study involved the assessment of the neuropsychological function by performing a psychometric test battery and blood sampling prior to and after administration of an amino acid solution mimicking the composition of the haemoglobin molecule or an identical placebo solution.

3.A.3.5 ORAL AMINO ACID SOLUTION

Simulation of the upper gastrointestinal bleed was by administration of an oral bolus of 75 grams of a specifically prepared solution (Nutricia Cuijk, The Netherlands, Product Number: 24143) that mimics the amino acid composition of the haemoglobin molecule (79;180) as detailed in 3.1.1.2.

3.A.3.6 MEASUREMENT OF NEUROPSYCHOLOGICAL FUNCTION

A construct-driven neuropsychological test battery was designed and used as described in section 3.1.2.

3.A.3.7 BLOOD SAMPLING AND ANALYSIS

A peripheral venous blood sample was taken for analysis of WBC, neutrophil count, CRP, ammonia, NO_x, and IL-6 at the beginning of each study immediately prior to the administration of the amino acid solution. Blood sampling was repeated at 4 hours after administration of the amino acid solution for analysis of ammonia and analysed as described in section 3.1.3.

3.A.4 STATISTICS AND DEFINITIONS

All the clinical and biochemical data were expressed as mean and standard error. The baseline neuropsychological function test scores were compared to a normal population and were corrected for age (184-187;194). Patients were considered to have mild minimal hepatic encephalopathy if their score was outside 2 standard deviations (2SD) of the population mean and severe if their score was outside 3 standard deviations (3SD). Following the amino acid solution or placebo solution, a deterioration or improvement in the score was noted. If the score deteriorated by more than 1 standard deviation (1SD) of the cirrhotic population mean in any of the neuropsychological function tests, the patient was considered to have had deterioration in their neuropsychological function. A deterioration of 2 standard deviations or more of the cirrhotic population mean was not used because of previous studies showing a relatively large value of the standard deviation from the mean. (52)

The clinical and biochemical data of the neuropsychological deteriorators and non-deteriorators were compared for normal distribution and equal variance before using parametric or non-parmetric statistical analyses using Student's t-test or the Mann Whitney test (Prism software version 3.0, GraphPad, San Diego USA). A p-value of <0.05 was considered significant. Unfortunately, the number of patients enrolled was insufficient to perform multivariate analysis to compare the severity of the underlying liver disease, ammonia, amino acid profile, neuropsychological function tests and multiple inflammatory markers.

3.A.5 RESULTS

3.A.5.1 PATIENTS

All 84 patients were clinically stable and had no evidence of overt hepatic encephalopathy or infection on clinical, biochemical or microbiological assessment (negative urine, sputum and blood cultures). All patients had biopsy proven cirrhosis of varying aetiologies. There were no significant differences in the clinical and laboratory parameters between the patients who had cirrhosis as a result of alcohol and other aetiologies. Table 4.1 shows the patient characteristics. Thirteen of the 84 had moderate ascites and 4 had tense ascites, but in all cases this had been longstanding and recent diagnostic ascitic taps had excluded spontaneous bacterial peritonitis on the basis of white cell count and culture.

Table 3.2

Patient Characteristics

Mean age (Range)		**n=84 (60 male, 24 female)**
		51.7 (26-79)
Aetiology	ALD	50
	PSC	5
	PBC	7
	HCV	9
	NASH	2
	Cryptogenic	8
	Autoimmune	3
Child Pugh	A	5
	B	51
	C	26
Ascites	None	23
	Mild	43
	Moderate	13
	Tense	4

3.A.5.2 BASELINE DATA

3.A.5.2.1 NEUROPSYCHOLOGICAL FUNCTION

3.A.5.2.1.1 TRAILS B TEST (TRB)

Thirty one of the 80 patients who completed the Trails B test had an abnormal score. A Trails B result was not obtained in 4 (2 receiving placebo and 2 receiving the amino acid solution). Seventeen had a score that was 2SD above the normal age-matched population mean but less than 3SD (mildly abnormal) and 14 had a score that was 3SD or greater above the normal age-matched population (severely abnormal). Patients with the abnormal tests had more markedly elevated inflammatory markers (WCC etc.), but the severity of liver disease and ammonia concentrations were similar in the 2 groups (Table 3.3).

3.A.5.2.1.2 THE DIGIT SYMBOL SUBSTITUTION TEST (DSST)

Seventy eight of the 83 patients who completed the test had a score which was within normal limits when compared to a normal age-matched population. A result was not obtained in 1 patient receiving the amino acid solution. The 5 abnormal scores were below 2SD but less than 3SD of the normal age-matched population mean. Two of these patients also had an abnormal TRB test result

3.A.5.2.1.3 REACTION TIME

Eighty three of the 84 patients who completed the reaction time test had a score which was within normal limits when compared to a normal age-matched population. The one abnormal score was above 2SD but less than 3SD of the normal age-matched population mean.

3.A.5.2.1.4 IMMEDIATE STORY RECALL SUBTEST OF THE RANDT MEMORY TEST

Eighty three of the 84 patients who completed the test had a score which was within normal limits when compared to a normal age-matched population. The one abnormal score was below 2SD but <3SD of the normal age-matched population mean.

Table 3.3

The Child Pugh score, plasma ammonia concentration and inflammatory mediators at baseline in the patients with cirrhosis who had a normal test result for the Trails B Test (TRB), a result which was >2SD outside the normal age-matched population mean and a result which was >3SD outside the normal age-matched population mean.

	Normal TRB time (secs)	Mildly abnormal TRB time (secs)	Severely abnormal TRB time (secs)
Child Pugh Score Δ	8.9 +/- 0.27	8.8 +/- 0.39	9.0 +/- 0.5
Ammonia (µmol/L)	75.95 +/- 3.16	70.71 +/- 4.18	75.57 +/-4.64
WCC (x 10^9/L)	7.29 +/- 0.42	6.63 +/-0.72	11.36 +/-1.37 ***
Neutrophils (%)	70.05 +/- 1.37	70.00 +/- 3.54	77.57 +/- 2.42 *
CRP (mmol/L)	16.94 +/- 1.62	12.12 +/-1.88	35.69 +/-7.45 **
NO_x (µmol/L)	19.15 +/-2.04	14.8 +/- 1.5	34.46 +/-7.16 *
IL-6 (pg/ml)	20.1 +/- 1.67	18.5 +/- 1.49	36.83 +/- 7.57 *

Δ The Child Pugh Score is derived from a score of 1-3 given for severity of ascites, hepatic encephalopathy, INR, albumin and bilirubin. The higher the score is, the more severe the liver disease.

Normal TRB score = a time (secs) which falls between the mean +/- 2 standard deviations of a normal age-matched population. Mildly abnormal TRB = a time which is >2 standard deviations of a normal age-matched population and severely abnormal TRB = a time which is >3 standard deviations of a normal age-matched population.

All values are in table are expressed as mean +/- standard error. * $p<0.05$, ** $p<0.001$, ***$p<0.0001$

3.A.5.3 RE-TESTING FOLLOWING ADMINISTRATION OF AMINO ACID SOLUTION

3.A.5.3.1 NEUROPSYCHOLOGICAL FUNCTION

None of the patients entered into the study showed any evidence of 'overt' hepatic encephalopathy either prior to or following the administration of the amino acid solution. Furthermore, none of the patients who received the placebo solution had deterioration in their neuropsychological test scores.

3.A.5.3.1.1 TRAILS B TEST

Trails B test scores were significantly better with patients in the placebo group. Overall, induced hyperammonemia resulted in a deterioration in the Trails B test in 2/58 (3.5%) patients tested. The deteriorators had significantly greater inflammatory markers compared with the non-deteriorators; WCC p=0.005; neutrophils p=0.03; IL-6 p=0.001, [Table 3.4 and Figure 3.2]. Neither baseline ammonia, nor severity of liver disease predicted neuropsychiatric response to induced hyperammonemia. However, the baseline neuropsychiatric test was predictive of patients that were more likely to deteriorate following induced hyperammonemia. In those that had a normal Trails B test, only 10/35 (28.6%) deteriorated; whereas in those induced with hyperammonemia 17/23 (74%) showed evidence of further deterioration in neuropsychiatric tests. Importantly, the patients with abnormal psychometric tests at baseline had significantly greater inflammatory markers at baseline; CRP p=0.04; WCC p=0.04; IL-6 p=0.04 and NO_x p=0.04.

Table 3.4

Child Pugh score, ammonia concentration (at 4 hours) and inflammatory mediators in the groups which had a deterioration in their neuropsychological function compared to those who did not 4 hours following the administration of the amino acid solution.

Neuropsychological Function Test		Deteriorators		Non-deteriorators	
		Mean	Standard Error (+/-)	Mean	Standard Error (+/-
Trails B Test (secs)	Child Pugh Score	9.04	0.33	8.74	0.26
	Ammonia (μmol/L)	92.27	4.3	88.44	4.38
	WCC (x 10^9 /L) **	22.98	5.23	7.3	0.42
	Neutrophils (%) *	67.87	2.2	54.92	5.08
	CRP (mmol/L)	27.08	4.72	17.68	2.58
	IL-6 (pg/ml) **	33.36	4.62	17.9	1.13
	NOx (μmol/L)	28.54	4.94	17.32	1.38
DSST Test Score	Child Pugh Score	9.46	0.41	8.76	0.22
	Ammonia (μmol/L)	89.91	7.14	89.42	3.42
	WCC (x 10^9 /L) **	10.89	1.34	7.44	0.42
	Neutrophils (%)	75.7	2.3	71.2	1.29
	CRP (mmol/L) ***	44.1	9.81	16.81	1.76
	IL-6 (pg/ml) ***	43.5	8.28	19.61	1.42
	NOx (μmol/L)	38.2	9.29	17.93	1.41
Choice Reaction Time (secs)	Child Pugh Score	8.67	0.55	8.89	0.22
	Ammonia (μmol/L)	84.44	5.2	90.35	3.47
	WCC (x 10^9 /L) **	12.33	1.64	7.37	0.39
	Neutrophils (%)	75.38	5.22	71.11	1.14
	CRP (mmol/L) *	49.56	12.85	17.17	1.58
	IL-6 (pg/ml) ***	49.71	8.74	19.32	1.29
	NOx (μmol/L) **	47.13	10.32	17.57	1.32
Immediate Story recall subtest of the Randt memory test	Child Pugh Score	9.09	0.29	8.87	0.29
	Ammonia (μmol/L)	79.1	3.8	74.32	2.82
	WCC (x 10^9 /L) *	9.11	0.79	6.62	0.31
	Neutrophils (%) **	75.47	1.67	68.43	1.21
	CRP (mmol/L) **	28.09	4.34	13.09	1.0
	IL-6 (pg/ml) ***	30.34	3.43	16.26	0.99
	NOx (μmol/L) **	27.91	3.63	14.2	0.77

*$p<0.05$, **$p<0.001$, ***$p<0.0001$

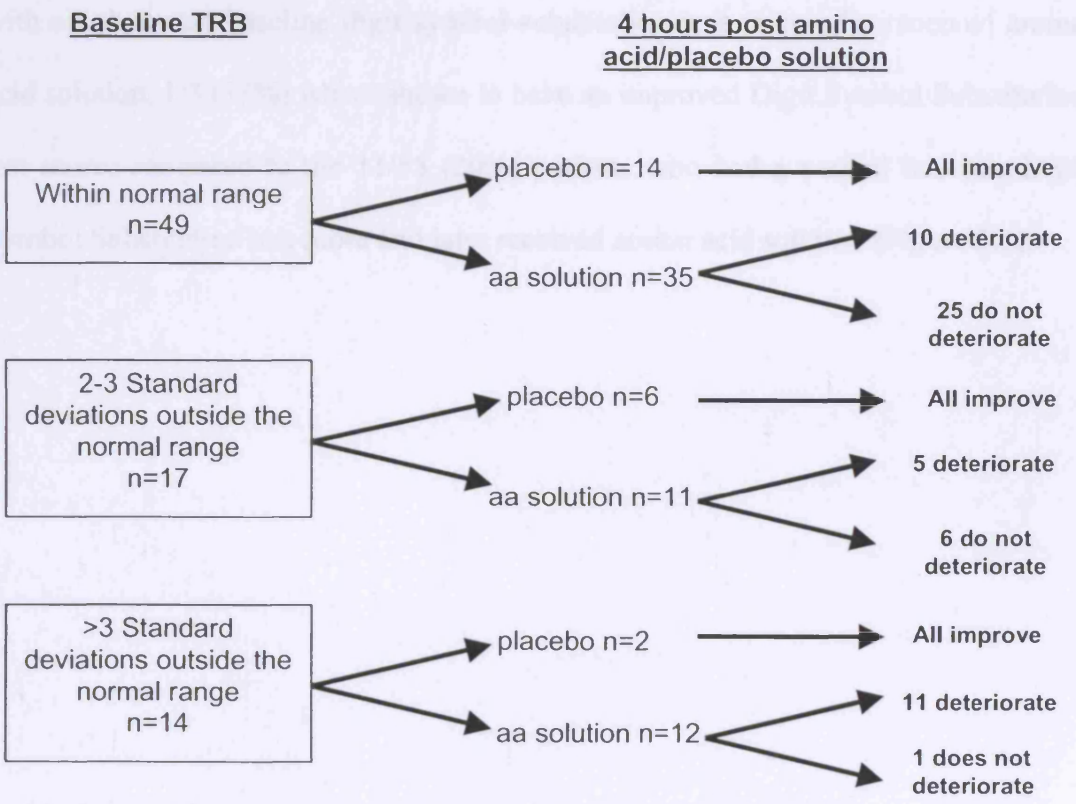

Figure 3.2

A diagram to show the outcome of the Trails B test (TRB) [secs] at baseline and 4 hours following administration of the amino acid (aa) or placebo solution.

3.A.5.3.1.2 THE DIGIT SYMBOL SUBSTITUTION TEST (DSST)

Digit Symbol Substitution test scores were significantly better with patients in the placebo group. The deteriorators (11/71) had significantly greater inflammatory markers compared with the non-deteriorators (WCC p=0.008; CRP p=0.0005; IL-6 p=0.0006). Neither baseline ammonia, nor severity of liver disease predicted neuropsychiatric response to induced hyperammonemia [Table 3.4]. In those patients with an abnormal baseline digit symbol substitution test score who received amino acid solution, 1/3 (33%) where shown to have an improved Digit Symbol Substitution test score; compared to the 11/55 (20%) patients who had a normal baseline Digit Symbol Substitution test score and later received amino acid solution (Figure 3.3).

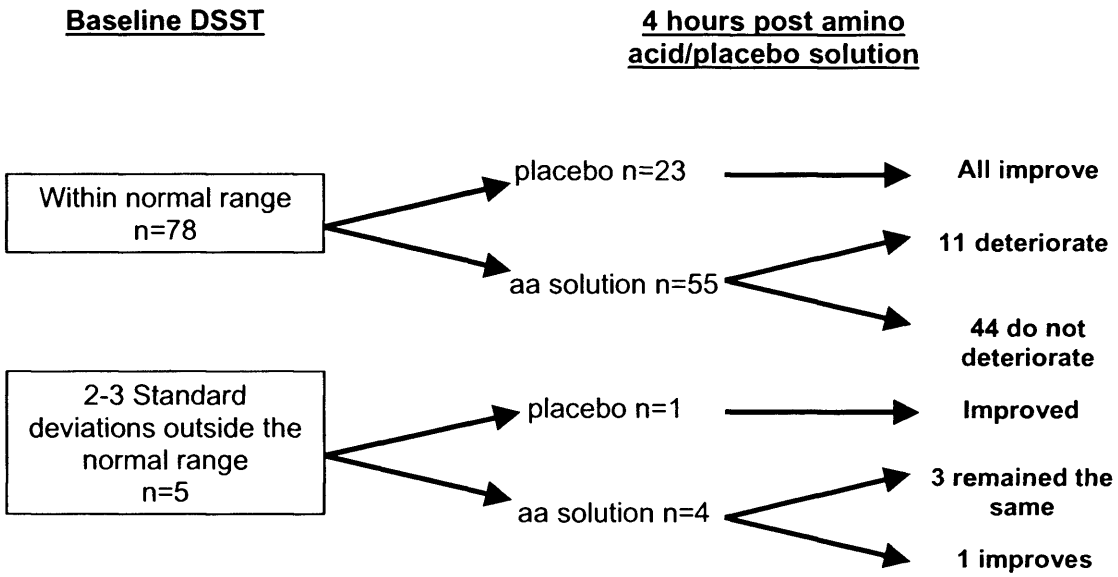

Figure 3.3

A diagram to show the outcome of the Digit symbol substitution test (DSST) at baseline and 4 hours following administration of the amino acid (aa) or placebo solution.

3.A.5.3.1.3 REACTION TIME

Reaction times were significantly better with patients in the placebo group. The deteriorators (9/84) had significantly greater inflammatory markers compared with the non-deteriorators (WCC p=0.004; CRP p=0.03; IL-6 p=0.0005 and NO_x p=0.006) [Table 3.4]. Neither baseline ammonia, nor severity of liver disease predicted neuropsychiatric response to induced hyperammonemia [Table 3.4]. In the 1 patient with an abnormal baseline reaction time who received amino acid solution, there was no deterioration in reaction time; compared to the 9/59 (15%) patients who had a normal baseline reaction time and later received amino acid solution [Figure 3.4]

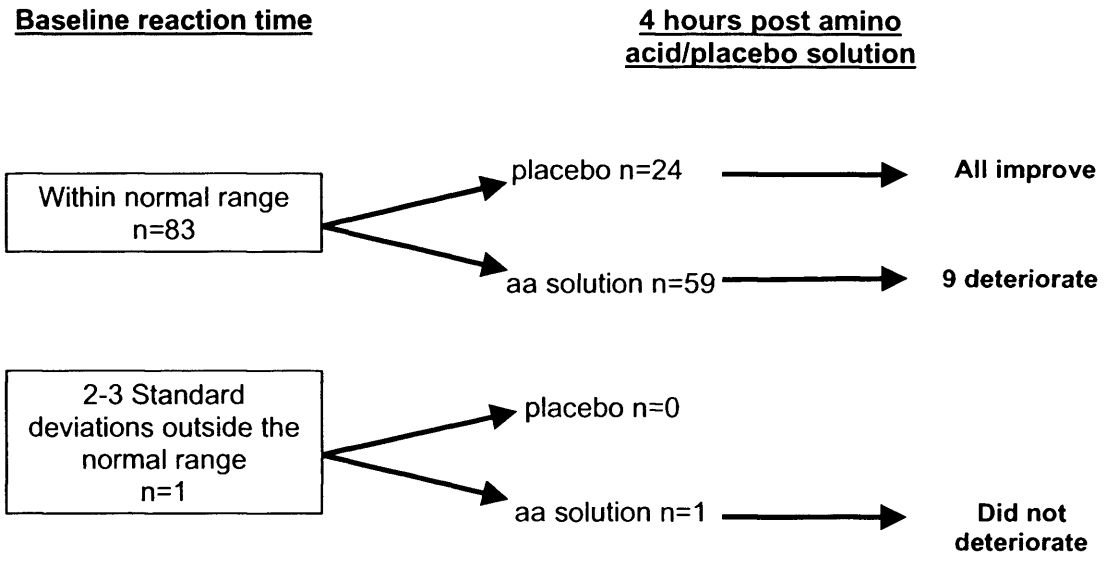

Figure 3.4

A diagram to show the outcome of the Choice reaction time test at baseline and 4 hours following administration of the amino acid (aa) or placebo solution.

3.A.5.3.1.4 IMMEDIATE STORY RECALL SUBTEST OF THE RANDT MEMORY TEST

Immediate story recall scores were significantly better with patients in the placebo group. The deteriorators (33/84) had significantly greater inflammatory markers compared with the non-deteriorators (CRP p=0.005; WCC p=0.02; neutrophil count p=0.0003; IL-6 p=0.0002; NO_x p=0.001). Neither baseline ammonia, nor severity of liver disease predicted neuropsychiatric response to induced hyperammonemia [Table 3.4]. In the 1 patient with an abnormal baseline immediate story recall score there was no change in the test score, but the patient only received placebo. In the patients who had a normal baseline immediate story recall score and later received amino acid solution, 33/60 (55%) showed a deterioration in their immediate story recall score [Figure 3.5].

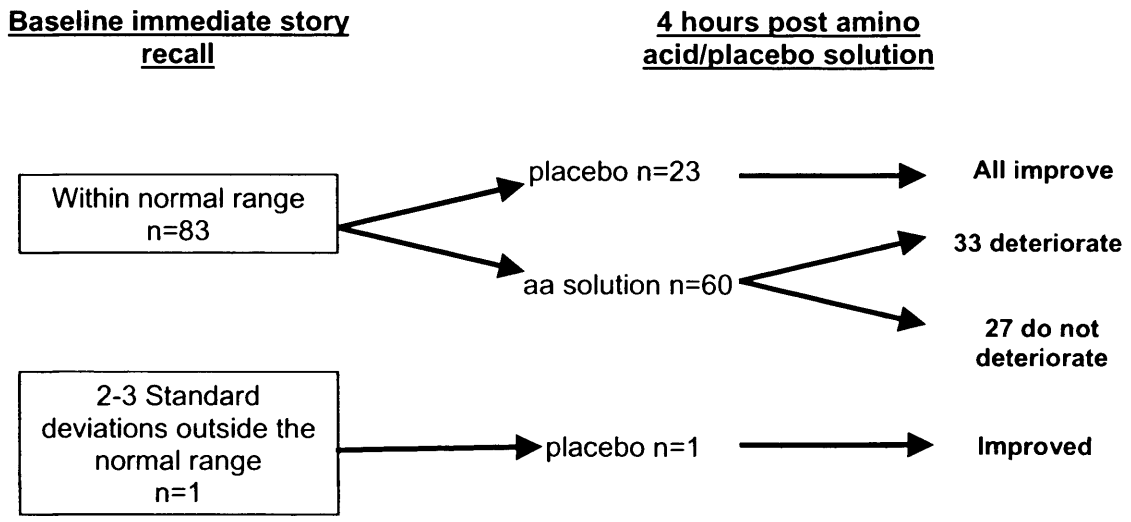

Figure 3.5

A diagram to show the outcome of the immediate story recall subtest of the Randt memory test at baseline and 4 hours following administration of the amino acid (aa) or placebo solution.

3.A.6 DISCUSSION

This study supports the conjecture for the importance of ammonia in the pathogenesis of hepatic encephalopathy, but suggests that the inflammatory response may be important in the determining the neuropsychiatric effects of ammonia rather than the severity of underlying liver disease or hyperammonemia. Also, it has been shown for the first time that those patients that have abnormal neuropsychiatric tests have more likelihood of further deterioration with induced hyperammonemia. As the patients with abnormal neuropsychiatric tests at baseline also had more marked inflammation, it is not possible to clarify whether the baseline mental or inflammatory states determines adverse neuropsychological effects of induced hyperammonemia.

An important observation of this study is that it demonstrates that some of the neuropsychological tests in the battery used are more useful in differentiating mental state at baseline, while other tests are more discriminating in patients with cirrhosis and ammonia-induced neuropsychological deterioration. The Trails B test was the only test in the battery which differentiated neuropsychological impairment between patients with cirrhosis in the basal state. The Trails B test reflects attention shift, but its execution is also influenced by visual search, psychometric speed, fine motor execution, and by a knowledge of, and familiarity with the alphabet sequence. (29) Why this test should be more sensitive than the Digit Symbol Substitution test is unclear, as this assesses visuomotor coordination and vigilance and is part of the recently recommended Psychometric Hepatic Encephalopathy Score (PHES) along with Number Connection Tests A and B, line tracing and serial dotting. However even the PHES score only correctly classified 63% of patients with cirrhosis initially which shows that no one neuropsychological test is entirely specific for diagnosing

minimal hepatic encephalopathy. (195) In a previous study it was noted that the immediate story recall subtest of the Randt memory test was not sensitive at detecting ammonia-induced deterioration of the mental state. (52) The explanation why this test should be normal in the basal state but deteriorate following induced-hyperammonemia is unclear but supports the idea that hyperammonemia may have a selective effect on the neuronal pathways controlling processes associated with memory and learning. (196)

The patients in this study did not show overt signs of infection and were clinically stable at the time of enrolment in this study. Despite this, several patients had raised inflammatory markers. The mechanism causing elevated inflammatory markers in the absence of overt infection is unclear, but may reflect chronic endotoxemia that is a well known feature of these patients. The relationship of raised inflammatory mediators in those who had abnormal neuropsychological function at baseline, and deteriorated following induced-hyperammonemia, suggests that inflammation may be synergistic and modulate the effects of hyperammonemia.

Further support for interaction between ammonia and inflammation is provided in a recent paper by Liu et al (121), who showed that alteration of gut flora with either administration of fibre and probiotics was associated with improvement in the severity of minimal hepatic encephalopathy compared with a control group. They showed that this improvement in minimal hepatic encephalopathy was associated with a reduction in endotoxaemia and ammonia concentration.

The specific mechanism by which inflammation and oxidative stress modulates neuropsychological function remains to be elucidated but recent work has highlighted several possible mechanisms. Firstly in the periphery, inflammatory mediators acting on vagal afferents will activate the nucleus tractus solitarius, the

primary projection of the vagus nerve (197) and subdiaphragmatic vagotomy will abrogate the induction of IL-1β messenger RNA in rat brain by peripheral IL-1β. (198) Secondly, brain endothelial cells have receptors for IL-1β and TNF-α. These can transduct signals which can culminate in the intracerebral synthesis of nitric oxide and prostanoids. (80) Perivascular cells of macrophage origin may be a target for these cytokine effects. (86) Thirdly, cytokines may enter the brain through the circumventricular organs (sites lacking a blood brain barrier) and diffuse directly into brain parenchyma. (80) This may alter glutaminergic neurotransmission (83) and increase the number of peripheral–type benzodiazepine binding sites which may alter cellular osmotic homeostasis. (84) Cytokines may also modulate ammonia diffusion and it has been shown that TNF-α and IL-6 increase fluid phase permeability and ammonia diffusion in CNS-derived endothelial cells. (85) High circulating levels of TNF-α following an intravenous bolus of endotoxin resulted in reduced cerebral blood flow and this might suggest why inflammation causes neuropsychological deterioration and changes in cerebral blood flow. (199) Fourthly, production of reactive oxygen species and increased protein tyrosine nitration by benzodiazepines may alter astrocyte function and contribute or precipitate episodes of hepatic encephalopathy. (200)

In summary, these data suggest that the presence and severity of minimal hepatic encephalopathy is independent of the degree of hyperammonemia and severity of liver disease but that there is an important synergistic role of inflammation in modulating the neuropsychological effects of ammonia.

STUDY B

AN INVESTIGATION INTO THE EXACERBATION OF THE NEUROPSYCHOLOGICAL EFFECTS INDUCED BY HYPERAMMONEMIA IN CIRRHOSIS DUE TO AN INCREASED SYSTEMIC INFLAMMATORY RESPONSE

This study has been published:

Systemic inflammatory response exacerbates the neuropsychological effects of induced hyperammonemia in cirrhosis. Shawcross DL, Davies NA, Williams R. and Jalan R. Journal of Hepatology 2004; 40:247-254. (192)

3.B.1 ABSTRACT

Background: Studies in acute liver failure show correlation between evidence of a systemic inflammatory response syndrome (SIRS) and progression of hepatic encephalopathy. In this study, the hypothesis that SIRS mediators, such as nitric oxide and proinflammatory cytokines, may exacerbate the neuropsychological effects of hyperammonemia in cirrhosis was tested.

Methods: Ten patients with cirrhosis were studied, 24-36 hours after admission with clinical evidence of infection, and following its resolution. Hyperammonemia was induced by oral administration of an amino acid solution mimicking haemoglobin composition. Inflammatory mediators, nitrate/nitrite, ammonia, amino acid profiles, and a battery of neuropsychological tests were measured.

Results: The hyperammonemia generated in response to administration of an amino acid solution was similar prior to and after resolution of the inflammation ($p=0.82$). With treatment of the infection there were significant reduction in WBC, CRP, nitrate/nitrite, IL-6, IL-1ß and TNF-α. Induced hyperammonemia resulted in significant worsening of the neuropsychological scores when patients showed evidence of SIRS but not after its resolution.

Conclusion: The significant deterioration of neuropsychological test scores following induced hyperammonemia during the inflammatory state, but not after its resolution, suggests that the inflammation and its mediators may be important in modulating the cerebral effect of ammonia in liver disease.

3.B.2 BACKGROUND

Hepatic encephalopathy is a neuropsychiatric syndrome, which incorporates a spectrum of manifestations, which include psychomotor dysfunction, impaired memory, increased reaction time, sensory abnormalities and poor concentration. This occurs on the background of severe liver dysfunction and has the potential for full reversibility. (27) Ammonia is detoxified in the brain by the synthesis of glutamine in astrocytes from amidation of glutamate by glutamine synthetase and this metabolic event is thought to be central in the pathogenesis of hepatic encephalopathy. (201) The prevailing hypothesis suggests that the accumulation of glutamine in the astrocytes induced by hyperammonemia produces osmotic stress and causes the astrocytes to swell. (49) However, a direct correlation between plasma ammonia concentrations and severity of hepatic encephalopathy is not found and additional factors may be important. In patients with acute liver failure, the presence of a systemic inflammatory response syndrome (SIRS) was recently shown to confer a poorer neurological outcome. (109) In cirrhosis, infection is a common precipitant of hepatic encephalopathy suggesting that inflammation may be important in its pathogenesis. Astrocytes belong to the macrophage lineage and therefore have an associated range of cytokine responses. Increased signalling factors such as nitric oxide and proinflammatory cytokines may be important in modulating the neuropsychological response to hyperammonemia. (80)

One of the most common precipitating events of hepatic encephalopathy in cirrhosis is upper gastrointestinal bleeding which produces hyperammonemia. (165) Simulating the metabolic effects of an upper gastrointestinal bleed by the oral administration of erythrocytes has been shown to induce hyperammonemia and

behavioural disturbance in portacaval shunted rats. (202) In a recently published placebo-controlled study, it was shown that simulating an upper gastrointestinal bleed by the oral administration of a specifically prepared amino acid solution identical to the amino acid profile of haemoglobin to patients with well-compensated cirrhosis, resulted in hyperammonemia but was not associated with significant deterioration in neuropsychological tests. However, the neuropsychological function in the group administered the placebo improved significantly suggesting that induced hyperammonemia produced a learning difficulty in the population studied. (79)

This study was designed to test the hypothesis that inflammatory mediators, such as nitric oxide and proinflammatory cytokines exacerbate the neuropsychological effects of hyperammonemia in patients with cirrhosis. We therefore evaluated the changes in neuropsychological function following induction of hyperammonemia by oral administration of a specifically prepared solution mimicking the amino acid composition of haemoglobin in patients with cirrhosis with evidence of systemic inflammatory response, (203) and after its resolution.

3.B.3 STUDY PROTOCOL

3.B.3.1 ETHICAL CONSIDERATIONS

These are described in section 3.1.1.3.

3.B.3.2 INCLUSION CRITERIA

Patients were included if they had clinical and histological evidence of cirrhosis and had a SIRS score of 2 or more. The components of SIRS include the following: temperature >38 ^{o}C or <36 ^{o}C; heart rate >90 beats per minute; tachypnoea >20 breaths per minute or $PaCO_2$ <4.3 kPa; white blood cell count (WBC) >12 x 10^9/L or the presence of >10% immature neutrophils.

3.B.3.3 EXCLUSION CRITERIA

Patients were excluded if they had clinical evidence of overt hepatic encephalopathy, (193) diabetes, cardiovascular disease, renal dysfunction (serum creatinine >150 μmol/l), serum sodium <130 mmol/L, serum potassium <3.2 mmol/L or >5 mmol/L, concomitant neurological disease, recent gastrointestinal bleeding (within the previous 4 weeks), malignancy or pregnancy. Patients had to be abstinent from alcohol and benzodiazepines for at least 1 month prior to the study.

3.B.3.4 STUDY PROTOCOL

Patients were studied within 24 – 36 hours after correction of volume and electrolyte disturbances and again after resolution of the inflammatory response (defined as normalisation of clinical indices of infection, WBC and C - reactive protein). All patients were studied following an overnight fast. Antibiotics were

commenced on the day of admission and the first study was performed on the following day. No patient received more than 3 doses of antibiotics prior to the first study being completed and all patients were given a 7-day course of a suitable antibiotic. The second study was performed on the day the patient was thought to be well enough for discharge [mean 9; range 7 – 12 days]. Each study involved assessment of the neuropsychological function and blood sampling prior to and after administration of the amino acid solution [Figure 3.6].

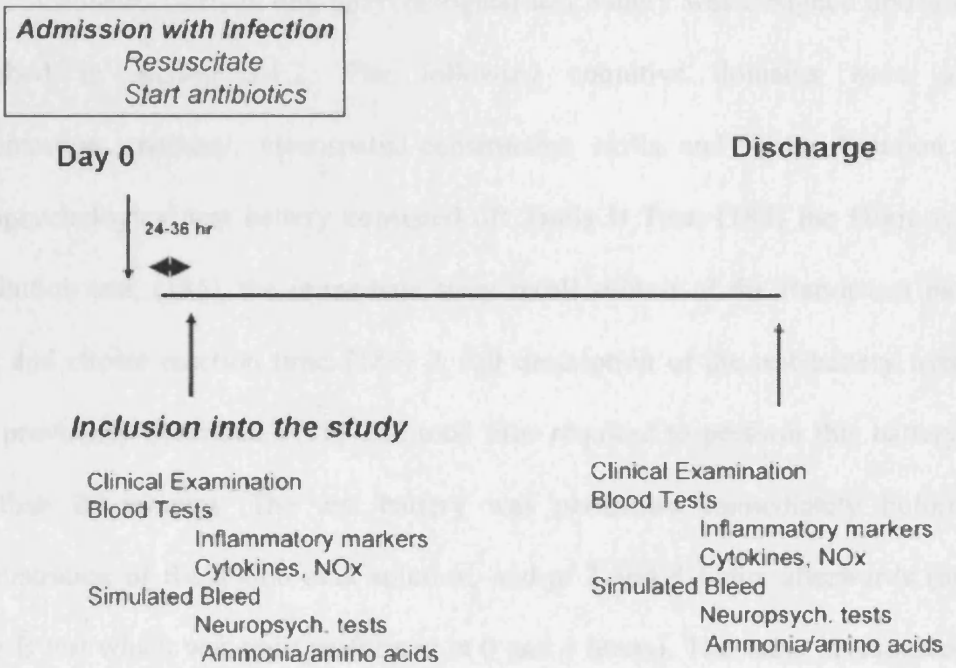

Figure 3.6

Summary of Study Design.

3.B.3.5 ORAL AMINO ACID SOLUTION

Simulation of the upper gastrointestinal bleed was by administration of an oral bolus of 75 grams of a specifically prepared solution as described in section 3.1.1.2.

3.B.3.6 MEASUREMENT OF NEUROPSYCHOLOGICAL FUNCTION

A construct-driven neuropsychological test battery was designed and used as described in section 3.1.2. The following cognitive domains were tested: concentration, memory, visuospatial-construction skills and motor function. The neuropsychological test battery consisted of: Trails B Test; (184) the Digit symbol substitution test; (185) the immediate story recall subtest of the Randt test battery; (187) and choice reaction time. (186) A full description of the test battery used has been previously described. (51) The total time required to perform this battery was less than 20 minutes. The test battery was performed immediately before the administration of the amino acid solution, and at 2 and 4 hours afterwards (except Trails B test which was only performed at 0 and 4 hours). The same investigator (Dr Rajiv Jalan) performed the neuropsychological tests and the patients had one practice session of each test. All the tests have been well validated and parallel forms were used.

3.B.3.7 BLOOD SAMPLING AND ANALYSIS

A peripheral venous blood sample was taken for analysis of WBC, neutrophil count, CRP, ammonia, amino acids, NO_x, IL-6, IL-1ß and TNF-α at the beginning of each study immediately prior to the administration of the amino acid solution. This was repeated after 2 and 4 hours for analysis of ammonia and amino acids as described in section 3.1.3.

3.B.4 STATISTICS

All the data are expressed as median and range. Results were compared using the Wilcoxon Sign Rank test. (Prism software version 3.0, GraphPad, San Diego USA). A p-value of <0.05 was considered significant.

3.B.5 RESULTS

3.B.5.1 PATIENTS

Twelve patients with cirrhosis were recruited from Edinburgh Royal Infirmary; of these ten completed the study and are the subject of this report. Two patients were excluded because of worsening in clinical condition with progression to renal dysfunction in one and development of 'overt' hepatic encephalopathy in the other. Each patient had end-stage biopsy-proven cirrhosis, was on the waiting list for an orthotopic liver transplant and had been admitted to the hospital with clinical evidence of mild SIRS. (203-205) The SIRS was due to confirmed infections. All patients were clinically stable and had no overt evidence of hepatic encephalopathy. Six of the patients were male (mean age 52; range 43 to 61). Patient details are summarised in Table 3.5.

Individual patient characteristics

Patient	Sex	Age	Aetiology	Source of sirs	Antibiotic	BMI	Pugh score	Severity (Child)	HE grade	Ascites
1	M	56	NASH	Urinary tract infection	Ciprofloxacin	26	9	B	0	Yes
2	M	45	PBC	Urinary tract infection	Ciprofloxacin	27	10	C	0	Yes
3	M	51	Autoimmune hepatitis	Spontaneous bacterial peritonitis	Ciprofloxacin	23	10	C	0	Yes
4	F	58	PBC	Chest infection	Cefuroxime	31	7	B	0	No
5	F	61	PSC	Spontaneous bacterial peritonitis	Ciprofloxacin	28	10	C	0	Yes
6	M	43	Cryptogenic	Urinary tract infection	Ciprofloxacin	23	9	B	0	Yes
7	F	49	Alcohol	Methicillin resistant *Staphylococcus aureus* bacteremia	Vancomycin	20	12	C	0	Yes
8	M	54	Alcohol	Spontaneous bacterial peritonitis	Ciprofloxacin	27	10	C	0	Yes
9	F	53	HCV	Source of infection unclear	Cefuroxime and Metronidazole	26	11	C	0	Yes
10	M	45	HCV	Chest infection	Cefuroxime	28	9	B	0	Yes

Table 3.5

A table to summarise the characteristics of the study patients.

3.B.5.2 CLINICAL AND BIOCHEMICAL INDICES

The median CRP [on admission: 55 mg/L (34 – 112) and post-antibiotic therapy: 20.5 mg/L (18 –31) {p=0.002}], WBC [admission: 14.2 x 10^9 /L (9 –23) and post: 9 x 10^9 /L (5.6 – 12.2) {p=0.002}] and neutrophil count [admission: 82 x 10^9 /L (78 – 82) and post: 69.5 x 10^9 /L (65 – 78) {p=0.002}] were reduced significantly with resolution of the inflammatory state.

No change was observed in Child Pugh Score (206) and the grade of hepatic encephalopathy remained unchanged at zero throughout the study. There was no significant change in liver function tests, albumin or prothrombin time between the 2 studies. The median bilirubin on admission was 78 μmol/l (56 – 132) and 81.5 (71 – 143) {p=0.106} in the post-inflammatory state. Table 3.6 outlines the clinical and biochemical indices of each patient.

Table 3.6

Temperature, heart rate, respiratory, mean arterial blood pressure, ammonia, bilirubin, CRP, WBC and neutrophil count before and following antibiotic therapy

Patient (pre/post treatment)		Temperature (°C)	Heart rate (beats per min)	Respiratory rate (breaths per min)	Mean arterial blood pressure (mmHg)	Ammonia (μmol/l)	Bilirubin (μmol/l)	CRP (mg/l)	WBC ($\times 10^9$/l)	Neutrophil count ($\times 10^9$/l)
1	Pre	38.1	89	22	67	64	67	67	13.2	11.75
	Post (day 9)	37	77	17	76	59	71	18	9	6.57
2	Pre	38.2	92	23	66	76	111	71	16	14.08
	Post (day 10)	36.5	81	17	71	69	121	23	12.2	9.52
3	Pre	38.2	99	19	77	78	56	54	23	20.93
	Post (day 8)	36.5	76	17	79	71	78	21	12	8.52
4	Pre	37.8	82	19[a]	77	56	132	112	15	10.09
	Post (day 12)	37	69	16	79	68	127	31	9	5.94
5	Pre	38.2	78	15	67	99	78	54	15	12.3
	Post (day 8)	37	70	17	72	88	82	9	9	5.85
6	Pre	37.5	78	21	71	112	78	78	12	10.44
	Post (day 7)	37	81	16	79	132	81	29	9	6.39
7	Pre	38.7	79	21	70	89	89	56	13.3	10.51
	Post (day 11)	37	71	17	72	98	78	13	8.9	6.05
8	Pre	38.3	81	23	78	91	78	41	9	7.11
	Post (day 7)	37.3	70	21	82	89	87	20	5.6	3.75
9	Pre	38.3	88	26	73	67	132	47	18.1	14.12
	Post (Day 9)	37.2	78	18	81	71	143	23	11.2	7.28
10	Pre	37.7	72	21	64	88	65	34	13	10.66
	Post (day 12)	37.1	73	21.17	73	76	78	11	8.7	6.18

[a] Patient 4 had $PaCO_2 < 4.3$ kPa, fulfilling 1 criterion for SIRS.

3.B.5.3 AMMONIA AND AMINO ACIDS

The median basal venous ammonia concentration was similar in the inflammatory state and following antibiotic therapy [83 (56 – 112) and 73.5 (59 – 132) μmol/L respectively). The ammonia generated in response to the simulated bleed did not differ between the 2 studies ($p=0.82$) [Figure 3.7].

The concentrations of leucine ($p<0.01$), valine and phenylalanine ($p<0.001$) increased following administration of the amino acid solution and the concentration of isoleucine decreased ($p<0.001$), but there was no difference between the inflammatory and post-inflammatory states [Table 3.7].

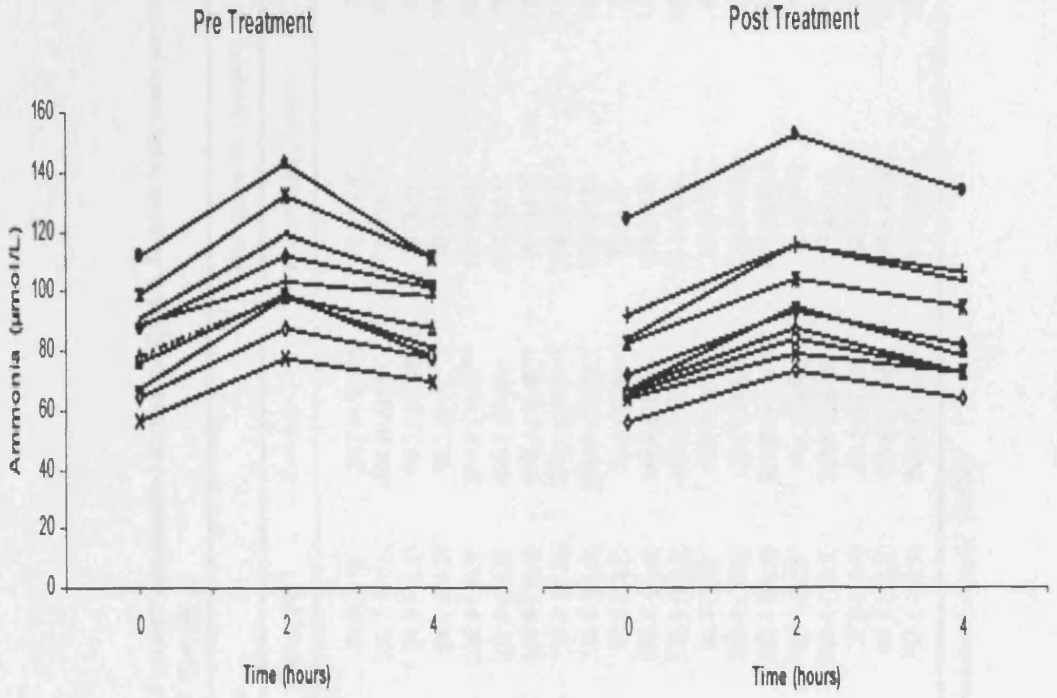

Figure 3.7

Change in venous ammonia concentration (µmol/L) in each of the ten patients administered the amino acid solution at 0, 2 and 4 hours in the study performed in the inflammatory state and then in the repeat study following antibiotic therapy (p = ns).

Table 3.7

Mean plasma amino acid profile (μmol/l) of the 10 patients administered the simulation at 0, 2 and 4h in the study performed in the inflammatory state and then in the repeat study following antibiotic therapy

Amino acid (μmol/l)	Pre-antibiotic treatment			Post-antibiotic treatment		
	Pre-simulated bleed	$T = 2$ h	$T = 4$ h	Pre-simulated bleed	$T = 2$ h	$T = 4$ h
Isoleucine	56.3 (3.9)	47.0 (4.5)	29.3 (4.8)***	72.7 (7.9)	35.5 (4.4)	35.6 (5.5)***
Leucine	108.4 (7.9)	332.7 (6.7)	354 (8.5)***	75.6 (6.1)	309.7 (7.8)	332.8 (9.1)***
Glutamate	72.1 (7.9)	91.0 (13.1)	99.2 (14.2)*	73 (3.3)	83 (5.8)	85 (9.5)*
Aspartate	63.3 (7.5)	99.1 (11.2)	95.3 (8.0)*	80 (7.9)	137 (11.1)	87 (7.5)**
Serine	157.3 (11.8)	236.6 (26.9)	234.1 (16.5)**	151 (6.6)	281 (9.9)	215 (14.5)*
Glutamine	716.0 (36.9)	625.0 (55.0)	805.5 (29.4)	524 (45.5)	714 (33.2)	739 (27.1)*
Histidine	106.6 (9.9)	224.0 (39.4)	200.1 (15.4)**	90 (14.9)	282 (34.6)	173 (15.4)***
Glycine	229.2 (19.0)	337.7 (37.4)	372.7 (14.0)**	226 (19.1)	431 (73.2)	326 (39.0)**
Threonine	196.7 (19.3)	324.0 (46.4)	334.5 (25.7)**	205 (24.6)	365 (49.7)	315 (34.2)**
Citrulline	69.9 (3.2)	67.2 (11.1)	75.2 (12.9)	51 (7.2)	71 (9.3)	79 (8.4)
Arginine	106.8 (11.4)	150.3 (22.6)	149.6 (17.6)	128 (15.6)	185 (26.1)	161 (21.8)
Alanine	379.9 (35.8)	536.9 (81.2)	412.6 (51.5)	314 (36.1)	647 (45.2)	421 (51.1)**
Taurine	50.1 (6.2)	48.4 (7.6)	50.8 (6.4)	45 (5.6)	41 (5.3)	32 (3.6)
Tyrosine	111.3 (7.1)	146.0 (20.9)	154.5 (18.1)**	118.0 (15.1)	159.3 (13.2)	160.4 (18.1)**
Valine	161.0 (11.0)	471.1 (46.1)	513.0 (47.1)***	131.3 (18.9)	490.1 (42.1)	413.4 (36)***
Methionine	43.6 (4.6)	53.3 (8.3)	41.3 (10.0)	44.1 (7.1)	50.7 (8.0)	39.2 (12.4)
Phenylalanine	141.1 (12.0)	249.1 (22.5)	259.9 (20.0)***	137.2 (4.6)	282.8 (13.9)	291 (20.1)***
Tryptophan	55.1 (6.7)	75.8 (16.9)	69.1 (15.4)*	62.3 (9.9)	86.1 (19.2)	64.6 (11.4)*
Ornithine	68.7 (6.9)	94.5 (12.2)	115.6 (21.0)	59.8 (10.6)	116.3 (11.1)	125.1 (19.1)
Lysine	210.2 (19.1)	332.1 (31.5)	319.6 (25.6)*	215.2 (14.3)	323.1 (31.0)	356.1 (24.5)*

*$P < 0.05$, **$P < 0.01$, ***$P < 0.001$. Data expressed as mean (SEM).

3.B.5.4 INFLAMMATORY MEDIATORS

Measured inflammatory markers, nitrate/nitrite, IL-6, IL-1ß and TNF-α were significantly reduced with resolution of the infection (nitrate/nitrite p=0.002, IL-6 p=0.002, IL-1ß p=0.031 and TNF-α p=0.031) [Figure 3.8]. IL-1ß and TNF-α levels were detectable in only 6 (patients 1,2,4,6,7 and 8). Patients 3 and 5 had undetectable levels of IL-1ß and TNF-α in both the inflammatory and post-inflammatory states. IL-1ß and TNF-α assays were not available in patients 9 and 10.

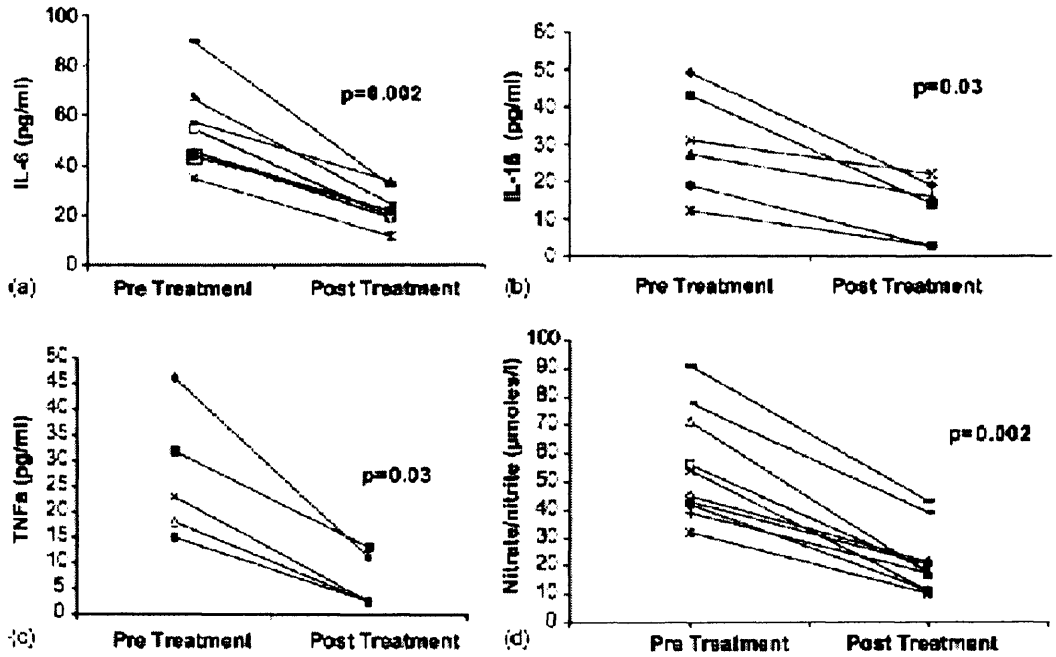

Figure 3.8

Measured concentrations of IL-6 (pg/ml), IL-1ß (pg/ml), TNF-α (pg/ml) and nitrate/nitrite (µmols/L) in each of patients in the inflammatory and the post-inflammatory state (TNF-α and IL-1ß were measured in only 8 patients and values were undetectable in 2 patients).

3.B.5.5 NEUROPSYCHOLOGICAL FUNCTION

None of the patients showed any evidence of an altered mental state or overt hepatic encephalopathy following the administration of the amino acid solution.

3.B.5.5.1 TRAILS B TEST

Data analysis could only be completed in 6 of the 10 patients. This is because the test has to be completed in 420 seconds and if the patient took any longer, the test was abandoned and a time of 420 seconds recorded. 4 of the patients took >420 seconds to complete the test at 0 and 4 hours following administration of the amino acid solution in the inflammatory state and 1 patient took >420 seconds to complete the test in both the studies. There were no significant differences in the time taken to complete the test between the inflammatory and post-inflammatory state both at baseline ($p=1$) and at 4 hours ($p=0.63$). There were however marked changes at baseline between the inflammatory and post-inflammatory state in individual patients, with 8 patients improving their performance time and 2 patients showing a marked deterioration [Figure 3.9].

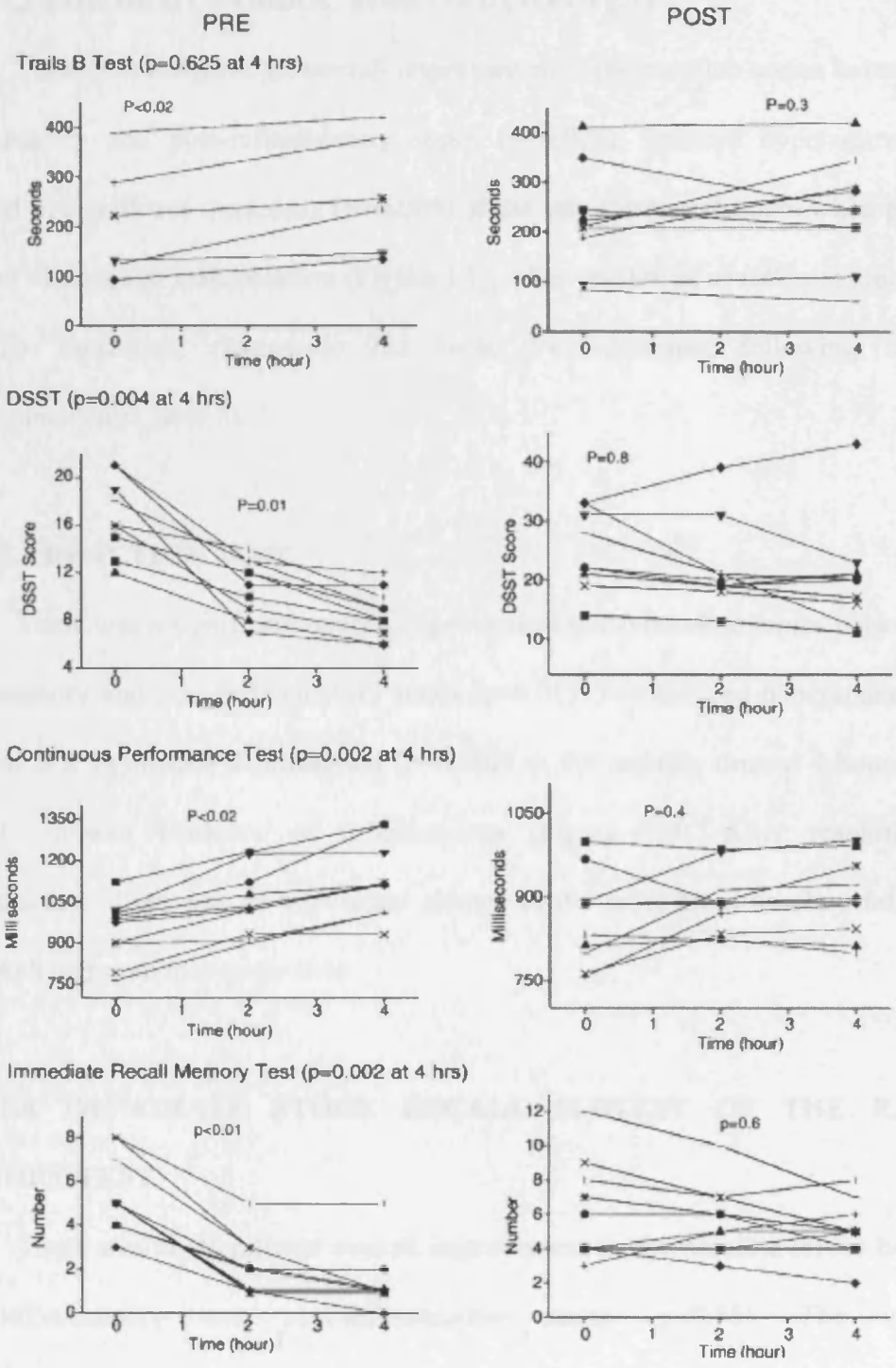

Figure 3.9 Change in neuropsychological function (Trails B test, Digit Symbol Substitution test, Choice reaction time (secs) and Immediate story recall) in patients administered the amino acid solution at 0, 2 and 4 hours performed in inflammatory state (pre) and in the post-inflammatory state. [Trails B test: data from 4 of the patients tested on admission are not shown as they took more than 420 seconds to complete the test at 0 and 4 hours following administration of the amino acid solution in the inflammatory state and 1 of them took more than 420 seconds to complete the test in both the studies]. The difference between groups was tested using the Wilcoxon Signed Rank test.

3.B.5.5.2 THE DIGIT SYMBOL SUBSTITUTION TEST

There was a significant overall improvement in the baseline scores between the inflammatory and post-inflammatory states (p=0.002). Induced hyperammonemia resulted in significant worsening (p=0.004) of the test scores at 4 hours when patients showed evidence of inflammation (Figure 3.9). After resolution of inflammation, there was no significant change in the score from baseline following induced hyperammonemia (p=0.8).

3.B.5.5.3 REACTION TIME

There was a significant overall improvement in the baseline scores between the inflammatory and post-inflammatory states (p=0.01). The induced hyperammonemia resulted in a significant deterioration (p=0.002) in the reaction time at 4 hours when patients showed evidence of inflammation (Figure 3.9). After resolution of inflammation, there was no significant change in the score from baseline following induced hyperammonemia (p=0.4).

3.B.5.5.4 IMMEDIATE STORY RECALL SUBTEST OF THE RANDT MEMORY TEST

There was no significant overall improvement in the baseline scores between the inflammatory and post-inflammatory states (p=0.58). The induced hyperammonemia resulted in a significant deterioration (p=0.002) in the number scored at 4 hours when patients showed evidence of inflammation (Figure 3.9). After resolution of inflammation, there was no significant change in the score from baseline following induced hyperammonemia (p=0.6).

3.B.6 DISCUSSION

The results of this study show that hyperammonemia induced by administration of an amino acid solution to cirrhotic patients, results in deterioration in neuropsychological function in the presence of a systemic inflammatory response. Following resolution of SIRS, there was no deterioration in neuropsychological function despite equivalent severity of induced hyperammonemia. We believe that these data provide supportive evidence suggesting that inflammation plays a crucial role in the neuropsychological effects of hyperammonemia in patients with cirrhosis.

The most important observation of this study is that the induction of a similar degree of hyperammonemia produced significant deterioration in all the neuropsychological function tests only in the inflammatory state. This suggests that inflammatory mediators may modulate the effects of hyperammonemia. SIRS is the clinical manifestation of inflammation and therefore the end product of the activation of a normally quiescent system comprising many components, including leucocytes, endothelial cells and cytokine networks. Patients performed significantly better at baseline in the post-inflammatory state in 2 of the 4 neuropsychological tests (DSST and Choice Reaction time). In the Trials B tests there were marked changes at baseline between the inflammatory and post-inflammatory state in individual patients, with 8 patients improving their performance time. The difference in the direction of the changes and the exclusion in the analysis of anyone taking longer than 420 seconds to complete the test (4 of the 8 patients who had an improvement in their performance time) is likely to explain the lack of statistically significant differences in the group when tested as a whole. The lack of significant improvement in overall baseline scores for the Immediate

Recall Memory test is also likely to be for similar reasons, where 4 patients showed a dramatic improvement, 3 remained the same and 3 marginally deteriorated.

The association between infection and impaired brain function is well recognised.(207) Septic encephalopathy can arise from the action of inflammatory mediators on the brain or a cytotoxic response by brain cells to these mediators. Septic encephalopathy is usually a sequelae of severe sepsis complicated by multiple organ failure and hypotension.(98) The patients in this study however, although fulfilling criteria for SIRS, had relatively mild infections and no evidence of 'overt' hepatic encephalopathy. We showed that resolution of inflammation was associated with improvement in the mental state despite similar liver function and ammonia concentration further highlighting the importance of inflammation in modulating derangement in neuropsychological dysfunction. It is not possible from the present study to define the neuropsychological effects of mild sepsis, which need to be further explored. Severe sepsis causes plasma and brain amino acids to become deranged with a decrease in branched chain amino acid's (e.g. isoleucine) and an increase in neutral amino acids in the brain similar to the findings in portosystemic encephalopathy.(99;100) In patients with sepsis it was shown that aromatic amino acids (e.g. phenylalanine) correlated with APACHE II scores and mortality. Scores were greater in shock patients with higher levels of ammonia and sulphur containing amino acids associated with a higher mortality rate.(101) However, amino acid derangements such as these could not be demonstrated in the present study, making it less likely that septic encephalopathy could explain our findings.

Studies in patients with acute liver failure have shown rapid progression to severe hepatic encephalopathy in those patients that have overt evidence of SIRS further suggesting a link between inflammation and hepatic encephalopathy. (109) The effect of inflammation on neuropsychological function in patients with cirrhosis has not been systematically studied. The patient population that we chose to study had evidence of SIRS fulfilling 2 or more criteria. Furthermore, all the patients had raised CRP, nitrate/nitrite and IL-6 values on admission, which significantly decreased following antibiotic therapy. It is unclear why 2 of the patients had undetectable levels (<5 pg/ml) of IL-1ß and TNF-α in the inflammatory state despite other markers of inflammation being raised. This however, is not an unusual finding in our experience of other, ongoing studies, and may reflect the fact that the cytokines are measured in peripheral blood rather than at sites of inflammation. In this context it is interesting that circulating soluble receptor levels (TNF-R1 and TNF-R2) are profoundly elevated in decompensated liver disease and the binding between TNF-α and its soluble receptors may mask TNF-α epitopes, thus making the antibody 'blind' to protein levels (Hodges S.J, personal communication).

Inflammation is associated with increased nitric oxide possibly by induction of nitric oxide synthase in response to proinflammatory cytokines. (208;209) We have shown in this study a significant reduction in the levels of nitrate/nitrite with resolution of inflammation.

The specific mechanism by which an inflammatory response modulates the neuropsychological response to hyperammonemia remains to be elucidated. There are several possibilities. First, recent work on cytokine effects on glutamate uptake by human

astrocytes has shown that proinflammatory cytokines inhibit astrocyte glutamate uptake by a mechanism involving nitric oxide resulting in altered glutaminergic neurotransmission.(83) Second, it has been shown that IL-1ß and TNF-α increase the expression of peripheral-type benzodiazepine binding sites in cultured astrocytes which may alter cellular osmotic homeostasis.(84) Third, it is possible that the difference in neuropsychological deterioration following the amino acid solution is related to changes in cerebral blood flow. Recent work by Moller et al. (199) has shown that high circulating levels of TNF-α following an intravenous bolus of endotoxin resulted in reduced cerebral blood flow. Fourth, it is possible that cytokines may modulate ammonia diffusion within the central nervous system. It has been shown that TNF-α and IL-6 increase fluid phase permeability and ammonia diffusion in central nervous system-derived endothelial cells.(85)

There has previously been doubt that the peripheral immune system could signal the brain. Cytokines (15 – 20 kD) cannot directly cross the blood brain barrier and, while it remains intact, these signalling proteins would be unable to have a direct affect. (210) Recent studies, however, suggested that peripheral cytokines can affect the brain by three routes (80): Firstly, peripheral tissues, innervated by the peripheral and autonomic nervous systems, can send direct signals to the brain via the vagus nerve. (211) Secondly, the brain vasculature can convey signals through secondary messengers, such as nitric oxide and prostaglandins by activation and induction of their synthesising enzymes (212) produced in response to cytokines binding to their receptors expressed in cerebral blood vessels. For example, in the brain, TNF-α and IL-1ß are potent stimuli for inducible nitric oxide synthase production. (213) Thirdly, cytokines can directly act at the level of the

brain parenchyma after crossing the blood brain barrier by active transport or after entering brain areas that lack a blood brain barrier.

In summary, the results of this study provide the first evidence that mediators of the systemic inflammatory response may modulate the neuropsychological effects of hyperammonemia in patients with cirrhosis.

Chapter 4

The effect of inflammation on the brain in a rat model of chronic liver disease

4.1 PREFACE

The results of both studies described in Chapter 3 provide good evidence that inflammation and infection are important in the pathogenesis of hepatic encephalopathy, thus supporting my first hypothesis (Q1; section 2.1). Moreover, as ammonia has been shown to be central in the pathogenesis of hepatic encephalopathy, the question of whether ammonia and inflammation act synergistically in the pathogenesis of hepatic encephalopathy is raised. This second hypothesis (Q2; section 2.1) will now be explored in this chapter using a rat model of chronic liver disease: the common bile duct ligated rat.

4.2 ABSTRACT

Background: There is growing evidence to support the role of inflammation as being important in increasing the susceptibility of the brain to the effects of hyperammonemia. This study tests the hypothesis that endotoxaemia induces brain oedema through inflammatory mediators, such as nitric oxide, in an animal model of cirrhosis, the bile duct ligated (BDL) rat.

Methods: Four weeks after bile duct ligation (BDL; n=12) or sham operation (n=14) adult Sprague Dawley rats were treated with endotoxin [lipopolysaccharide (LPS), 0.5 mg/kg, IP)] or saline, and sacrificed 3 hours later. Plasma ammonia and nitrite/nitrate concentrations as well as samples of the frontal cortex and cerebellum were obtained for the measurement of brain water, nitrotyrosine and histopathology.

Results: Plasma ammonia levels were significantly higher in BDL rats than sham-operated controls and did not change significantly with the administration of LPS in either group. LPS administration increased brain water in both BDL and sham-operated groups ($p=0.004$ and $p=0.03$ respectively); this was associated with coma in BDL rats, but had no such effect on sham-operated controls. Injection of LPS led to collapsed brain microvessels and astrocyte swelling predominantly in cirrhotic rats. Plasma nitrite/nitrate levels increased significantly in both LPS treated groups compared to the non-LPS treated controls ($p<0.01$), but frontal cortex nitrotyrosine levels only increased in the cirrhotic rats injected with LPS compared to non-LPS treated cirrhotic rats ($p<0.005$).

Conclusions: Injection of LPS into cirrhotic rats causes worsening cytotoxic brain oedema and coma, potentially related to the formation of reactive nitrogen species leading to nitration of brain proteins.

4.3 BACKGROUND

The susceptibility of the brain to the effects of hyperammonemia is variable and the ammonia concentration alone cannot account for the degree of brain swelling in acute liver failure. Recently, attention has been focused on inflammation as being critical in the manifestation of intracranial hypertension and hepatic encephalopathy in acute liver failure. (214) Sepsis is a well described and frequent precipitant of hepatic encephalopathy and recent studies have suggested a rapid progression in the severity of hepatic encephalopathy in those patients with acute liver failure that have a more marked inflammatory response. (109) Takada et al. (215) showed in a pig model of acute liver failure that animals administered LPS and amatoxin intraportally developed greater intracranial hypertension than animals given amatoxin alone, even though ammonia concentrations were similar in both groups.

Astrocytes have a repertoire of cytokine responses and have the ability to synthesise interleukin-1β in response to peripheral inflammation, (216) which may induce soluble mediators such as nitric oxide, superoxide and prostaglandins, which may make the brain more susceptible to the effects of hyperammonemia. Cytokines may modulate the expression of glutamate receptors on the astrocyte and recent work on human astrocytes has shown that proinflammatory cytokines inhibit astrocyte glutamate uptake by a mechanism involving nitric oxide.(83) Furthermore, cerebral blood flow is likely to be critical, and Moller et al. (199) have shown that high circulating levels of TNF-α, following an intravenous bolus of endotoxin, resulted in decreased cerebral blood flow, whilst cerebral oxidative metabolism remained unchanged. Sharshar et al. have also

recently published a study in which they demonstrated neuronal and glial apoptosis in the brain autonomic centres in patients who died of septic shock. Immunohistochemical analysis showed expression of TNF-α in glial cells and of inducible nitric oxide synthase within the vascular endothelium. The intensity of apoptosis correlated with endothelial expression of inducible nitric oxide synthase and not with TNF-α. (82)

Recently, Jalan et al. reported a correlation between the severity of increased intracranial hypertension and the circulating levels of proinflammatory cytokines in patients with acute liver failure. (73) Furthermore, an increased production of brain cytokines in a group of acute liver failure patients with uncontrolled intracranial hypertension was observed. Moreover, in patients with cirrhosis, I have demonstrated in chapter 4 that induced hyperammonemia resulted in significant worsening of neuropsychological function in those patients with evidence of an inflammatory response due to bacterial infection but not after resolution of the infection following antibiotic therapy. (192) However, the importance of the inflammatory response in the pathogenesis of hepatic encephalopathy, though indicated by such observations, lacks experimental evidence and the mechanism remains undefined. More specifically, although we know that ammonia is central to the pathogenesis of hepatic encephalopathy and that inflammation modulates the cerebral effects of ammonia in cirrhosis, direct evidence supporting the synergistic effects of ammonia and inflammation/infection are lacking.

The aim of this collaborative study was to explore the hypothesis that the inflammatory response induced by administration of bacterial cell wall lipopolysaccharide (LPS) exacerbates brain oedema in cirrhosis. This study was performed using the bile duct ligated rat (BDL) model of cirrhosis as it has been well

characterized by our group (217) and the cirrhosis is known to progress to jaundice and ascites.

Chronic bile duct ligation (BDL) in the rat is a very frequently used technique which produces an experimental model of liver cirrhosis with cholestasis. (218) It reproduces some of the human features of cirrhosis and is known to progress to jaundice and ascites. Chronic BDL induces a circulatory hyperdynamic state, with arterial hypotension and increased cardiac output, similar to that found in other experimental models of cirrhosis and in cirrhotic patients. There is also concomitant sodium retention and activation of the intrarenal hormones, plasma renin activity, aldosterone and angiotensin II. (219) This is associated with portal hypertension and an excessive production of vasodilator substances, such as nitric oxide and bile acids, and a reduced pressor response to circulating endogenous vasoconstrictors. (220) Creatinine, urea, bilirubin and liver function tests are higher in BDL rats than weight matched controls. Plasma glucose and haematocrit are always lower in BDL rats. (219)

Complete diversion of bile from the gut lumen changes the bacterial flora and causes loss of mucosal integrity which decreases endotoxin inactivation leading to portal bacteremia and endotoxemia. This occurs in the BDL cirrhotic rat, in which endotoxin concentration in the portal blood is increased approximately 7-fold at 3 weeks after BDL. Increased systemic endotoxin levels have also been reported in patients with cirrhosis. (221) Furthermore, sepsis and associated endotoxemia occur in approximately 40% of hospitalised patients with cirrhosis and is a major cause of death. (126) BDL rats are markedly sensitive to lipopolysaccharide (LPS). This is associated with an enhanced TNF-α response and increased lipid peroxidation. (217) LPS is a component of the outer

membrane of gram-negative bacteria. Macrophage and endothelial cells of the hepatic sinusoids are the major sites of clearance of LPS from the circulation, most of which appears to originate from the digestive tract. Interaction of macrophages with LPS results in increased production of reactive oxygen intermediates and of proinflammatory cytokines. (222)

Nitric oxide reacts in biological systems with oxygen, superoxide and transition metals to form reactive nitrogen species that can support nitrosylation reactions with nucleophiles such as thiol groups to form S-nitrosothiols, or can lead to the nitration of amino acids such as tyrosine. The S-nitrosylation of extracellular proteins, such as albumin, gives rise to a circulating pool of nitric oxide, which may release nitric oxide directly, or transfer nitric oxide into the intracellular milieu via transnitrosylation reactions with cell surface thiols, thus affecting vascular and platelet function. (223-226) In BDL rats, Ottesen et al. have shown that hepatic nitrotyrosine levels were increased compared to controls and that this was further increased after the administration of LPS. Therefore, there is likely to be increased formation of S-nitrosothiols and nitrotyrosine in these rats which is markedly upregulated during endotoxaemia.

It has been shown that bile duct ligation induces hepatic encephalopathy in rats as evidenced by a decrease in motor activities. (227) Furthermore, it has been shown that motor activities correlate with the neurobehaviour score. (228) However, the chronic administration of a non-selective nitric oxide synthase inhibitor, N^{ω} – nitro – L-arginine methyl ester (L-NAME), does not have any significantly detrimental or therapeutic effects on the severity of encephalopathy in BDL rats. (227)

Modulation of soluble guanylate cyclase by nitric oxide is altered in brain from cirrhotic patients. Rodrigo et al. using rat bile duct ligation, alone or combined with diet-induced hyperammonemia for 7-10 days tried to reproduce the alterations in nitric oxide modulation of soluble guanylate cyclase found in brains from cirrhotic patients. Soluble guanylate cyclase activity was measured under basal conditions and in the presence of nitric oxide in the cerebellum and cerebral cortex of controls, bile duct ligated without or with hyperammonemia and hyperammonemia without bile duct ligation. In the cerebellum, activation of soluble guanylate cyclase by nitric oxide was significantly lower in bile duct ligated rats with or without hyperammonemia than in control rats. In the cerebral cortex activation of soluble guanylate cyclase by nitric oxide was higher in rats with bile duct ligation with hyperammonemia but not without hyperammonemia than in control rats. The combination of bile duct ligation and hyperammonemia reproduced the alterations in the modulation of soluble guanylate cyclase by nitric oxide found in cerebral cortex and cerebellum of cirrhotic patients while bile duct ligation or hyperammonemia alone reproduced the effects in cerebellum but not in cerebral cortex. (229)

4.4 METHODS

4.4.1 EXPERIMENTAL CONDITIONS

All animal experiments were conducted according to Home Office guidelines under the UK Animals in Scientific Procedures Act 1986. Male Sprague-Dawley rats (body weight 230 – 280 g) were obtained from the comparative biological unit at the Royal Free and University College Medical School (Royal Free Campus, London, UK). All animals were housed in the comparative biological unit and given free access to normal rodent chow and water, with a light:dark cycle of 12 hours, at a temperature of 19-23 °C, and humidity of approximately 50%.

4.4.2 COMMON BILE DUCT LIGATION

All rats underwent bile duct ligation to induce biliary cirrhosis or a sham operation. A midline abdominal incision was made under anaesthesia. The common bile duct was isolated, triply ligated with 3-0 silk, and sectioned between ligatures. After bile duct ligation all animals continued to gain weight. Overall mortality was less than 10% and the infrequent deaths occurred within 36 hours of surgery. Control rats underwent a sham procedure in which the common bile duct was located but not ligated.

4.4.3 ANIMAL STUDY PROTOCOL

The rats were anaesthetised (pentobarbital) and sacrificed 28 days following common bile duct ligation or sham surgery. Subgroups of rats received

lipopolysaccharide (*Salmonella typhimurium* 0.5 mg/kg) which was administered by intraperitoneal injection 3 hours before sacrifice. After this time point, animals were sacrificed by full exsanguinations under anaesthesia (60mg/kg Inactin; 5-ethyl 5-[1-methylpropyl] -2- thiobarbituric acid). Blood was then withdrawn from the descending aorta until full exsanguination into tubes containing 68 iu lithium heparin and then immediately centrifuged. The plasma was then stored at -80°C until assay. The whole brain was collected immediately for estimation of the brain water content in the forebrain and cerebellum.

Six rats were perfused with 100 -150 ml sodium cacodylate buffer (Agar Scientific) [2M pH 7.2-7.4] followed by 200 ml of half strength Karnovskys fixative mix (1% formaldehyde and 2.5% glutaraldehyde) (230;231) to fix brain tissue for light microscopy. A midline incision from the base of the abdomen to the rib cage was made exposing the xiphoid sternum. Then using Spencer Wells forceps to lift the xiphoid sternum, the diaphragm and rib cage were incised to expose the heart. The perfusion was performed via a cannula inserted into the left cardiac ventricle at a constant pressure of 100-110 mmHg as illustrated in Figure 4.1. The brain was then removed and stored in half-strength Karnovskys fixative until examination of brain histology at a later date.

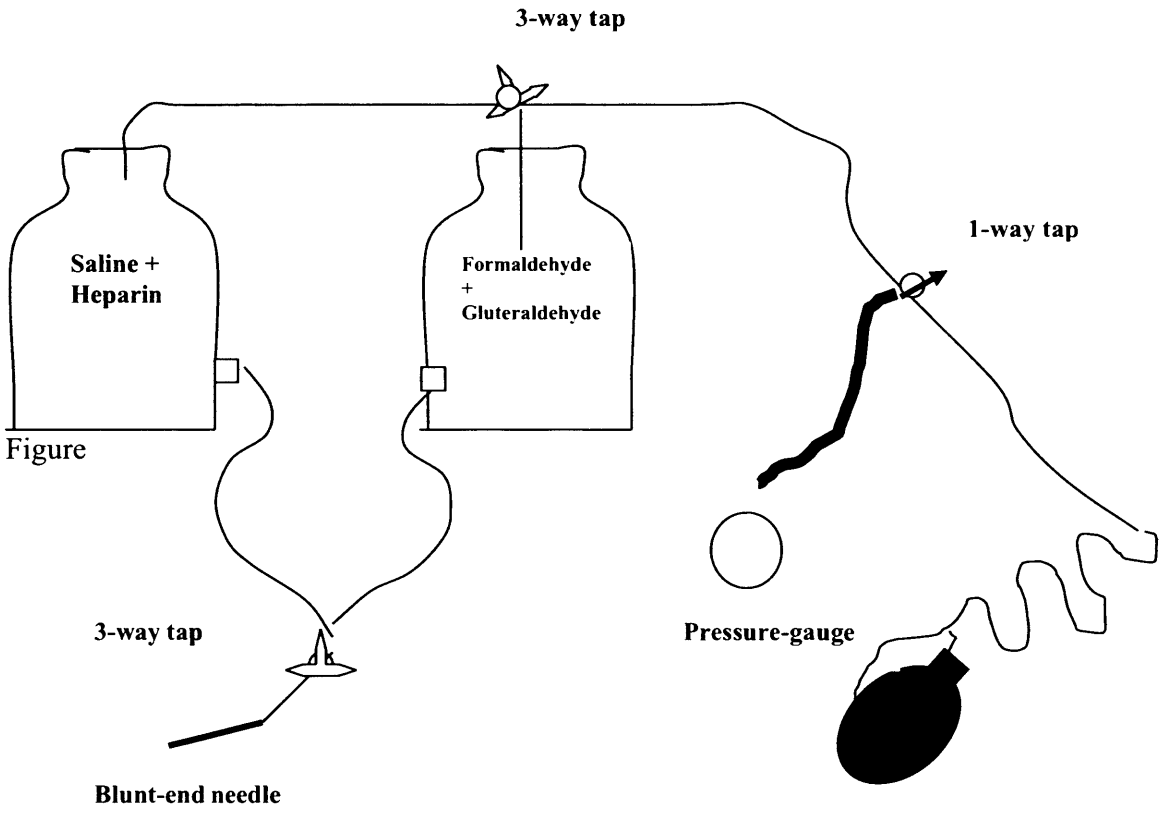

Figure

Figure 4.1

A diagram to illustrate the perfusion & fixation of the rat brain for light microscopy

4.4.4 MONITORING OF LEVEL OF CONSCIOUSNESS

The conscious levels of rats used in this study were rated using an established neurological scale. (232)

4.4.5 MEASUREMENT OF BRAIN WATER

This was performed by a gravimetric technique and is illustrated in Figure 4.2. This allows the percent gram water per gram tissue of samples less than 2 mm^3 to be determined within minutes to an accuracy of greater than 1%. (233)

1. Two mixtures of kerosene and bromobenzene were used in the preparation of the gradient. One litre of mixture A was prepared from 735.6 mls of kerosene and 264.4 mls bromobenzene to give a specific gravity of 0.9750. One litre of mixture B was prepared from 608.8 mls kerosene and 391.2 mls of bromobenzene to give a specific gravity of 1.0650.

2. A flask containing 100mls of mixture B was placed 40 cm above an empty 100ml graduated cylinder. 100mls of mixture A was then placed 43cm above mixture B.

3. The fluid kinetics of this system is such that a linear gradient column is produced if the outflow from the constantly mixed Mixture B to a 100 ml graduated cylinder is exactly twice the outflow from A to B. This was accomplished by using equal lengths of polyethylene outflow tubing of length 90 cm and internal diameter 0.76mm from flask B to the graduated cylinder and a single length of tubing from Flask A to Flask B. By this technique, the specific gravity at the very bottom of the graduated cylinder is equal to that of Mixture B (1.065), while the

specific gravity at the top is equal to the arithmetic mean of the two solutions (1.020).

4. A steady flow to the surface of the graduated cylinder was maintained by gradually lowering the cylinder in 2 mm increments as the fluid level increased. When a cylinder volume of 100ml was reached the tubes were clamped. The gradient was then permitted to stabilize for 15 minutes and calibrated with standards made up of potassium sulphate (K_2S0_4) of known specific gravity.

5. The concentrations of the K_2S0_4 solutions were 5.99, 5.34, 4.7 and 3.4 g/100ml, corresponding to specific gravities of 1.045, 1.040, 1.030 and 1.025. One drop of each standard was gently placed in the column by means of a small syringe. The depth of equilibration was recorded at the end of 2 minutes.

6. The specific gravity of forebrain and cerebellum was measured in 2 mm^3 pieces of tissue and placed gently in the column by needle tip. The depth of equilibration was recorded at the end of 2 minutes. Six pieces for each brain area were recorded.

7. The specific gravity of the samples was calculated using the gradient of the line ($y= mx + c$) generated from a graph of the specific gravity of the K_2S0_4 standards (x axis) and the column position (y axis).

8. Using a constant (c) to represent the specific gravity of the solid component (1.298 in rat frontal cortex and 1.269 in rat cerebellum) the percentage brain water can be calculated using the following formula:

$$[c/(c-1)] / SpG] - [1/(c-1)] \times 100\%$$

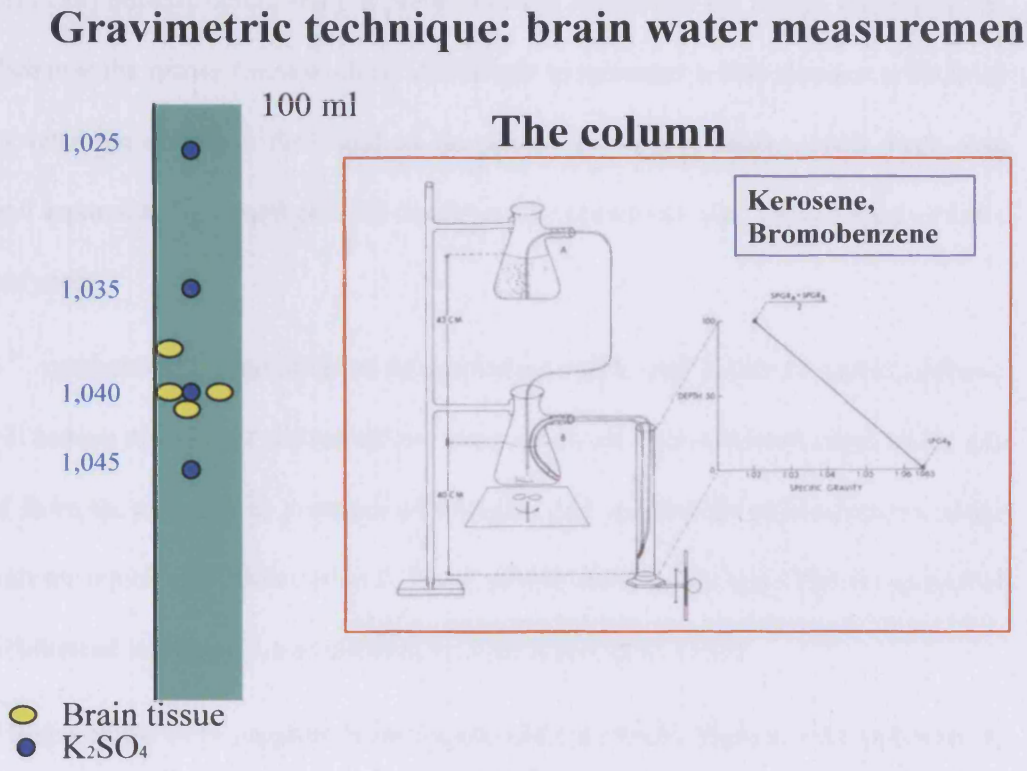

Figure 4.2

Diagrammatic representation of the experimental setup for the gravimetric technique which allows the measurement of brain specific gravity from which brain water content can be calculated.

4.4.6 METHOD FOR SENSITIVE AND SPECIFIC MEASUREMENT OF NITRITE IN PLASMA USING A CHEMILUMINESCENCE ASSAY (234)

As mentioned the combined NO_2/NO_3 levels were determined using a modified Greiss test (190) but this determination predominantly represents the nitrate content in the sample, because the nitrite fraction alone is difficult to measure in this manner as its level is usually near the detection threshold of the assay. Therefore, nitrite levels were also determined separately by a method with much greater sensitivity (ca. 5nM), using a Nitric Oxide analyzer:

I^{3-}, synthesised by the addition of potassium iodide and iodide to acetic acid and water, will reduce nitrite (but not nitrate) to nitric oxide gas. The released nitric oxide gas is carried from the solution in a stream of nitrogen gas into the chemiluminescent nitric oxide analyser which can detect from 0.3 to 1 pmole nitric oxide gas. The instrumental setup is illustrated in Figure 3.4 as detailed by Samouilov et al. (235)

All chemicals were supplied from Sigma-Aldrich (Poole, Dorset, UK) and were of the highest laboratory grade.

1. A stock solution of 180 ml of I_3^- reagent was prepared from 2g potassium iodide and 1.3g of iodine dissolved in 40 ml double distilled water. 140 ml of acetic acid was then added and mixed thoroughly for 30 minutes.

2. Nitrogen gas was bubbled through the 9 ml I_3^- reagent in a glass purge vessel. The vessel is linked to a trap containing 15 ml of 1M sodium hydroxide and is then connected to the chemiluminescent nitric oxide analyser (Sievers, Model 280, Boulder, Colorado, USA) as illustrated in Figure 4.3.

3. The system was then allowed to reach steady baseline.

4. One hundred µL of plasma was diluted 1 in 4 with phosphate buffered saline.

5. This was placed in a Whatman 12 kD molecular weight cut off filter and spun at 18,900 g for 30 minutes at 4 °C.

6. Ten µL of the filtered plasma was then injected via a syringe into the purge vessel. The nitric oxide released then passes into the nitric oxide analyser to produce an optical signal which is detected by a photomultiplier tube.

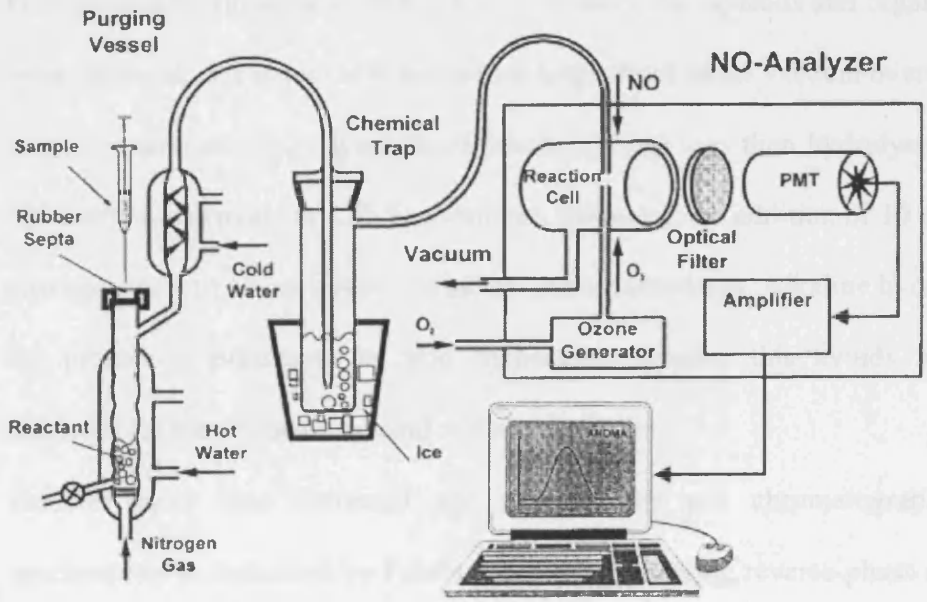

Figure 4.3

A schematic diagram of the chemiluminescence instrumental setup (235)

4.4.7 MEASUREMENT OF BRAIN TISSUE NITROTYROSINE LEVELS

Nitrotyrosine levels were measured by a stable isotope dilution gas chromatography mass spectrometry method following the extraction of tissue or plasma proteins and alkaline hydrolysis. (236)This was only performed on tissue samples from the frontal cortex in the sham-operated and BDL animals.

All chemicals were supplied from Sigma-Aldrich (Poole, Dorset, UK) and were of the highest laboratory grade.

1. Brain proteins were precipitated from brain tissue that was initially homogenised in 13 ml of chloroform:methanol (2:1) with a blade homogeniser on ice, followed by the addition of 2 ml of saline and further homogenisation.
2. Following centrifugation at 3000 g for 30 minutes, the aqueous and organic layers were removed, and the protein precipitate lyophilised under vacuum overnight.
3. A known amount of the lyophilised protein (2 mg) was then hydrolysed in 1ml 4M sodium hydroxide at 120 °C overnight, following the addition of 10 ng [C^{13}_9]-nitrotyrosine and 10 µg [D4]-tyrosine as internal standards. Alkaline hydrolysis of the protein is preferable to acid hydrolysis, because this avoids artifactual formation of nitrotyrosine by acid and nitrate/nitrite.
4. Samples were then extracted and analysed by gas chromatography mass spectrometry as described by Frost et al. (236), following reverse-phase columnic chromatograph purification using LC18 and ENV+ cartridge extraction and derivatization to the heptafluorobutyric amide and tertbutyldimethylsilyl derivatives. This method has an intra-assay and inter-assay variation of < 4% and

5% respectively. All results are expressed in relation to dry weight of protein as measured by direct weighing prior to hydrolysis.

4.4.8 TISSUE PREPARATION FOR LIGHT MICROSCOPY AND HISTOPATHOLOGICAL ASSESSMENT

This was performed at St George's University Hospital in the Department of Anatomy, Basic Medical Sciences Division by Gavin Wright, Ceri Davies and Heather Brooks.

4.5 EXPERIMENTAL PROTOCOL

In brief, all rats underwent bile duct ligation to induce biliary cirrhosis or a sham operation. Twenty eight days after surgery, the rats were randomized into 4 groups as summarised in table 4.1 below.

Animal and Study Condition	No of animals studied
Sham operated	7
Sham + Lipolysaccharide	7
Bile duct ligated	6
Bile Duct Ligated + Lipopolysaccharide	6

Table 4.1

BDL or sham operated rats were injected with LPS (*Salmonella typhimurium*, 0.5 mg/kg intra-peritoneally made up to 0.5 mls in saline) or given 0.5 mls saline alone. The rats were allowed free access to food and water for a period of 3 hours post-intervention in a temperature controlled environment and were then sacrificed by exsanguinations under terminal anaesthesia (Hyponorm 400 μL/kg intraperitoneally, Janssen Pharmaceutica, Belgium). Blood was withdrawn from the descending aorta into heparin containing tubes until full exsanguination, centrifuged, and the plasma collected and stored at -80 °C until assayed.

The conscious levels of rats used in this study was rated using an established neurological scale. (232) Immediately after death, the whole brain was rapidly removed and 2 mm^3 samples were dissected from the frontal cortex (grey matter) and the cerebellar cortex. Brain tissue water content (as a measure of cerebral oedema) was determined using a gravimetric technique. (233) Ammonia was measured in the heparinised plasma using a modified indophenol detection method (237) as detailed in section 3.1.3.2. Combined nitrite/nitrate levels were determined using a modified Greiss test (189) as detailed in section 3.1.3.3. Nitrite concentrations were measured in the filtrate by chemiluminescence. (234) Measurement of brain tissue nitrotyrosine levels were performed on brain homogenates. (236)

Histopathological assessment of brain tissue for high power scanning light microscopy was performed on a further 16 rats as the necessary perfusion and fixation process, makes it impossible to use serum or brain tissue for the other measurements described above.

4.6 STATISTICS

The data are expressed as the mean and standard error of the mean for each group of animals. The significance of any differences seen was tested with the unpaired t-test and Mann Whitney test, indicated in figure legends; <0.05 was taken to be statistically significant. Software used included Microsoft Excel 2003 (Microsoft Corp., Redmond, WA) and GraphPad Prism 4.0 (GraphPad Software, Inc., San Diego, CA).

4.7 RESULTS

4.7.1 RATS

All rats continued to gain weight following surgery. Rats were weighed immediately before sacrifice. BDL rats were found to be marginally heavier compared to sham –operated controls (BDL mean 320 g; n=12; sham mean 296 g; n=14); p=0.01. The difference was attributed to the presence of ascites. At day 28, all BDL rats were deeply jaundiced. All rats remained alive at 3 hours post injection of saline or LPS.

4.7.2 CONSCIOUS LEVEL

BDL rats had a marked deterioration in their conscious level following injection of LPS, with all reaching pre-coma stages at the 3 hour sacrifice time point. The BDL and sham-operated rats administered saline and the sham-operated rats administered LPS remained fully alert.

4.7.3 BRAIN WATER

There was a significant increase in the water content of the frontal cortex of BDL rats administered LPS compared to BDL rats given saline (p=0.004) as measured by gravitometry. There was also a significant increase in the water content within the frontal cortex of sham-operated rats administered LPS compared to sham-operated administered saline (p=0.03) using this technique. There was no significant difference in the brain water content between non-LPS treated groups (BDL/sham-operated and saline) or between the LPS administered groups (BDL/sham-operated and LPS); p=0.07

respectively [Figure 4.4]. There was no effect of LPS on cerebellar water content [Figure 4.5].

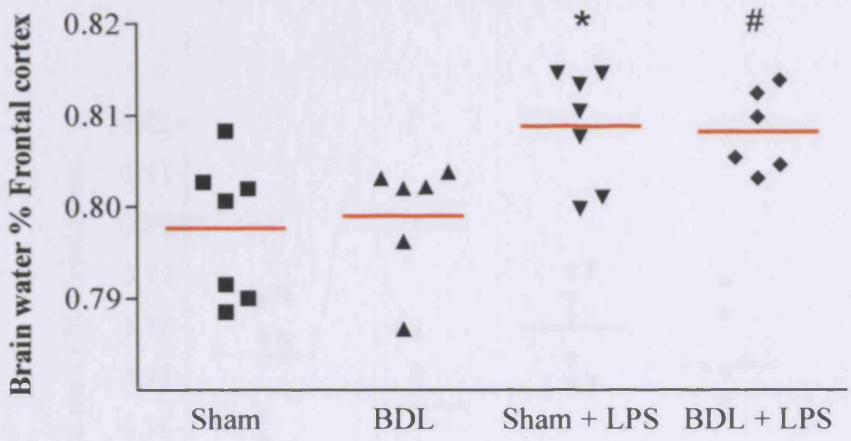

* P<0.03: Sham versus sham + LPS animals

# P<0.004: BDL versus BDL + LPS animals

Figure 4.4

Frontal cortex brain water content

There was a significant increase in percentage water content with LPS administration in both BDL and sham-operated rats (BDL + LPS compared to BDL + saline rats, p<0.004# and sham-operated + LPS compared to sham-operated + saline rats, p<0.03 * respectively, as determined using Mann-Whitney test to compare groups.

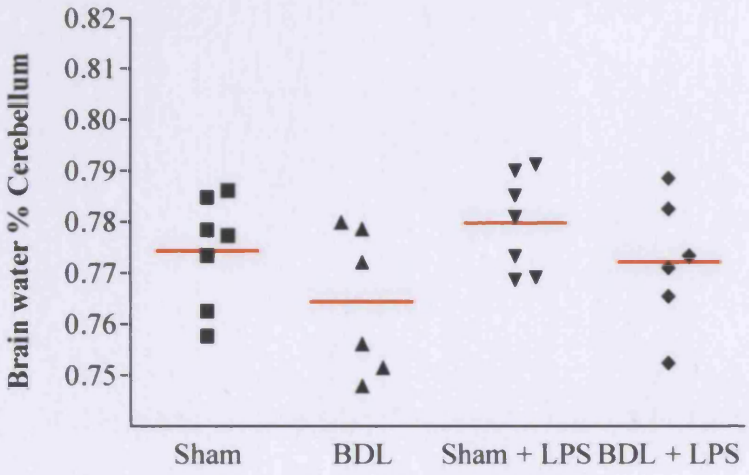

Figure 4.5

Cerebellar brain water content

In the cerebellum of both BDL and sham-operated rats, there was no significant increase in percentage water content following administration of LPS or saline.

4.7.4 PLASMA AMMONIA

The plasma ammonia concentration in BDL rats with saline or LPS was significantly higher than in sham-operated and saline treated rats (mean +/- SEM: BDL 173 +/- 12.4 μmol/L versus sham-operated 134 +/- 12 μmol/L); p=0.035 [Figure 4.6]. Following injection of LPS there was no change in plasma ammonia concentrations compared to BDL rats (p=0.7) or sham-operated rats (p=0.08) administered saline.

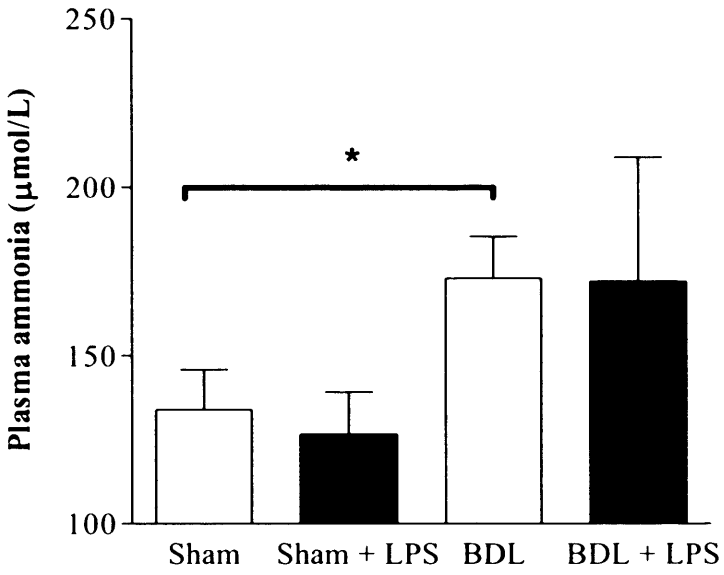

* p=0.035; Sham vs. BDL

Figure 4.6

Plasma ammonia levels

The plasma ammonia levels were significantly higher in saline-treated BDL: rats compared to saline-treated sham-operated rats ($p<0.035$*, as determined using Mann Whitney test to compare groups). LPS treatment did not significantly affect plasma ammonia levels in either BDL or sham-operated rats.

4.7.5 PLASMA NITRITE/NITRATE

The plasma concentration of nitrite and nitrate [Figure 4.7] was significantly higher in rats treated with LPS compared to the non-LPS administered groups (BDL and LPS versus BDL; $p<0.008$ and saline and sham-operated and LPS versus sham-operated and saline; $p<0.018$). BDL rats, with or without LPS, also had higher levels of nitrite/nitrate compared to sham-operated and saline rats; $p<0.06$. Similarly, the BDL/sham-operated rats treated with LPS also had higher plasma nitrite values compared to the BDL/sham-operated and saline treated rats; $p<0.05$, respectively [Figure 4.8].

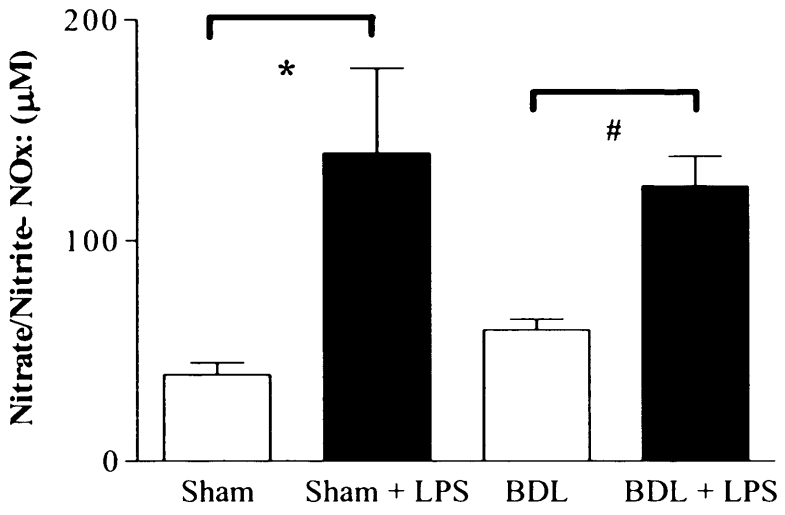

* p<0.018: Sham versus sham + LPS

# p<0.008: BDL versus BDL + LPS

Figure 4.7

Plasma nitrite/nitrate levels

There was a significant increase in plasma nitrite/nitrate levels with administration of LPS in BDL/sham-operated rats compared to BDL/sham-operated rats (in BDL + LPS compared to BDL + saline rats; $p<0.008$ # and sham-operated + LPS compared to sham-operated + saline rats; $p<0.018$ * respectively) as determined using the Mann-Whitney test to compare groups.

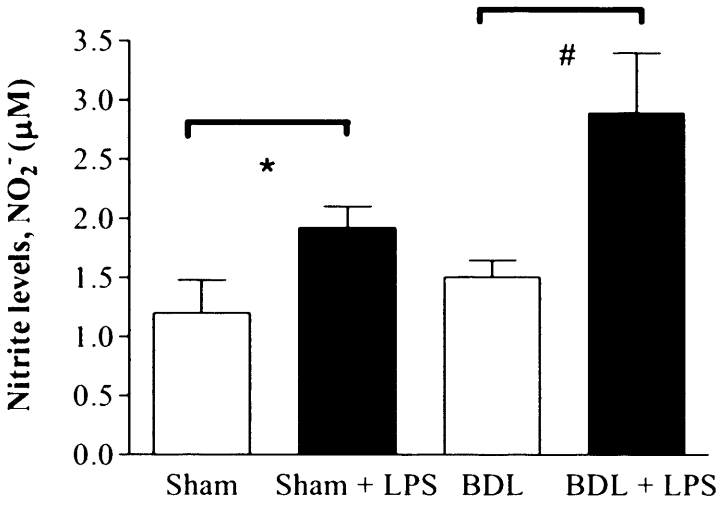

* p=0.045: Sham vs Sham + LPS

p=0.04: BDL vs BDL + LPS

Figure 4.8

Plasma nitrite levels

There was a significant increase in plasma nitrite levels in LPS treated BDL rats versus saline treated BDL rats; $p<0.04$ # and also, LPS treated sham-operated rats compared to saline treated sham-operated rats; $p<0.045$ *, as determined using the unpaired t test to compare groups.

4.7.6 BRAIN NITROTYROSINE/TYROSINE RATIO

A significantly increased nitrotyrosine/tyrosine ratio (NT/T) was present in the BDL rats administered LPS, compared to saline administered to BDL; $p<0.005$ # and sham-operated rats; $p<0.04$ * respectively [Figure 4.9]. There was no difference in the NT/T ratio between saline administered to BDL and sham-operated rats; $p=0.3$. Administration of LPS to sham-operated rats did not increase the NT/T ratio compared to saline administered sham-operated rats; $p=0.8$.

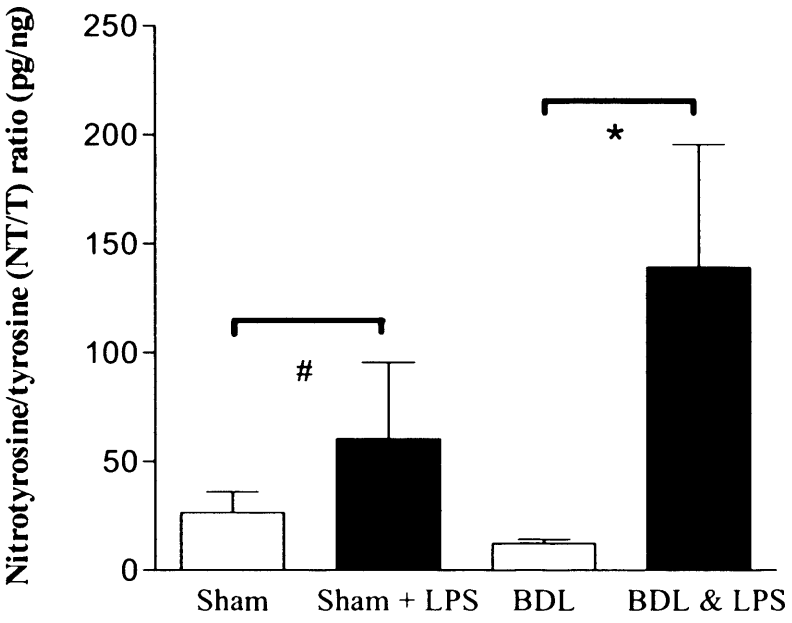

* p<0.005: BDL versus BDL + LPS
# p<0.04 sham versus sham +LPS

Figure 4.9

Brain Nitrotyrosine/Tyrosine ratio

There was a significant increase in the brain nitrotyrosine/tyrosine ratio in LPS treated BDL rats compared to saline-treated BDL; p<0.05 # and sham-operated rats; p<0.04 * as determined using the Mann-Whitney test to compare groups.

4.7.7 HIGH POWER LIGHT MICROSCOPY OF THE BRAIN

Light microscopy of BDL rat forebrain revealed partially collapsed venules, perivascular oedema and neuronal oedema [Figure 4.11]. When given LPS, massive perivascular oedema was seen accompanied by completely collapsed venules and neuronal death [Figure 4.13]. Sham-operated forebrain did not show any evidence of venule collapse or oedema [Figure 4.10], but when given LPS, the forebrain was observed to develop mild perivascular oedema [Figure 4.12].

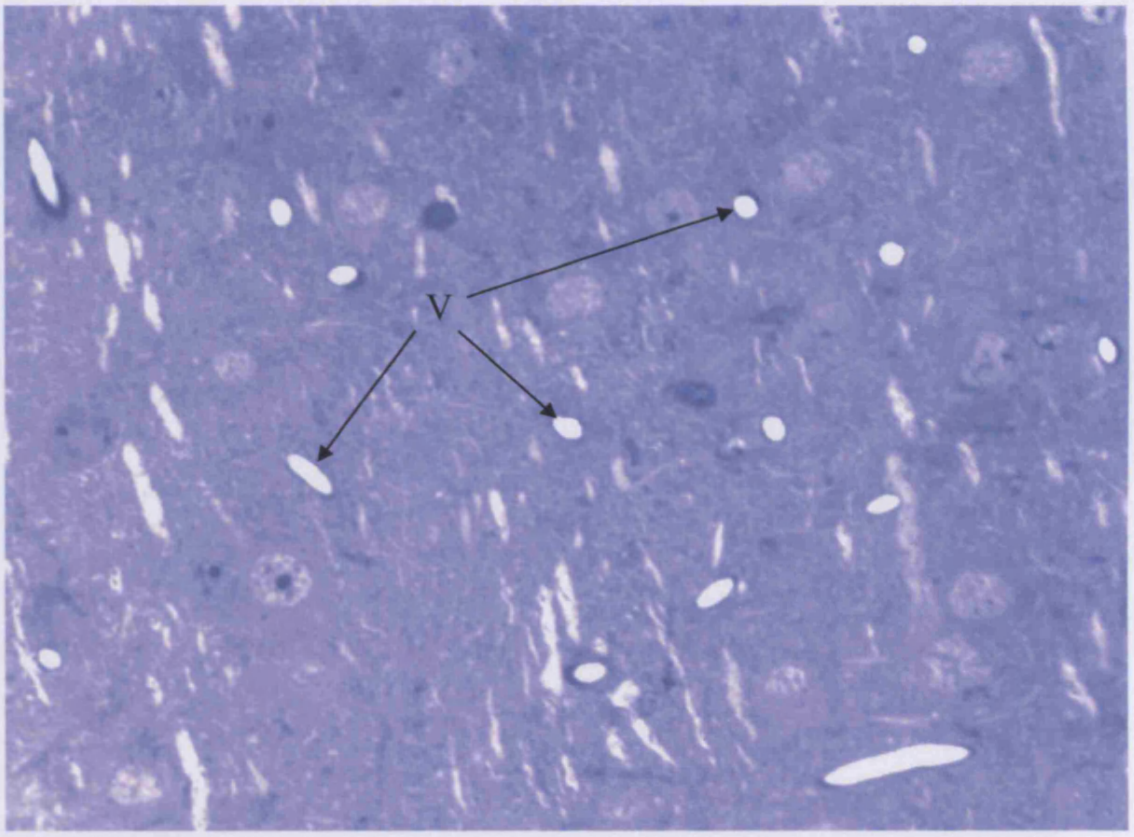

Figure 4.10

A scanning light micrograph (magnification x 200) of a sham-operated rat forebrain showing 3 normal venules (V).

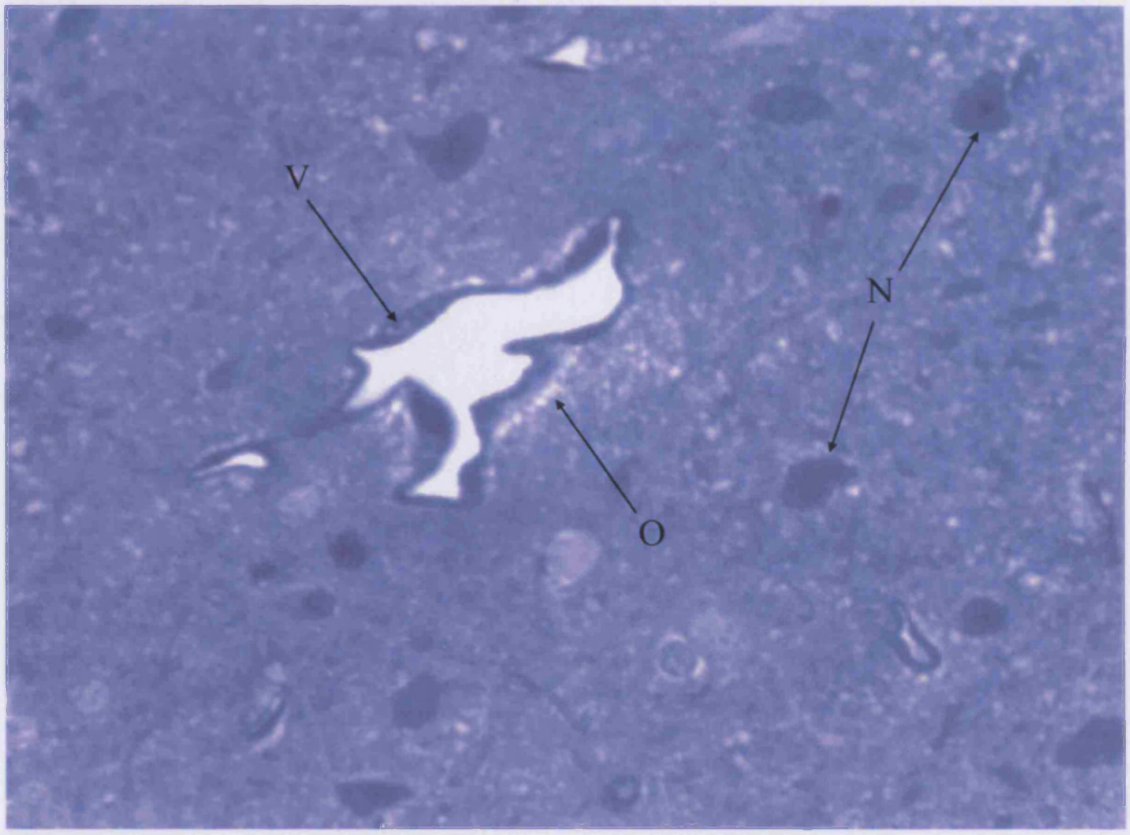

Figure 4.11

A scanning light micrograph (magnification x 200) of a BDL rat forebrain showing a partially collapsed vessel (V), perivascular oedema and neuronal swelling.

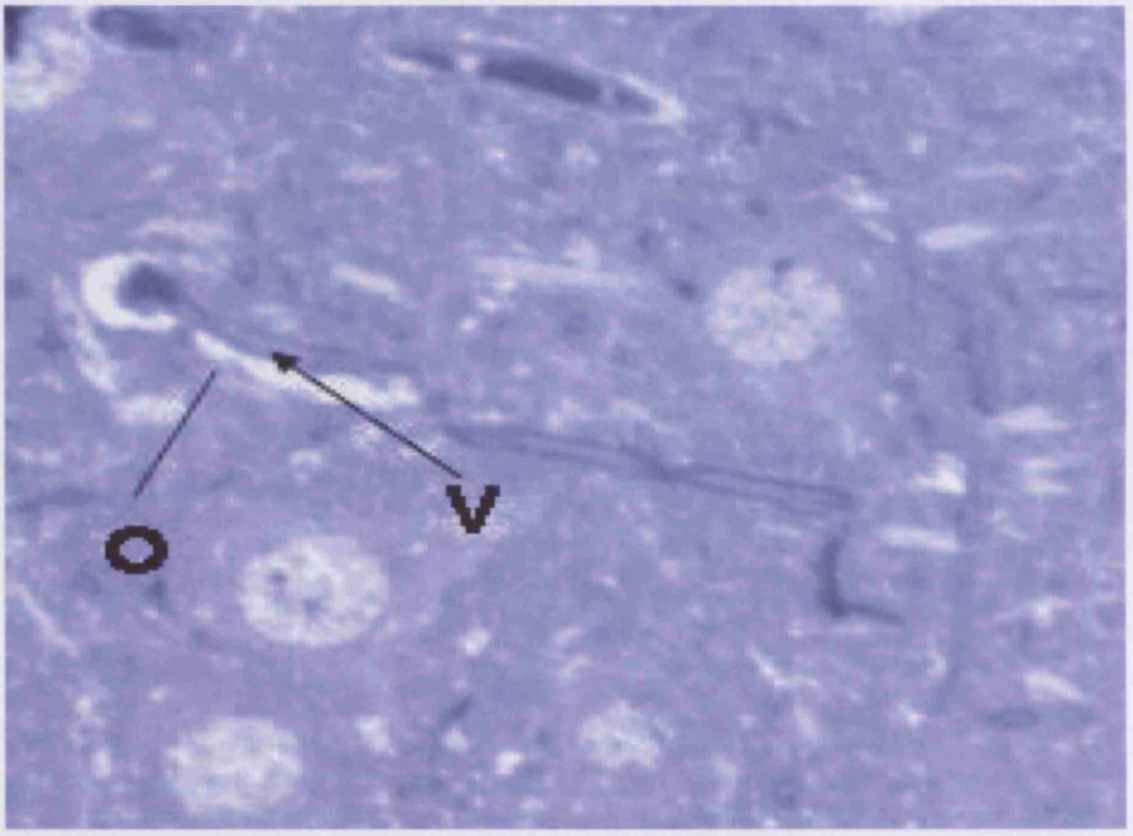

Figure 4.12

A scanning light micrograph (magnification x 200) of a sham-operated rat forebrain 3 hours after the administration of LPS showing venule (V) collapse and mild perivascular oedema (O).

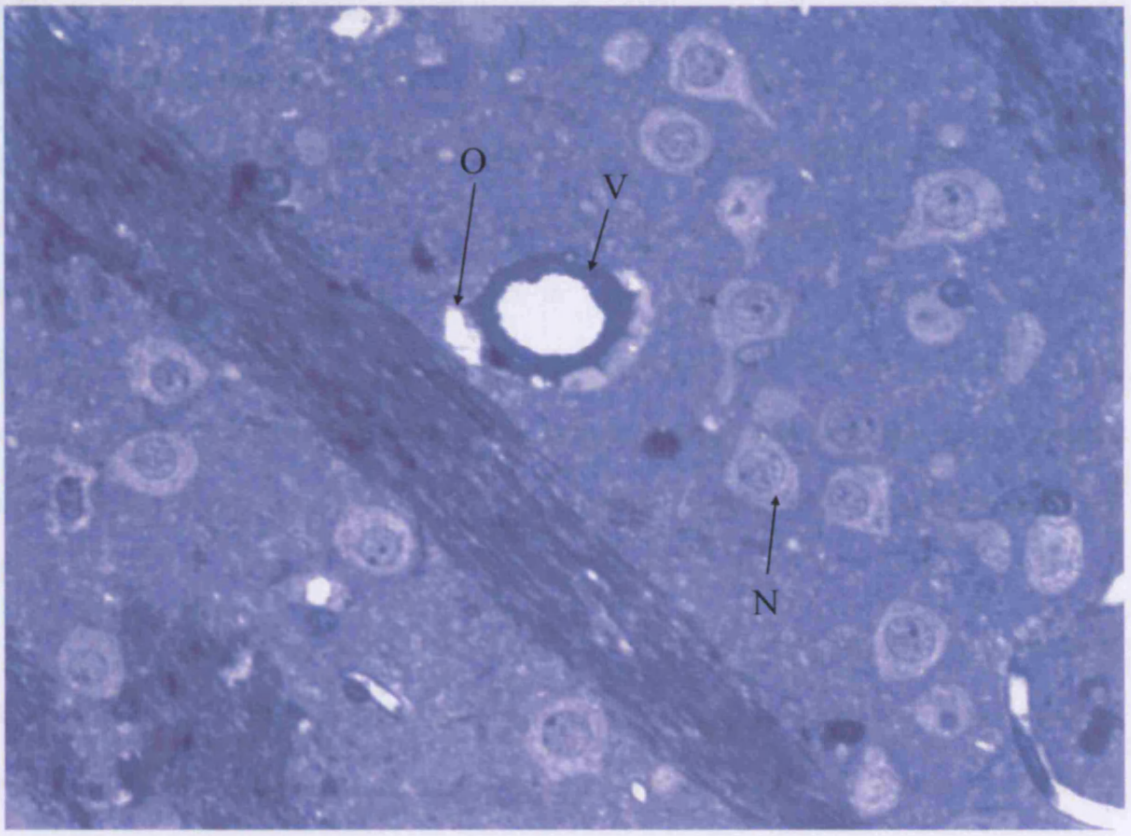

Figure 4.13

A scanning light micrograph (magnification x 200) of a BDL rat forebrain 3 hours after the administration of LPS showing massive perivascular oedema (O) surrounding a venule (V) and severe neuronal oedema (N).

4.8 DISCUSSION

This study has explored whether an inflammatory stimulus in cirrhotic rats would produce cerebral oedema. The data arising from this study has shown that although BDL and sham-operated rats had similar brain water content 3 hours after administration of LPS compared to their saline counterparts, the BDL and LPS rats reached pre-coma stages, whereas the mental state of the LPS treated sham-operated rats remained unchanged in this time. High power light microscopy suggests that forebrain oedema is perivascular in origin and related to astrocyte swelling. An increase in forebrain water is a hallmark of advanced cerebral changes in acute liver failure. Recent studies have indicated that patients with cirrhosis have low-grade cerebral oedema (238;239). This study describes low-grade brain oedema in cirrhotic rats, similar to the low-grade oedema observed in cirrhotic patients. This cerebral oedema worsened after the administration of LPS.

These data did not show any differences in the basal brain water content between BDL rats and sham-operated controls as measured by the gravimetric technique however; histopathologically there is evidence of astrocyte swelling and brain oedema. Following the induction of endotoxemia with LPS, the brain water content rose in the frontal cortex but not the cerebellum in all animals and this was accompanied by evidence of worsening astrocyte swelling and brain oedema histopathologically. There were no significant differences between the plasma ammonia values in each group, which would suggest that there is no direct relationship between the plasma ammonia concentration and brain water content. The observation of a similar increase in brain water and astrocytic swelling in both the sham-operated (normal ammonia) and the BDL rats (high ammonia) following

the administration of LPS, suggests that inflammatory mechanisms are likely to be important in the pathogenesis of brain swelling.

An interesting observation of this study is that there is brain swelling with endotoxaemia in the control animals. This demonstrates the importance of inflammation in brain swelling in the absence of liver dysfunction and is likely to be explained by the development of a septic encephalopathy. The association between infection and impaired brain function has been recognized for a long time since it was first described by Hippocrates 2000 years ago. (207) Septic encephalopathy can arise from the action of inflammatory mediators on the brain or a cytotoxic response by brain cells to these mediators. Septic encephalopathy is usually a sequelae of severe sepsis complicated by multiple organ failure and hypotension. (98)

In the presence of liver dysfunction, urea synthesis is impaired and the brain acts as a major alternative ammonia detoxification pathway. Astrocytes, which provide physical and nutritional support for neurons also eliminate ammonia by the synthesis of glutamine through amidation of glutamate. Accumulation of glutamine in astrocytes, induced by hyperammonemia, produces osmotic stress and causes the astrocytes to swell. (49) In acute liver failure, astrocytes swell and cytotoxic brain oedema develops. This observation has been replicated in cultured astrocytes exposed to high concentrations of ammonia. (32) In chronic liver disease, astrocytes show the characteristic morphological features of Alzheimer Type II astrocytosis. Astrocytes exhibit a large swollen nucleus, prominent nucleolus, margination of the chromatin pattern and marked enlargement of the cytoplasm associated with a proliferation of cytoplasmic organelles which has also been replicated in astrocytes exposed chronically to ammonia. (33) This may not however

equate to overt cell swelling and it may therefore perhaps not be surprising that the BDL animals did not exhibit increased brain water content (as measured by the gravimetric technique) 28 days following surgery. No significant change was observed in the water content of tissue collected from the cerebellum, which was utilised as a control tissue as it is devoid of astrocytes and therefore may not be expected to display cell swelling in this model.

The BDL rats administered LPS showed universal deteriorating levels of consciousness (to pre-coma and coma stages) as has previously been observed (217). In the BDL/sham operated rats administered saline and the sham-operated rats administered LPS, no change in conscious level occurred. This is despite the LPS treated sham-operated rats and saline BDL rats showing some evidence of brain swelling and astrocyte oedema. It is therefore possible that in the BDL rats hyperammonemia in some way acts synergistically with the systemic inflammatory response to alter the level of consciousness. This concept fits with the observation in chapter 4 in cirrhotic patients, where induction of hyperammonemia resulted in neuropsychological deterioration when the patients were infected and showed evidence of an inflammatory response. (192) Following resolution of infection, similarly induced hyperammonemia did not result in an alteration in neuropsychological function supporting the hypothesis that ammonia and inflammation may be synergistic. Furthermore, the suggestion of synergy between hyperammonemia and inflammation is supported by the recent observation that BDL rats that were fed a high ammonia diet (and which showed evidence of a low level of inflammation), developed increases in brain water (240).

Harry et al. have previously shown that the administration of LPS resulted in a sustained increase in TNF-α and F2 isoprostanes in the BDL rats 3 hours after the administration of LPS (217). In sham-operated rats administered LPS, the increase in both TNF- α and isoprostanes was transient. In support of this observation, we observed that both the BDL and sham-operated rats administered LPS had higher nitrite/nitrate and nitrite. These observations indicate that in this model of cirrhosis an altered response to injury may contribute to the differences in the observed conscious level and cerebral oedema in the BDL rats administered LPS compared to the sham-operated rats administered LPS. In order to explore whether this altered peripheral inflammatory response was reflected in the brain, nitrosylation of protein in the brain was measured. The observation of increased brain nitrotyrosine/tyrosine ratio in the BDL animals given LPS argues that the exacerbated inflammatory response on a background of hyperammonemia may play an important role in the clinical presentation in these rats. Stimulation of astrocytes in culture with LPS results in upregulation of inducible nitric oxide that culminates in increased production of nitric oxide. (91) A similar phenomenon is observed with ammonia. Schleiss et al. have provided evidence of protein tyrosine nitration in ammonia-treated cultured astrocytes and also *in vivo* in brains of rats treated with an ammonia load. (92) Similarly, LPS itself can lead to nitrosylation of proteins in the brain. (241) Furthermore, the addition of ammonia to astrocyte cultures generates reactive oxygen species, a process involving the synthesis of glutamine. Treatment of astrocytes with glutamine also increases free radical production. (93) As most of the glutamine in astrocytes is metabolised by mitochondrial phosphate-activated glutaminase, breakdown of glutamine could result in release of high levels of ammonia in

mitochondria, which is a likely to increase reactive oxygen species. It is conceivable that hyperammonemia and LPS together provide an environment for nitrosylation of brain proteins and act as an important pathway in producing alteration in the mental state. Though an increase in nitrotyrosine/tyrosine ratio in the LPS treated sham-operated rats was observed, this was not significantly different to the nitrotyrosine/tyrosine ratio in saline treated BDL/sham operated rats.

The mechanisms leading to increased protein nitrosylation are thought to involve formation of peroxynitrite. This is formed from the combination of superoxide and nitric oxide. Peroxynitrite, in the presence of carbon dioxide can modify tissue proteins to form nitrotyrosine which may mediate nitric oxide-induced blood brain barrier damage. (96) An increase in the permeability of the inner mitochondrial membrane to small solutes (mitochondrial permeability transition) results from oxidative and nitrosative stress and ammonia has been recently shown to induce similar changes in cultured astrocytes. (97) Increased cerebral nitric oxide, increased markers of oxidative stress and nitrotyrosine accumulation within brain microvessels have been associated with raised intracranial pressure and brain oedema in models of ammonia-induced brain oedema (76). However, evidence implicating activation of nitric oxide synthase (NOS) in ammonia-induced brain oedema is not universal, with the role of nitric oxide being refuted due to the failure of NOS inhibitors to impact on the development of brain oedema and cerebral hyperemia (120).

In conclusion, this study provides further evidence to indicate that on a background of cirrhosis with hyperammonemia, inflammation has an important synergistic role in the development of hepatic encephalopathy. Although the exact

mechanism of how ammonia and LPS produce cerebral oedema and coma is not clear, these data support an important role for the nitrosylation of brain proteins.

4.9 FUTURE AVENUES OF STUDY

In order to further investigate the synergistic nature of the relationship between ammonia and inflammation, it would have been interesting to co-administer ammonia and endotoxin in the BDL model and compare this to sham-operated controls. The problem with achieving this is that the animals do not tolerate this toxic combination well and many succumbed in pilot studies. It might be argued that this can be overcome by sacrificing the animals after a shorter time period or by using lower doses of ammonia and endotoxin. However, this may not allow sufficient time for brain oedema to develop. One possible way of overcoming this problem may have been to feed the rats on a diet rich in ammonia or ammonia generating nitrogenous compounds, rendering them hyperammonemic. This should allow ample time for astrocyte swelling to develop as the rats will be adjusted to a chronic level of hyperammonemia.

Another aspect of this investigation that deserves further study is the origin of the nitric oxide. Western blots of homogenized brain tissue would allow the identification of tissue nitric oxide synthase isoforms; defining the relative amounts of inducible, endothelial and neuronal nitric oxide synthase. Furthermore, immunohistochemistry performed on the sections obtained for high resolution light microscopy would indicate the location of these nitric oxide synthases within the brain.

Finally, although the brain tissue sections visualized under light microscopy are highly informative and clearly demonstrate astrocyte swelling, it would be even better if the blood brain barrier could be visualized by electron microscopy in these animal models in the presence and absence of endotoxaemia. Contact and communication between the

neurovascular unit, which is a dynamic structure consisting of vascular endothelial cells, pericytes, and closely juxtaposed astrocytes and neurons, modulates cerebral blood flow and influences the permeability properties of the blood brain barrier. Electron microscopy utilizing intravascular ionic tracers such as lanthanum nitrate, would allow detection of blood brain barrier integrity to paracellular movement and would allow visualization of the tight junctions which may allow the study of the effect of hyperammonemia and inflammation on the tight junction proteins such as claudin and occludin.

Chapter 5

The effect of ammonia on neutrophil function: an observational study

5.1 PREFACE

Thus far it has been shown that inflammation is an important determinant of the presence and severity of minimal hepatic encephalopathy. Furthermore, the change in neuropsychological function following induced hyperammonemia was greater in those with more severe inflammation. Following on from this, patients with cirrhosis were studied 24-36 hours after admission with clinical evidence of infection, and following its resolution. Significant deterioration of neuropsychological test scores following induced hyperammonemia during the inflammatory state, but not after its resolution, suggested that inflammation and its mediators may be important in modulating the cerebral effect of ammonia in liver disease. Moreover, in an animal model of cirrhosis, the BDL rat, increased brain water and astrocyte swelling which was exacerbated by endotoxin and was accompanied by a rise in nitric oxide and brain nitrotyrosine, but not in plasma ammonia, suggested that inflammation may play an important synergistic role with ammonia in the pathogenesis of hepatic encephalopathy. These findings provide strong supportive evidence for my hypothesis as stated in chapter 2 [Figure 2.1].

If inflammation modulates the cerebral effects of ammonia, then a key question to then go on to ask is how is the metabolism of ammonia affected by the presence of inflammation or infection? If one takes a step back from this supposition, then it might be logical to question whether ammonia itself may impair immunity and predispose an individual to the development of infection or sepsis. This led onto the development of the third hypothesis [Figure 2.1], that ammonia impairs neutrophil function. This hypothesis will be tested in the following 2 chapters of this thesis [Chapters 5 & 6].

5.2 ABSTRACT

Background: In patients with cirrhosis, hyperammonemia is commonly associated with hepatic encephalopathy and accompanies gastrointestinal bleeding, both conditions being associated with a high incidence of sepsis and mortality. We aimed to determine whether incubation of normal neutrophils with ammonia concentrations similar to that found in cirrhosis impaired phagocytosis and influenced resting and E.coli-induced oxidative burst. **Methods:** Whole blood from 12 healthy volunteers was incubated for 90 minutes at 37°C with 0 - 500 μM ammonium chloride (NH_4Cl). Quantification of phagocytosis was performed using the Phagotest® which utilises an opsonised FITC-labeled E.coli. Quantification of oxidative burst was determined using the Burstest® which measures the percentage of neutrophils which produce reactive oxidants. Isolated neutrophils were then labeled with anti-CD16-R-PE antibodies and analysed using flow cytometry. The pH was monitored and did not change. Myeloperoxidase activity was also measured. **Results:** Phagocytosis was significantly impaired by 12-20% following incubation with 75 μM NH_4Cl ($p<0.0005$). Spontaneous respiratory burst increased by 10.7% ($p<0.0005$) and myeloperoxidase activity likewise with 75μM NH_4Cl ($p<0.001$). Furthermore, neutrophils increased in volume by 2 % (on flow cytometry), suggesting cell swelling. Ammonia-induced apoptosis or necrosis was excluded by staining with propidium iodide and annexin V-FITC. **Conclusions:** Hyperammonemia impaired neutrophil phagocytosis and induced spontaneous oxidative burst. The mechanisms have yet to be fully elucidated but cell swelling and activation of key oxidative enzymes were important. Consequently, in the presence of hyperammonemia neutrophils may be unable to respond to microbial challenge, in part accounting for the increased susceptibility to infection.

5.3 BACKGROUND

Our group has recently shown that neutrophil dysfunction with high resting oxidative burst and reduced phagocytic capacity is present in patients with cirrhosis and alcoholic hepatitis which was associated with a significantly greater risk of infection, organ failure and mortality (131).

Furthermore, pilot studies performed by our group suggested that phagocytosis and oxidative burst in normal neutrophils may be impaired by micromolar concentrations of ammonia. The exact mechanism of action underlying this is unclear but could conceivably involve the inhibition of glutaminase. However, published data suggests that glutaminase is usually inhibited by millimolar rather than micromolar concentrations of ammonium chloride (139) which might suggest alternative mechanisms. It is also known that in astrocyte cultures, exposure to ammonia results in cytosolic alkalinization leading to calcium-dependent release of glutamate. (55) It is therefore reasonable to postulate that ammonia may cause cytosolic alkalinization in neutrophils as well. Ammonia freely passes into the neutrophil cytosol and one possibility is that it may alter the activity of intracellular signalers such as mitogen-activated protein (MAP) kinases, p38-MAP kinase ($p38^{-MAPK}$), Jun-kinase (JNK) and extracellular signal-regulated kinase (ERK) (179).

As neutrophil function is impaired in cirrhosis, I hypothesise that, as hyperammonemia is invariably present in acute and chronic liver dysfunction, that hyperammonemia impairs the ability of neutrophils to function normally. The aim of this study was therefore to characterize some aspects of neutrophil morphology and function in the presence of ammonia, such as phagocytosis and oxidative burst.

Phagocytosis was assessed using a test kit (Phagotest ®) which was devised to test the phagocytic activity in various congenital and acquired neutrophil abnormalities (242) and to evaluate the effect of drugs. Abnormal phagocytosis can occur with a variety of clinical disorders (242). The defects can be associated with the neutrophil itself or with an immunoglobulin or complement defect. Known inborn defects are actin dysfunction, tuftsin deficiency and complement receptor C3bi deficiency. These deficiencies can result in increased susceptibility to infection due to defective neutrophil phagocytosis. Acquired defects associated with altered phagocytic activity can be observed in trauma, diabetes, renal failure and infection. The Phagotest ® also allows the study of phagocytic activity of HL-60 promyelocytic leukaemia cells or of isolated monocytes or macrophages.

Oxidative burst activity was assessed using a test kit (Burstest®) which was devised to investigate the altered oxidative burst activity found in various disorders and to evaluate the effect of drugs. Reduced or missing burst activity is observed in inborn defects like chronic granulomatous disease (CGD). This is a heterogenous group of inherited disorders that usually manifests itself during the first 2 years of life. (242) The disease is characterized clinically by repeated and life-threatening infections caused by bacterial and fungal organisms. These infections typically consist of pneumonia, lymphadenitis or abscesses involving the lymph nodes, lung and liver. The NADPH oxidase is the enzyme system responsible for producing superoxide anion, which is quickly converted to hydrogen peroxide and hydroxyl radicals. Abnormalities in the constituent peptides of NADPH oxidase enzyme system lead to the dysfunctions characteristic of CGD. Neutrophils from CGD patients fail to produce a significant

oxidative burst following stimulation. The Burstest® is a rapid and sensitive method for the diagnosis of CGD and for the detection of X-linked carriers.

5.4 METHODS

5.4.1 AMMONIA INCUBATION

1. Venous blood was collected from 12 healthy fully consented individuals in 4 ml vacuum tubes containing 68 iu lithium heparin (BD Vacutainer®). On average 30mls was collected and placed immediately in ice for 10 minutes to pre-cool the neutrophils to 0 ^{o}C.

2. The stock ammonia solution used was prepared from 50mls of a 1M solution of NH_4Cl (Sigma) [2.67 grams in 50 mls ddH_20]. From this a 10 mM NH_4Cl solution was prepared by adding 0.5 mls of the 1M solution to 49.5 mls double distilled water (ddH_20).

3. Two mls of heparinised whole blood was then incubated at 37 ^{o}C in a water bath (Grant Instruments, Cambridge, UK) with 0, 25, 50, 75, 100, 125, 150, 250, 300 or 500 µmol NH_4Cl for 90 minutes after gentle mixing on a blood rotator (SB1, Stuart Scientific) for 1 minute. 5ml Falcon polystyrene round bottom tubes 12 x 75mm (Becton Dickinson; UK) were used. Each concentration was tested in triplicate. An incubation time of 90 minutes was chosen on the basis of pilot studies which showed that neutrophils incubated, with and without ammonia, did not die or begin to apoptose until at least 5 hours following venesection. As the neutrophil isolation, preparation and flow cytometry steps take a minimum of 2 hours, incubation of the neutrophils for longer than 90 minutes would have compromised the health of the neutrophils.

4. The blood was gently re-mixed on the blood rotator for a further 1 minute after 30 and 60 minutes incubation in the water bath.

5.4.2 NEUTROPHIL ISOLATION

5.4.2.1 NEUTROPHIL ISOLATION USING PHAGOTEST® AND BURSTESTS®

1. After pre-incubation, 100 µL of blood was pipetted into 5ml Falcon polystyrene round bottom tubes 12 x 75mm (Becton Dickinson, UK) tubes.

2. These were then treated with 20 µL of E.coli (concentration 2 x 10^9 bacteria) or 20 µL of neutrophil wash solution and incubated in the water bath for 20 minutes according to the manufacturer's instructions (Phagotest® and Burstest®).

3. 100 µL of tryptan blue was then added to each tube to quench neutrophil phagocytosis in the case of the Phagotest® and re-incubation in the water bath with 20 uL of substrate in the case of the Burstest®.

4. The tubes were then filled with 2 mls of neutrophil wash solution [Phosphate Buffered Saline (PBS) – salts (0.1M Sodium dihydrogen orthophosphate, 0.1M sodium chloride and 0.1M disodium hydrogen orthophosphate) reconstituted in 1000mls double distilled water (ddH_20)] and centrifuged (Biofuge Primo R, Heraeus) with 20 x 75mm tube carriers at 4 °C at 516 g for 5 minutes. The supernatant was then removed carefully and the cells re-washed with a further 2 mls of washing solution. The supernatant was once again removed after centrifugation.

5. The tubes were then centrifuged at 4 °C at 516 g and the lysing solution was removed. The cells (leucocytes) were then washed twice as before with neutrophil washing solution.

6. After the final wash, the supernatant was removed and 20 µl of anti- CD16-PE IgG_1 or 20 µl of neutrophil wash solution was added in the case of the Phagotest® and Burstest®. The tubes were then placed in a dark cupboard at room temperature for 1 hour.

7. The leucocytes were then re-washed twice with neutrophil wash solution.

8. After the second wash the supernatant was removed and the cells were re-suspended in 60 µl of neutrophil wash solution.

5.4.2.2 NEUTROPHIL ISOLATION USING POLYMORPHOPREP ™

Polymorphoprep ™ (Axis Shield, Norway) is a ready made, sterile and endotoxin tested solution for the isolation of polymorphonuclear granulocytes from whole blood. The solution contains sodium diatrizoate 13.8% (w/v) and dextran 500 8% (w/v). Using a mixture of sodium metrizoate and Ficoll (Lymphoprep), Boyum (243) developed a one-step centrifugal technique for the isolation of mononuclear cells. In this technique the polymorphonuclear cells are centrifuged to the bottom of the tube together with the erythrocytes. Polymorphoprep™, is a further development of this method. The mononuclear and the polymorphonuclear leucocytes are separated into 2 distinct bands free from red blood cells.

1. Venous blood was collected from 12 healthy fully consented individuals in 4 ml vacuum tubes containing 68 iu lithium heparin (BD Vacutainer®) and used immediately. This was not pre-chilled as in the previous isolation method.

2. Five mls of blood was layered with a pipette over 5 mls of the polymorphoprep ™ in a 12ml Falcon Tube taking particular care not to mix the blood with the separation fluid.

3. The samples were then centrifuged (Biofuge Primo R, Heraeus) with 4 x 15ml tube carriers for 690 g for 35 minutes at 18 °C.

4. After centrifugation, 2 leucocyte bands were visible. The top band at the sample/medium interface consists of mononuclear cells and the lower band of polymorphonuclear cells. The erythrocytes were pelleted at the bottom of the tube. The polymorphonuclear band was harvested using a Pasteur pipette and diluted by the addition of one volume of neutrophil wash solution at 50% of the normal concentration in order to restore osmolality [Figure 5.1].

5. The cells were then washed twice with neutrophil wash solution, centrifuged at 516 g for 5 minutes and resuspended in 60 µL of neutrophil wash solution.

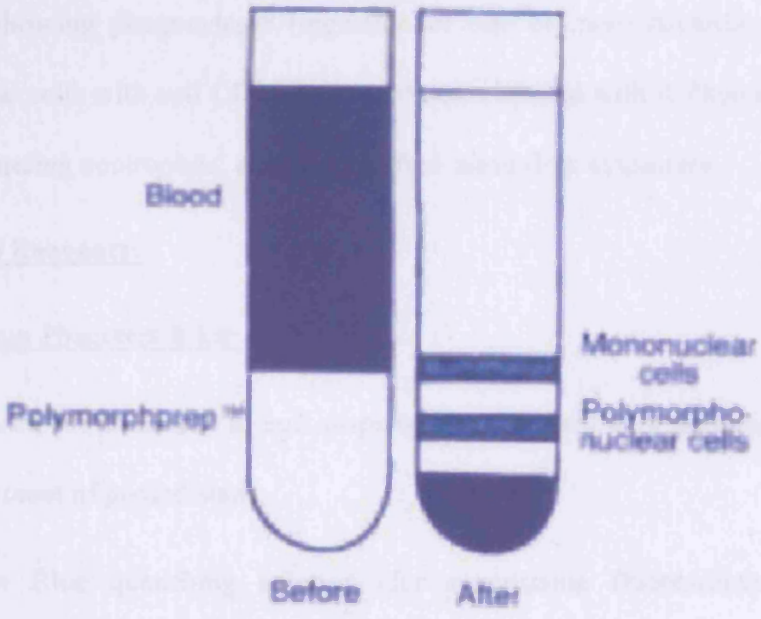

Figure 5.1

Isolation of polymorphonuclear cells before and after centrifugation, using the polymorphprep™ method.

5.4.3 NEUTROPHIL FUNCTION TESTS

5.4.3.1 PHAGOTEST® (Orpegen Pharma, Heidelberg, Germany): QUANTIFICATION OF PHAGOCYTIC ACTIVITY OF NEUTROPHILS IN HEPARINISED WHOLE BLOOD

This *in vitro* test allows the quantitative determination of leukocyte phagocytosis in heparinised whole blood. This measures the overall percentage of monocytes and granulocytes showing phagocytosis (ingestion of one or more bacteria per cell). By incubating these cells with anti CD16 IgG_1 antibodies labeled with R Phycoerythrin (PE), leucocytes including neutrophils, can be identified using flow cytometry.

Materials and Reagents:

Contained within Phagotest ® kit:

- Opsonised FITC-labeled E. coli suspension (opsonised with immunoglobulin and complement of pooled sera).
- Tryptan Blue quenching solution (for suppressing fluorescence of bacteria attached to the outside of the cell).
- Lysing solution (contains diethylenglycol and formaldehyde).
- Neutrophil wash solution [Phosphate Buffered Saline (PBS) – salts (0.1M Sodium dihydrogen orthophosphate, 0.1M sodium chloride and 0.1M disodium hydrogen orthophosphate) reconstituted in 1000mls double distilled water (ddH_2O)].

Other:

- Anti- CD16-PE IgG_1(IOTest®, Beckman Coulter)

Method:

The Phagotest™ was performed according to the manufacturer's instructions, briefly:

1. Venous blood was collected from 12 fully consented healthy individuals in 4ml vacuum tubes containing 68 iu lithium heparin (BD Vacutainer®). On average 30mls was collected and placed immediately in ice for 10 minutes to pre-cool the neutrophils to 0 °C.
2. Neutrophil washing salts were re-constituted with 1000mls ddH_20.
3. The opsonised E. coli and tryptan blue were pre-cooled on ice.
4. Fifty mls of lysing solution was prepared by adding 45 mls of ddH_20 to 5mls stock solution.
5. After pre-incubation with ammonia, 100 µL of blood was pipetted into tubes [5ml Falcon polystyrene round bottom tubes 12 x 75mm (Becton Dickinson)] A-D to quantify the phagocytosis. A-D were done in triplicate. Tubes B-D were used as the controls to set flow cytometry parameters.
6. Twenty µL of E.coli or 20 µL of neutrophil wash solution was then added to the 100 µL of blood in tubes A-D as shown in Table 3.1 and incubated in the waterbath for 20 minutes.
7. One hundred µL of tryptan blue was then added to each tube to quench the neutrophil phagocytosis.
8. The tubes were then filled with 2 mls of neutrophil wash solution and centrifuged at 4 °C at 516 g for 5 minutes. The supernatant was then removed carefully and

the cells re-washed with a further 2 mls of washing solution. The supernatant was once again removed after centrifugation.

9. Two mls of lysing solution was then added to lyse the red blood cells. The tubes were placed on the blood rotator to thoroughly mix the lysing solution with the blood cells for 5 mins and then left standing for a further 20 minutes.

10. The tubes were then centrifuged at 4 ^{o}C at 516 g and the lysing solution was removed. The cells (leucocytes) were then washed twice as before with neutrophil washing solution.

11. After the final wash, the supernatant was removed and 20 µL of anti- CD16-PE IgG_1 or 20 µL of neutrophil wash solution was added to tubes A-D as per Table 5.1. The tubes were then placed in a dark cupboard at room temperature for 1 hour.

12. The leucocytes were then re-washed twice with neutrophil wash solution.

13. After the second wash the supernatant was removed and the cells were re-suspended in 60 µL of neutrophil wash solution.

Tube No	Blood	E.coli - FITC	Anti- CD16-PE
A (Test sample)	100 µL	Yes	Yes
B	100 µL	No	Yes
C	100 µL	No	No
D	100 µL	Yes	No

Table 5.1

The experimental protocol for the phagocytosis experiments.

5.4.3.2 FLOW CYTOMETRY AND THE PHAGOTEST®

The cells were then analysed by flow cytometry [Fluorescent Activated Cell Sorting] (FACScan™, Becton Dickinson, UK) using Cellquest™ software using the blue-green excitation light (488 nm argon-ion laser) by forward scatter (FL1) and side scatter (FL2), and by FITC (FL1) and CD16-PE (FL2) on the gated population of granulocytes [Figure 5.2]. The control samples (B-D) were used to set markers for FL1 and FL2 so that less than 1% of the events are positive. The percentage of phagocytosing cells in the test sample could then be determined by counting the number of events above this marker position i.e. in the upper right quadrant [Figure 5.3]. The mean fluorescence correlated with the number of bacteria per individual granulocyte (geometric mean of fluorescence intensity).

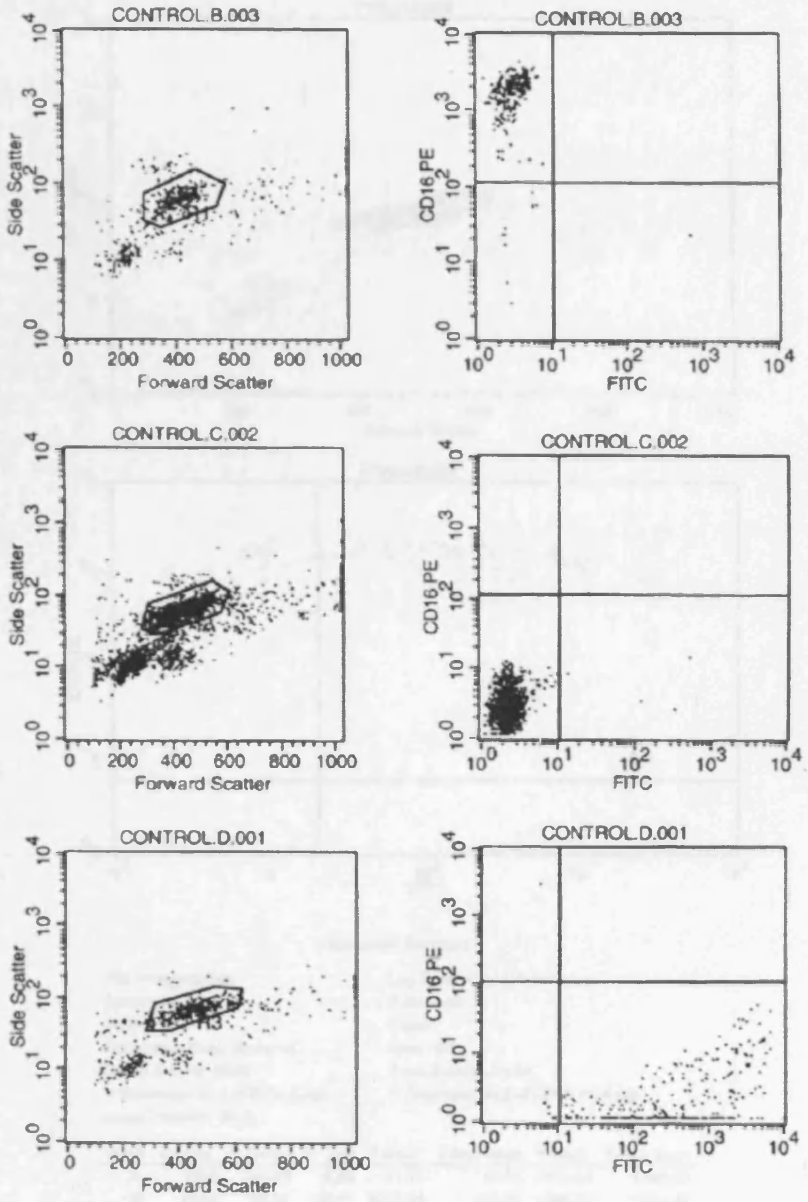

Figure 5.2

Plots generated from flow cytometry illustrating the gated population of granulocytes (left hand columns) and the plots obtained from the control samples [tube B (anti-CD16-PE control; top right plot), tube C (double negative control; middle right plot) and tube D (E.Coli control; bottom right plot)]

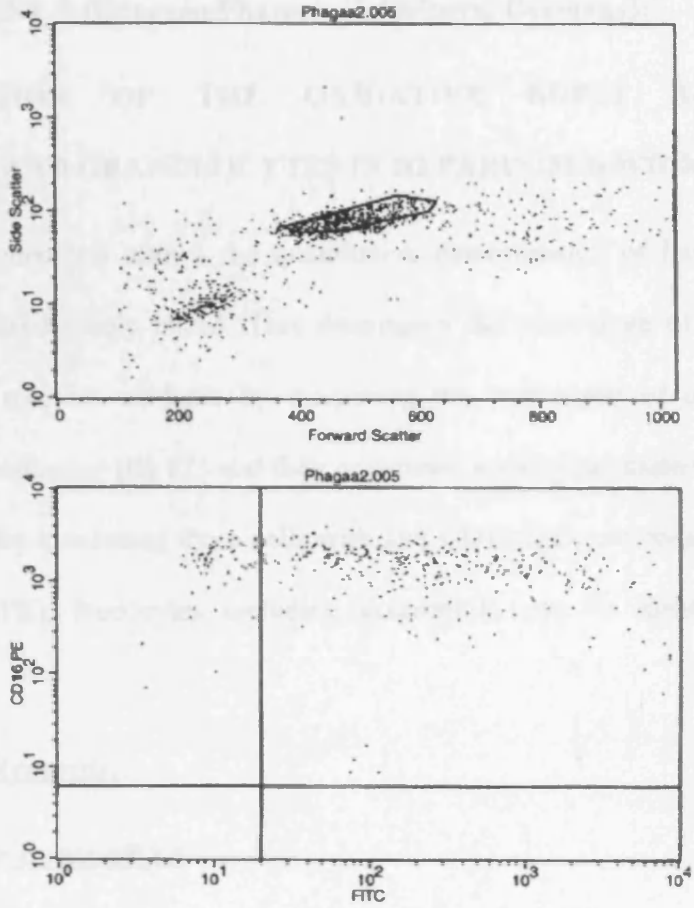

Quadrant Statistics

File: Phagaa2.005
Log Data Units: Linear Values
Sample ID:
Patient ID:
Tube:
Panel:
Acquisition Date: 29-Apr-4
Gate: G6
Gated Events: 8340
Total Events: 21699
X Parameter: FL1-H FITC (Log)
Y Parameter: FL2-H CD16 PE (Log)
Quad Location: 20, 6

Quad	Events	% Gated	% Total	X Mean	X Geo Mean	Y Mean	Y Geo Mean
UL	1358	16.28	6.26	11.17	10.51	1618.48	1586.84
UR	6965	83.51	32.10	1087.95	325.27	1525.92	1254.47
LL	1	0.01	0.00	9.06	9.06	1.20	1.20
LR	16	0.19	0.07	1198.09	337.54	2.80	2.46

Figure 5.3

A typical plot obtained from a test sample. In this case 83.51% of the neutrophils have undergone phagocytosis and have been gated in the right upper quadrant (lower panel).

5.4.3.3 BURSTEST ® (Orpegen Pharma, Heidelberg, Germany):

QUANTIFICATION OF THE OXIDATIVE BURST ACTIVITY OF MONOCYTES AND GRANULOCYTES IN HEPARINISED WHOLE BLOOD

This *in vitro* test allows the quantitative determination of leukocyte oxidative burst in heparinised whole blood. This determines the percentage of phagocytic cells which produce reactive oxidants by measuring the conversion of dihydrorhodamine (DHR) 123 to rhodamine (R) 123 and their enzymatic activity calculated as the amount of R 123 per cell. By incubating these cells with anti-CD16 IgG_1 antibodies labeled with R Phycoerythrin (PE), leucocytes including neutrophils, can be identified using flow cytometry.

Materials and Reagents:

Contained within Burstest® kit

- Opsonised non-labeled E. coli suspension (opsonised with immunoglobulin and complement of pooled sera).
- 100 µL containing the chemotactic synthetic peptide formyl-Met-Leu-Phe (fMLP) (200 x stock solution, 1mM). fMLP is a synthetic peptide that mimics the activity of bacterially-derived peptides with formylated N-terminal methionine groups.
- 100 µL containing phorbol 12-myristate 13-acetate (PMA) [200 x stock solution, 1.62mM]. PMA activates protein kinase C.
- Substrate disk (DHR 123) reconstituted in 1 ml of neutrophil washing solution.
- Lysing solution (contains diethylenglycol and formaldehyde).

- Neutrophil wash solution [Phosphate Buffered Saline (PBS) – salts (0.1M Sodium dihydrogen orthophosphate, 0.1M sodium chloride and 0.1M disodium hydrogen orthophosphate) reconstituted in 1000mls double distilled water (ddH_20)].

Other:

- Anti- CD16-PE IgG_1(IOTest®, Beckman Coulter)

Method:

The Burstest™ was performed according to the manufacturer's instructions, briefly:

1. Venous blood was collected from 12 fully consented healthy individuals in 4 ml vacuum tubes containing 68 iu lithium heparin (BD Vacutainer®). On average 30 mls was collected and placed immediately in ice for 10 minutes to pre-cool the neutrophils to 0 °C.

2. Neutrophil washing salts were re-constituted with 1000 mls ddH_20.

3. The opsonised E. coli was pre-cooled on ice.

4. Five µL of the PMA stock solution was added to 1ml of neutrophil wash solution.

5. Five µL of the fMLP stock solution was added to 1ml of neutrophil wash solution.

6. Fifty mls of lysing solution was prepared by adding 45 mls of ddH_20 to 5mls stock solution.

7. After pre-incubation with ammonia, 100 µL of blood was pipetted into tubes 5ml Falcon polystyrene round bottom tubes 12 x 75mm (Becton Dickinson) 1–7 to quantify the oxidative burst. 1-7 were done in triplicate. Tubes 3-7 were used as controls. 8.

Twenty μL of E.coli or 20 μL of neutrophil wash solution or 5 μL PMA (high neutrophil control stimulus) or 5 μL fMLP (low neutrophil control stimulus) was then added to the 100 μL of blood in tubes 1-7 as per Table 5.2 and incubated in the waterbath for 20 minutes.

9. Twenty μL of the substrate (DHR 123) was then added to tubes 1, 2, 3, 4 and 6 and 20 μL of neutrophil washing solution was added to tubes 5 and 7. The tubes were then incubated for a further 20 minutes in the waterbath.

10. The tubes were then filled with 2 mls of neutrophil wash solution and centrifuged at 4 ^{o}C at 516 g for 5 minutes. The supernatant was then removed carefully and the cells re-washed with a further 2mls of washing solution. The supernatant was once again removed after centrifugation.

11. Two mls of lysing solution was then added to lyse the red blood cells. The tubes were placed on the blood rotator to thoroughly mix the lysing solution with the blood cells for 5 mins and then left standing for a further 20 minutes.

12. The tubes were then centrifuged at 4 ^{o}C at 516 g and the lysing solution was removed. The cells (leucocytes) were then washed twice as before with neutrophil washing solution.

13. After the final wash, the supernatant was removed and 20 μL of anti- CD16-PE IgG_1 or 20 μL of neutrophil wash solution was added to tubes 1-7 described in Table 5.2. The tubes were then placed in a dark cupboard at room temperature for 1 hour.

14. The leucocytes were then re-washed twice with neutrophil wash solution.

15. After the second wash the supernatant was removed and the cells were re-suspended in 60 µL of neutrophil wash solution.

Tube No	Blood	E.coli - FITC	PMA/fMLP	Substrate	Anti- CD16-PE
1 (Test Sample)	100 µL	YES		YES	YES
2 (Resting oxidative burst)	100 µL	NO		YES	YES
3 (High neutrophil stimulus)	100 µL	NO	PMA	YES	YES
4 (low neutrophil stimulus)	100 µL	NO	fMLP	YES	YES
5	100 µL	NO		NO	YES
6	100 µL	YES		YES	NO
7	100 µL	NO		NO	NO

Table 5.2

The experimental protocol for the oxidative burst experiments.

5.4.3.4 FLOW CYTOMETRY AND THE BURSTEST®

The cells were then analysed by flow cytometry [Fluorescent Activated Cell Sorting] (FACScan™, Beckton Dickinson, UK) using Cellquest™ software using the blue-green excitation light (488 nm argon-ion laser) by forward scatter (FL1) and side scatter (FL2), and by R 123 (FL1) and CD16-PE (FL2) on the gated population of granulocytes. The control samples (tubes 5-7) were used to set markers for FL1 and FL2 so that less than 1% of the events are positive. The percentage of granulocytes that have produced reactive oxygen metabolites in the test sample could then be determined by counting the number of events above this marker position i.e. in the upper right quadrant (Figure 5.4). The mean fluorescence correlated with the oxidation quantity per individual leucocyte. Figure 5.5 shows the resting oxidative burst plots obtained and Figure 5.6 shows the plot obtained from PMA (high neutrophil stimulus) and fMLP (low neutrophil stimulus). Figure 5.7 shows the plots obtained from the control tubes used to set the flow cytometry parameters.

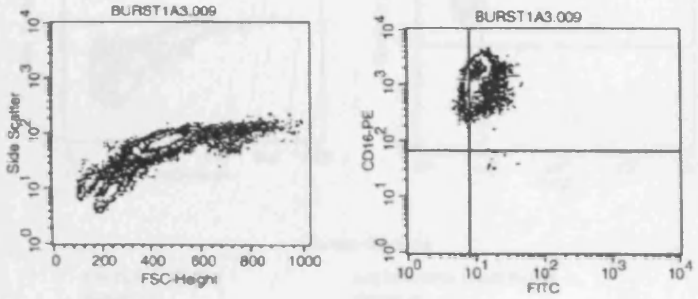

Quadrant Statistics

File: BURST1A3.009
Log Data Units: Linear Values
Sample ID:
Patient ID:
Tube:
Panel:
Acquisition Date: 19-Feb-4
Gate: G4
Gated Events: 10376
Total Events: 24248
X Parameter: FL1-H FITC (Log)
Y Parameter: FL2-H CD16-PE (Log)
Quad Location: 8, 65

Quad	Events	% Gated	% Total	X Mean	X Geo Mean	Y Mean	Y Geo Mean
UL	1658	15.98	6.84	6.96	6.90	829.03	882.07
UR	8486	81.78	35.00	14.66	13.20	1477.17	1198.93
LL	24	0.23	0.10	6.61	6.53	38.62	32.11
LR	208	2.00	0.86	22.36	19.79	41.15	37.84

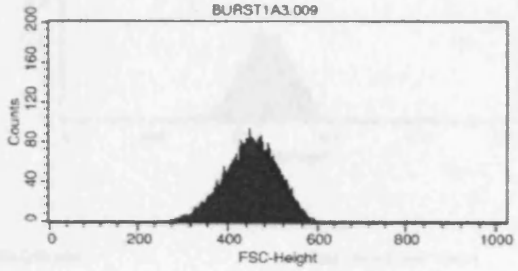

Histogram Statistics

File: BURST1A3.009
Log Data Units: Linear Values
Sample ID:
Patient ID:
Tube:
Panel:
Acquisition Date: 19-Feb-4
Gate: G4
Gated Events: 10376
Total Events: 24248
X Parameter: FSC-H FSC-Height (Linear)

Marker	Left, Right	Events	% Gated	% Total	Mean	Geo Mean	CV	Median	Peak Ch
All	0, 1023	10376	100.00	42.79	446.86	443.27	12.47	449.00	445

Figure 5.4

A typical plot obtained from FITC-labeled, E.coli challenged neutrophils. In this case 81.78% of neutrophils have undergone oxidative burst and have been gated in the right upper quadrant (top right panel).

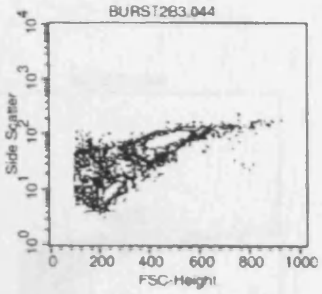

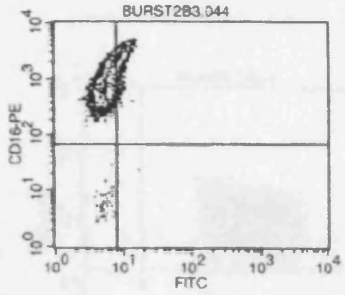

Quadrant Statistics

File: BURST2B3.044
Sample ID:
Tube:
Acquisition Date: 19-Feb-4
Gated Events: 10091
X Parameter: FL1-H FITC (Log)
Quad Location: 8, 65

Log Data Units: Linear Values
Patient ID:
Panel:
Gate: G4
Total Events: 19233
Y Parameter: FL2-H CD16-PE (Log)

Quad	Events	% Gated	% Total	X Mean	X Geo Mean	Y Mean	Y Geo Mean
UL	6745	66.84	35.07	5.67	5.50	952.61	774.61
UR	2688	26.64	13.98	10.25	10.06	2605.56	2219.62
LL	546	5.41	2.84	5.44	5.25	12.87	8.32
LR	112	1.11	0.58	12.11	11.57	22.06	18.00

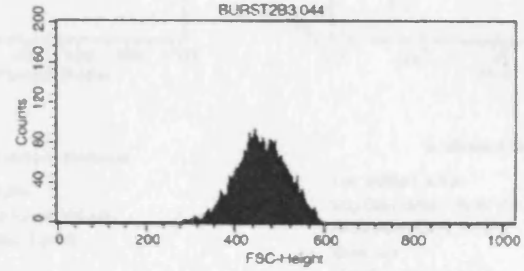

Histogram Statistics

File: BURST2B3.044
Sample ID:
Tube:
Acquisition Date: 19-Feb-4
Gated Events: 10091
X Parameter: FSC-H FSC-Height (Linear)

Log Data Units: Linear Values
Patient ID:
Panel:
Gate: G4
Total Events: 19233

Marker	Left, Right	Events	% Gated	% Total	Mean	Geo Mean	CV	Median	Peak Ch
All	0, 1023	10091	100.00	52.47	454.54	451.44	11.55	455.00	442

Figure 5.5

A typical plot obtained from a FITC-labeled tube with no bacteria added (resting burst activity). In this case, 26.64% of neutrophils have undergone oxidative burst in the resting state and have been gated in the right upper quadrant (top right panel).

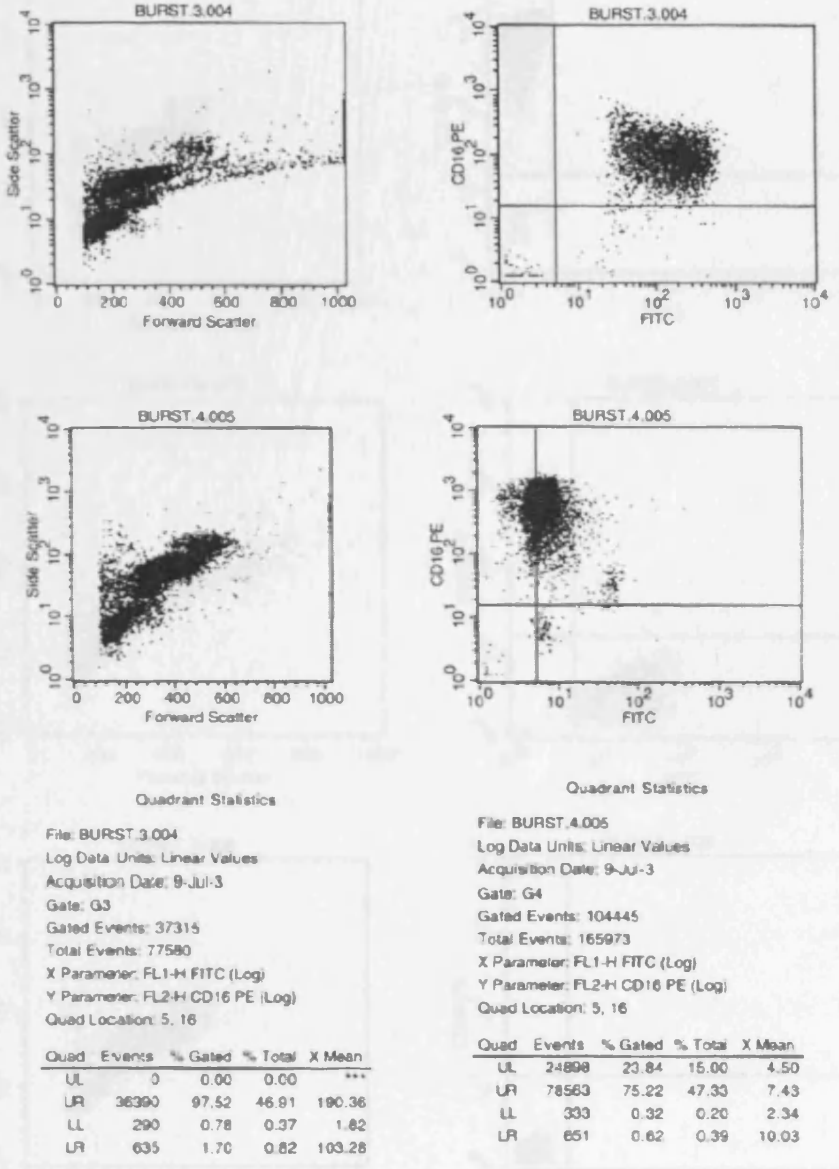

Quadrant Statistics

File: BURST.3.004
Log Data Units: Linear Values
Acquisition Date: 9-Jul-3
Gate: G3
Gated Events: 37315
Total Events: 77580
X Parameter: FL1-H FITC (Log)
Y Parameter: FL2-H CD16 PE (Log)
Quad Location: 5, 16

Quad	Events	% Gated	% Total	X Mean
UL	0	0.00	0.00	***
UR	36390	97.52	46.91	190.36
LL	290	0.78	0.37	1.82
LR	635	1.70	0.82	103.28

Quadrant Statistics

File: BURST.4.005
Log Data Units: Linear Values
Acquisition Date: 9-Jul-3
Gate: G4
Gated Events: 104445
Total Events: 165973
X Parameter: FL1-H FITC (Log)
Y Parameter: FL2-H CD16 PE (Log)
Quad Location: 5, 16

Quad	Events	% Gated	% Total	X Mean
UL	24898	23.84	15.00	4.50
UR	78563	75.22	47.33	7.43
LL	333	0.32	0.20	2.34
LR	651	0.62	0.39	10.03

Figure 5.6

A typical plot obtained from a FITC-labeled tube exposed to PMA (high neutrophil stimulus) and fMLP (low neutrophil stimulus). In this case, 97.52% of neutrophils have undergone oxidative burst with PMA and 75.22% with fMLP.

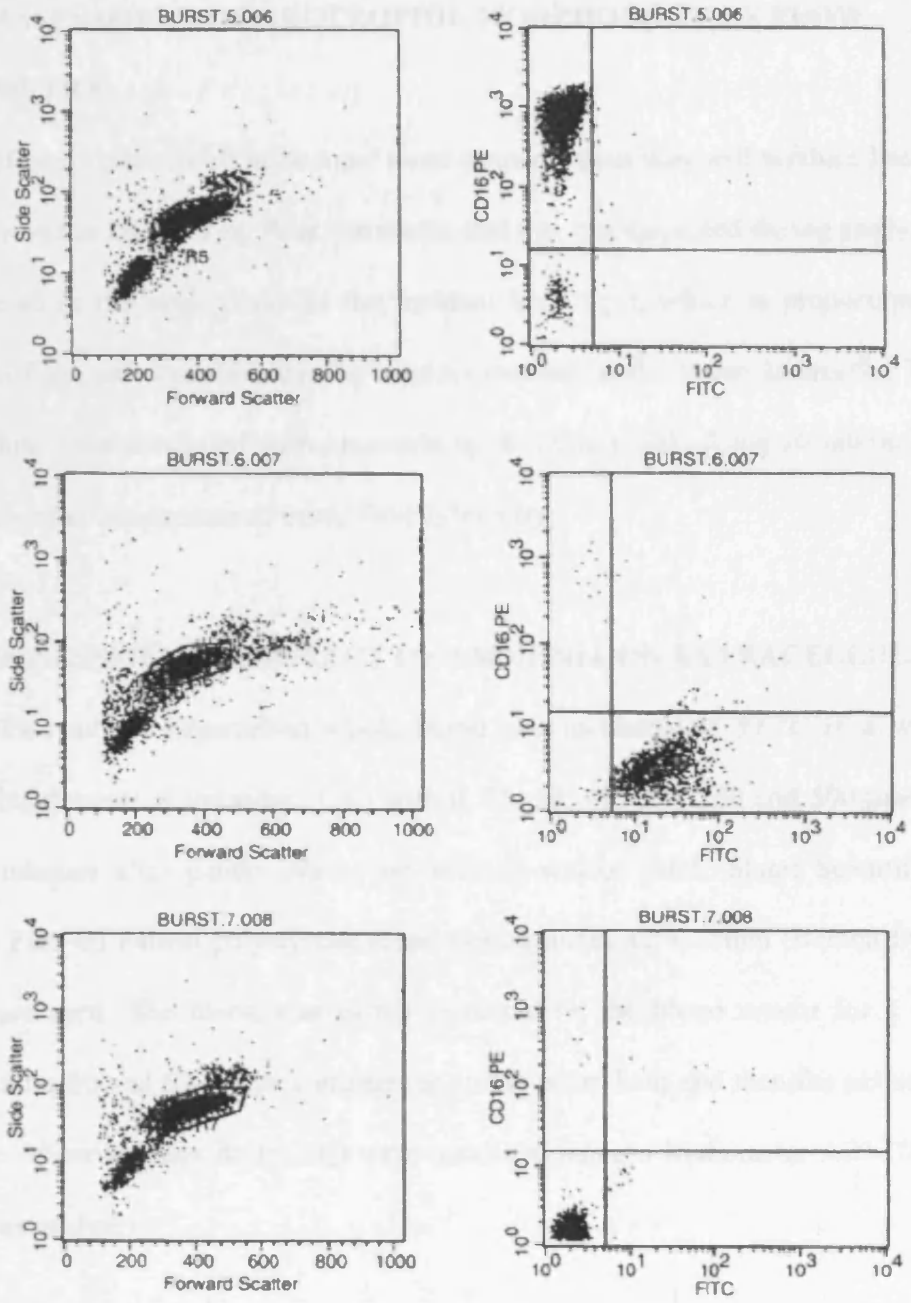

Figure 5.7

Plots generated from flow cytometry used to set the flow cytometry parameters. The top panels show the anti-CD16-PE control, the middle panels show the E.Coli control and the lower panels show the double negative control.

5.4.3.5 ASSESSMENT OF NEUTROPHIL MORPHOLOGY BY FLOW CYTOMETRY

If neutrophils swell or become more rounded, then they will produce less forward scatter from the laser during flow cytometry and this can measured during analysis. Light is scattered in the same plane as the incident laser light, which is proportional to the volume of the cell therefore can be used to measure cell volume indirectly. Therefore neutrophils were incubated with ammonia up to 75 μM NH_4Cl for 90 minutes and the forward scatter was measured using flow cytometry.

5.4.3.6 ASSESSMENT OF EFEECT OF AMMONIA ON EXTRACELLULAR pH

Two mls of heparinised whole blood was incubated at 37 ^{o}C in a water bath (Grant Instruments, Cambridge, UK) with 0, 25, 50, 75, 100, 250 and 500 μmol NH_4Cl for 90 minutes after gentle mixing on a blood rotator (SB1, Stuart Scientific) for 1 minute. Five ml Falcon polystyrene round bottom tubes 12 x 75mm (Becton Dickinson, UK) were used. The blood was gently re-mixed on the blood rotator for a further 1 minute after 30 and 60 minutes incubation in the water bath and then the pH and partial pressure of carbon dioxide (pCO_2) were measured using a Radiometer ABL 700 Series blood gas analyzer.

5.4.3.7 ASSESSMENT OF NEUTROPHIL APOPTOSIS/DEATH

5.4.3.7.1 TRYPAN BLUE EXCLUSION TEST

After diluting trypan blue (Sigma) 1 in 10 with neutrophil wash solution, 400 μL of diluent was added to 400 μL of neutrophils re-suspended in wash solution which had

been pre-incubated with 0 or 500 μM NH_4Cl and isolated. Twenty microlitres of neutrophil mixture was then examined on a haemocytometer slide (Assistent, Thoma) and the number of blue-stained cells counted under a light microscope. Blue-stained cells were counted as non-viable.

5.4.3.7.2 ANNEXIN V-FITC AND PROPIDIUM IODIDE

To ensure that neutrophil function was not impaired through the induction of apoptosis, an experiment was performed using Annexin V-FITC (BD Pharminogen) and Propidium Iodide [BD Pharminogen]. Annexin V-FITC is a sensitive probe for identifying apoptotic cells (244-246) and binds negatively charged phospholipid surfaces (Kd of ~ 5 x 10^{-2}) (247) with a higher specificity for phosphatidylserine than most other phospholipids. Phosphatidylserine is principally associated with the inner leaflet of the plasma membrane bilayer. Annexin V-FITC is used quantitatively to determine the percentage of cells undergoing apoptosis. Therefore, it relies on the property of cells to lose membrane asymmetry in the early phases of apoptosis. In apoptotic cells, the membrane phospholipid phosphatidylserine is translocated from the inner leaflet of the plasma membrane to the outer leaflet, thereby exposing phosphatidylserine to the external environment. Propidium iodide is used to assess plasma membrane integrity in Annexin V apoptosis assays (246). It is a fluorescent dye that stains DNA. It does not cross the plasma membrane of cells that are viable or in the early stages of apoptosis because they maintain plasma membrane integrity. In contrast those cells in the late stages of apoptosis or already dead have lost plasma membrane integrity and are permeable to propidium iodide. Propidium iodide is detected in the orange range of the spectrum using a 562-588

nm band pass filter. Cells that stain positive for Annexin V-FITC and negative for propidium iodide are undergoing apoptosis. Cells that remain positive for both Annexin-V-FITC and propidium iodide are either in the end stage of apoptosis, undergoing necrosis, or already dead. Cells that stain negative for both are alive and not undergoing measurable apoptosis.

Two experiments were performed. The first assessed apoptosis/cell death and the duration of incubation with ammonia, and the second assessing the relationship between concentration of ammonia and apoptosis/cell death.

5.4.3.7.2.1 APOPTOSIS/ DEATH AND TIME

1. Four mls of blood was collected in a heparinised tube and immediately 2 mls of blood was aliquoted into 2 x 5ml Falcon polystyrene round bottom tubes 12 x 75mm (Becton Dickinson, UK) and incubated in a water bath at 37 °C. One tube contained 100 µL of 10mM NH_4Cl giving a final concentration of 500 µM NH_4Cl and the other 100 µL of neutrophil wash solution as a control. A positive control was also prepared which consisted of 20 µL of lipopolysaccharide (E. coli 0111:B4, Sigma) 5 mg/mL in 2 mls of blood. All the tubes were left to incubate in the waterbath for 30 mins.

2. One hundred µL of blood was then removed immediately and every 30 mins thereafter for 5 hours with gentle inversion of the tube every 30 mins at sampling.

3. The red cells in the timed samples were lysed with 2 mls of lysing solution. The tubes were gently mixed for 1 minute by inversion and then left standing for a further 20 minutes.

4. The tubes were then centrifuged at 4 °C at 516 g and the lysing solution was removed. The cells (leucocytes) were then washed twice as before with neutrophil washing solution.

4. After the final wash, the supernatant was removed and the cells were re-suspended in 100 µL of binding buffer (10mM Hepes/NAOH, pH 7.4, 140mM NaCl, 2.5 mM $CaCl_2$).

5. In a FACS tube, 5 µL of Annexin V-FITC and 10 µL of propidium iodide were added and gently mixed. The tubes were then incubated for 15 minutes at room temperature (20-25 °C) in the dark. Control tubes containing neither Annexin V-FITC nor propidium iodide (double negative), Annexin V-FITC only and propidium iodide only were also prepared to set the flow cytometry parameters.

6. The tubes were then analysed by flow cytometry.

5.4.3.7.2.2. APOPTOSIS AND AMMONIA CONCENTRATION

Following the same protocol above, an experiment was performed in which 2 mls of blood was incubated at 37 °C in a waterbath for 90 minutes with varying concentrations of ammonia ranging from 0 to 500 µM NH_4Cl.

5.4.3.8 ASSESSMENT OF CD11b EXPRESSION

The Phagotest® and Burstest® were repeated using anti-CD11b (BD Pharminogen) instead of anti-CD16 as a neutrophil marker. CD11b (or C3b receptor) is the alpha chain of the integrin Mac-1, a ligand for the intercellular adhesion molecule (ICAM). This was performed to assess whether ammonia impairs the expression of this neutrophil cell surface marker, as this receptor allows the neutrophil to bind to ICAM-1

on the endothelium which is a critical step in allowing the neutrophil to bind and transmigrate the endothelium. (248;249)

5.4.4 ASSESSMENT OF LEUCOCYTE AMMONIA CONTENT

1. Six mls of blood was collected in a heparinised tube and immediately 2 mls of blood was aliquoted into 3 x 5 ml Falcon polystyrene round bottom tubes 12 x 75 mm (Becton Dickinson, UK) in a water bath at 37 °C. One tube contained 100 µL of 10 mM NH_4Cl giving a final concentration of 500 µM NH_4Cl, one tube contained 15 µL of 10mM NH_4Cl with 85 µL of neutrophil wash solution giving a final concentration of 75 µM NH_4Cl and the other 100 µL of neutrophil wash solution as a control.

2. The blood was incubated at 37 °C in a water bath for 90 minutes after gentle mixing on a blood rotator for 1 minute. The blood was gently re-mixed on the blood rotator for a further 1 minute after 30 and 60 minutes incubation in the water bath.

3. The red cells were lysed with 2 mls of lysing solution. The tubes were gently mixed for 1 min by inversion and then left standing for a further 20 minutes.

4. The tubes were then centrifuged at 4 °C at 316 g and the lysing solution was removed. The cells (leucocytes) were then washed twice as before with neutrophil washing solution.

4. After the final wash, the supernatant was removed and the cells were re-suspended in 400 µL neutrophil wash solution.

5. Twenty µL was then added to a haemocytometer (Assistent, Thoma) and the numbers of cells were counted under a light microscope.

6. Fifty µL was then removed from each sample and added to 15 µL of 5% trichloroacetic acid.

7. This was then freeze thawed three times in a -80 °C freezer to homogenize the cells and then spun in a microcentrifuge at 11,200 g at 4 °C for 10 minutes.

8. Fifty µL of the supernatant was pipetted out onto a 96 well plate at 30 °C for 3 hours in 200 µL of a solution containing phenol (10 mM), nitroprusside (10 mM), sodium hypochlorite (10 mM) solution and sodium hydroxide (0.5 mM).

9. The blue colour formed by reaction of ammonia with phenol and hypochlorite was then measured colorimetrically at 630nm. This was read in a 96 well plate reader (Tecan Sunrise, Salzburg, Austria).

10. Each sample was analysed in duplicate and compared to an ammonium chloride standard curve (Figure 3.1).

11. The ammonia content of each neutrophil was then calculated in nM.

5.4.5 CO-INCUBATION WITH AMMONIA AND DIFLUOROMETHYL ORNITHINE (DFMO) AND OXIDATIVE BURST

1. Two mls of heparinised whole blood was incubated at 37 °C in a waterbath with either 10 mM DFMO (Sigma) or with 100 µL of neutrophil washing solution as a control, and 75 µM NH_4Cl for 90 minutes after gentle mixing on a blood rotator for 1 minute. Mixing was repeated for 1 minute after 30 and 60 minutes incubation.

2. The Burstest® was then performed and the results were analysed by flow cytometry.

5.4.6 MYELOPEROXIDASE ASSAY

This is a classical guaiacol peroxidation assay.(250;251) It is affected by the presence of even a small number of eosinophils since eosinophils have an even higher peroxidase activity (EPO) and content than neutrophils, therefore this assay utilizes 3-amino-1,2,4-triazole [AMT] (Sigma) which inhibits EPO.

1. Blood was incubated with 0, 75 or 300 μM ammonia for 90 mins and the neutrophils were isolated using polymorphoprep™ .
2. The neutrophils were then re-suspended in 400 μL of neutrophil wash solution and then 20 μL was placed on a haemocytometer and the cells counted under a light microscope.
3. The myeloperoxidase buffer was then prepared by adding 0.02% w/v cetyltrimethylammonium bromide [CTAB] (Sigma) and 13 mM guaiacol (sigma) to 200 mls of phosphate-buffered saline, pH 7.0.
4. Three mls of MPO buffer was then added to a cuvette, along with 50,000 neutrophils and 6 μL of 2 mM AMT.
5. The reaction was then started by adding 4 μL of 1 μM of hydrogen peroxide (Sigma) whilst the reaction mixture was maintained at 37 °C by a heated mount and the increase in optical density was followed kinetically at 470 nm using a spectrophotometer.

5.5 RESULTS

In the presentation of this work on neutrophils, there are components of the research that employ by the very nature of the methodology, a mixed granulocyte or leucocyte population. When the former is the case, the term neutrophils will be used in the description as >95% of the cells isolated are likely to be neutrophils (the remaining small fraction of granulocytes will be basophils and eosinophils). In the later case, the cell population will be identified as leucocytes, 70% of which will be neutrophils, the remainder of which will be mainly lymphocytes.

5.5.1 AMMONIA AND PHAGOCYTOSIS

Phagocytosis was significantly impaired by 12-20% following incubation with 75 μM NH_4Cl (0 versus 75 μM NH_4Cl; $p<0.0005$ Mann Whitney). The critical ammonia concentration which had a significant effect on phagocytosis was 75 μM and the additional effect of 100 - 500 μM was only marginally more detrimental. Two distinct neutrophil populations were seen, one functioning more optimally than the other. [Figure 5.8] The sub-optimal population increased with rising ammonia concentration. That is, the number of neutrophils which were CD16 positive (functional) but did not express FITC, increased with rising ammonia concentration. This can be seen clearly in Figure 5.9 which shows that only 59.63% of neutrophils are 'optimally' phagocytosing (neutrophils fall in the right upper quadrant) whilst 35.99% are falling in the left upper quadrant (sub-optimal) following incubation with 500 μM NH_4Cl.

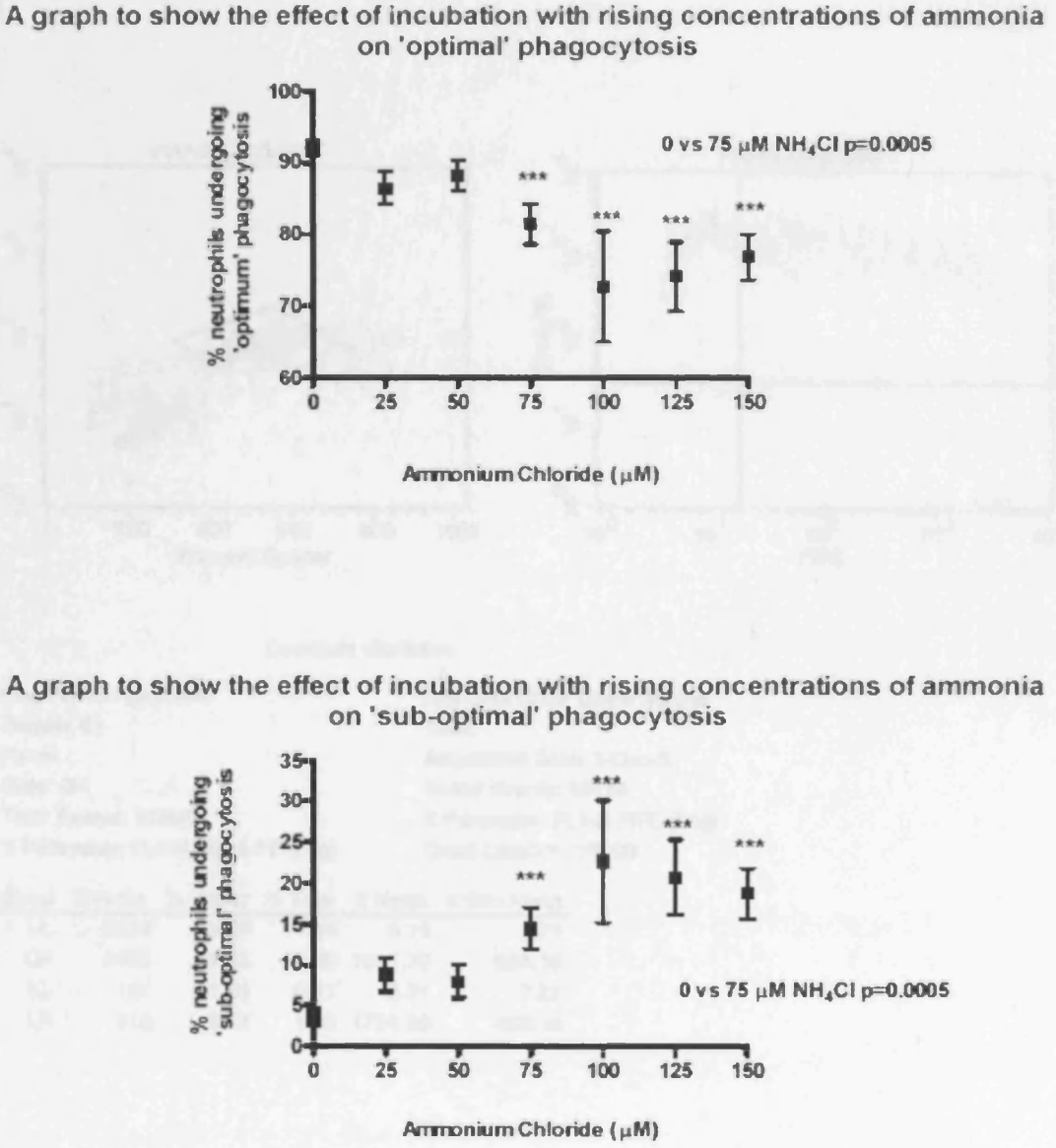

Figure 5.8

Graphs showing the percentage of neutrophils undergoing 'optimal' (above) and 'sub-optimal' (below) phagocytosis, following incubation with 0 – 150 μM ammonium chloride (NH_4Cl).

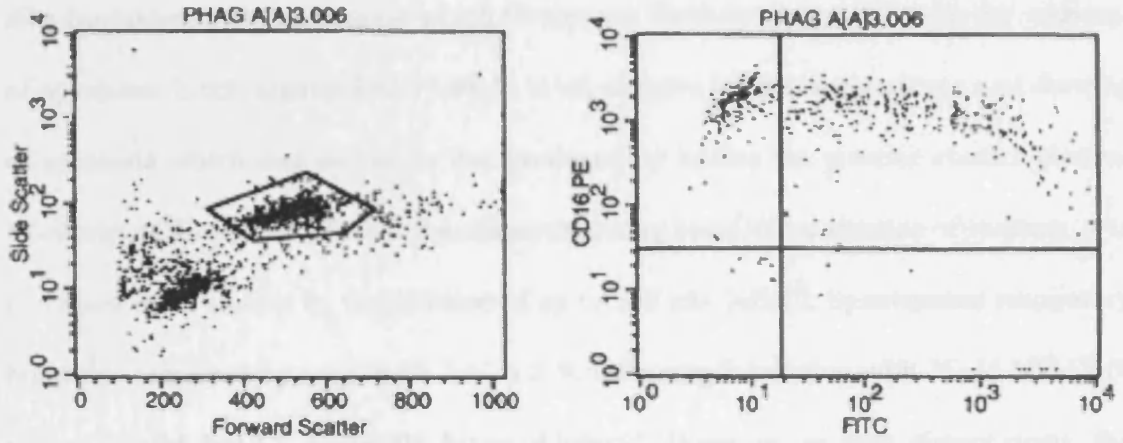

Quadrant Statistics

File: PHAG A[A]3.006
Sample ID:
Panel:
Gate: G4
Total Events: 30865
Y Parameter: FL2-H CD16 PE (Log)
Log Data Units: Linear Values
Tube:
Acquisition Date: 8-Dec-3
Gated Events: 10154
X Parameter: FL1-H FITC (Log)
Quad Location: 18, 30

Quad	Events	% Gated	% Total	X Mean	X Geo Mean
UL	3654	35.99	11.84	8.19	7.71
UR	6055	59.63	19.62	1011.79	294.18
LL	127	1.25	0.41	9.21	7.27
LR	318	3.13	1.03	1758.90	453.16

Figure 5.9

Typical flow cytometry plots to demonstrate the 'optimal' (top right quadrant of top right cytometry plot [UR]) and 'sub-optimal' (top left quadrant of top right cytometry plot [UL]) neutrophil populations following incubation for 90 minutes with 500 μM ammonium chloride (NH_4Cl).

5.5.2 AMMONIA AND OXIDATIVE BURST

Oxidative burst was determined using the Burstest® (Orpegen Pharma) which measures the percentage of neutrophils that produce reactive oxidants converting dihydrorhodamine to rhodamine which fluoresces. Oxidative burst following the addition of opsonised E.coli approached 95-98 % in all samples in both the presence and absence of ammonia which was similar to that produced by adding the positive control phorbol 12-myristate 13-acetate (PMA). Spontaneous resting burst in the absence of bacteria, was increased in all studies by the addition of up to 500 μM NH_4Cl. Spontaneous respiratory burst was increased by a mean 10.7 +/- 1.8 % following incubation with 75μM NH_4Cl (0 versus 75 μM NH_4Cl; $p<0.0005$ Mann Whitney). However, as with phagocytosis, the critical ammonia concentration which had a significant effect on inducing spontaneous respiratory burst was 75 μM and the additional effect of 100 - 500 μM was only marginally greater.

5.5.3 AMMONIA AND NEUTROPHIL MORPHOLOGY ASSESSED BY FLOW CYTOMETRY

Following isolation and incubation with 75μM NH_4Cl for 90 minutes the forward scatter of the neutrophils was measured using flow cytometry. The mean of the forward scatter and standard error for 100,000 gated neutrophils was 509 +/- 4.9 for controls versus 502.7 +/- 3.8 for neutrophils incubated with 75 μM NH_4Cl ($p=0.02$ Mann Whitney). The ammonia-incubated neutrophils were 2 % bigger than controls on flow cytometry of 100,000 gated neutrophils, most likely to represent cell swelling.

5.5.4 THE EFEECT OF AMMONIA ON EXTRACELLULAR pH

The pH and partial pressure of carbon dioxide (pCO_2) were measured using a Radiometer ABL 700 Series blood gas analyzer on whole blood samples with 0 - 500 μM NH_4Cl, to assess for changes in extracellular pH resulting from incubating whole blood, and thus the neutrophils, with ammonia. There were no detectable differences in either extracellular pH or pCO2 between controls and whole blood incubated with up to 500 μM NH_4Cl from which the neutrophils were isolated 90 minutes later [Figure 5.10].

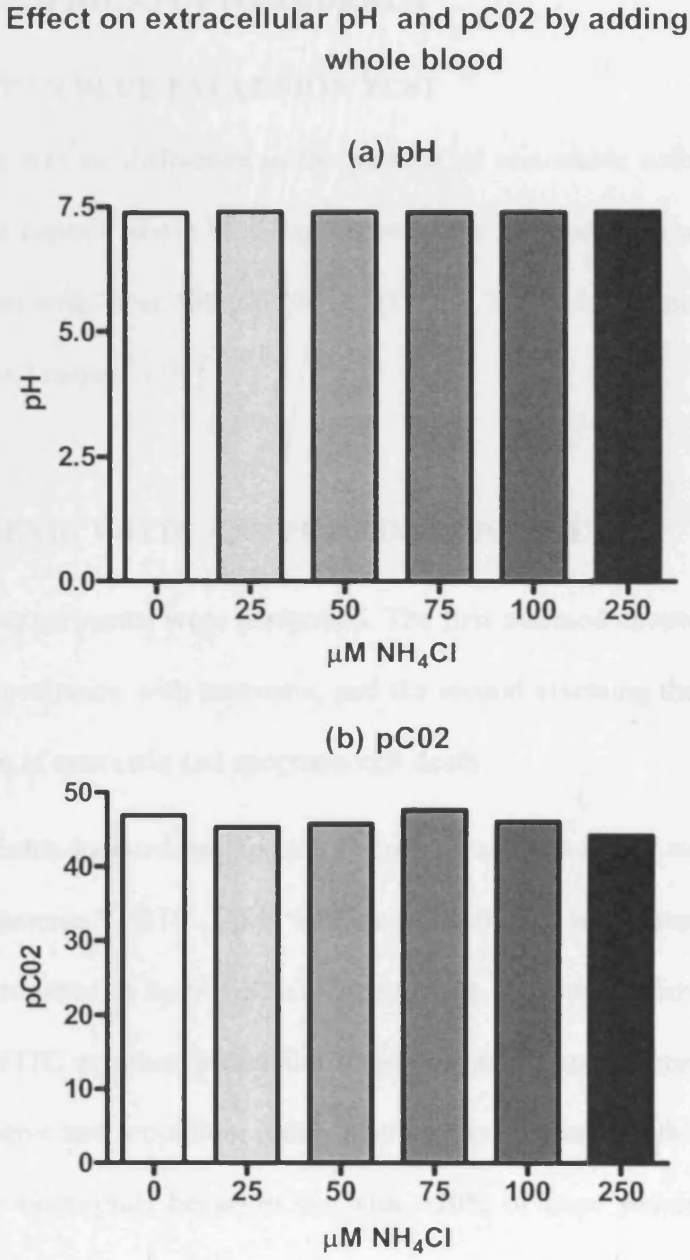

Figure 5.10

Graphs to show the effect on extracellular (a) pH and (b) pCO2 of adding 0 – 500 μM NH_4Cl to whole blood from which the neutrophils are isolated.

5.5.5 NEUTROPHIL APOPTOSIS/DEATH

5.5.5.1 TRYPAN BLUE EXCLUSION TEST

There was no difference in the number of non-viable cells between neutrophils isolated from control whole blood and neutrophils isolated from whole blood incubated for 90 minutes with 75 or 500 μM NH_4Cl [1.57, 1.78 and 1.77% non-viable for 0, 75 and 500 μM NH_4Cl respectively].

5.5.5.2 ANNEXIN V-FITC AND PROPIDIUM IODIDE

Two experiments were performed. The first assessed apoptosis/cell death and the duration of incubation with ammonia, and the second assessing the relationship between concentration of ammonia and apoptosis/cell death.

Ammonia-induced apoptosis or necrosis was excluded by staining with propidium iodide and annexin V-FITC. Up to 5 hours of incubation in a waterbath at 37 °C with 75 μM NH_4Cl resulted in only 1-2% of neutrophils showing evidence of early apoptosis (annexin V-FITC positive, propidium iodide negative) and necrosis/cell death (annexin V-FITC positive and propidium iodide positive) as measured with flow cytometry. After 5 hours, the neutrophils began to die with >20% of them staining positive with both annexin V-FITC and propidium iodide as measured with flow cytometry. Furthermore, incubation with ammonia for up to 120 minutes at concentrations of NH_4Cl up to 500 μM did not induce apoptosis or cell death and this cannot therefore account for the impairment in phagocytosis or increase in spontaneous respiratory burst activity.

5.5.6 NEUTROPHIL CD11b EXPRESSION

The Phagotest® and Burstest® were repeated using anti-CD11b (BD Pharminogen) instead of anti-CD16 as a neutrophil marker. This was performed to assess whether ammonia impaired the expression of this neutrophil cell surface marker, as this receptor allows the neutrophil to bind to ICAM-1 on the endothelium which is a critical step in allowing the neutrophil to bind and transmigrate the endothelium. Incubation with up to 500 μM NH_4Cl however, did not alter the expression of CD11b during phagocytosis and oxidative burst tests as analysed by flow cytometry.

5.5.7 INTRACELLULAR NEUTROPHIL AMMONIA CONCENTRATION

The intracellular neutrophil ammonia concentration was calculated from 7.6×10^6 granulocytes isolated with Polymorphoprep™. The mean intracellular neutrophil ammonia concentration following 90 minute incubation with and without ammonia, were 0.26 nM in controls and 0.32 nM following incubation with both 75 μM and 500 μM NH_4Cl. This demonstrates that ammonia is taken up by the neutrophil during the incubation period but that this does not rise beyond 0.32 nM with increasing extracellular ammonia concentration.

5.5.8 DIFLUOROMETHYLORNITHINE HYDROCHLORIDE (DFMO) AND OXIDATIVE BURST

Whole blood was incubated with the ornithine decarboxylase inhibitor DFMO with and without 75 μM NH_4Cl. DFMO partially inhibits respiratory burst which is crucial in the production of polyamines and reactive oxygen species. The ammonia-

induced increase in spontaneous burst activity was prevented by the addition of DFMO and both control and ammonia-incubated neutrophils showed reduced respiratory burst [Figure 5.11]. Therefore the inhibition of ornithine decarboxylase negated the increased spontaneous respiratory burst activity induced by ammonia. DFMO did not affect phagocytosis.

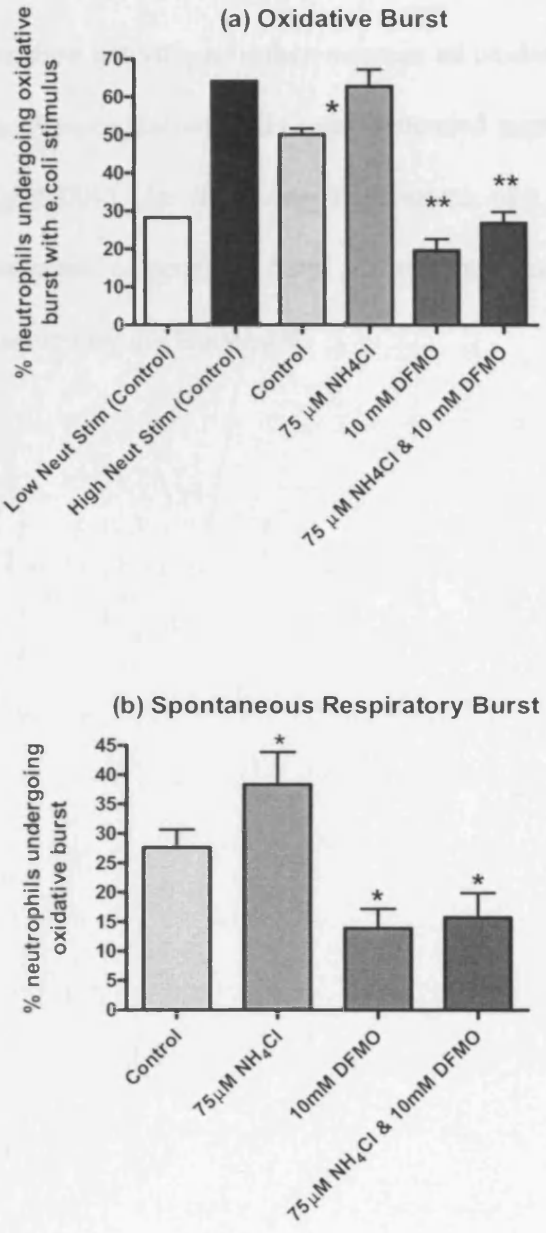

Figure 5.11

Graphs showing the effect of incubation of 75 μM NH_4Cl on (a) induced and (b) spontaneous oxidative burst with and without the ornithine decarboxylase inhibitor DFMO.

* $p < 0.05$; ** $p < 0.001$

5.5.9 AMMONIA AND MYELOPEROXIDASE ACTIVITY

Myeloperoxidase activity, a further measure of oxidative burst, was measured by the classical guaiacol peroxidation assay and increased significantly with incubation of 75 μM NH_4Cl ($p<0.001$). In the same experiment, the percentage of neutrophils undergoing spontaneous respiratory burst at rest increased from 6.54 to 21.62% ($p<0.0005$), as measured by the Burstest®.

5.6 DISCUSSION

These observational studies examining the effect of ammonia on neutrophil function have shown that the presence of ammonia is detrimental to the ability of neutrophils to phagocytose and that ammonia induces spontaneous respiratory burst in unstimulated neutrophils. Myeloperoxidase activity, a measure of oxidative burst, increased significantly in the presence of ammonia but an inhibitor of ornithine decarboxylase, an enzyme crucial in the production of polyamines and reactive oxygen species, prevented ammonia-induced increases in respiratory burst activity. This occurred in the absence of an extracellular pH change, and without any evidence of increased apoptosis or early cell death. The intracellular ammonia concentration has been shown to rise and the neutrophil morphology changes, with cells appearing to become more rounded as a result of swelling on flow cytometry. Furthermore, the expression of CD11b surface receptors did not change in the presence of ammonia making it unlikely that the ability of the neutrophil to bind to ICAM-1 on the endothelium is impaired.

These studies provide the first direct evidence that ammonia, in concentrations which are commonly found in both acute and chronic liver dysfunction, impairs the morphology and function of neutrophils in the absence of the other physiological and biological factors which may contribute to neutrophil dysfunction in liver disease. Therefore, the presence of hyperammonemia is likely to represent yet another insult on these already poorly functioning neutrophils, reducing the response to microbial challenge and increasing susceptibility to infection. Hyperammonemia is commonly associated with hepatic encephalopathy and accompanies gastrointestinal bleeding, both conditions being associated with a high incidence of sepsis and mortality (124). Therefore

one might postulate that in addition to infection making a cirrhotic individual more susceptible to the cerebral effects of hyperammonemia, that hyperammonemia itself might also make them more susceptible to the development of infection. Moreover, as ammonia induces spontaneous respiratory burst in resting neutrophils, then this may account in part for the raised levels of proinflammatory cytokines and inflammatory markers measured in cirrhotic individuals even in the absence of overt infection when repeated cultures are negative. This adds another dimension to the synergistic relationship between ammonia and infection in the pathogenesis of hepatic encephalopathy and supports my hypothesis.

Clearly these studies are observational ones and the mechanisms which lead to the ammonia-induced impairment in neutrophil function have yet to be fully elucidated. The changes in neutrophil morphology shown on flow cytometry hint that neutrophil swelling could be important in their reduced ability to phagocytose but also the activation of key oxidative enzymes must be important. We had hoped to have examined the morphological changes in the neutrophils more specifically with electron microscopy before and after incubation with ammonia, allowing for the cytoskeleton and cell volumes to be observed, however, the images obtained showed that the cell membranes had been damaged in the processing of the neutrophils for electron microscopy.

Ammonia freely passes into the neutrophil cytosol and one possibility is that it may activate intracellular signalers such as mitogen-activated protein (MAP) kinases; p38-MAP kinase ($p38^{-MAPK}$), Jun-kinase (JNK) and extracellular signal-regulated kinase (ERK) (179). Inflammatory stimuli activate these four major signaling intracellular signaling pathways: the nuclear factor-κB (NFκB) and the 3 MAPK kinase pathways

($p38^{-MAPK}$, ERK and JNK). All 4 pathways drive transcription of inflammatory genes which are central to the inflammatory response. Exploration of the influence of ammonia on these signaling pathways poses an interesting mechanistic approach, although as ammonia freely passes into the neutrophil cytosol, many essential pathways, key to the successful functioning of a neutrophil, are likely to be affected in some way or other.

In conclusion, ammonia impairs neutrophil phagocytosis and induces oxidative burst in unstimulated neutrophils. The mechanisms have yet to be fully elucidated but cell swelling and activation of key oxidative enzymes are important. Consequently, in the presence of hyperammonemia neutrophils may be unable to respond to microbial challenge, in part accounting for the increased susceptibility to infection. In the 6^{th} chapter of this thesis, I chose to explore one specific area in relation to elucidating a possible mechanism of action involving the effect of ammonia on the mitogen-activated kinases.

Chapter 6

The effect of ammonia on neutrophil function: an investigation into a p38^{-MAPK} dependent mechanism

6.1 BACKGROUND

It has already been shown in chapter 5 that phagocytosis is impaired by 12-20% following incubation with 75 μM NH_4Cl ($p<0.0005$; Mann Whitney) and that spontaneous respiratory burst was increased by 10.7 +/- 1.8 % ($p<0.0001$; Mann Whitney). If the $p38^{-MAPK}$ signaling pathway plays an important role in inflammation and also acts as an osmoregulator, activated in response to increased cell hydration, it is conceivable that it could have an important role in the ammonia-induced impairment of neutrophil function. As neutrophils have also been shown to morphologically change by becoming more rounded and thus most likely to have swollen in response to exogenous ammonia. The hypothesis was developed that $p38^{-MAPK}$ signaling is involved in the ammonia-induced impairment of neutrophil function. In the first study of this chapter the impact of modulators of $p38^{-MAPK}$ activity influence on ammonia-induced phagocytosis has been investigated and comparable experiments on resting respiratory burst in unstimulated neutrophils explored.

6.2 ABSTRACT

Background: It has been previously shown that phagocytosis is impaired following incubation with 75 μM ammonia [$p<0.0005$] and that spontaneous respiratory burst was increased ($p<0.0005$). The $p38^{-MAPK}$ signaling pathway plays an important role in inflammation and acts as an osmoregulator, activated in response to increased cell hydration. As neutrophils were also found to swell in response to exogenous ammonia, it was hypothesised that $p38^{-MAPK}$ signalling is involved in the ammonia-induced impairment of neutrophil function. **Aims:** To determine whether specific modulators of $p38^{-MAPK}$ activity influence ammonia-induced phagocytosis or resting oxidative burst.

Methods: Whole blood from healthy volunteers was incubated for 90 mins at 37°C with 75μM NH_4Cl with or without a specific p38 agonist (1μM isoproterenol) or antagonist (10μM SB203580). Quantification of phagocytosis was performed using the Phagotest® utilizing opsonised FITC-labeled E.Coli. Oxidative burst was determined using the Burstest® which measures the percentage of neutrophils that produce reactive oxidants. Isolated neutrophils were then labeled with anti-CD16-R-PE antibodies and analyzed using flow cytometry. **Results:** 75 μM NH_4Cl impaired phagocytosis by 18.4% and caused cell swelling, this was further exacerbated by the addition of SB203580. The p38 agonist prevented the ammonia-induced impairment of phagocytosis and resulted in 2.5% cell shrinkage. Spontaneous respiratory burst was induced by ammonia but the p38 agonist was not protective. **Conclusions:** The $p38^{-MAPK}$ pathway is important in the ammonia-induced impairment of phagocytosis. $p38^{-MAPK}$ agonist prevents neutrophils from swelling in the presence of ammonia and improves phagocytosis.

6.3 METHODS

6.3.1 AMMONIA AND CELL INTRACELLULAR SIGNALLING

As part of the investigation to elucidate the mechanisms by which ammonia impairs neutrophil function experiments were performed to explore the effects of ammonia incubation on leucocyte intracellular signal pathways using specific and non-specific agonists and antagonists of the intracellular signalers ERK2, JNK, MAPK and in particular $p38^{-MAPK}$.

6.3.1.1 CELL SIGNALLING INHIBITORS USED IN THIS STUDY

6.3.1.1.1 SB 203580

[4-(4-Fluorophenyl)-2-(4-methylsulfinylphenyl)-5(4-pyridyl)1H-imidazole (Calbiochem, San Diego, California) is a highly specific, cell-permeable inhibitor of $p38^{-MAPK}$ (IC_{50}=34 nM). It is also known as reactivating kinase and cytokine synthesis anti-inflammatory drug binding protein) (252). It does not significantly inhibit JNK or $p42^{-MAPK}$ even at 100 μM. It has been shown to inhibit IL-1 and TNF-α release from lipopolysaccharide-stimulated human monocytes. It was also shown to be an effective inhibitor of inflammatory cytokine production in vivo in both mice and rats. (253)

6.3.1.1.2 PD 98059

[2'-amino-3'-methoxyflavone] (Calbiochem) is a selective and cell-permeable inhibitor of MAP kinase (MEK) that acts by inhibiting the activation of MAP kinase and subsequent phosphorylation of MAP kinase substrates. (254)

6.3.1.1.3 SP 600125

[anthra(1,9-cd)pyrazol-6(2H)-one; 1,9-pyrazoloanthrone] (Calibiochem) is a potent, cell-permeable, selective and reversible inhibitor of c-Jun N-terminal kinase (JNK) (IC_{50}= 40 nM for JNK-1 and JNK-2 and 90 nM for JNK-3. The inhibition is competitive with respect to ATP. It exhibits over 300-fold greater selectivity for JNK as compared to ERK1 and p38-MAPK. (255) It inhibits the phosphorylation of c-Jun and blocks the expression of IL-2, IFN-γ, TNF-α and COX-2 in synovial cells and blocked IL-1-induced accumulation of phosphor-Jun and induction of c-Jun transcription. (256)

6.3.1.1.4 UO 126

[1,4-diamino-2,3-dicyano-1,4-bis(2-aminophenylthio) butadiene is a potent and specific inhibitor of MEK1 (IC_{50} = 72 nM) and MEK2 (IC_{50}= 58 nM). The inhibition is non-competitive with respect to MEK substrates, ATP and ERK. It has very little effect on the other kinases, such as ERK, JNK, MEK, MKK-3 and MKK-6. (257;258) It acts as an immunosuppressant by effectively blocking IL-2 synthesis and T-cell proliferation without affecting the long-term outcomes of either T cell activation or tolerance. (259)

6.3.1.2 CELL SIGNALLING AGONISTS USED IN THIS STUDY

6.3.1.2.1 PHORBOL 12-MYRISTATE 13-ACETATE (PMA)

This is a non-specific agonist of all the intracellular signalers including ERK2, JNK, MAPK and $p38^{-MAPK}$ as it activates protein kinase C.

6.3.1.2.3 ISOPROTERENOL

This β-adrenergic agonist increases the activity of the stress-activated $p38^{-MAPK}$ over 10-fold in freshly isolated rat epididymal fat cells. Stimulation of $p38^{-MAPK}$ is rapid, sustained for at least 60 mins and sensitive to the specific $p38^{-MAPK}$ inhibitor, SB 203580. Half-maximal stimulation occurs at 13 nM and the effect is achieved via increases in the activity of cyclic-AMP dependent protein kinase. It has no effect on JNK. (260)

6.3.2 CO-INCUBATION OF NEUTROPHILS WITH CELL SIGNALING AGONISTS AND INHIBITORS AND AMMONIA

1. Two mls of heparinised whole blood was incubated at 37 °C in a waterbath with either 50 μM PD98059 (Calbiochem), 10 μM UO126 (Calbiochem), 10 μM SB203580 (Calbiochem) and 10 μM SP600125 (Calbiochem) dissolved in dimethyl sulfoxide (DMSO), and 75 μM NH_4Cl for 90 mins after gentle mixing on a blood rotator for 1 minute. Control samples were incubated with an equivalent volume of DMSO. Mixing was repeated for 1 minute after 30 and 60 mins incubation.

2. PMA (a non-specific activator of protein kinase C) and isoproterenol (specific agonist of $p38^{-MAPK}$) were used as positive controls.

3. The Phagotest® and Burstest® were then performed and the results were analysed by flow cytometry.

6.4 PROTOCOL

Heparinised whole blood from 3 healthy volunteers was incubated for 90 minutes at 37°C with 75 μM NH_4Cl with or without a specific $p38^{-MAPK}$ agonist (1 μM isoproterenol) or $p38^{-MAPK}$ antagonist (10 μM SB203580; Calbiochem. Quantification of phagocytosis was performed using the Phagotest® (Orpegen Pharma) utilizing opsonised FITC-labelled E.coli. Quantification of oxidative burst was determined using the Burstest® (Orpegen Pharma) which measures the percentage of neutrophils that produce reactive oxidants converting dihydrorhodamine to rhodamine which fluoresces. Isolated neutrophils were then labeled with anti-CD16-R-Phycoerythrin antibodies and analysed using flow cytometry. The pH was monitored and did not change by adding NH_4Cl.

6.5 RESULTS

6.5.1 AMMONIA AND INTRACELLULAR SIGNALLING INHIBITORS

Initial pilot studies were performed to look at the effect of 4 different inhibitors on the intracellular signaling pathways. In theses studies, UO126 an ERK2 inhibitor, PD98059 a MEK inhibitor and SP60025 a JNK inhibitor had no effect on phagocytosis or respiratory burst, in both the presence and absence of ammonia. However, co-incubating healthy neutrophils with the specific $p38^{-MAPK}$ inhibitor SB203580, resulted in phagocytosis being dramatically impaired. It was therefore decided that all further studies would be focused on the role of $p38^{-MAPK}$ in phagocytosis and respiratory burst in the presence and absence of ammonia.

6.5.2 AMMONIA, PHAGOCYTOSIS AND $p38^{-MAPK}$ ANTAGONISM

Incubation of neutrophils with 75 μM NH_4Cl impaired phagocytosis by 18.4 % ($p<0.05$) with the percentage of neutrophils undergoing phagocytosis being 91.09 % with 0 μM NH_4Cl and 71.81 % with 75 μM NH_4Cl respectively. Co-incubation with the $p38^{-MAPK}$ antagonist SB203580 (75 μM NH_4Cl + 10 μM SB203580) exacerbated this further with only 64.43 % ($p<0.05$) of neutrophils undergoing phagocytosis [Figure 6.1].

6.5.3 AMMONIA, OXIDATIVE BURST AND $p38^{-MAPK}$ ANTAGONISM

Incubation of neutrophils with 75 μM NH_4Cl, with and without the $p38^{-MAPK}$ antagonist SB203580, did not alter the number of neutrophils undergoing oxidative burst with E.coli which approached 95% in all groups [Figure 6.2]. Spontaneous respiratory

burst in unstimulated neutrophils was however induced by 75 μM NH_4Cl (4.74% in controls versus 9.66% in those incubated with ammonia; $p<0.05$). The $p38^{-MAPK}$ antagonist SB203580 prevented the ammonia-induced increase in spontaneous respiratory burst reducing the levels back to those in controls (4.98 %) [Figure 6.3].

6.5.4 AMMONIA, PHAGOCYTOSIS AND SPECIFIC $p38^{-MAPK}$ AGONISM

The specific $p38^{-MAPK}$ agonist isoproterenol (1 μM) prevented the ammonia-induced impairment of phagocytosis with 75 μM NH_4Cl (91.09 % of control neutrophils undergoing phagocytosis versus 95.69 % incubated with ammonia and $p38^{-MAPK}$ agonist) [Figure 6.1].

6.5.5 AMMONIA, OXIDATIVE BURST AND SPECIFIC $p38^{-MAPK}$ AGONISM

Incubation of neutrophils with 75 μM NH_4Cl, with and without the specific $p38^{-MAPK}$ agonist 1 μM isoproterenol, did not alter the number of neutrophils undergoing oxidative burst with E. coli which approached 95% in all groups [Figure 6.2]. In the unstimulated neutrophils, the percentage undergoing spontaneous respiratory burst was not altered by co-incubation with the specific $p38^{-MAPK}$ agonist [Figure 6.3].

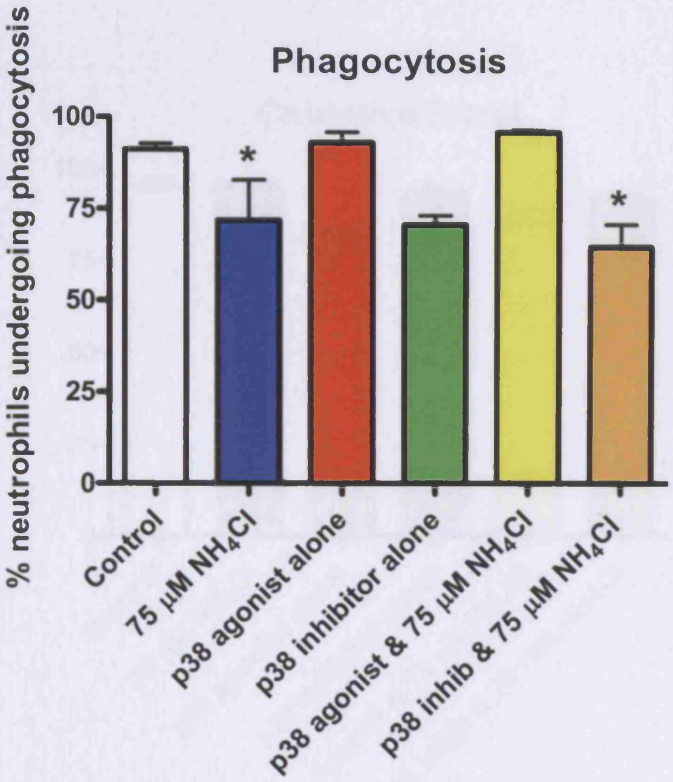

Figure 6.1

Bar graph representing the effect of the specific $p38^{-MAPK}$ agonist isoproterenol (1 μM) and the specific $p38^{-MAPK}$ antagonist SB203580 (10 μM) on the percentage of neutrophils undergoing phagocytosis with and without 75 μM NH_4Cl.

* $p<0.05$

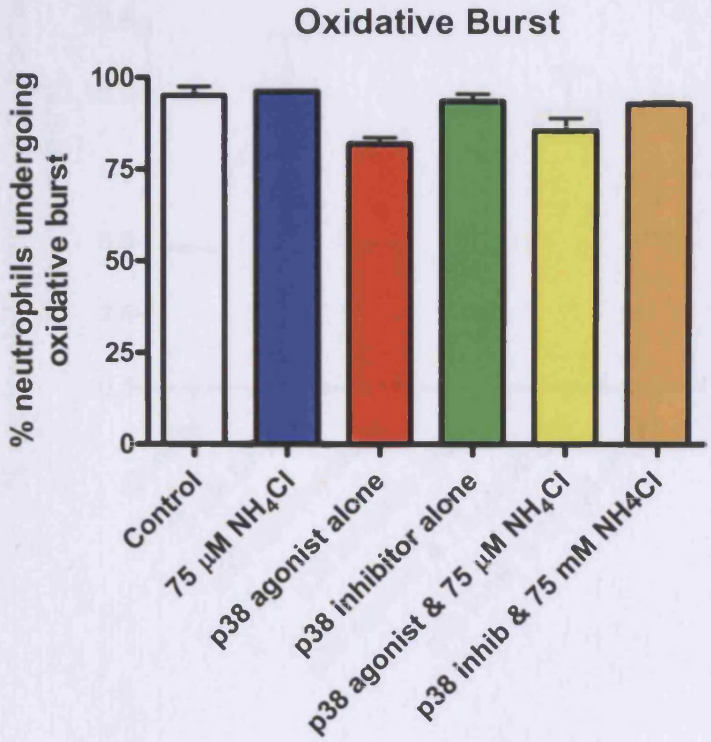

Figure 6.2

Bar graph representing the effect of the specific $p38^{-MAPK}$ agonist isoproterenol (1 μM) and the specific $p38^{-MAPK}$ antagonist SB203580 (10 μM) on the percentage of neutrophils undergoing oxidative burst with and without 75 μM NH_4Cl.

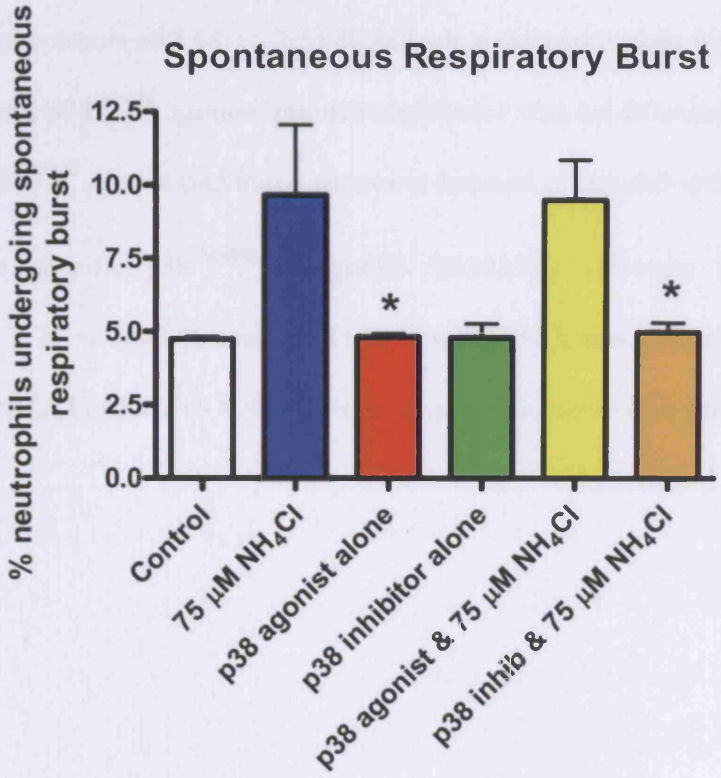

Figure 6.3

Bar graph representing the effect of the specific p38^{-MAPK} agonist isoproterenol (1 μM) and the specific p38^{-MAPK} antagonist SB203580 (10 μM) on the percentage of unstimulated neutrophils undergoing spontaneous respiratory burst with and without 75 μM NH_4Cl.

* $p<0.05$

6.5.6 NEUTROPHIL SWELLING AND $p38^{-MAPK}$

Neutrophils exposed to 75 μM NH_4Cl increased in volume (as measured by a reduction in forward scatter on flow cytometry of an average of 100,000 neutrophils) by 2.01 +/- 0.36 %. The specific $p38^{-MAPK}$ agonist isoproterenol led to cell shrinkage compared to controls of 2.48 +/- 2.55 % and when the neutrophils were co-incubated with ammonia and $p38^{-MAPK}$ agonist, the neutrophil size was no different to controls showing that the $p38^{-MAPK}$ agonist prevented ammonia-induced neutrophil swelling.

The specific $p38^{-MAPK}$ antagonist SB203580 however, increased neutrophil volume by 2.74 +/- 0.43 % compared to controls, which was exacerbated by the addition of 75 μM NH_4Cl to 5.16 +/- 0.92 % preventing normal neutrophil osmoregulation.

6.6 DISCUSSION

In conclusion, this study demonstrates that the ammonia-induced impairment in phagocytosis is exacerbated by the addition of the specific $p38^{-MAPK}$ antagonist SB203580 and prevented by the addition of a $p38^{-MAPK}$ agonist suggesting that $p38^{-MAPK}$ plays a pivotal role in the ammonia-induced alterations in neutrophil function, which may have a significant relationship to neutrophil function in the hyperammonaemic liver disease patient. As $p38^{-MAPK}$ is an important cell osmoregulator, then its inhibition may be preventing the neutrophil from regulating its water uptake and excretion and thus explains why the neutrophil increases in volume on flow cytometry.

As the addition of a $p38^{-MAPK}$ agonist abrogates the ammonia-induced impairment in phagocytosis, this would imply that ammonia either inhibits $p38^{-MAPK}$ directly or its metabolism within the cell leads to the production of a substance which exerts an osmotic effect within the neutrophil; a potential candidate is glutamine. This has been shown to be the case in the astrocyte which contains glutamine synthetase, which in the presence of ammonia, amidates glutamate to form glutamine. Glutamine exerts an osmotic effect within the astrocyte, causing it to take in water and thus swell (49). Glutamine has been shown to exert many of its biological effects through a swelling-induced activation of ERK and $p38^{-MAPK}$ signaling in rat hepatocytes (154-157) and vom Dahl et al. have shown in the perfused rat liver with hypoosmotic exposure, that $p38^{-MAPK}$ (but not Erks or PI-3-kinase) is critical in cell volume regulation (157) and that cell hydration controls autophagosome formation in rat liver in a microtubule-dependent way downstream from $p38^{-MAPK}$ activation (261). Hepatocytes express both glutamine synthetase and glutaminase, but in neutrophils however, the dominant enzyme is glutaminase, which is

necessary to break glutamine down to glutamate, lactate and aspartate which are important fuels for the neutrophil (138;139). Therefore, the production of glutamine by neutrophils in response to exogenous ammonia is unlikely. Furthermore, the addition of the glutamine synthetase inhibitor (methionine sulphoxamine) in pilot studies, made no difference to neutrophil function in both the presence and absence of ammonia. This therefore leads us to the conclusion that ammonia inhibits $p38^{-MAPK}$ activation directly or through another metabolic derivative other than glutamine, which consequently impairs neutrophil osmoregulation.

Conversely, in regard to the ammonia-induced increase in resting respiratory burst, the $p38^{-MAPK}$ agonist made no difference at all. However, the $p38^{-MAPK}$ antagonist SB203580 prevented the ammonia-induced increase in spontaneous respiratory burst reducing the levels back to those seen in controls. This implies that $p38^{-MAPK}$ is important in the activation of background spontaneous respiratory burst and that its inhibition can abrogate the increased spontaneous respiratory burst induced by ammonia. However, inhibition of $p38^{-MAPK}$ did not alter the number of neutrophils undergoing respiratory burst with E.coli. This would imply that other protein kinases and enzymes important in the oxidative burst such as myeloperoxidase, are also activated in the presence of the bacteria so that the absence of $p38^{-MAPK}$ makes very little difference to the final outcome.

In conclusion, the $p38^{-MAPK}$ signaling pathway is important in ammonia-induced impairment of neutrophil phagocytosis. Ammonia reduces the ability of neutrophils to phagocytose, as the neutrophil in no longer able to osmoregulate and consequently swells; this can be overcome by adding a $p38^{-MAPK}$ agonist. Inhibition of $p38^{-MAPK}$ however, also reduces the number of neutrophils undergoing spontaneous respiratory

burst which has been shown to increase in the presence of ammonia. Therefore, ammonia is also likely to separately activate key oxidative enzymes such as myeloperoxidase within 90 minutes (as shown in chapter 6), which have more of an immediate influence on the spontaneous neutrophil respiratory burst rate than $p38^{-MAPK}$ activation, which leads to the transcription of inflammatory genes e.g. TNF-α maximal at 24 hours (150;151). It is possible that these mechanisms may, in part, account for the increased susceptibility to infection found in patients with cirrhosis.

Chapter 7

An investigation into the influence of inflammation on ammonia uptake in muscle

7.1 BACKGROUND

If inflammation modulates the cerebral effects of ammonia, then a key question to answer is how is the metabolism of ammonia affected by the presence of inflammation or infection? The muscle is an important organ in total body ammonia metabolism. As described earlier, the muscle may be an important site for ammonia detoxification and a potential therapeutic target for ammonia reduction in liver disease. By exploring how the muscle metabolism of ammonia is modulated by inflammation, it was anticipated that potential mechanisms might be further elucidated. The hypothesis to be tested was that muscle metabolism of ammonia is modulated by inflammation.

Studies were performed using chick embryo primary muscle cell cultures and later with cultures of the immortilized murine myofibroblast cell line C2C12 exploring whether ammonia metabolism, as measured by stable amino acid isotopes, could be altered by the addition of an inflammatory stimulus such as lipopolysaccharide.

7.2 METHODS

7.2.1 MUSCLE CELL CULTURE

7.2.1.1 CHICK EMBRYO PRIMARY MUSCLE CELLS

All the following methods were performed in a Laminar Airflow Cabinet (Microflow Biological Safety) to maintain sterility, adhering to a strict aseptic technique.

7.2.1.2 COLLAGEN PREPARATION FROM RAT TAILS (262)

1. Rat tails were washed in 70% ethanol for 30 minutes.

2. The skin was stripped away and the tendons removed. The tendons were then placed in sterile 0.1% ethanoic acid solution at 4 °C for at least 24 hours.

3. The resulting suspension was centrifuged at 18,000G for 1 hour, the supernatant was decanted and diluted 1:5 with sterile ddH_20 and stored at 4 °C until required.

7.2.1.3 CHICK EMBRYO EXTRACT (CEE)

This was prepared by squeezing 9-12 day old chick embryos through a 50 ml syringe followed by the addition of an equal volume of Earle's Balanced Salt Solution (EBSS) [Table 7.1]. (263)

	F.Wt	mM	g/litre
NaCl	58.44	116.35	6.80
KCl	74.55	5.4	0.40
Glucose	180.2	5.55	1.00
$MgSO_4$	246.5	0.81	0.20
NaH_2PO_4	137.99	0.9	0.124
$NaHCO_3$	84.01	26	2.184
$CaCl_2$	147	1.2	0.176

Table 7.1

Earle's Balance Salt Solution

After standing for 2 hours at room temperature (20 – 22 °C), the extract was either centrifuged immediately or stored at -20 °C. Centrifugation was carried out for 1 hour at 4 °C and 18,000G and the supernatant was stored at -20 °C until use.

7.2.1.4 PREPARATION OF TRYPSIN SOLUTION

This was prepared in a calcium and magnesium-free EBSS to a concentration of 0.1% and sterilised by filtration.

7.2.1.5 PREPARATION OF CULTURE MEDIUM

Eagle's minimum essential growth medium (MEM) (264) [Dulbecco's Eagle's MEM with glutamax I (L-alanyl-L-glutamine) without sodium pyruvate with 4500 mg/L glucose with pyridoxine (GibcoBRL)] was used for culturing chick skeletal muscle cells and the following was added to 500 ml:

- 75 mls horse sera (Invitrogen; UK)
- 25 mls CEE

- 5 mls glutamine (Sigma; UK)
- 500 mcg penicillin G (Sigma; UK)
- 125 mcg streptomycin (Sigma; UK)

7.2.1.6 TISSUE CULTURE OF CHICK EMBRYO SKELETAL MUSCLE

Chick skeletal muscle myotubes were grown according to the procedures of Harvey and Dryden (265) in which single cell suspensions of myoblasts were obtained using the method of Konigsberg et al. (266) Chick embryos of 10-12 days incubation age were used for all cultures.

1. After removal of the embryo from the egg and immediate decapitation, extra-embryonic membranes and gross debris were removed, the legs were severed from the body at the level of the ischial crests.
2. The skin was then peeled away from both legs. The muscle tissue was then teased away from the bone and connective tissue and minced with a pair of fine scissors.
3. The pulped muscle tissue was then placed in 10 ml of 0.1% trypsin solution for 30 minutes at 37 ^{o}C and shaken every 10 minutes for 5 seconds.
4. The enzymatic reaction was stopped by the addition of 10 mls of cold MEM containing fetal calf sera (Invitrogen; UK).
5. Dissociation of cell aggregates was aided by sucking the solution 3 or 4 times in and out of a 10 ml pipette. The cell suspension was then filtered through 2 layers of cotton gauze to remove large cell and remaining tissue aggregates.

6. The filtrate was then centrifuged for 15 minutes at 516 g. The supernatant was then decanted and the myoblasts resuspended in 10 mls of whole MEM. The number of cells was then counted using a haemocytometer.
7. Cultures were grown in 35 mm plastic Petri dishes (Sterilin; UK) that had been pre-coated with 1 ml of collagen solution and dried overnight in an oven at 50 °C.
8. Cells were plated out with a density of 5 x 10^6 cells/ml, with 2 mls media being added to each plate.
9. The cultures were then incubated at 37 °C in a humid atmosphere of 5% CO_2 in air. The medium was then changed every 2 to 3 days.
10. Cultures were treated with whole MEM media containing cytosine arabinoside (Sigma; UK) 10^{-5} after 4 to 5 days for 24 hours after the beginning of rapid myoblast fusion. (267). In muscle cells DNA synthesis ceases after fusion (266;268), therefore this treatment greatly reduces contamination with actively replicating cells, such as fibroblasts, which could otherwise overgrow the cultures.
11. Once treated with cytosine arabinoside, the cultures were allowed to settle for 24 to 48 hours before being challenged. A picture of the cultured muscle cells is shown in Figure 7.1.

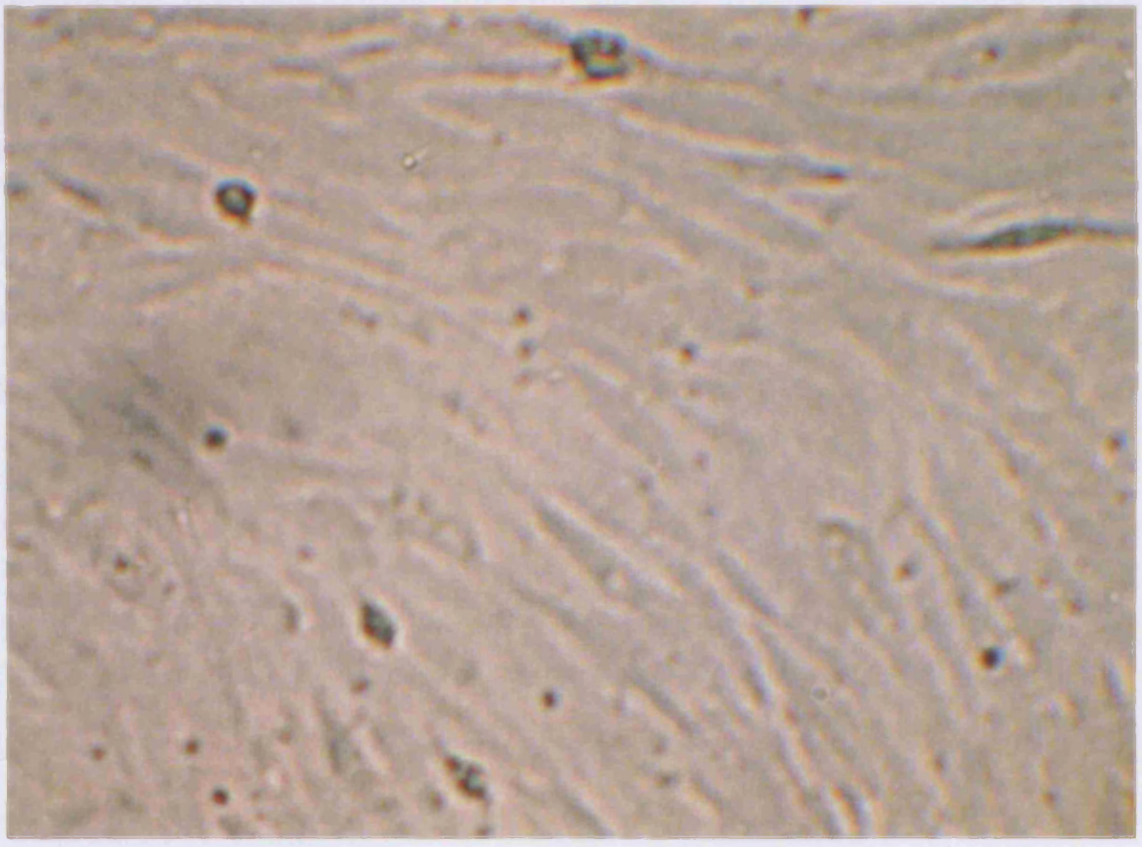

Figure 7.1

A scanning light micrograph of a chick embryo primary muscle cell culture (x 200 magnification; Biorad Radiance 2000; UK)

7.2.2 CHALLENGE OF CULTURED MUSCLE CELLS WITH AMMONIA, GLUTAMATE AND LOLA

The muscle cells were pre-incubated for 1 hour with 2 mls of media containing either 10 mM glutamate (147 mg in 100 mls) (Sigma; UK), 10 mM LOLA (530 µL in 100 mls) (Merz Pharmaceuticals, Frankfurt, Germany) and ^{3}H Glutamate (1 µCurie/ml) (Amersham; UK). The plates were then washed with 2 mls of MEM and then incubated for 2 hours with 0, 25, 50 or 100 µM NH_4Cl (Sigma; UK) in 2 mls MEM. The supernatant was then collected and frozen at -80 °C and the culture plates were stored at -80 °C for later analysis.

7.2.3 MEASUREMENT OF ^{3}H- GLUTAMATE IN CELL LYSATES

The cells were lysed with 150 µL cell lysis buffer (300 µL of 0.1% triton w/v (Sigma; UK) in 30 mls PBS) and scraped from the Petri dishes using a cell scraper. The lysis mixture was centrifuged at 1000g for 15 mins at 4 °C before 5 µL of the supernatant was loaded onto a silica thin layer chromatography (TLC) (Kieselgel 60, Merck, Darmstadt, Germany) plate and run to separate the glutamine from the glutamate. Non-radiaoactive glutamate and glutamine was spotted onto the sample spot (2 µL, 1mM solutions) for identification purposes. The solvent eluent mixture consisted of 5 mls formic acid, 15 mls methanol, 25 mls acetaldehyde and 10 mM hexanesulphonic acid (Sigma, UK). The plates were then developed in a fume cupboard using Ninhydrin spray reagent (0.5% ninhydrin in butanol, Sigma; UK) and dried. The spot was then scratched off and added to 8 mls of scintillation fluid (™Ultimo Gold, Packard Bioscience, UK). The count was then measured on a Liquid Scintillation Analyser (Tri-Carb 2100 TR,

Hewlett Packard Bioscience, UK; Program 3). An example of a developed TLC plate is shown in Figure 7.2.

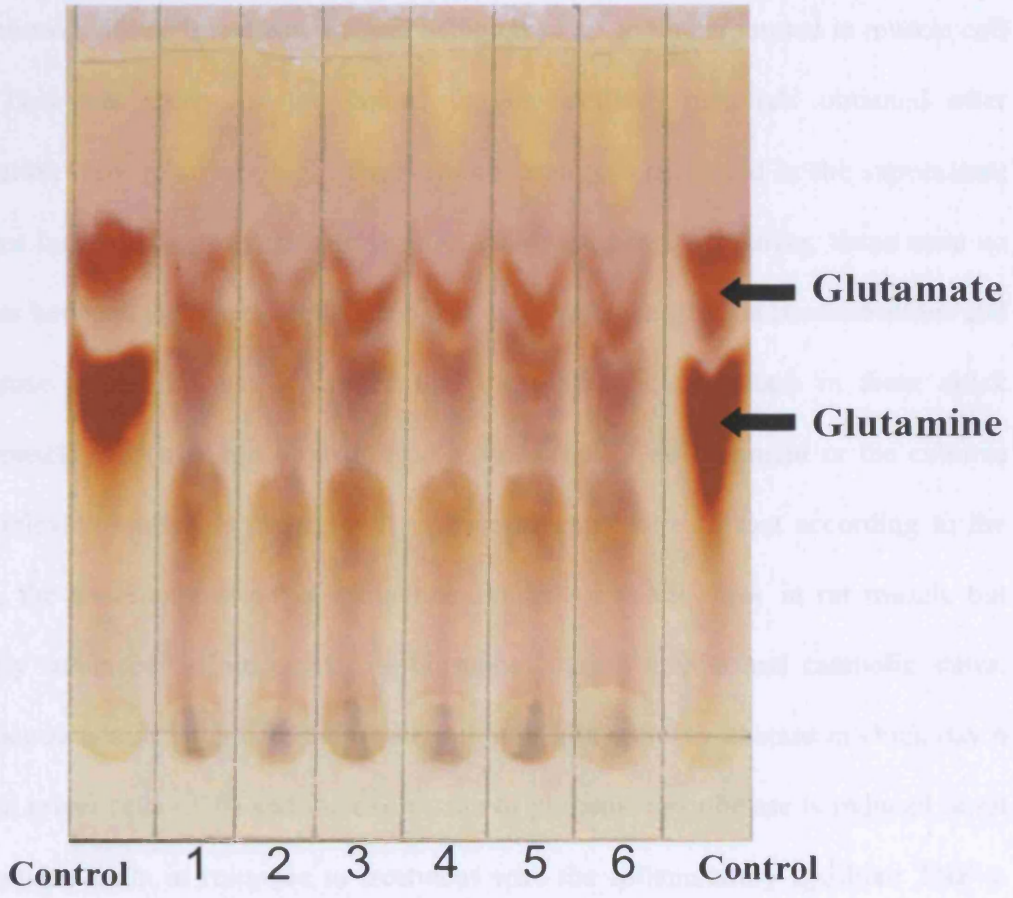

Figure 7.2

A diagram showing a picture of a typical developed TLC plate for 6 samples of muscle cell lysate as compared with glutamate and glutamine controls on either side.

7.2.4 CULTURE OF C2C12 MURINE MYOFIBROBLAST CELL LINE

Unfortunately, there was no evidence of the presence of either glutamate or glutamine in the muscle cell lysate as the radioactivity of the different spots was very low. This suggested that glutamine synthetase was absent or expressed at very low concentrations, with the glutamate instead being taken up and incorporated in muscle cell protein. This was likely as the counts for the pelleted materials obtained after centrifugation were relatively high. Furthermore, ammonia measured in the supernatant and lysates incubated with glutamate or LOLA did not differ. Moreover, there were no differences between the muscle cells incubated with varying ammonia concentrations and ^{3}H-glutamate. From this we concluded that the glutamine synthetase in these chick embryo muscle cells may not be expressed at this stage of development or the cultures lack the relevant stimuli in order for it to become expressed. In fact according to the literature, the basal expression of glutamine synthetase is very low in rat muscle but remarkably enhanced by glucocorticoid hormones during trauma and catabolic states. (269) Glucocorticoids potentiate the transcription of glutamine synthetase in chick day 6 embryonic retina cells (270) and the expression of glutamine synthetase is induced in rat skeletal muscle cells in response to treatment with the inflammatory cytokine TNF-α. (271) Therefore, we attempted to stimulate the muscle cells with 50 nM dexamethasone (Sigma; UK) added to the culture medium from day 7 onwards to encourage the expression of glutamine synthetase, prior to challenging them with ammonia and amino acids. Despite attempting this on several occasions, it was still not possible to demonstrate any convincing evidence that any substantial glutamine synthetase activity was present in the muscle cells.

Following the disappointing results obtained from the initial pilot experiments using the chick embryo muscle cell cultures, we reverted to culturing an established muscle cell line to see if the resultant myotubes were more likely to or could be induced to express glutamine synthetase. These cells were obtained from Dr Jim Owen at the Institute for Liver Studies at the Royal Free Hospital.

7.2.4.1 CULTURE METHOD

Cells were grown in 75 ml vented sterile culture flasks (Fisher Scientific) in 25mls Eagle's minimum essential growth medium (MEM) (264) [Dulbecco's Eagle's MEM with glutamax I (L-alanyl-L-glutamine) without sodium pyruvate with 4500 mg/L glucose with pyridoxine (GibcoBRL)] and the following was added to 500 ml:

- 10% fetal calf serum (Invitrogen; UK)
- 5 mls glutamine (Sigma; UK)
- 500 mcg penicillin G (Sigma; UK)
- 125 mcg streptomycin (Sigma; UK)

1. Cells were grown in an incubator at 37 ^{o}C in a humid atmosphere of 5% CO_2 in air until they became confluent [Figure 7.3]. The medium was then changed every 24 hours.

2. Cultures were treated with whole MEM media containing cytosine arabinoside (Sigma, UK) 10^{-5} for 24 hours as before to reduce the number of fibroblasts and encourage the growth of myotubes. Once treated with cytosine arabinoside, the cultures were allowed to settle for 24 before being challenged.

3. Some muscle cultures were treated with 50nM dexamethasone added to the culture medium from day 7 onwards to see if this would further stimulate the expression of glutamine synthetase. (270)

4. Tetrodotoxin (120 μL of 100 nM) [Alomone Labs; Jerusalem, Israel] was added to every 200 mls of culture medium from day 7 onwards to prevent contraction of the myotubes away from the culture flask.

5. Myotubes were cultured with 5 mM glutamate-enriched culture media or 5 mM LOLA-enriched media or plain media for 24 hours prior to challenge with ammonia.

6. At this point there was a move away from using radioactive glutamate and toward $^{2\text{-}15}N$- stable nitrogen isotope containing glutamate.

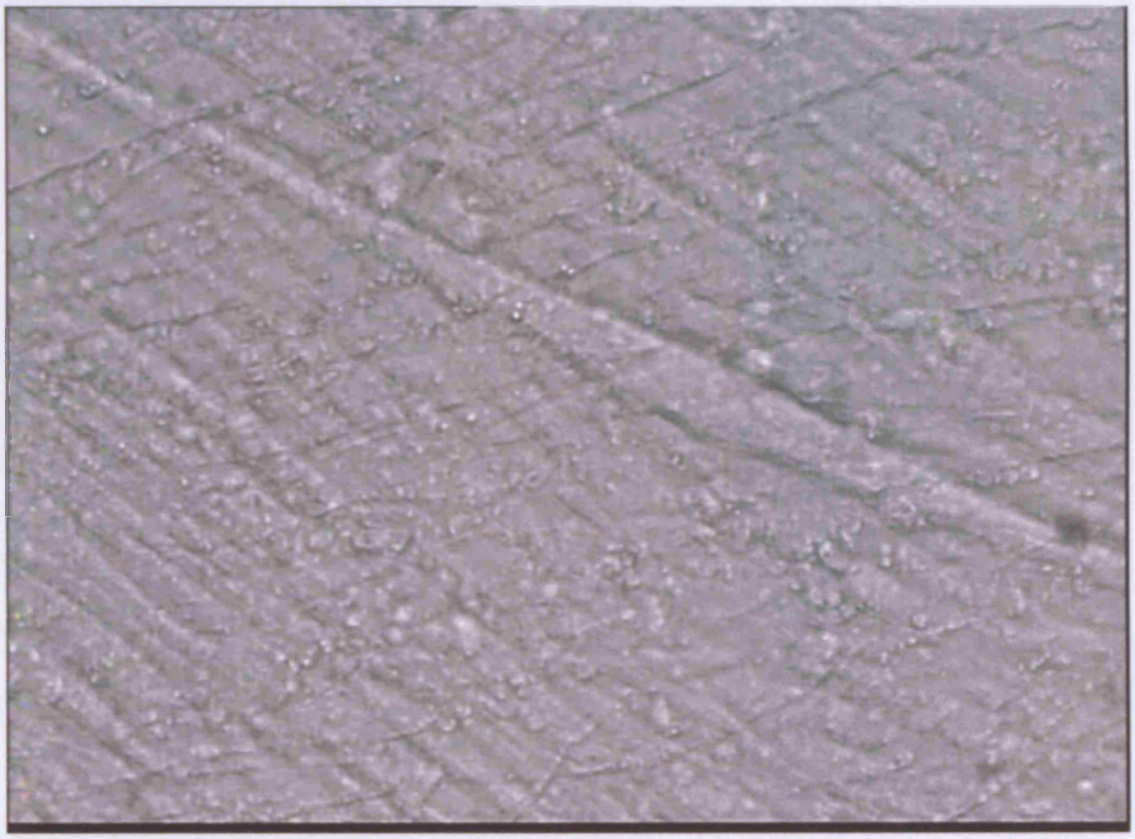

Figure 7.3

A scanning light micrograph of C2C12 myotubes (x 200 magnification; Biorad Radiance 2000; UK)

7.2.5 CHALLENGE OF CULTURED MUSCLE CELLS WITH AMMONIA AND $^{2-15}$N-GLUTAMATE

1. Twelve flasks of myotubes were then incubated for 6 hours with 100 μM $^{2-15}$N-glutamate (obtained from N.E.P Deutz, Academic Department of Surgery, Maastricht University, The Netherlands) and 100 μM glutamate (Sigma; UK) +/- 500 μM NH_4Cl +/- 3 mM methionine sulfoxime (an inhibitor of glutamine synthetase) [Sigma; UK].
2. Four flasks containing media only (no myotubes) were used as controls. Five hundred microlitre aliquots of supernatant were removed at t = 0 hrs and then hourly for a total of 6 hours.
3. Eighty microlitres of 33% w/v sulphosalicylic acid was added to each aliquot and the samples were then stored at -80 °C for later determination of amino acid concentration by high-performance liquid chromatography and liquid chromatography mass spectrometry (Pharmacia, Woerden, The Netherlands). This was performed at The Department of Surgery, Maastricht University, Maastricht, The Netherlands by Dr H. van Eijk and Dr N.E.P Deutz. (191)
4. Fifty microlitres of supernatant was also removed at each time point for ammonia determination using the method detailed in section 3.1.3.2.
5. Following challenge, cells were washed 3 times with PBS and then removed from the flasks using a cell scraper and lysed with cell lysis buffer (300 μL of 0.1% triton w/v in 30 mls PBS; pH 7.4) and stored at -80 °C for later analysis.

7.2.6 GLUTAMINE SYNTHETASE ACTIVITY ASSAY

Glutamine synthetase catalyses the formation of L-Glutamine from L-Glutamate and NH^{4+}. This enzyme also exerts a glutamyl-transferase activity that produces gamma-glutamyl-hydroxamate from glutamine and hydroxylamine. This gamma-glutamyl-transfer reaction can be used to determine glutamine synthetase activity by colorimetric assay (272). All chemicals used were from Sigma; UK.

1. Muscle lysate was homogenised in ice-cold Tris buffer (pH 7.0) and centrifuged at 4500 g at 4 °C for 20 minutes.
2. A reaction mix including 0.05 M imidazole, 0.05 M imidazole-L-glutamine, 25 mM sodium arsenate, 2 mM manganese chloride, 0.16 mM adenosine diphosphate and 25 mM hydroxylamine was mixed and pre-warmed to 37 °C.
3. Fifty microlitres of the lysate was added to 25 µL of the reaction mix and incubated for 30 minutes at 37 °C.
4. The reaction was stopped by the addition of 2.42% ferric chloride, 1.45% trichloroacetate and 1.2% hydrochloric acid.
5. The reaction product gamma-glutamyl-hydroxamate forms a purplish brown complex in the presence of trivalent ion. The increase in optical density was followed kinetically at 540 nm using a spectrophotometer over 30 minutes.
6. The experiment was then repeated in the presence of 3 mM methionine sulphoxamine.

7.3 RESULTS AND DISCUSSION

Once again, the data obtained from the repeat studies performed on the C2C12 murine myofibroblast line did not show any convincing evidence of any detectable glutamine synthetase activity. Figure 7.4 below shows that at most there was 20% glutamine synthetase activity which was not inhibited by methionine sulphoxamine.

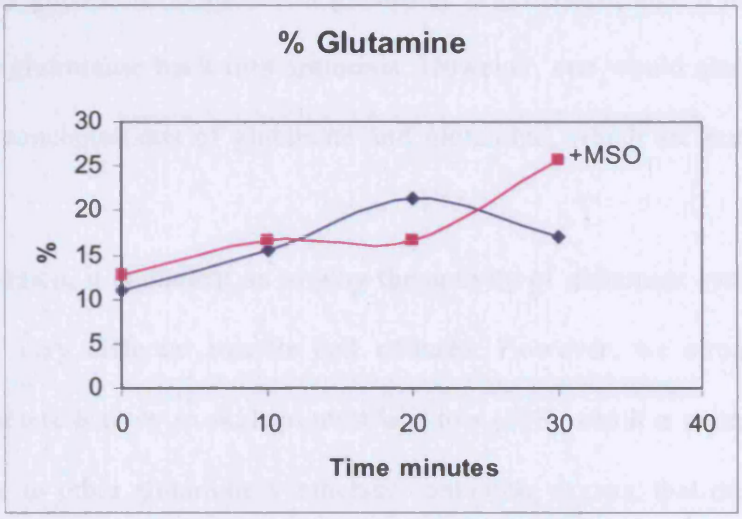

Figure 7.4

A graph showing the percentage glutamine generated from a colorimetric glutamine synthetase activity assay with (pink line) and without methionine sulfoxamine (MSO) [dark blue line] over 30 minutes.

Furthermore, there was no evidence of incorporation of glutamate (as measured by high performance liquid chromatography) or $^{2\text{-}15}$N-glutamate (as measured by liquid chromatography mass spectrometry), or the production of glutamine at 6 hours as shown in Figure 7.5. Likewise, there was no drop seen in ammonia concentration over time [Figure 7.6]. Surprisingly, an increase in ammonia concentration was seen in the muscle cells grown in a LOLA-enriched media. A possible explanation for this could come from the fact that the muscle cells were able to take up the ornithine and convert it to glutamate and subsequently glutamine. If sufficient glutamine is generated, then it may breakdown via the enzyme glutminase back into ammonia. However, one would also expect to see changes in the concentrations of glutamate and glutamine, which are not seen in these studies.

In conclusion, it is unclear as to why the activity of glutamine synthetase was so low in these 2 very different muscle cell cultures. However, we already know that glutamine synthetase activity in skeletal muscle is low (158), and it is mainly by virtue of its mass relative to other glutamine synthetase containing organs, that muscle is one of the principle glutamine synthesizing organs. If one did find a way to upregulate the expression of this enzyme, then this *in vitro* model could represent a potential way to study the role of ammonia in the modulation of muscle ammonia metabolism in the future.

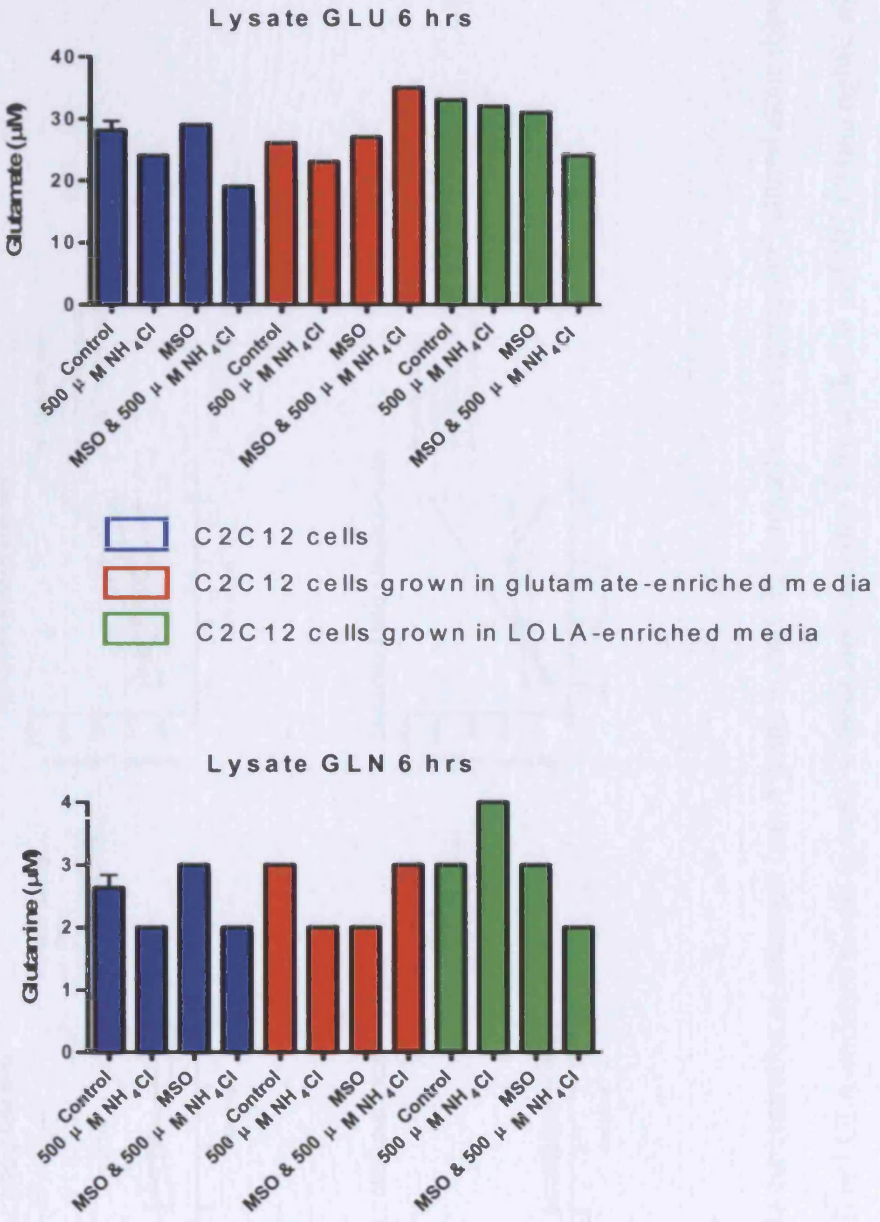

Figure 7.5

Bar graphs to show the change in concentration of glutamate (GLU) [top] and glutamine (GLN) [bottom] at 6 hours in the C2C12 muscle cell lysates cultured alone (blue), in glutamate-enriched media (red) or LOLA-enriched media (green), with or without the presence of 500 μM NH_4Cl and/or 3 mM methionine sulfoxamine (MSO).

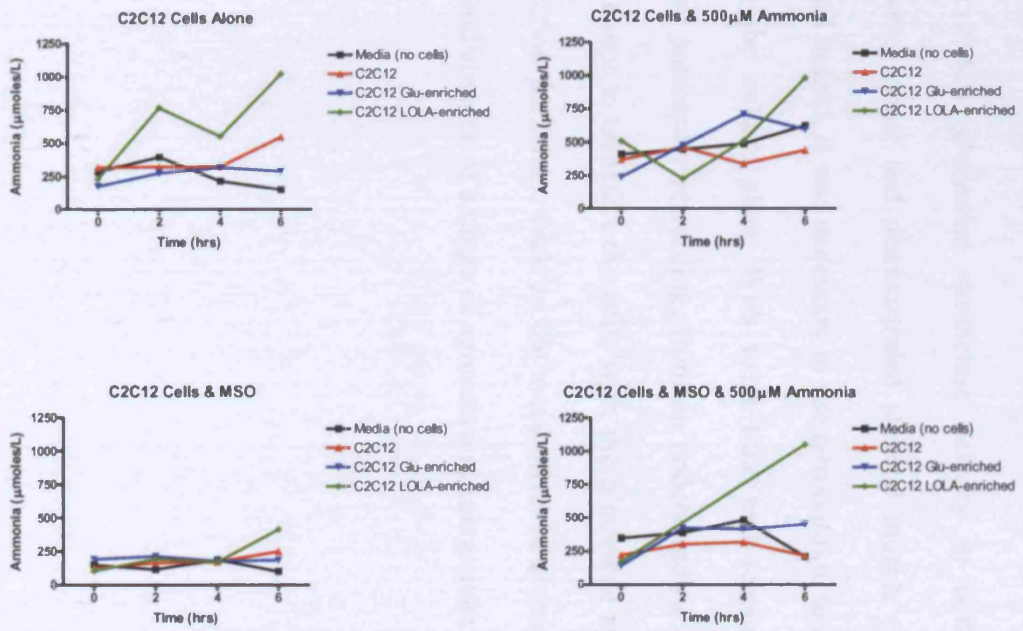

Figure 7.6

Line graphs to show the change in concentration of ammonia over 8 hours in the C2C12 muscle cell supernatant cultured alone (blue), in glutamate-enriched media (red) or LOLA-enriched media (green), without ammonia (top left), with 500 µM NH_4Cl (top right), with 3 mM methionine sulfoxamine (MSO) [bottom left] or both (bottom right)

7.4 CONCLUDING REMARKS

While the culture of both primary chick skeletal muscle myotubes and C2C12 murine-derived myotubes was a potentially interesting direction to take the metabolic aspects of the overall study, it was unfortunate that the resulting experimental data demonstrated a low glutamine synthetase activity in both systems. The cultures themselves were robust and demonstrated skeletal muscle cell striations. They were contractile, and indeed, it was necessary to use tetrodotoxin to maintain an intact lawn of myotubes on the culture plate. With extra time and resources it would have been interesting and potentially rewarding, from an understanding of metabolic processes in muscle, to attempt to transfect the cells with the glutamine synthetase gene. This may remain a direction for future work on the metabolism of ammonia by skeletal muscle in the presence and absence of a range of agonists and antagonists.

Chapter 8

Summary

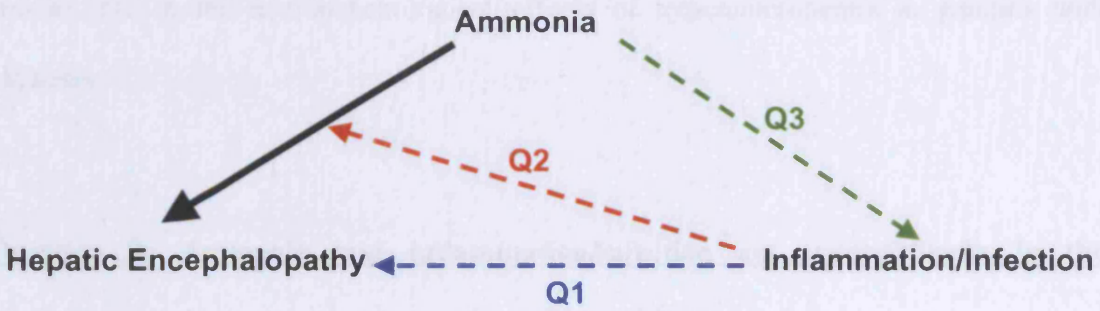

Figure 8.1

Hypothesis

Each of the 3 hypotheses illustrated above has now been explored and tested.

Question 1: Inflammation and infection are important in the pathogenesis of hepatic encephalopathy [Chapter 3].

The data presented from the clinical studies have confirmed the importance of ammonia in the pathogenesis of hepatic encephalopathy, but suggests that the inflammatory response may be important in determining the neuropsychiatric effects of ammonia rather than the severity of underlying liver disease or hyperammonemia. Also, it has been shown for the first time that those patients that have abnormal neuropsychiatric tests have more likelihood of further deterioration with induced hyperammonemia. Furthermore, it has been shown that hyperammonemia induced by administration of an amino acid solution to patients with cirrhosis, results in deterioration in neuropsychological function in the presence of a systemic inflammatory response. Following resolution of the systemic inflammatory response, there was no deterioration in neuropsychological function despite equivalent severity of induced hyperammonemia.

Therefore, these data provide supportive evidence suggesting that inflammation plays a crucial role in the neuropsychological effects of hyperammonemia in patients with cirrhosis.

Question 2: Ammonia and inflammation/infection act synergistically in the pathogenesis of hepatic encephalopathy [Chapter 4]

Ammonia and inflammation were shown to be synergistic in the bile duct ligated (BDL) rat which showed increased brain water and astrocyte swelling exacerbated by endotoxin and accompanied by a rise in nitric oxide and brain nitrotyrosine, but not in plasma ammonia, suggesting nitric oxide may play an important synergistic role in the pathogenesis of hepatic encephalopathy. The BDL rats administered LPS showed universal deteriorating levels of consciousness (to pre-coma and coma stages). In the BDL/sham operated rats administered saline and the sham-operated rats administered LPS, no change in conscious level occurred. This is despite the LPS treated sham-operated rats and saline BDL rats showing some evidence of brain swelling and astrocyte oedema. It is therefore possible that in the BDL rats hyperammonemia in some way acts synergistically with the systemic inflammatory response to alter the level of consciousness. This concept fits with the observation in cirrhotic patients, where induction of hyperammonemia resulted in neuropsychological deterioration when the patients were infected and showed evidence of an inflammatory response. Following resolution of infection, similarly induced hyperammonemia did not result in an alteration in neuropsychological function supporting the hypothesis that ammonia and inflammation may be synergistic. Furthermore, the suggestion of synergy between

hyperammonemia and inflammation is supported by the recent observation that BDL rats that were fed a high ammonia diet (and which showed evidence of a low level of inflammation), developed increases in brain water (240).

Question 3: Ammonia impairs neutrophil function [Chapters 5 and 6]

The data obtained from the studies incubating normal neutrophils with ammonia concentrations typically found in cirrhotic patients showed that ammonia impaired neutrophil phagocytosis and induced spontaneous oxidative burst. The $p38^{-MAPK}$ signaling pathway has been shown to play an important role in ammonia-induced impairment of neutrophil phagocytosis. Ammonia reduced the ability of neutrophils to phagocytose, possibly because the neutrophil was no longer able to osmoregulate and consequently swelled; this can be overcome by adding a $p38^{-MAPK}$ agonist. Inhibition of $p38^{-MAPK}$ however, also reduced the number of neutrophils undergoing spontaneous respiratory burst which has been shown to increase in the presence of ammonia. Therefore, ammonia is also likely to separately activate key oxidative enzymes such as myeloperoxidase within 90 minutes, which have more of an immediate influence on the spontaneous neutrophil respiratory burst rate than $p38^{-MAPK}$ activation, which leads to the transcription of inflammatory genes e.g. TNF-α maximal at 24 hours (150;151). It is possible that these mechanisms may, in part, account for the increased susceptibility to infection found in patients with cirrhosis.

Question 4: An investigation into the influence of inflammation on ammonia uptake in muscle (Chapter 7)

By exploring how the muscle metabolism of ammonia is modulated by inflammation, it was hoped that potential mechanisms might be further elucidated. Studies were performed using chick embryo primary muscle cell cultures and later with cultures of a C2C12 murine myoblast cell line exploring whether ammonia metabolism, as measured by stable amino acid isotopes, could be altered by the addition of an inflammatory stimulus such as lipopolysaccharide. Unfortunately, there were severe methodological failures in these studies in that the muscle cell cultures had low levels of activity of the enzyme glutamine synthetase, essential to the conversion of glutamate and ammonia into glutamine. Despite attempts to upregulate this enzyme with dexamethasone, levels of the enzyme were insufficient to assess the metabolism of ammonia into glutamine within the muscle cell making it extremely difficult to explore whether ammonia metabolism could be modulated in the presence of inflammation.

In conclusion, this thesis has illustrated I believe, the important factors that modulate the manifestation of symptoms of hepatic encephalopathy in cirrhosis, the most important of which is the synergistic role of inflammation and ammonia. Furthermore, the ammonia-induced impairment of neutrophil function may, in part, account for the increased susceptibility to infection found in cirrhotic patients.

PERSPECTIVES FOR THE FUTURE

This thesis has explored the synergistic relationship between ammonia and inflammation in the molecular pathogenesis of hepatic encephalopathy. The importance of the role of ammonia has been previously highlighted with respect to both its direct neurotoxicity and on brain swelling through its detoxification to glutamine in the astrocyte, the cell most often implicated in the pathogenesis of hepatic encephalopathy. Therefore, one might say that the key to understanding the pathogenesis of hepatic encephalopathy is to explore the story of the 'sick astrocyte'. This thesis has demonstrated factors that are critical in modulating the manifest symptoms of hepatic encephalopathy, the most important of which is the synergistic role of inflammation in modulating the cerebral effects of ammonia. Furthermore, the production of reactive oxygen species and increased protein tyrosine nitration may alter astrocyte function and contribute or precipitate episodes of hepatic encephalopathy. However, little is really understood about the underlying mechanisms which control ammonia handling in the brain in an inflammatory milieu.

One aspect of the findings of this thesis that is worthy of further attention is the origin of the nitric oxide, shown to be important in mediating the synergistic relationship between of ammonia and inflammation. Future studies which could include Western blots of homogenized brain tissue would allow the identification of tissue nitric oxide synthase isoforms; defining the relative amounts of inducible, endothelial and neuronal nitric oxide synthase. Furthermore, immunohistochemistry performed on the sections obtained for

high resolution light microscopy would indicate the location of these nitric oxide synthases within the brain.

Another avenue of investigation should be the study of the blood brain barrier. Although the brain tissue sections visualized under light microscopy are highly informative and clearly demonstrate astrocyte swelling, it would be even better if the blood brain barrier could be visualized by electron microscopy in these animal models in the presence and absence of endotoxaemia. Contact and communication between the neurovascular unit, which is a dynamic structure consisting of vascular endothelial cells, pericytes, and closely juxtaposed astrocytes and neurons, modulates cerebral blood flow and influences the permeability properties of the blood brain barrier. Electron microscopy utilizing intravascular ionic tracers such as lanthanum nitrate, would allow detection of blood brain barrier integrity to paracellular movement and would allow visualization of the tight junctions which may allow the study of the effect of hyperammonemia and inflammation on the tight junction proteins such as claudin and occludin.

Finally, perhaps a really novel study to undertake would be to investigate the role of $p38^{-MAPK}$ in ammonia-induced astrocyte swelling. $p38^{-MAPK}$ has already been shown to be important in glutamine-induced hepatocyte swelling and these findings have been mirrored in the neutrophil which has been shown to swell following ammonia incubation, an observation which is prevented by a specific $p38^{-MAPK}$ agonist isoproterenol. Novel strategies such as utilising $p38^{-MAPK}$ agonists in therapies for hepatic encephalopathy might also be explored in the future.

We have so far only uncovered the tip of the iceberg in terms of understanding the operative mechanisms involved in the pathogenesis of hepatic encephalopathy but I very

much look forward to seeing this exciting area of research move forward over the next few years.

References

Reference List

1. Budge E. Gods of the Egyptians. New York, USA: Dover Publications, 1985.
2. Pickett J, et al. The American Heritage Dictionary of the English Language. Fourth Edition ed. Boston: Houghton Mifflin Co, 2000.
3. Todes D. Pavlov's Physiology Factory: Experiment, Interpretation, Laboratory Enterprise. Baltimore and London: The John Hopkins University Press, 2002.
4. Hahn M, Massen O, Nencki M, Pavlov I. Die Eck'sche fistel zwischen der unteren hohlvene und der pfortader und ihre folgen fur den organismus. Arch Exp Pathol Pharm 1893; 32:161-210.
5. Nencki M, Zaleski J. Ueber die Bestimmung des Ammoniaks in Thierischen Fluessigkeiten und Geweben. Archiv fuer experimentelle pathologie und pharmakologie 1895; 36:385-396.
6. Nencki M, Pawlow J, Zaleski J. Ueber den ammoniakgehalt des blutes under der organe und die harnstoffbildung bei den saugethieren. Archiv fuer experimentelle pathologie und pharmakologie 1896; 37:26-51.
7. Shawcross DL, Olde Damink SWM, Butterworth RF, Jalan R. Ammonia and Hepatic Encephalopathy: The More Things Change, the More They Remain the Same. Metab Brain Dis 2005; 20(3):169-179.
8. Hagen S, Wu H, Morrison S. NH(4)Cl inhibition of acid secretion: possible involvement of an apical (+) channel in bullfrog oxyntic cells. Am J Physiol Gastrointest Liver Physiol 2000; 279(2):G400-G410.

9. Neiger R, Simpson K. Helicobacter infection in dogs and cats: facts and fiction. J Vet Intern Med 2000; 14(2):125-133.
10. Vasconez C, Ignasi Elizalde J, Llach J, Gines A, de la Rosa C, Fernadez R et al. Helicobacter pylori, hyperammonemia and subclinical portosystemic encephalopathy: effects of eradication. Journal of Hepatology 1999; 30:260-264.
11. Floch M, Katz J, Conn H. Qualitative and quantitative relationships of the faecal flora in cirrhotic patients with portal systemic encephalopathy and following portacaval anastomosis. Gastroenterology 1970; 59:70-75.
12. Weber FJ, Veach G. The importance of the small intestine in gut ammonium production in the fasting dog. Gastroenterology 1979; 77:235-240.
13. Nance F, Kayfman H, Kline D. Role of urea in the hyperammonemia of germ-free Eck fistula dogs. Gastroenterology 1974; 66:108-112.
14. Schalm S, van der Mey T. Hyperammonemia coma after hepatectomy in germ-free rats. Gastroenterology 1979; 77:231-234.
15. Windmueller H. Glutamine utilization by the small intestine. Adv Enzyme Regul 1982; 53:210-237.
16. Owen E, Tyor M, Flanagan J, Berry J. The kidney as a source of blood ammonia in patients with liver disease: the effect of acetazolamaide. J Clin Invest 1960; 39:288-294.
17. Webster L, Gabuzda G. Ammonium uptake by the extremities and brain in hepatic coma. J Clin Invest 1958; 37:414-424.

18. Lockwood A, McDonald J, Reiman R, Gelbard A, Laughlin J, Duffy T et al. The dynamics of ammonia metabolism in man. Effects of liver disease and hyperammonemia. J Clin Invest 1979; 63:449-460.

19. Owen E, Mozzoli M, Reichle F, Kreulen T, Owen R, Boden G et al. Hepatic and renal metabolism before and after portosystemic shunts in patients with cirrhosis. J Clin Invest 1985; 76:1209-1217.

20. Dejong C, Deutz N, Soeters P. Renal ammonia and glutamine metabolism during liver insufficiency-induced hyperammonemia in the rat. J Clin Invest 1993; 92:2834-2840.

21. Olde Damink S, Deutz N, Redhead D, Hayes P, Soeters P, Jalan R. Interorgan ammonia and amino acid metabolism in metabolically stable patients with cirrhosis and a TIPSS. Hepatology 2002; 36:1163-1171.

22. Olde Damink S, Jalan R, Deutz N, Redhead D, Dejong C, Hynd P et al. The kidney plays a major role in the hyperammonemia seen after a simulated or actual upper gastrointestinal bleeding in patients with cirhosis. Hepatology 2003; 37:1277-1285.

23. Gabuzda GJ, Jr., Phillips GB, Davidson CS. Reversible toxic manifestations in patients with cirrhosis of the liver given cation-exchange resins. N Engl J Med 1952; 246(4):124-130.

24. Phillips G, Schwartz R, Gabuzda G, Davidson C. The syndrome of impending hepatic coma in patients with cirrhosis of the liver given certain nitrogenous substances. New England Journal of Medicine 1952; 247:239-246.

25. Sherlock S. Pathogenesis and management of hepatic coma. Am J Med 1958; 24(5):805-813.

26. Stahl J. Studies of the blood ammonia in liver disease. Its diagnostic, prognostic, and therapeutic significance. Ann Intern Med 1963; 58:1-24.

27. Ferenci P, Lockwood A, Mullen K, Tater R, Weissenborn K, Blei A et al. Hepatic Encephalopathy - Definition, nomenclature, diagnosis and quantification: Final report of the Working Party at the 11th World Congress of Gastroenterology, Vienna, 1998. Hepatology 2002; 35:716-721.

28. Amodio P, Del Piccolo F, Marchetti P, Angeli P, Iemmolo R, Caregaro L et al. Clinical features and survivial of cirrhotic patients with subclinical cognitive alterations detected by the number connection test and computerized psychometric tests. Hepatology 1999; 29(6):1662-1667.

29. Amodio P, Montagnese S, Gatta A, Morgan MY. Characteristics of minimal hepatic encephalopathy. Metab Brain Dis 2004; 19(3-4):253-267.

30. Schomerus H, Hamster W, Blunck H, Reinhard U, Mayer K, Dolle W. Latent portasystemic encephalopathy. I. Nature of cerebral functional defects and their effect on fitness to drive. Dig Dis Sci 1981; 26(7):622-630.

31. Sen S, Williams R, Jalan R. The pathophysiological basis of acute-on-chronic liver failure. Liver 2002; Suppl 2:5-13.

32. Norenberg M. Hepatic Encephalopathy: Studies with astrocyte cultures. In: Norenberg M, Hertz L, Schousboe A, editors. The Biochemical Pathology of Astrocytes. New York: Alan R. Liss, 1988: 451-464.

33. Butterworth RF, Giguere JF, Michaud J, Lavoie J, Layrargues GP. Ammonia: key factor in the pathogenesis of hepatic encephalopathy. Neurochem Pathol 1987; 6(1-2):1-12.

34. Desjardins P, Bandeira P, Rao VL, Butterworth RF. Portacaval anastomosis causes selective alterations of peripheral-type benzodiazepine receptor expression in rat brain and peripheral tissues. Neurochem Int 1999; 35(4):293-299.

35. Chan H, Butterworth RF. Evidence for an astrocytic glutamate transporter deficit in hepatic encephalopathy. Neurochem Res 1999; 24(11):1397-1401.

36. Belanger M, Desjardins P, Chatauret N, Butterworth RF. Loss of expression of glial fibrillary acidic protein in acute hyperammonemia. Neurochem Int 2002; 41(2-3):155-160.

37. McCarty JH. Cell biology of the neurovascular unit: implications for drug delivery across the blood-brain barrier. Assay Drug Dev Technol 2005; 3(1):89-95.

38. Lockwood A, Yap E, Wong W. Cerebral ammonia metabolism in patients with severe liver disease and minimal hepatic encephalopathy. Journal of Cerebral Blood Flow and Metabolism 1991; 11:337-341.

39. Hamm S, Dehouck B, Kraus J, Wolburg-Buchholz K, Wolburg H, Risau W et al. Astrocyte mediated modulation of blood-brain barrier permeability does not correlate with a loss of tight junction proteins from the cellular contacts. Cell Tissue Res 2004; 315(2):157-166.

40. Kato M, Hughes RD, Keays RT, Williams R. Electron microscopic study of brain capillaries in cerebral edema from fulminant hepatic failure. Hepatology 1992; 15(6):1060-1066.

41. Bassett ML, Mullen KD, Scholz B, Fenstermacher JD, Jones EA. Increased brain uptake of gamma-aminobutyric acid in a rabbit model of hepatic encephalopathy. Gastroenterology 1990; 98(3):747-757.

42. Michalak A, Rose C, Butterworth J, Butterworth RF. Neuroactive amino acids and glutamate (NMDA) receptors in frontal cortex of rats with experimental acute liver failure. Hepatology 1996; 24(4):908-913.

43. Schafer DF, Fowler JM, Munson PJ, Thakur AK, Waggoner JG, Jones EA. Gamma-aminobutyric acid and benzodiazepine receptors in an animal model of fulminant hepatic failure. J Lab Clin Med 1983; 102(6):870-880.

44. Ahboucha S, Butterworth RF. Pathophysiology of hepatic encephalopathy: a new look at GABA from the molecular standpoint. Metab Brain Dis 2004; 19(3-4):331-343.

45. Butterworth RF. Pathophysiology of hepatic encephalopathy: a new look at ammonia. Metab Brain Dis 2002; 17(4):221-227.

46. Lockwood AH, McDonald JM, Reiman RE, Gelbard AS, Laughlin JS, Duffy TE et al. The dynamics of ammonia metabolism in man. Effects of liver disease and hyperammonemia. J Clin Invest 1979; 63(3):449-460.

47. Dejong C, Kampman M, Deutz N, Soeters P. Cerebral cortex ammonia and glutamine metabolism during liver insufficiency-induced hyperammonemia in the rat. J Neurochem 1992; 59:1071-1079.

48. Clemmesen J, Larsen F, Kondrup J, Hansen B, Ott P. Cerebral herniation in patients with acute liver failure is correlated with arterial ammonia concentration. Hepatology 1999; 29:648-653.

49. Haussinger D, Kircheis G, Fischer R, Schleiss F, vom Dahl S. Hepatic encephalopathy in chronic liver disease: a clinical manifestation of astrocyte swelling and low grade oedema? Journal of Hepatology 2000; 32:1035-1038.

50. Cordoba J, Alonso J, Rovira A, Jacas C, Sanpedro F, Castells L et al. The development of low-grade cerebral oedema in cirrhosis is supported by the evolution of 1H-magnetic resonance abnormalities after liver transplantation. Journal of Hepatology 2001; 35:598-604.

51. Balata S, Olde Damink S, Ferguson K, Marshall I, Hayes P, Deutz N et al. Induced hyperammonemia alters neuropsychology, brain MR spectroscopy and magnetization transfer in cirrhosis. Hepatology 2003; 37:931-939.

52. Shawcross DL, Balata S, Olde Damink SW, Hayes PC, Wardlaw J, Marshall I et al. Low myo-inositol and high glutamine levels in brain are associated with neuropsychological deterioration after induced hyperammonemia. Am J Physiol Gastrointest Liver Physiol 2004; 287(3):G503-G509.

53. Cordoba J, Gottstein J, Blei A. Chronic hyponatremia exacerbates ammonia-induced brain oedema in rats after portacaval anastomosis. Hepatology 1998; 29(4):589-594.

54. Szerb JC, Butterworth RF. Effect of ammonium ions on synaptic transmission in the mammalian central nervous system. Prog Neurobiol 1992; 39(2):135-153.

55. Rose C, Kresse W, Kettenmann H. Acute insult of ammonia leads to calcium-dependent glutamate release from cultured astrocytes: An effect of pH. J Biol Chem 2005.

56. Michalak A, Rose C, Butterworth J, Butterworth RF. Neuroactive amino acids and glutamate (NMDA) receptors in frontal cortex of rats with experimental acute liver failure. Hepatology 1996; 24(4):908-913.

57. Albrecht J, Jones EA. Hepatic encephalopathy: molecular mechanisms underlying the clinical syndrome. J Neurol Sci 1999; 170(2):138-146.

58. Jones EA. Potential mechanisms of enhanced GABA-mediated inhibitory neurotransmission in liver failure. Neurochem Int 2003; 43(4-5):509-516.

59. Ahboucha S, Pomier-Layrargues G, Butterworth RF. Increased brain concentrations of endogenous (non-benzodiazepine) GABA-A receptor ligands in human hepatic encephalopathy. Metab Brain Dis 2004; 19(3-4):241-251.

60. Erceg S, Monfort P, Hernandez-Viadel M, Rodrigo R, Montoliu C, Felipo V. Oral administration of sildenafil restores learning ability in rats with hyperammonemia and with portacaval shunts. Hepatology 2005; 41(2):299-306.

61. Lai JC, Cooper AJ. Brain alpha-ketoglutarate dehydrogenase complex: kinetic properties, regional distribution, and effects of inhibitors. J Neurochem 1986; 47(5):1376-1386.

62. Hindfelt B, Plum F, Duffy T. Effect of acute ammonia intoxication on cerebral metabolism in rats with portacaval shunts. J Clin Invest 1977; 59(3):386-396.

63. Yao H, Sadoshima S, Fujii K, Kusuda K, Ishitsuka T, Tamaki K et al. Cerebrospinal fluid lactate in patients with hepatic encephalopathy. Eur Neurol 1987; 27(3):182-187.

64. Therrien G, Giguere JF, Butterworth RF. Increased cerebrospinal fluid lactate reflects deterioration of neurological status in experimental portal-systemic encephalopathy. Metab Brain Dis 1991; 6(4):225-231.

65. Zwingmann C, Chatauret N, Leibfritz D, Butterworth RF. Selective increase of brain lactate synthesis in experimental acute liver failure: results of a [H-C] nuclear magnetic resonance study. Hepatology 2003; 37(2):420-428.

66. Desjardins P, Belanger M, Butterworth RF. Alterations in expression of genes coding for key astrocytic proteins in acute liver failure. J Neurosci Res 2001; 66(5):967-971.

67. Bergeron M, Reader TA, Layrargues GP, Butterworth RF. Monoamines and metabolites in autopsied brain tissue from cirrhotic patients with hepatic encephalopathy. Neurochem Res 1989; 14(9):853-859.

68. Norenberg MD. Astrocytic-ammonia interactions in hepatic encephalopathy. Semin Liver Dis 1996; 16(3):245-253.

69. Rama Rao KV, Chen M, Simard JM, Norenberg MD. Increased aquaporin-4 expression in ammonia-treated cultured astrocytes. Neuroreport 2003; 14(18):2379-2382.

70. Manley GT, Binder DK, Papadopoulos MC, Verkman AS. New insights into water transport and edema in the central nervous system from phenotype analysis of aquaporin-4 null mice. Neuroscience 2004; 129(4):983-991.

71. Rao V, Butterworth R. Neuronal nitric oxide synthase and hepatic encephalopathy. Metab Brain Dis 1998; 13:175-189.

72. Mulligan SJ, MacVicar BA. Calcium transients in astrocyte endfeet cause cerebrovascular constrictions. Nature 2004; 431(7005):195-199.

73. Jalan R, Olde Damink SW, Hayes PC, Deutz NE, Lee A. Pathogenesis of intracranial hypertension in acute liver failure: inflammation, ammonia and cerebral blood flow. J Hepatol 2004; 41(4):613-620.

74. Vaquero J, Chung C, Blei AT. Cerebral blood flow in acute liver failure: a finding in search of a mechanism. Metab Brain Dis 2004; 19(3-4):177-194.

75. Magistretti PJ, Pellerin L, Rothman DL, Shulman RG. Energy on demand. Science 1999; 283(5401):496-497.

76. Master S, Gottstein J, Blei AT. Cerebral blood flow and the development of ammonia-induced brain edema in rats after portacaval anastomosis. Hepatology 1999; 30(4):876-880.

77. Guevara M, Bru C, Gines P, Fernandez-Esparrach G, Sort P, Bataller R et al. Increased cerebrovascular resistance in cirrhotic patients with ascites. Hepatology 1998; 28(1):39-44.

78. Ahl B, Weissenborn K, van den HJ, Fischer-Wasels D, Kostler H, Hecker H et al. Regional differences in cerebral blood flow and cerebral ammonia metabolism in patients with cirrhosis. Hepatology 2004; 40(1):73-79.

79. Jalan R, Olde Damink S, Lui H, Glabus M, Deutz N, Hayes P et al. Oral amino acid load mimicking haemoglobin results in reduced regional cerebral perfusion

and deterioration in memory tests in patients with cirrhosis of the liver. Metabolic Brain Disease 2003; 18:37-49.

80. Licinio J, Wong M. Pathways and mechanisms for cytokine signalling of the central nervous system. J Clin Invest 1997; 100:2941-2947.

81. Hosoi T, Okuma Y, Nomura Y. The mechanisms of immune-to-brain communication in inflammation as a drug target. Curr Drug Targets Inflamm Allergy 2002; 1(3):257-262.

82. Sharshar T, Gray F, Lorin de la Grandmaison G, Hopkinson N, Ross E, Dorandeau A et al. Apoptosis of neurons in cardiovascular autonomic centres triggered by inducible nitric oxide synthase after death from septic shock. Lancet 2003; 363:1799-1805.

83. Hu S, Sheng W, Ehrlich L, Peterson P, Chao C. Cytokine effects on glutamate uptake by human astrocytes. Neuroimmunomodulation 2000; 7:153-159.

84. Oh YJ, Francis JW, Markelonis GJ, Oh TH. Interleukin-1-beta and tumor necrosis factor-alpha increase peripheral-type benzodiazepine binding sites in cultured polygonal astrocytes. J Neurochem 1992; 58(6):2131-2138.

85. Duchini A, Govindarajan S, Santucci M, Zampi G, Hofman FM. Effects of tumor necrosis factor-alpha and interleukin-6 on fluid-phase permeability and ammonia diffusion in CNS-derived endothelial cells. J Investig Med 1996; 44(8):474-482.

86. Schiltz JC, Sawchenko PE. Signaling the brain in systemic inflammation: the role of perivascular cells. Front Biosci 2003; 8:s1321-s1329.

87. Fong Y, Tracey KJ, Moldawer LL, Hesse DG, Manogue KB, Kenney JS et al. Antibodies to cachectin/tumor necrosis factor reduce interleukin 1 beta and

interleukin 6 appearance during lethal bacteremia. J Exp Med 1989; 170(5):1627-1633.

88. de Vries HE, Blom-Roosemalen MC, van Oosten M, de Boer AG, van Berkel TJ, Breimer DD et al. The influence of cytokines on the integrity of the blood-brain barrier in vitro. J Neuroimmunol 1996; 64(1):37-43.

89. Didier N, Romero IA, Creminon C, Wijkhuisen A, Grassi J, Mabondzo A. Secretion of interleukin-1beta by astrocytes mediates endothelin-1 and tumour necrosis factor-alpha effects on human brain microvascular endothelial cell permeability. J Neurochem 2003; 86(1):246-254.

90. Falsig J, Latta M, Leist M. Defined inflammatory states in astrocyte cultures: correlation with susceptibility towards CD95-driven apoptosis. J Neurochem 2004; 88(1):181-193.

91. Korcok J, Wu F, Tyml K, Hammond RR, Wilson JX. Sepsis inhibits reduction of dehydroascorbic acid and accumulation of ascorbate in astroglial cultures: intracellular ascorbate depletion increases nitric oxide synthase induction and glutamate uptake inhibition. J Neurochem 2002; 81(1):185-193.

92. Schliess F, Gorg B, Fischer R, Desjardins P, Bidmon HJ, Herrmann A et al. Ammonia induces MK-801-sensitive nitration and phosphorylation of protein tyrosine residues in rat astrocytes. FASEB J 2002; 16(7):739-741.

93. Murthy C, Bai G, Dombro R, Norenberg M. Ammonia-induced swelling in primary cultures of rat astrocytes: Role of free radicals. Soc.Neurosci.Abstr. 26, 1893. 2000.

Ref Type: Abstract

94. Sonnewald U, Westergaard N, Jones P, Taylor A, Bachelard HS, Schousboe A. Metabolism of [U-13C5] glutamine in cultured astrocytes studied by NMR spectroscopy: first evidence of astrocytic pyruvate recycling. J Neurochem 1996; 67(6):2566-2572.

95. Yudkoff M, Nissim I, Pleasure D. Astrocyte metabolism of [15N]glutamine: implications for the glutamine-glutamate cycle. J Neurochem 1988; 51(3):843-850.

96. Tan KH, Harrington S, Purcell WM, Hurst RD. Peroxynitrite mediates nitric oxide-induced blood-brain barrier damage. Neurochem Res 2004; 29(3):579-587.

97. Rama Rao KV, Jayakumar AR, Norenberg MD. Induction of the mitochondrial permeability transition in cultured astrocytes by glutamine. Neurochem Int 2003; 43(4-5):517-523.

98. Papadopoulos MC, Davies DC, Moss RF, Tighe D, Bennett ED. Pathophysiology of septic encephalopathy: a review. Crit Care Med 2000; 28(8):3019-3024.

99. Freund HR, Ryan JA, Jr., Fischer JE. Amino acid derangements in patients with sepsis: treatment with branched chain amino acid rich infusions. Ann Surg 1978; 188(3):423-430.

100. Basler T, Meier-Hellmann A, Bredle D, Reinhart K. Amino acid imbalance early in septic encephalopathy. Intensive Care Med 2002; 28(3):293-298.

101. Sprung CL, Cerra FB, Freund HR, Schein RM, Konstantinides FN, Marcial EH et al. Amino acid alterations and encephalopathy in the sepsis syndrome. Crit Care Med 1991; 19(6):753-757.

102. Marcaida G, Felipo V, Hermenegildo C, Minana MD, Grisolia S. Acute ammonia toxicity is mediated by the NMDA type of glutamate receptors. FEBS Lett 1992; 296(1):67-68.

103. Rao KV, Norenberg MD. Cerebral energy metabolism in hepatic encephalopathy and hyperammonemia. Metab Brain Dis 2001; 16(1-2):67-78.

104. Guerrini VH. Effect of antioxidants on ammonia induced CNS-renal pathobiology in sheep. Free Radic Res 1994; 21(1):35-43.

105. Jalan R, Olde Damink SW, Deutz NE, Hayes PC, Lee A. Moderate hypothermia in patients with acute liver failure and uncontrolled intracranial hypertension. Gastroenterology 2004; 127(5):1338-1346.

106. Globus MY, Alonso O, Dietrich WD, Busto R, Ginsberg MD. Glutamate release and free radical production following brain injury: effects of posttraumatic hypothermia. J Neurochem 1995; 65(4):1704-1711.

107. Takada Y, Ishiguro S, Fukunaga K, Gu M, Tangiguchi H, Seino K-I et al. Increased intracranial pressure in a porcine model of fulminant hepatic failure using amatoxin and endotoxin. Journal of Hepatology 2001; 34:825-831.

108. Sen S, Rose C, Davies N, Williams R, Butterworth R, Revhaug A et al. Albumin dialysis reduces brain water and intracranial pressure in acute liver failure: a randomised controlled study in a pig model. Hepatology 38 Suppl. 1[4]. 2003.

Ref Type: Abstract

109. Rolando N, Wade J, Davalos M, Wendon J, Philpott-Howard J, Williams R. The systemic inflammatory response syndrome in acute liver failure. Hepatology 2000; 32:734-739.

110. Vacquero J, Polson J, Chung C, Helenowski I, Schiodt F, Reisch J et al. Infection and the progression of hepatic encephalopathy in acute liver failure. Gastroenterology 2003; 125:755-764.

111. Jalan R, Olde Damink SW, Hayes PC, Deutz NE, Lee A. Pathogenesis of intracranial hypertension in acute liver failure: inflammation, ammonia and cerebral blood flow. J Hepatol 2004; 41(4):613-620.

112. Jalan R, Olde Damink S, Lee A, Hayes P, Williams R. Brain production of inflammatory cytokines in patients with acute liver failure and uncontrolled intracranial hypertension. Hepatology 38, 548A. 2003.

Ref Type: Abstract

113. Jalan R, Olde Damink S, Sen S, Mookerjee RP, Hayes PC, Deutz N. Arginine, citrulline and nitric oxide metabolism in patients with liver failure and the effect of intervention with hypothermia, MARS and transplantation. Hepatology 40[4 Suppl. 1]. 2004.

Ref Type: Abstract

114. Aggarwal S, Kramer D, Yonas H, Obrist W, Kang Y, Martin M et al. Cerebral hemodynamic and metabolic changes in fulminant hepatic failure: a retrospective study. Hepatology 1994; 19(1):80-87.

115. Jalan R, Olde Damink S, Deutz N, Lee A, Hayes P. Treatment of uncontrolled intracranial hypertension in acute liver failure with moderate hypothermia. Lancet 1999; 354:1164-1168.

116. Jalan R, Pollok A, Shah SH, Madhavan K, Simpson KJ. Liver derived pro-inflammatory cytokines may be important in producing intracranial hypertension in acute liver failure. J Hepatol 2002; 37(4):536-538.

117. Brunk UT. On the origin of lipofuscin; the iron content of residual bodies, and the relation of these organelles to the lysosomal vacuome. A study on cultured human glial cells. Adv Exp Med Biol 1989; 266:313-320.

118. Rao VL, Audet RM, Butterworth RF. Increased nitric oxide synthase activities and L-[3H]arginine uptake in brain following portacaval anastomosis. J Neurochem 1995; 65(2):677-678.

119. Vaquero J, Chung C, Cahill ME, Blei AT. Pathogenesis of hepatic encephalopathy in acute liver failure. Semin Liver Dis 2003; 23(3):259-269.

120. Larsen F, Gottstein J, Blei A. Cerebral hyperemia and nitric oxide synthase in rats with ammonia-induced brain edema. J Hepatol 2001; 34:548-554.

121. Liu Q, Duan ZP, Ha dK, Bengmark S, Kurtovic J, Riordan SM. Synbiotic modulation of gut flora: effect on minimal hepatic encephalopathy in patients with cirrhosis. Hepatology 2004; 39(5):1441-1449.

122. Borzio M, Salerno F, Piantoni L, Cazzaniga M, Angeli P, Bissoli F et al. Bacterial infection in patients with advanced cirrhosis: a multicentre prospective study. Dig Liver Dis 2001; 33(1):41-48.

123. Fernandez J, Navasa M, Gomez J, Colmenero J, Vila J, Arroyo V et al. Bacterial infections in cirrhosis: epidemiological changes with invasive procedures and norfloxacin prophylaxis. Hepatology 2002; 35(1):140-148.

124. Wong F, Bernardi M, Balk R, Christman B, Moreau R, Garcia-Tsao G et al. Sepsis in cirrhosis: report on the 7th meeting of the International Ascites Club. Gut 2005; 54(5):718-725.

125. Nolan J. The role of endotoxin in liver injury. Gastroenterology 1975; 69:1346-1356.

126. Bode C, Kugler V, Bode J. Endotoxemia in patients with alcoholic and non-alcoholic cirrhosis and in subjects with no evidence of chronic liver disease following acute alcohol excess. Journal of Hepatology 1987; 4:8-14.

127. Rajkovic IA, Williams R. Mechanisms of abnormalities in host defences against bacterial infection in liver disease. Clin Sci (Lond) 1985; 68(3):247-253.

128. Rajkovic IA, Williams R. Abnormalities of neutrophil phagocytosis, intracellular killing and metabolic activity in alcoholic cirrhosis and hepatitis. Hepatology 1986; 6(2):252-262.

129. Navasa M, Feu F, Garcia-Pagan J, Jimenez W, Llach J, Rimola A et al. Hemodynamic and humoral changes after liver transplantation in patients with cirrhosis. Hepatology 1993; 17(3):355-360.

130. Trevisani F, Castelli E, Foschi FG, Parazza M, Loggi E, Bertelli M et al. Impaired tuftsin activity in cirrhosis: relationship with splenic function and clinical outcome. Gut 2002; 50(5):707-712.

131. Mookerjee R, Stadlbauer V, Lidder S, Wright G, Hodges S, Davies N et al. Neutrophil dysfunction in alcoholic hepatitis superimposed on cirrhosis is reversible and predicts outcome. Hepatology. In press.

132. Lee W, Harrison R, Grinstein S. Phagocytosis by neutrophils. Microbes and Infection 2003; 5:1299-1306.

133. Baldridge C, Gerard R. The extra respiration of phagocytosis. Am J Physiol 1933; 103:235.

134. Sbarra A, Karnovsky M. The biochemical basis of phagocytosis: I. Metabolic changes during the ingestion of particles by polymorphonuclear leukocytes. J Biol Chem 1959; 234:1355.

135. Dahlgren C, Karlsson A. Respiratory burst in human neutrophils. Journal of Immunological Methods 1999; 232:3-14.

136. Hellstrand K, Asea A, Dahlgren C, Hermodsson S. Histaminergic regulation of NK cells. Role of monocyte-derived reactive oxygen metabolites. J Immunol 1994; 153:4940.

137. Lundqvist Gustafsson H, Bengtsson T. Activation of the granule pool of the NADPH-oxidase accelerates apoptosis in human neutrophils. J Leukoc Biol 1999; 65:196.

138. Pithon-Curi T, Trezena A, Tavares-Lima W. Evidence that glutamine is involved in neutrophil function. Cell Biochemistry and Function 2002; 20:81-86.

139. Pithon Curi T, De Melo M, Azevedo R, Zorn T, Curi R. Glutamine utilization by rat neutrophils: presence of phosphate-dependent glutaminase. Am J Physiol 1997; 273:C1124-C1129.

140. Garcia C, Pithon-Curi T, Firmano M, Pires de Mel M, Newsholme P, Curi R. Effects of adrenaline on glucose and glutamine metabolism and superoxide production by rat neutrophils. Clinical Science 1999; 96:549-555.

141. Ogle C, Ogle J, Mao J, Simon J, Noel J, Li B et al. Effect of glutamine on phagocytosis and bacterial killing by normal and paediatric burn patient neutrophils. J Parent Ent Nutr 1994; 18:128-133.

142. Moinard C, Chauveau B, Walrand S, Felgines C, Chassagne J, Caldefie F et al. Phagocyte functions in stressed rats: comparison of modulation by glutamine, arginine and ornithine 2-oxoglutarate. Clinical Science 1999; 97:59-65.

143. Moinard C, Caldefie F, Walrand S, Tridon A, Chassagnes J, Vasson M-P. Effects of ornithine 2-oxoglutarate on neutrophils in stressed rats: evidence for the involvement of nitirc oxide and polyamines. Clinical Science 2002; 102:287-295.

144. Ono K, Han J. The p38 signal transduction pathway: activation and function. Cell Signal 2000; 12(1):1-13.

145. Kumar S, Boehm J, Lee JC. p38 MAP kinases: key signalling molecules as therapeutic targets for inflammatory diseases. Nat Rev Drug Discov 2003; 2(9):717-726.

146. Saklatvala J. The p38 MAP kinase pathway as a therapeutic target in inflammatory disease. Curr Opin Pharmacol 2004; 4(4):372-377.

147. Han J, Lee JD, Tobias PS, Ulevitch RJ. Endotoxin induces rapid protein tyrosine phosphorylation in 70Z/3 cells expressing CD14. J Biol Chem 1993; 268(33):25009-25014.

148. Han J, Lee JD, Bibbs L, Ulevitch RJ. A MAP kinase targeted by endotoxin and hyperosmolarity in mammalian cells. Science 1994; 265(5173):808-811.

149. Hale KK, Trollinger D, Rihanek M, Manthey CL. Differential expression and activation of p38 mitogen-activated protein kinase alpha, beta, gamma, and delta in inflammatory cell lineages. J Immunol 1999; 162(7):4246-4252.

150. Akgul C, Moulding D, Edwards S. Molecular control of neutrophil apoptosis. FEBS Lett 2001; 487:318-322.

151. Doyle S, O'Connell R, Miranda G, Vaidya S, Chow E, Liu P et al. Toll-like receptors induce a phagocytic gene program through p38. J Exp Med 2004; 199(1):81-90.

152. Xiao Y, Malcolm K, Worthen G, Gardai S, Schiemann W, Fadok V et al. Cross-talk between ERK and p38 MAPK mediates selective suppression of pro-inflammatory cytokines by transforming growth factor-beta. The Journal of Biological Chemistry 2002; 277(17):14884-14893.

153. Alvarado-Kristensson M, Melander F, Leandersson K, Ronnstrand L, Wernstedt C, Andersson T. p38-MAPK Signals Survival by Phosphorylation of Caspase-8 and Caspase-3 in Human Neutrophils. J Exp Med 2004; 199(4):449-458.

154. Haussinger D, Graf D, Weiergraber O. Glutamine and cell signaling in the liver. J Nutr 2001; 131:2509S-2514S.

155. Haussinger D, Schliess F. Osmotic induction of signaling cascades: role in regulation of cell function. Biochem Biophys Res Commun 1999; 255(3):551-555.

156. Haussinger D, Schliess F, Dombrowski F, Vom DS. Involvement of p38MAPK in the regulation of proteolysis by liver cell hydration. Gastroenterology 1999; 116(4):921-935.

157. Vom DS, Schliess F, Graf D, Haussinger D. Role of p38(MAPK) in cell volume regulation of perfused rat liver. Cell Physiol Biochem 2001; 11(6):285-294.

158. Lund P. A radiochemical assay for glutamine synthetase, and activity of the enzyme in rat tissues. Biochem J 1970; 118:35-39.

159. Ganda OP, Ruderman NB. Muscle nitrogen metabolism in chronic hepatic insufficiency. Metabolism 1976; 25(4):427-435.

160. Eriksson LS, Broberg S, Bjorkman O, Wahren J. Ammonia metabolism during exercise in man. Clin Physiol 1985; 5(4):325-336.

161. Barrett EJ, Revkin JH, Young LH, Zaret BL, Jacob R, Gelfand RA. An isotopic method for measurement of muscle protein synthesis and degradation in vivo. Biochem J 1987; 245(1):223-228.

162. Bessman SP, Bessman AN. The cerebral and peripheral uptake of ammonia in liver disease with an hypothesis for the mechanism of hepatic coma. J Clin Invest 1955; 34(4):622-628.

163. Bessman SP, Bradley JE. Uptake of ammonia by muscle; its implications in ammoniagenic coma. N Engl J Med 1955; 253(26):1143-1147.

164. Tyor MP, Owen EE, Berry JN, Flanagan JF. The relative role of extremity, liver, and kidney as ammonia receivers and donors in patients with liver disease. Gastroenterology 1960; 39:420-424.

165. Bessman A, Hawkins R. The relative effects of enterically administered plasma and packed cells on circulating blood ammonia. Gastroenterology 1963; 45:368-373.

166. Clemmesen JO, Kondrup J, Ott P. Splanchnic and leg exchange of amino acids and ammonia in acute liver failure. Gastroenterology 2000; 118(6):1131-1139.

167. Desjardins P, Rao K, Michalak A, Rose C, Butterworth R. Effect of portacaval anstomosis on glutamine synthetase protein and gene expression in brain, liver and skeletal muscle. Metab Brain Dis 1999; 14(4):273-280.

168. Chabrier G, Schlienger JL, Imler M. [Study of muscular metabolism of ammonia in the posterior limbs of the intact rat]. C R Seances Soc Biol Fil 1982; 176(5):716-722.

169. Hills A, Reid E, Kerr W. Circulatory transport of L-glutamine in fasted mammals: cellular sources of urine ammonia. American Journal of Physiology 1967; 223:1470-1476.

170. Fine A. The effects of ammonia infusion on ammonia and glutamine metabolism by liver and muscle in the normal dog. Contrib Nephrol 1985; 47:1-8.

171. Deutz N, Dejong C, Reijven P, Soeters P. In vivo ammonia and glutamine flux measurements during hyperammonemia in rats and pigs. Prog Hepatol Encephal Metabol Nitr Exchange 1991;329-339.

172. Dejong C, Kampman M, Deutz N, Soeters P. Altered glutamine metabolism in rat portal drained viscera and hindquarter during hyperammonemia. Gastroenterology 1992; 102:936-948.

173. Rees C, Oppong K, Al-Mardini H, Hudson M, Record C. Effect of L-ornithine-L-aspartate on patients with and without TIPS undergoing glutamine challenge: a double blind, placebo controlled trial. Gut 2002; 47:571-574.

174. Staedt U, Leweling H, Gladisch R, Kortsik C, Hagmuller E, Holm E. Effects of ornithine aspartate on plasma ammonia and plasma amino acids in patients with cirrhosis. A double-blind, randomised study using a four-fold crossover design. J Hepatol 1993; 19(3):24-30.

175. Kircheis G, Nilius R, Held C, Berndt H, Buchner M, Gortelmeyer R et al. Therapeutic efficacy of L-ornithine-L-aspartate infusions in patients with cirrhosis and hepatic encephalopathy: results of a placebo-controlled double-blind study. Hepatology 1997; 25(6):1351-1360.

176. Rose C, Michalak A, Pannunzio P, Therrien G, Quack G, Kircheis G et al. L-ornithine-Laspartate in experimental portal-systemic encephalopathy: therapeutic efficacy and mechanism of action. Metab Brain Dis 1998; 13(2):147-157.

177. Stauch S, Kircheis G, Adler G, Beckh K, Ditschuneit H, Gortelmeyer R et al. Oral L-ornithine-L-aspartate therapy of chronic hepatic encephalopathy: results of a placebo-controlled double-blind study. J Hepatol 1998; 28(5):856-864.

178. Groeneweg M, Quero J, De Bruijn I, Hartmann I, Essink-bot M, Hop W et al. Subclinical hepatic encephalopathy impairs daily functioning. Hepatology 1998; 28:45-49.

179. Stein B, Gamble J, Pitson S, Vadas M, Khew-Goodhall Y. Activation of endothelial extracellular signal-regulated kinase is essential for neutrophil transmigration: potential involvement of a soluble neutrophil factor in endothelial activation. J Immunol 2003; 171(11):6097-6104.

180. Hill R, Koningsberg W. The structure of human haemoglobin. The Journal of Biological Chemistry 1962; 237:3151-3156.

181. Douglass A, Al-Mardini H, Record C. Amino acid challenge in patients with cirrhosis: a model for the assessment of treatments for hepatic encephalopathy. Journal of Hepatology 2001; 34:658-664.

182. Oppong K, Al-Mardini H, Thick M, Record C. Oral glutamine challenge in patients with cirrhosis pre- and post- liver transplantation: a psychometric and analysed EEG study. Hepatology 1997; 26:870-876.

183. Masini A, Efrati C, Merli M, Nicolao F, Amodio P, Del Piccolo F et al. Effect of the blood ammonia elevation following orla glutamine load on the psychometric performance of cirrhotic patients. Metab Brain Dis 2003; 18:27-35.

184. Davies A. The influence of age on trail making test performance. J Clin Psychol 1968; 24:96-98.

185. Hindmarch I. Psychomotor function and psychoactive drugs. Br J Clin Pharmacol 1980; 10:189-209.

186. Frith C, Leary J, Cahill C, Johnstone E. Performance on psychological tests. Demographic and clinical correlates of the results of these tests. Br J Psychiatry Suppl 1991; 26-9:44-46.

187. Randt C, Brown E, Osborne D. A memory test for longitudinal measurement of mild to moderate defects. Clinical Neuropsychology 1980; II:184-197.

188. Gips CH, Wibbens-Alberts M. Ammonia determination in blood using the TCA direct method. Clin Chim Acta 1968; 22(2):183-186.

189. Miranda KM, Espey MG, Wink DA. A rapid, simple spectrophotometric method for simultaneous detection of nitrate and nitrite. Nitric Oxide 2001; 5(1):62-71.

190. Giovannoni G, Land J, Keir G, Thompson E, Heales S. Adaptation of the nitrate reductase and Griess reaction methods for the measurement of serum nitrate plus nitrite levels. Ann Clin Biochem 1997; 34(Pt 2):193-198.

191. van Eijk HM, Rooyakkers DR, Deutz NE. Rapid routine determination of amino acids in plasma by high-performance liquid chromatography with a 2-3 microns Spherisorb ODS II column. J Chromatogr 1993; 620(1):143-148.

192. Shawcross D, Davies N, Williams R, Jalan R. Systemic inflammatory response exacerbates the neuropsychological effects of induced hyperammonemia in cirrhosis. Journal of Hepatology 2004; 40(2):247-254.

193. Conn H, Lieberthal M. The hepatic coma syndromes and lactulose. Baltimore: Williams and Wilkins, 1979, 1979.

194. O'Carroll RE, MacLeod D. Moderate altitude has no effect on choice reaction time in international rugby players. Br J Sports Med 1997; 31(2):151-152.

195. Weissenborn K, Ennen J, Schomerus H, Ruckert N, Hecker H. Neuropsychological characterization of hepatic encephalopathy. Journal of Hepatology 2001; 34:768-773.

196. Amodio P, Marchetti P, Del Piccolo F, Campo G, Rizzo C, Lemmolo R et al. Visual attention in cirrhotic patients: a study on covert visual attention requiring orienting. Hepatology 1998; 27:1517-1523.

197. Wan W, Wetmore L, Sorensen CM, Greenberg AH, Nance DM. Neural and biochemical mediators of endotoxin and stress-induced c-fos expression in the rat brain. Brain Res Bull 1994; 34(1):7-14.

198. Hansen MK, Taishi P, Chen Z, Krueger JM. Vagotomy blocks the induction of interleukin-1beta (IL-1beta) mRNA in the brain of rats in response to systemic IL-1beta. J Neurosci 1998; 18(6):2247-2253.

199. Moller K, Strauss G, Qvist J, Fonsmark L, Knudsen G, Larsen F et al. Cerebral blood flow and oxidative metabolism during human endotoxaemia. J of Cerebral Blood Flow and Metab 2002; 22:1262-1270.

200. Gorg B, Foster N, Reinehr R, Bidmon HJ, Hongen A, Haussinger D et al. Benzodiazepine-induced protein tyrosine nitration in rat astrocytes. Hepatology 2003; 37(2):334-342.

201. Butterworth R. Pathophysiology of hepatic encephalopathy: the ammonia hypothesis revisited. In: Bengtsson F JBATeale, editor. Hepatic. Boca Raton, CRC Press, 1993: 9-24.

202. Olde Damink S, Dejong C, Deutz N, Soeters P. Effects of simulated upper gastrointestinal haemorrhage on ammonia and related amino acids in blood and brain of chronic portacaval-shunted rats. Metabolic Brain Disease 1997; 12:121-135.

203. Members of the American College of Chest Physicians/Society of Critical Care Medicine Consensus Conference Committee. American College of Chest Physicians/Society of Critical Care Medicine Consensus Conference: definitions for sepsis and organ failure and guidelines for the use of innovative therapies in sepsis. Crit Care Med 1992; 20:864-874.

204. Rolando N, Ellis A, De Groote D, Wendon J, Williams R. Correlation of serial cytokine levels with progression to coma (grade IV) in patients with acute liver failure. Hepatology 22, 366A. 1995.

Ref Type: Abstract

205. Rangel-Fausto M, Pittet D, Costigan M, Hwang T, Davis C, Wenzel R. The natural history of the systemic inflammatory response (SIRS). A prospective study. JAMA 1995; 273:117-123.

206. Pugh R, Murray-Lyon I, Dawson J, Pietroni M, Williams R. Transection of the oesophagus for bleeding oesphageal varices. Br J Surg 1973; 60(8):646-649.

207. Chadwick J, Mann W. The Medical Works of Hippocrates. Oxford: Blackwell, 1950.

208. Moncada S, Higgs A. The L-arginine-nitric oxide pathway. N Engl J Med 1993; 329:2002-2012.

209. Goulis J, Patch D, Burroughs AK. Bacterial infection in the pathogenesis of variceal bleeding. Lancet 1999; 353(9147):139-142.

210. Banks WA, Kastin AJ. Relative contributions of peripheral and central sources to levels of IL-1 alpha in the cerebral cortex of mice: assessment with species-specific enzyme immunoassays. J Neuroimmunol 1997; 79(1):22-28.

211. Watkins LR, Maier SF, Goehler LE. Cytokine-to-brain communication: a review & analysis of alternative mechanisms. Life Sci 1995; 57(11):1011-1026.

212. Romero L, Tatro J, Field J, Reichlin S. Roles of IL-1 and TNF-alpha in endotoxin-induced activation of nitric oxide synthase in cultured rat astrocytes. Am.J.Physiol. 270[Abstract], R326-R332. 1996.

Ref Type: Abstract

213. Wong M, Maier S, Goehler L. Inducible nitric oxide synthase gene expression in the brain during systemic inflammation. Nat Med 1996; 2:581-584.

214. Jalan R, Williams R. The inflammatory basis of intracranial hypertension in acute liver failure. Journal of Hepatology 2001; 34:548-554.

215. Takada Y, Ishiguro S, Fukunaga K, Gu M, Tangiguchi H, Seino K-I et al. Increased intracranial pressure in a porcine model of fulminant hepatic failure using amatoxin and endotoxin. Journal of Hepatology 2001; 34:825-831.

216. Norenberg M. A light and electron microscopic study of experiemental portal-systemic (ammonia) encephalopathy. Lab Invest 1977; 36:618-627.

217. Harry D, Anand R, Holt S, Davies S, Marley R, Fernando B et al. Increased sensitivity to endotoxemia in the bile duct-ligated cirrhotic rat. Hepatology 1999; 30(5):1198-1205.

218. Kountouras J, Billing B, Scheuer P. Prolonged bile duct ligation obstruction: a new experimental model of cirrhosis in the rat. Br J Exp Pathol 1984; 65:305-311.

219. Martinez-Prieto C, Ortiz M, Fortepiani L, Ruiz-Macia J, Atucha N, Garcia-Estan J. Haemodynamic and renal evolution of the bile duct-ligated rat. Clinical Science 2000; 98:611-617.

220. Green J, Better O. Systemic hypotension and renal failure in obstructive jaundice - mechanistic and therapeutic aspects. J Am Soc Nephrol 1995; 5:1853-1871.

221. Grinko I, Geerts A, Wisse E. Experimental biliary fibrosis correlates with increased numbers of fat-storing and Kupffer cells and portal endotoxemia. J Hepatol 1995; 23:449-458.

222. Manchay C, Vogel S. Interactions of lipopolysaccharide with macrophages. Immunol Series 1994; 60:63-81.

223. Kelm M. Nitric oxide metabolism and breakdown. Biochim Biophys Acta 1999; 1411(2-3):273-289.

224. Jourd'heuil D, Hallen K, Feelisch M, Grisham MB. Dynamic state of S-nitrosothiols in human plasma and whole blood. Free Radic Biol Med 2000; 28(3):409-417.

225. Keaney JF, Jr., Simon DI, Stamler JS, Jaraki O, Scharfstein J, Vita JA et al. NO forms an adduct with serum albumin that has endothelium-derived relaxing factor-like properties. J Clin Invest 1993; 91(4):1582-1589.

226. Simon DI, Stamler JS, Jaraki O, Keaney JF, Osborne JA, Francis SA et al. Antiplatelet properties of protein S-nitrosothiols derived from nitric oxide and endothelium-derived relaxing factor. Arterioscler Thromb 1993; 13(6):791-799.

227. Chan CY, Huang SW, Wang TF, Lu RH, Lee FY, Chang FY et al. Lack of detrimental effects of nitric oxide inhibition in bile duct-ligated rats with hepatic encephalopathy. Eur J Clin Invest 2004; 34(2):122-128.

228. Chu CJ, Lee FY, Wang SS, Chang FY, Lin HC, Wu SL et al. Establishment of an animal model of hepatic encephalopathy. Zhonghua Yi Xue Za Zhi (Taipei) 2000; 63(4):263-269.

229. Rodrigo R, Jover R, Candela A, Compan A, Saez-Valero J, Erceg S et al. Bile duct ligation plus hyperammonemia in rats reproduces the alterations in the modulation of soluble guanylate cyclase by nitric oxide in brain of cirrhotic patients. Neuroscience 2005; 130(2):435-443.

230. Karnovsky MJ. A formaldehyde-glutaraldehyde fixature of high osmolality for use in electron microscopy. J Cell Biol 1965; 27:137A-138A.

231. Graham RC, Jr., Karnovsky MJ. The early stages of absorption of injected horseradish peroxidase in the proximal tubules of mouse kidney: ultrastructural cytochemistry by a new technique. J Histochem Cytochem 1966; 14(4):291-302.

232. Matkowskyj KA, Marrero JA, Carroll RE, Danilkovich AV, Green RM, Benya RV. Azoxymethane-induced fulminant hepatic failure in C57BL/6J mice: characterization of a new animal model. Am J Physiol 1999; 277(2 Pt 1):G455-G462.

233. Marmarou A, Poll W, Shulman K, Bhagavan H. A simple gravimetric technique for measurement of cerebral oedema. Journal of Neurosurgery 1978; 49:530-537.

234. Yang BK, Vivas EX, Reiter CD, Gladwin MT. Methodologies for the sensitive and specific measurement of S-nitrosothiols, iron-nitrosyls, and nitrite in biological samples. Free Radic Res 2003; 37(1):1-10.

235. Samouilov A, Zweier JL. Development of chemiluminescence-based methods for specific quantitation of nitrosylated thiols. Anal Biochem 1998; 258(2):322-330.

236. Frost MT, Halliwell B, Moore KP. Analysis of free and protein-bound nitrotyrosine in human plasma by a gas chromatography/mass spectrometry method that avoids nitration artifacts. Biochem J 2000; 345 Pt 3:453-458.

237. Gips CH, Reitsema A, Wibbens-Alberts M. Preservation of urine for ammonia determination with a direct method. Clin Chim Acta 1970; 29(3):501-505.

238. Cordoba J, Alonso J, Rovira A, Jacas C, Sanpedro F, Castells L et al. The development of low-grade cerebral oedema in cirrhosis is supported by the

evolution of 1H-magnetic resonance abnormalities after liver transplantation. Journal of Hepatology 2001; 35:598-604.

239. Cordoba J, Sanpedro F, Alonso J, Rovira A. Proton Magnetic Resonance in the study of Hepatic Encephalopathy in Humans. Metabolic Brain Disease 2002; 17(4):415-429.

240. Jover R, Rodrigo R, Felipo V, Insausti R, Saez-Valero J, Garcia-Ayllon MS et al. Brain edema and inflammatory activation in bile duct ligated rats with diet-induced hyperammonemia: A model of hepatic encephalopathy in cirrhosis. Hepatology 2006; 43(6):1257-1266.

241. Lee JC, Cho GS, Kim HJ, Lim JH, Oh YK, Nam W et al. Accelerated cerebral ischemic injury by activated macrophages/microglia after lipopolysaccharide microinjection into rat corpus callosum. Glia 2005; 50(2):168-181.

242. Donadebian H. Congenital and acquired neutrophil abnormalities. In: Klempner M, et al., editors. Phagocytes and Disease. New York: Kluwer, Dordrecht Boston, 1989: 103-118.

243. Boyum A. Separation of leukocytes from blood and bone marrow. Introduction. Scand J Clin Lab Invest Suppl 1968; 97:7.

244. Vermes I, Haanen C, Steffens-Nakken H, Reutelingsperger C. A novel assay for apoptosis. Flow cytometric detection of phosphatidylserine expression on early apoptotic cells using fluorescein labelled Annexin V. J Immunol Methods 1995; 184(1):39-51.

245. Homburg CH, de Haas M, dem Borne AE, Verhoeven AJ, Reutelingsperger CP, Roos D. Human neutrophils lose their surface Fc gamma RIII and acquire Annexin V binding sites during apoptosis in vitro. Blood 1995; 85(2):532-540.

246. Martin SJ, Reutelingsperger CP, McGahon AJ, Rader JA, van Schie RC, LaFace DM et al. Early redistribution of plasma membrane phosphatidylserine is a general feature of apoptosis regardless of the initiating stimulus: inhibition by overexpression of Bcl-2 and Abl. J Exp Med 1995; 182(5):1545-1556.

247. Andree HA, Reutelingsperger CP, Hauptmann R, Hemker HC, Hermens WT, Willems GM. Binding of vascular anticoagulant alpha (VAC alpha) to planar phospholipid bilayers. J Biol Chem 1990; 265(9):4923-4928.

248. Muller WA, Randolph GJ. Migration of leukocytes across endothelium and beyond: molecules involved in the transmigration and fate of monocytes. J Leukoc Biol 1999; 66(5):698-704.

249. Schenkel AR, Mamdouh Z, Muller WA. Locomotion of monocytes on endothelium is a critical step during extravasation. Nat Immunol 2004; 5(4):393-400.

250. Cramer R, Soranzo MR, Dri P, Menegazzi R, Pitotti A, Zabucchi G et al. A simple reliable assay for myeloperoxidase activity in mixed neutrophil-eosinophil cell suspensions: application to detection of myeloperoxidase deficiency. J Immunol Methods 1984; 70(1):119-125.

251. Chance B, Mahely A. Methods in enzymology. In: Colowick S, Kaplan N, editors. Methods in Enzymology, Volume 2. New York: Academic Press, 1955: 764.

252. LoGrasso PV, Frantz B, Rolando AM, O'Keefe SJ, Hermes JD, O'Neill EA. Kinetic mechanism for p38 MAP kinase. Biochemistry 1997; 36(34):10422-10427.

253. Badger AM, Bradbeer JN, Votta B, Lee JC, Adams JL, Griswold DE. Pharmacological profile of SB 203580, a selective inhibitor of cytokine suppressive binding protein/p38 kinase, in animal models of arthritis, bone resorption, endotoxin shock and immune function. J Pharmacol Exp Ther 1996; 279(3):1453-1461.

254. Dudley DT, Pang L, Decker SJ, Bridges AJ, Saltiel AR. A synthetic inhibitor of the mitogen-activated protein kinase cascade. Proc Natl Acad Sci U S A 1995; 92(17):7686-7689.

255. Bennett BL, Sasaki DT, Murray BW, O'Leary EC, Sakata ST, Xu W et al. SP600125, an anthrapyrazolone inhibitor of Jun N-terminal kinase. Proc Natl Acad Sci U S A 2001; 98(24):13681-13686.

256. Han Z, Boyle DL, Chang L, Bennett B, Karin M, Yang L et al. c-Jun N-terminal kinase is required for metalloproteinase expression and joint destruction in inflammatory arthritis. J Clin Invest 2001; 108(1):73-81.

257. Duncia JV, Santella JB, III, Higley CA, Pitts WJ, Wityak J, Frietze WE et al. MEK inhibitors: the chemistry and biological activity of U0126, its analogs, and cyclization products. Bioorg Med Chem Lett 1998; 8(20):2839-2844.

258. Favata MF, Horiuchi KY, Manos EJ, Daulerio AJ, Stradley DA, Feeser WS et al. Identification of a novel inhibitor of mitogen-activated protein kinase kinase. J Biol Chem 1998; 273(29):18623-18632.

259. DeSilva DR, Jones EA, Favata MF, Jaffee BD, Magolda RL, Trzaskos JM et al. Inhibition of mitogen-activated protein kinase kinase blocks T cell proliferation but does not induce or prevent anergy. J Immunol 1998; 160(9):4175-4181.

260. Moule S, Denton R. The activation of p38 MAPK by the beta-adrenergic agonist isoproterenol in rat epididymal fat cells. FEBS Lett 1998; 439:287-290.

261. Vom DS, Dombrowski F, Schmitt M, Schliess F, Pfeifer U, Haussinger D. Cell hydration controls autophagosome formation in rat liver in a microtubule-dependent way downstream from p38MAPK activation. Biochem J 2001; 354(Pt 1):31-36.

262. Ehrmann RL, Gey GO. The growth of cells on a transparent gel of reconstituted rat-tail collagen. J Natl Cancer Inst 1956; 16(6):1375-1403.

263. Earle W. Production of malignancy in vitro. The mouse fibroblast cultures and the changes seen in the living cells. J Nat Cancer Inst 1943; 4:167-212.

264. Eagle G. Amino acid metabolism in mammalian cell cultures. Science 1959; 130:432-437.

265. Harvey AL, Dryden WF. Depolarization, desensitization and the effects of tubocurarine and neostigmine in cultured skeletal muscle. Eur J Pharmacol 1974; 27(1):5-13.

266. Konigsberg IR, McElvain N, Tootle M, Herrmann H. The dissociability of deoxyribonucleic acid synthesis from the development of multinuclearity of muscle cells in culture. J Biophys Biochem Cytol 1960; 8:333-343.

267. Graham FL, Whitmore GF. The effect of-beta-D-arabinofuranosylcytosine on growth, viability, and DNA synthesis of mouse L-cells. Cancer Res 1970; 30(11):2627-2635.

268. Stockdale FE, Holtzer H. DNA synthesis and myogenesis. Exp Cell Res 1961; 24:508-520.

269. Chandrasekhar S, Souba WW, Abcouwer SF. Identification of glucocorticoid-responsive elements that control transcription of rat glutamine synthetase. Am J Physiol 1999; 276(2 Pt 1):L319-L331.

270. Patejunas G, Young AP. Constitutive and glucocorticoid-mediated activation of glutamine synthetase gene expression in the developing chicken retina. J Biol Chem 1990; 265(25):15280-15285.

271. Chakrabarti R. Transcriptional regulation of the rat glutamine synthetase gene by tumor necrosis factor-alpha. Eur J Biochem 1998; 254(1):70-74.

272. Minet R, Villie F, Marcollet M, Meynial-Denis D, Cynober L. Measurement of glutamine synthetase activity in rat muscle by a colorimetric assay. Clin Chim Acta 1997; 268(1-2):121-132.

ACKNOWLEDGEMENTS

It would have been impossible to undertake this Ph.D without the selfless support and encouragement of a large number of people who I would like to give my grateful thanks.

Firstly, I would like to thank my Supervisor Dr Rajiv Jalan who during his Ph.D, undertook along with Steven Olde Damink, much of the research into Hepatic Encephalopathy and Interorgan Ammonia Metabolism which has laid down the foundation stones on which I've based much of my studies and consequently this thesis. Since the first day that I began working for him at the Middlesex Hospital in 2001, he has continuously supported me clinically and academically in following a career in Academic Hepatology. Furthermore, he has been the senior author on all of my original publications and reviews.

I undertook this research as a member of The Liver Failure Group at the Institute of Hepatology. The Liver Failure Group are unique, in that aside from being extremely hardworking, gifted scientists and clinicians, they also serve as a close knit family and incredible support network in difficult times. In particular, I would like to thank Stephen Hodges, a very Senior Scientist in the lab who has been unfailing in his support as a surrogate supervisor, having been a constant source of ideas and laboratory-based technical help, as well as proof-reading this thesis several times over! Other members of the Liver Failure Group that I'd like to acknowledge are Nathan Davies, another Senior Scientist, who is gifted at being able to fix any computer or program, as well as offer unending laboratory technical help. Also, Sister Lisa Cheshire, a Senior Clinical

Hepatology Research Nurse, made performing any clinical study easy with her fantastic efficiency and patient bedside skills; a wonderful friend and colleague. I'd also like to thank Suki Lidder, who has now moved to Chicago for teaching me how to isolate neutrophils and use flow cytometry, and whose early pilot neutrophil studies led on to the work performed in this thesis. I'd also like to mention Dr Sambit Sen, Dr Raj Mookerjee, Dr Gavin Wright, Dr Vanessa Stadlbauer and Dr Antonio Bertoletti for their help and support.

I'd also like to thank my second supervisor Mick Deutz and the Department of Academic Surgery in Maastricht University who performed HPLC and LCMS on my samples and provided me with the glutamate stable isotope. In particular, I'd like to thank Dr Hans van Eijk and Dr Gabrie Ten Haave for their laboratory support, particularly in the processing of the muscle cell samples.

The clinical studies employed patients from Edinburgh Royal Infirmary Liver Outpatients on the waiting list for liver transplantation under the directorship of Professor Peter Hayes. Dr Jalan performed all the neuropsychological function tests with guidance from Karen Ferguson and I'd like to thank them all for their help.

For the BDL studies, all the light microscopy and histology was performed at St George's University Department of Anatomy, Basic Medical Sciences Division by Gavin Wright, Ceri Davies and Heather Brooks. I'd also like to thank Dave Harry, A. Mani and Professor Kevin Moore at the Royal Free and University College Medical School who provided and housed the animals and performed the nitrotyrosine measurements.

The neutrophil mechanistic studies would have been impossible to perform without the expert help and guidance of Andy Pitsillides and Caroline Wheeler-Jones who provided the p38-MAPK inhibitors.

Of course, this work would not have been possible without funding which was gratefully received from The Foundation for Liver Research for 3 years. Furthermore, I'd like to acknowledge Merz and Axcan for the financial support they gave me in paying for my university fees and allowing me to present my research at International meetings such as the AASLD.

Lastly and most importantly, I'd like to thank my family, friends and in particular, Craig, the love of my life who has never stopped believing in me and has put up with doing all the household chores, cooking and making me endless cups of tea throughout the last year.